



UNIVERSITÀ  
degli STUDI  
di CATANIA

DEPARTMENT OF BIOMEDICAL AND BIOTECHNOLOGICAL SCIENCES  
PH.D. IN BIOTECHNOLOGY  
CURRICULUM IN MOLECULAR BIOTECHNOLOGY

XXXVI CYCLE

---

*Greta Paternò*

---

REVEALING THE POTENTIAL OF ASTROCYTE-DERIVED  
EXTRACELLULAR VESICLES:  
A NEW FRONTIER TO BOOST BRAIN REPAIR IN  
PARKINSON'S DISEASE

---

Ph.D. Thesis

Tutor:  
Prof. Nunzio Iraci  
Co-Tutor:  
Dr. Loredana Leggio

Coordinator:  
Prof. Vito De Pinto

---

Academic years 2020/23

# Table of content

<i>Abstract</i> .....	5
<i>Keywords and abbreviations</i> .....	6
<i>Affiliations</i> .....	8
<b>1. Introduction</b> .....	<b>9</b>
<b>1.1 Parkinson’s Disease (PD)</b> .....	<b>9</b>
1.1.1 Milestones of PD history .....	10
1.1.2 PD pathology: interplay between genetic and environmental factors ...	13
1.1.2.1 PD and $\alpha$ -Syn.....	17
1.1.2.2 PD and Mitochondrial dysfunction .....	19
1.1.2.3 PD and Neuroinflammation .....	20
1.1.2.4 PD and Gut microbiota.....	22
1.1.3 Clinical features and diagnosis .....	23
1.1.4 Therapeutic approaches for the treatment of PD.....	25
<b>1.2 Glial cells: a turning point in the therapeutic strategy of PD</b> .....	<b>31</b>
1.2.1 Glia history .....	32
1.2.2 Microglia.....	33
1.2.3 Macroglia .....	35
1.2.3.1 RGCs, oligodendrocytes and ependymal cells .....	35
1.2.3.2 Astrocytes .....	37
1.2.4 The “bad” and the “good” side of glial cells in the context of PD.....	39
1.2.5 The role of CCL3 chemokine in astrocyte stimulation .....	42
<b>1.3 Extracellular Vesicles (EVs)</b> .....	<b>44</b>
1.3.1 Historical background .....	46
1.3.2 EV biogenesis.....	48
1.3.2.1 EV purification methods .....	52
1.3.3 EV cargoes .....	54
1.3.4 EV secretion.....	58
1.3.5 Mechanisms of EV signaling with target cells .....	62

<b>1.3.6 Therapeutic potential of EVs .....</b>	<b>66</b>
<b>1.3.7 Dual role of astrocyte-derived EVs in PD .....</b>	<b>72</b>
<b>1.4 PD experimental model.....</b>	<b>76</b>
<b>2. Aims of the study and methods.....</b>	<b>80</b>
<b>3. Results.....</b>	<b>82</b>
<b>3.1 MPP<sup>+</sup> neurotoxin induces mitochondrial toxicity on RA-differentiated SH-SY5Y cell line .....</b>	<b>82</b>
<b>3.2 EVs released by nigrostriatal astrocytes preserve cell death and mitochondrial function in a cellular model of PD .....</b>	<b>85</b>
<b>3.3 An analytical model for quantifying EV uptake mechanism by differentiated SH-SY5Y cell line .....</b>	<b>90</b>
<b>4. Conclusions and future perspectives .....</b>	<b>92</b>
<b>5. References .....</b>	<b>98</b>
<b>6. Research articles.....</b>	<b>131</b>
<b>7. List of publications .....</b>	<b>183</b>
<b>8. Meetings and educational workshops.....</b>	<b>185</b>

## Sintesi

La malattia di Parkinson (MP), dopo l'Alzheimer, è il disturbo neurodegenerativo più diffuso, con la comparsa di disturbi sia motori che non-motori. Il processo degenerativo è caratterizzato dalla perdita dei neuroni dopaminergici del mesencefalo ventrale (VMB) e delle loro proiezioni nello striato (STR), con conseguente riduzione della dopamina. Ad oggi, le cause della MP sono ancora poco note, e non esistono terapie curative. In questo contesto, un ruolo essenziale viene svolto dalla glia, mediante una segnalazione bidirezionale con i neuroni. Astrociti e microglia sono in grado di rispondere al danno cerebrale con il rilascio di fattori neurotrofici e pro-infiammatori, che possono favorire la neuroprotezione, oppure contribuire alla neurodegenerazione. I meccanismi molecolari che regolano questo complesso *signaling* intercellulare non sono, tuttavia, ancora chiari. Negli ultimi 15-20 anni le vescicole extracellulari (EVs) sono emerse come importanti mediatori della comunicazione intercellulare, implicati in processi fisiologici e patologici. Le EVs sono nanostrutture membranose rilasciate da tutti i tipi di cellule, ed in grado di trasferire alle cellule bersaglio diverse classi di molecole. Le EVs sono anche una promettente fonte di nuovi biomarcatori e potenziali nanoterapeutici innovativi, poiché in grado di veicolare molecole ad azione farmacologica in maniera mirata.

Nel contesto della MP, le EVs prodotte dalla glia presentano ruoli controversi, riflettendo di fatto il comportamento delle cellule donatrici. In particolare, gli astrociti "attivati" dalla chemochina CCL3, proteggono i neuroni dopaminergici danneggiati, come dimostrato sia in modelli *in vitro* che *in vivo* di MP. Ciò avviene attraverso l'attivazione di un *cross-talk* astrocita-neurone, in cui le EVs potrebbero svolgere un ruolo chiave.

Obiettivo principale di questo progetto di dottorato è stato proprio quello di studiare le EVs nigrostriatali ed il loro ruolo nella MP. In particolare, abbiamo caratterizzato le EVs derivanti dagli astrociti del sistema nigrostriatale (VMB e STR), ed analizzato il loro ruolo nella comunicazione intercellulare astrocita-neurone. Per fare questo, abbiamo anche perfezionato un modello cellulare di MP, che è stato poi dissezionato mediante respirometria ad alta risoluzione.

Dai risultati è emerso che gli astrociti del VMB producono più vescicole rispetto allo STR e ad altre regioni cerebrali, e rispondono al trattamento con CCL3 incrementando la produzione di EVs. Abbiamo inoltre studiato il potenziale neuroprotettivo delle EVs derivanti dagli astrociti nigrostriatali su modelli *in vitro* di MP. Le analisi hanno mostrato che, sebbene tutte le EVs siano in grado di contrastare l'apoptosi indotta da H<sub>2</sub>O<sub>2</sub>, quelle derivanti dagli astrociti pretrattati con CCL3 hanno un effetto neuroprotettivo maggiore, confermando il potenziale terapeutico di tale citochina. Inoltre, a seguito dell'esposizione a MPP<sup>+</sup>, tutte le EVs sono in grado di ripristinare la funzionalità del complesso I della catena di trasporto degli elettroni, ma solo le EVs derivanti dagli astrociti del VMB ristabiliscono pienamente i livelli di ATP. Questi risultati enfatizzano le diversità regionali astrocitarie nel sistema nigrostriatale, anche per la secrezione e la funzione delle EVs, con importanti implicazioni applicative per il PD. Per lo sviluppo di nuovi approcci terapeutici è necessario poi comprendere le dinamiche molecolari di interazione ed assorbimento delle EVs da parte dei neuroni bersaglio. Per quantificare in maniera diretta il livello di *uptake* delle vescicole nel tempo, a partire dai dati di laboratorio, abbiamo infine sviluppato un modello matematico che possa essere utile per ottimizzare la progettazione di studi traslazionali basati sull'uso delle EVs.

Nel lungo termine, le conoscenze derivanti da questa linea di ricerca potranno avere ricadute importanti, non solo accrescendo la comprensione dei meccanismi molecolari alla base del complesso *cross-talk* glia-neuroni, ma anche implementando la progettazione di terapie innovative basate sull'utilizzo delle EVs per il trattamento della MP.



## Abstract

Parkinson's disease (PD) is the second most common neurodegenerative disorder after Alzheimer's disease, defined by motor and non-motor symptoms. The degenerative process is characterized by the loss of dopaminergic (DAergic) neurons in the ventral midbrain (VMB) and their projections in the striatum (STR), resulting in a reduction of dopamine levels. To date the causes of PD are still poorly understood, and there are no therapies able to stop or reverse the pathology.

In this context, a pivotal role is played by the glial compartment, through a bi-directional signaling with neurons. Indeed, astrocytes and microglia are able to respond to brain damage by releasing neurotrophic and pro-inflammatory factors. Depending on the context, these factors can either promote neuroprotection or contribute to neurodegeneration. However, the molecular mechanisms regulating this complex intercellular signaling are not yet clear. In the last 15-20 years, extracellular vesicles (EVs) have emerged as important mediators of intercellular communication, both in physiological and pathological conditions. EVs are membranous nanostructures released by all cell types, and they are able to transfer different classes of molecules to target cells. They are also considered a promising source of new biomarkers and potential innovative nanotherapeutics, delivering pharmacologically active molecules in a targeted manner.

In the context of PD, glia-derived EVs have controversial role, reflecting the behavior of donor cells. In particular, astrocytes “activated” by CCL3 chemokine, protect damaged DAergic neurons both in *in vivo* and *in vitro* PD models. This is possible thanks to the astrocyte-neuron cross-talk, where EVs may play a key role.

The main objective of this doctoral project was to study nigrostriatal EVs and their role in PD. Specifically, EVs derived from astrocytes of the nigrostriatal system (VMB and STR) were characterized, and their role in astrocyte-neuron intercellular communication was analyzed. In order to do this, we also developed a PD cellular model, dissected by high-resolution respirometry.

Results indicated that VMB astrocytes release more vesicles than STR and other brain regions, and are able to respond to CCL3 treatment by increasing EV production. Moreover, we also studied the neuroprotective potential of nigrostriatal astrocyte-derived EVs in *in vitro* PD models. Analyses showed that EVs from CCL3 pre-treated astrocytes had a greater neuroprotective effect against H<sub>2</sub>O<sub>2</sub>-induced apoptosis, confirming the therapeutic potential of this cytokine. Furthermore, after exposure to MPP<sup>+</sup>, all EVs recovered electron transport chain complex I functionality, but only VMB astrocyte-derived EVs fully restored ATP levels.

These findings show astrocyte regional diversities in the nigrostriatal system, both in term of EV secretion and function, with significant implications for PD. To develop new therapeutic approaches, understanding the molecular dynamics of EV interaction and uptake by target neurons is crucial. In order to do this, a mathematical model was developed based on laboratory data, useful for optimizing translational studies using EVs. In the long term, knowledge stemming from this research may have significant implications, not only enhancing the understanding of molecular mechanisms underlying the complex glia-neuron crosstalk but also implementing the design of innovative therapies using EVs for PD treatment.

# Keywords and abbreviations

## Keywords

Extracellular Vesicles – Exosomes – Parkinson’s Disease – Astrocytes – Mitochondria  
– ODE based uptake model

## Abbreviations

$\alpha$ -Syn	$\alpha$ -Synuclein
$\alpha$ Syn-SAA	$\alpha$ -Syn seeding amplification assay
6-OHDA	6-hydroxydopamine
AADC	Aromatic L-amino acid decarboxylase
ACM	Astrocyte Conditioned Media
AD	Alzheimer's Disease
AF4	Asymmetric Field Flow Fractionation
ApoD	Apolipoprotein D
ARRDC1	Arrestin Domain-Containing Protein 1
AS-EVs	Astrocytes derived Extracellular Vesicles
BBB	Blood Brain Barrier
BDNF	Brain-Derived Neurotrophic Factor
bFGF	Basic Fibroblast Growth Factor
CCL3	Chemokine (C-C motif) ligand 3
COMT	Catechol-O-Methyltransferases
COX-2	Cyclooxygenase-2
circRNAs	Circular RNAs
CNS	Central Nervous System
DAergic	Dopaminergic
DAT	Dopamine Transporter
DBS	Deep Brain Stimulation
DIA	Developmentally Induced Astrocyte
DJ-1	Protein Deglycase-1
dUC	Differential Ultracentrifugation
ESCRT	Endosomal Sorting Complexes Required for Transport
ETS	Electron Transport System
EVs	Extracellular Vesicles
ENS	Enteric Nervous System
FGF-2	Fibroblast Growth Factor-2
GBA	Glucocerebrosidase
GDNF	Glial-Derived Neurotrophic Factor
GFAP	Glial Fibrillary Acidic Protein
GWAS	Genome-Wide Association Studies
H <sub>2</sub> O <sub>2</sub>	Hydrogen Peroxide
hESCs	Human Embryonic Stem Cells
hPSCs	Human Induced Pluripotent Stem Cells
HRR	High Resolution-Respirometry
HSPs	Heat Shock Proteins
IL-1 $\beta$	Interleukin 1 $\beta$
IL-6	Interleukin 6
ILV	Intraluminal Vesicles
IFC	Imaging Flow Cytometry
IFN- $\gamma$	Interferon-gamma
IG-TEM	Immunogold-Labeling Transmission Electron Microscopy
iPSC	Induced Pluripotent Stem Cells
LC/MS	Liquid Chromatography Mass Spectrometry
lncRNAs	Long non-coding RNAs
LRRK2	Leucine-rich-repeat kinase 2

MAO-B	Monoamine Oxidase inhibitors type B
MAP2	Microtubule-Associated Protein 2
MDVs	Mitochondrial-Derived Vesicles
MHC	Major Histocompatibility Complex
miRNAs	Micro RNAs
MISEV	Minimal Information for Studies of Extracellular Vesicles
MPP <sup>+</sup>	1-methyl-4-phenylpyridinium
MQC	Mitochondrial Quality Control
MPTP	1-methyl-4-phenyl-1,2,3,6-tetrahydropyridine
MSCs	Mesenchymal Stem Cells
MVBs	Multivesicular Bodies
ncRNAs	Non-coding RNAs
NDs	Neurodegenerative Diseases
NeuN	Neuronal Nuclei
NF- $\kappa$ B	Nuclear Factor $\kappa$ B
NGF	Nerve Growth Factor
NGS	Next Generation Sequencing
NLRP3	NOD-like receptor family pyrin domain containing 3
NO	Nitric Oxide
NSCs	Neural Stem Cells
NTA	Nanoparticle Tracking Analysis
O <sub>2</sub>	Oxygen
OPCs	Oligodendrocytes Precursor Cells
PASADENA	Phase 2 Study of Prasinezumab in Early PD
PD	Parkinson's Disease
PET	Positron emission tomography
PINK1	PTEN-induced putative kinase
PR	Plate reader
PRKN	Parkin
PrP	Prion Protein
RA	Retinoic Acid
RBP <sub>s</sub>	RNA-binding proteins
RGCs	Radial Glial Cells
ROS	Reactive Oxygen Species
SDHA	Succinate Dehydrogenase complex flavoprotein subunit A
SEC	Size Exclusion Chromatography
sEVs	Small Extracellular Vesicles
SIA	Stimulus-Induced Astrocyte
siRNAs	Short interfering RNA
SNpc	Substantia Nigra pars compacta
SPARK	Study of Parkinson's Efficacy of Nilotinib
sRNA-seq	small RNA-sequencing
STR	Striatum
SUIT	Substrate-Uncoupler-Inhibitor Titration
SVZ	Subventricular Zone
TEM	Transmission Electron Microscopy
TFF	Tangential Flow Filtration
TH	Tyrosine Hydroxylase
TNF- $\alpha$	Tumor Necrosis Factor- $\alpha$
tRFs	tRNA-derived fragments
VEGF	Vascular-Endothelial Growth Factor
VMB	Ventral Midbrain
VPS35	Vacuolar Protein Sorting 35
WB	Western Blot

# **Affiliations**

## **2020-2023 PhD Student**

Department of Biomedical and Biotechnological Sciences, Biology and Genetics Section,  
Biological Tower, University of Catania, Via S. Sofia 87, 95123 Catania, Italy

## **Sept 2023-Dec 2023 Internship student**

Institut Pasteur, Membrane Traffic and Pathogenesis Unit, Université Paris Cité, CNRS  
UMR 3691, F-75015 Paris, France.

# 1. Introduction

## 1.1 Parkinson's Disease (PD)

Parkinson's disease (PD) is the most common age-dependent movement disorder and the second most prevalent chronic neurodegenerative disease (ND), after Alzheimer's disease (AD) [1]. PD affects about 1–2% of the population over the age of 65, and 5% over the age of 85. Seven to ten million people worldwide are currently affected by PD, and its incidence is predicted to rise over the next 20 years, with significant socio-economic issues [2]. The pathology occurs in both male and female, but it is not gender-neutral, with a notable sex difference in its prevalence. Indeed, in the range of 45–54 years, PD onset is equal in both men and women (corresponding to 1% of affected population), but then the 4% of men versus 2% of women develop the pathology at the age of 85 [3].

The exact causes and mechanisms responsible for the PD onset and progression, and the sex difference, are not fully understood [4]. Over 90% of PD cases are considered sporadic or idiopathic, with the remaining cases being early-onset familial PD, indicating a potential inheritance of these risk factors. Current evidence suggests that PD pathophysiology involves a complex interplay between genetic susceptibility and a range of environmental factors, especially aging, oxidative stress and inflammation [5]. This results in an altered regulation of key pathways linked to oxidative stress, mitochondrial dysfunction, protein misfolding and aggregation, which finally leads to the progressive loss of dopaminergic (DAergic) neurons [6], [7]. Other conditions, such as the specific gastrointestinal microbiota composition, have recently been linked to PD [8], [9]. Indeed, numerous pathologies, such as cancer, inflammation, and other NDs, have been demonstrated to be significantly influenced by gut microbiota [8], [9]. In particular, the network called "gut-brain axis" seems to be particularly important in regulating the brain through a two-way interaction with the neurological, neuroendocrine, and immunological systems [10].

All these aspects reflect the difficulties encountered for the development of effective therapies. Indeed, the available treatments relieve the motor symptoms only temporarily, while they are not able to stop or reverse the neurodegenerative process.

### 1.1.1 Milestones of PD history

The British physician James Parkinson was the first who described the clinical signs and symptoms of PD as a "*shaking palsy*" in 1817. In his work, he described people with trembling at rest, shuffling gait, stopped posture, sleep disorders, and constipation. He also observed the progressive nature of the disease and the resulting disability [11]. Subsequently, in 1872, the neurologist Jean Martin Charcot deeply investigated on the disease, adding bradykinesia and rigidity to the list of symptoms, and renaming it as "*Parkinson's disease*", to recognize the significant research findings gained by James Parkinson [12]. In 1893, Blocq and Marinescu observed resting tremors in a patient with parkinsonian symptoms, which were attributed to a tuberculous granuloma affecting the ipsilateral *Substantia Nigra pars compacta* (SNpc) in the brain [13]. Brissaud suggested that this region might be the affected site in PD pathology [14]. Two decades later, in 1912, Frederic Lewy detected eosinophilic inclusion bodies within neurons in specific brain nuclei, subsequently recognized as Lewy bodies, establishing them as the distinctive pathological hallmark of PD [15]. His discovery was then supported by Trétiakoff in 1919, which observed a significant loss of neuromelanin and the presence of cytoplasmic inclusions (Lewy bodies) in the SNpc of PD patients [16]. But we need to wait until the 1953 to have the most comprehensive pathological examination of PD, and the exact identification of brain stem lesions, carried out by Greenfield and Bosanquet [17]. However, although diagnostic criteria were established, there was still more to be investigated and, importantly, there was the need to find an effective treatment. To this end, the discovery of dopamine, in the late 1950s and early 1960s, added new key points to the understating of PD pathophysiology and symptomatology. In particular, Carlsson reported the functional role of dopamine as an independent neurotransmitter involved in motor control, and not just a precursor of noradrenaline and adrenaline. Moreover, he defined the effectiveness of L-Dopa (L-3,4-dihydroxyphenylalanine) - the precursor of dopamine - in reversing reserpine-induced motor deficits in rat PD model [18].

In 1960 Ehringer and Hornykiewicz, showed dopamine deficits in both the striatum (STR) and SNpc of parkinsonian brains [19]. Considering that dopamine is not able to cross the Blood-Brain Barrier (BBB), one year later, in 1961, Hornykiewicz had the groundbreaking idea to administer L-Dopa to Parkinsonian patients. Twenty patients received intravenous L-Dopa doses ranging from 50 to 150 mg, leading to what is now known as "*The Dopamine miracle*". This treatment resulted in either complete deletion

or significant relief from akinesia, establishing L-Dopa as the first effective therapy for PD [20]. The identification of the DAergic deficit in PD and the development of dopamine replacement therapy had a great impact on PD research. In support to this, in 1967, Cotzias and his collaborators, discovered that L-Dopa could have an important impact on parkinsonian symptoms, and since then L-Dopa became the gold standard for medical therapy [21]. Simultaneous with Hornykiewicz's discoveries, during the 1960s, Hoehn and Yahr introduced a staging system for the disease. They differentiated between unilateral disease (Stage I) and bilateral disease (Stage II-IV), highlighting the emergence of postural reflex impairment as a pivotal clinical milestone (Stage III) [22]. These findings established the basis for future inquiries into the complex molecular mechanisms underlying the development and advancement of PD. Indeed, new pharmacological and surgical approaches to treat PD motor symptoms were developed in the following decades [23].

A crucial breakthrough occurred in 1983, when Langston and colleagues reported acute parkinsonism in drug users which accidentally ingesting synthetic heroin contaminated with 1-methyl-4-phenyl-1,2,3,6-tetrahydropyridine (MPTP) [24]. MPTP is able to cross the BBB and reach glial cells where it is oxidated by monoamine oxidase type b (MAO-B) into 1-methyl-4-phenylpyridinium (MPP<sup>+</sup>). Then, via the dopamine transporter (DAT), it is taken up by DAergic neurons where it induces a sequence of changes in the mitochondrial matrix and the electron transport chain, finally leading to DAergic neuron degeneration [25], [26]. This unexpected outbreak of parkinsonism among drug users provided a potential link between MPTP and Parkinson's-like symptoms [27]. This discovery was a significant breakthrough as it provided a toxin to create animal PD models for experimental purposes (see **Section 1.4**).

Later, despite the successes of pharmacological dopamine treatments, the exploration of cell-based dopamine replacement approaches led to largely disappointing results. For this reason, in 1995, the Deep Brain Stimulation (DBS), which involves the electrical stimulation to modulate brain activity, became effective for the treatment of PD (see **Section 1.1.4**) [28]. In the late 1990s, thanks to the progress of the genetic analysis techniques, the discovery of mutations in the SNCA gene, encoding  $\alpha$ -synuclein ( $\alpha$ -Syn), were defined as the first genetic cause of PD [29].  $\alpha$ -Syn was subsequently identified as the primary component of Lewy bodies [30]. All these findings led to Braak pathological staging of the disease, and the discovery of various other PD-related gene mutations (PINK1, LRRK2, Parkin, DJ1, etc., see **Section 1.1.2**) [31].

Moreover, with advancements in genetics and molecular techniques like CRISPR, researchers developed transgenic animal models based on PD-associated mutations [32]. These models have opened avenues for studying  $\alpha$ -Syn aggregation, potential therapeutics, biomarkers, and novel targets for disease intervention. These new models, together with the established animal models - based on neurotoxins like MPTP - offered valuable insights into potential new targets for the disease. Indeed, in 2012 there was the first clinical trial in phase I for PD immunotherapy [33], [34]. The experimental vaccine, developed by AFFiRiS in Vienna, comprised short peptide fragments specifically engineered to stimulate the body's immune response, prompting the antibodies to target and remove native  $\alpha$ -Syn proteins that are either trapped in cell membranes or spreading among cells [34]. In 2017, AFFiRiS announced that the vaccine is safe in people with PD, and effectively causes an immune response, leading to the production of antibodies against the toxic form of  $\alpha$ -Syn. However, they are still waiting to see if this approach actually slows down the PD progression [35].

Recently, it was also explored the link between alterations in gut microbiota and PD [36], in order to decipher pre-symptomatic phases for the development of specific therapies [37]. In addition, less invasive treatments such as  $\gamma$  knife (or focused ultrasound) for PD motor symptoms have been proposed [38]. These advances represent the cutting edge of technology for PD diagnosis, clinical assessment, and treatment (**Figure 1**).



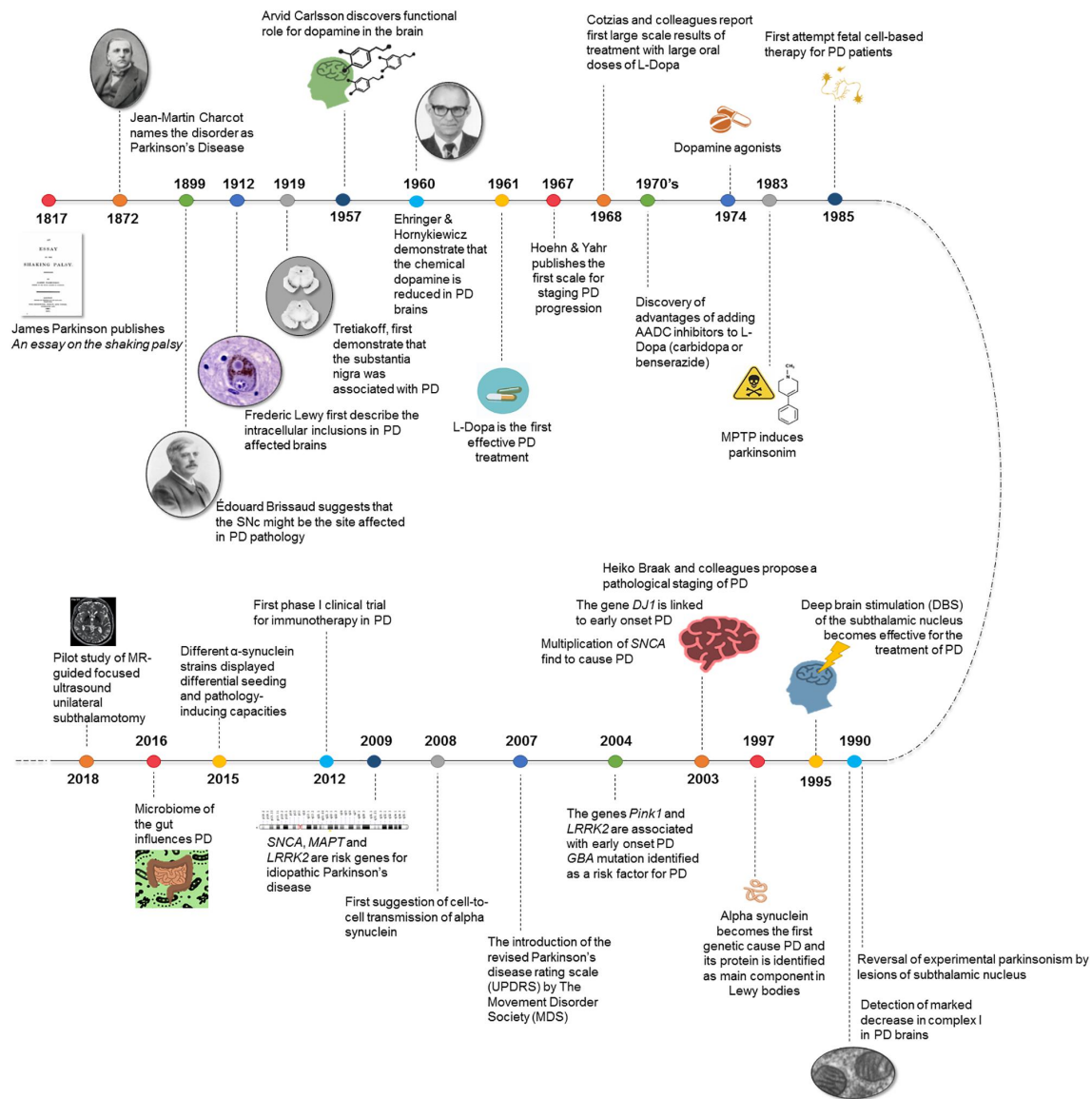


**Figure 1.** This schematic diagram provides an overview of pivotal milestones and breakthroughs in the field of PD research throughout history. (Source: <https://doi.org/10.3389/fnana.2018.00113>).

### 1.1.2 PD pathology: interplay between genetic and environmental factors

Despite the numerous advances made over more than a century of research, the exact mechanism(s) responsible for the pathogenesis of PD are still unknown. It has been proposed that PD onset and development is the result of a complex interplay between genetic and environmental factors (including aging, neuroinflammation, oxidative stress, mitochondrial dysfunction, misfolded proteins, exposure to neurotoxic substances), collectively referred to as the "environmentome", encompassing all potential causative and protective elements [39]–[41]. All together these factors, contribute to the progressive

loss of DAergic neuronal cell bodies in the SNpc within the ventral midbrain (VMB), and their axons which project in the STR region, with consequent dopamine depletion, resulting in disrupted signaling throughout the basal ganglia circuitry [42]–[44]. The basal ganglia, a group of interconnected nuclei located deep within the brain, play a crucial role in controlling movement, posture, and a range of other motor functions. Consequently, the loss of dopamine-producing neurons leads to a reduction of motor functions and a progressive impairment of other autonomic, cognitive and behavioral functions [42]–[44] (**Figure 2**).

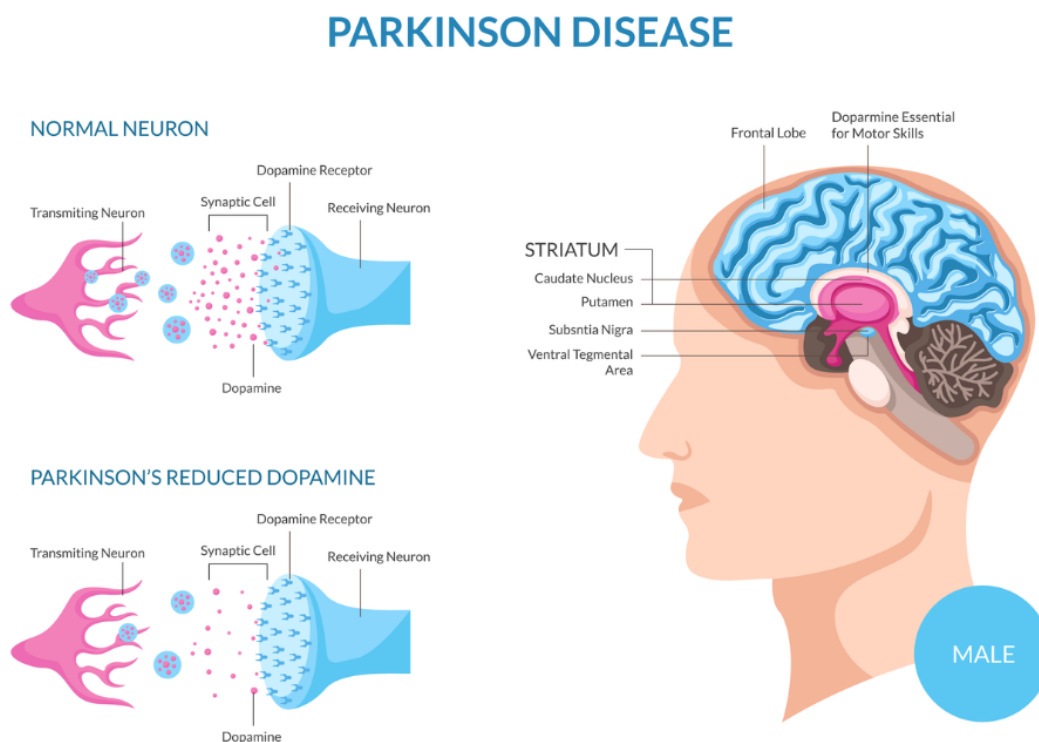


**Figure 2.** Dopamine level in normal and Parkinson’s affected neurons. In normal neurons: dopamine production and release are robust, maintaining a delicate balance in neurotransmission. Dopamine levels remain relatively stable, ensuring efficient signaling between neurons. In Parkinson's affected neurons: dopamine-producing neurons are progressively lost due to the neurodegenerative nature of the disease. This loss leads to a significant reduction in dopamine levels, disrupting the balance of neurotransmitters. The consequent lower dopamine levels result in motor symptoms characteristic of PD, such as tremors, rigidity, and bradykinesia. (Source: <https://www.fionawaring.com/recent-articles/parkinsons>).

While the environment is characterized by continual, long-term fluctuations that eventually accumulate into diverse, challenging-to-assess effects, a growing body of knowledge focuses on stable genetic information [45]. To date, PD has been linked to rare variants in over twenty genes. Nonetheless, the significance of many of these genes and their variants is a subject of intense debate, and some of them lack the support of

functional validation studies (**Table 1**). Currently, the most notable mutations are found in genes such as SNCA, leucine-rich-repeat kinase 2 (LRRK2), PTEN-induced putative kinase (PINK1), parkin (PRKN), deglycase (DJ-1), vacuolar protein sorting 35 gene (VPS35), and glucocerebrosidase (GBA), accounting for ~10% of cases, known as familial PD [39]. Some of these mutations lead to juvenile forms of the disease, hastened motor symptom progression, rapid cognitive decline, and a severe clinical course [46]. Additionally, mutations in genes like DJ-1, PINK1 and Parkin have been linked to mitochondrial and mitophagy processes. Meanwhile, mutations in other genes like GBA, LRRK2, and VPS35 are presumed to play a role in lysosomal and trafficking pathways. The remaining 90% of cases are classified as idiopathic or sporadic PD [47]. However, the assertion that PD typically develops spontaneously or has an unknown cause is debated. Indeed, a recent study showed that a significant portion of PD cases is influenced by genetic risk factors, as identified through Genome-Wide Association Studies (GWAS) [48]. GWAS facilitated a shift away from candidate-based assessment, where single genes or, more frequently, single variants were scrutinized, to the capacity to simultaneously explore the majority of common variations in the human genome without any specific hypotheses. The most extensive meta-analysis of GWAS has identified 90 independent risk factors responsible for 16-36% of hereditary risk [48].

**Table 1.** Summary of all the mutations that have been linked to PD. (Source: <https://pubmed.ncbi.nlm.nih.gov/31521533/>).

	Mutation	Note	Year of discovery	Proposed disease mechanism	Inheritance	Frequency	Nominated by GWAS	Multiple independent families reported*	Functional evidence†	Negative reports published‡	Confidence as actual PD gene§	
	SNCA	Missense or multiplication	Often with dementia	1997, 2003	Gain of function or overexpression	Dominant	Very rare	Yes	++	++	+	Very high
	PRKN	Missense or loss of function	Often early onset	1998	Loss of function	Recessive	Rare	No	++	++	+	Very high
	UCHL1	Missense	..	1998	Loss of function?	Dominant	Unclear	No	-	+	--	Low
	PARK7	Missense	Often early onset	2003	Loss of function	Recessive	Very rare	No	++	++	+	Very high
	LRRK2	Missense	..	2004	Gain of function	Dominant	Common	Yes	++	++	+	Very high
	PINK1	Missense or loss of function	Often early onset	2004	Loss of function	Recessive	Rare	No	++	++	+	Very high
	POLG	Missense or loss of function	Atypical PD	2004	Loss of function?	Dominant	Rare	No	++	+	+	High
	HTRA2	Missense	..	2005	Unclear	Dominant	Unclear	No	-	+	--	Low
	ATP13A2	Missense or loss of function	Atypical PD	2006	Loss of function	Recessive	Very rare	No	++	++	+	Very high
	FBXO7	Missense	Often early onset	2008	Loss of function	Recessive	Very rare	No	++	++	+	Very high
	GIGYF2	Missense	..	2008	Unclear	Dominant	Unclear	No	+	+	--	Low
	GBA	Missense or loss of function	..	2009	Likely loss of function	Dominant (incomplete penetrance)	Common	Yes	++	++	+	Very high
	PLA2G6	Missense or loss of function	Often early onset	2009	Loss of function	Recessive	Rare	No	++	++	+	Very high
	EIF4G1	Missense	..	2011	Unclear	Dominant	Unclear	No	-	+	--	Low
	VPS35	Missense	..	2011	Loss of function	Dominant	Very rare	No	++	+	+	Very high
	DNAJC6	Missense or loss of function	Often early onset	2012	Loss of function	Recessive	Very rare	No	++	+	+	High
	SYNJ1	Missense or loss of function	Often atypical PD	2013	Loss of function	Recessive	Very rare	No	++	+	+	High
	DNAJC13	Missense	Same family as TMEM230	2014	Unclear	Dominant	Unclear	No	+	+	-	Low
	TMEM230	Missense	Same family as DNAJC13	2016	Loss of function?	Dominant	Unclear	No	-	+	-	Low
	VPS13C	Missense or loss of function	..	2016	Loss of function	Recessive	Rare	Yes	++	+	+	High
	LRP10	Missense or loss of function	..	2018	Loss of function?	Dominant	Unclear	No	-	+	--	Low

GWAS=genome-wide association study, PD=Parkinson's disease. \*In this column, ++ denotes ≥4 families reported; + denotes ≥2 and <4 families reported; - denotes 1 family reported; -- denotes no reported families. †In this column, ++ denotes ≥4 disease-related reports; + denotes ≥1 and <4 disease-related reports; - denotes no disease-related reports. ‡Reports that could not replicate the finding that this gene is a PD gene. In this column, + denotes no negative reports; - denotes ≥1 and <4 negative reports; -- denotes ≥4 negative reports. §Sum of the scores in the three preceding columns, with each + adding 1 and each - subtracting 1; very high denotes a score of ≥5; high denotes a score of 4; medium denotes a score of 2 or 3; low denotes a score of <1.

Recent advances in single-cell RNA sequencing technologies allowed Kamath and Abdulraouf to unveil cell-type-specific changes, defining ten transcriptionally-distinct populations in human DAergic neurons [49]. Among these, a single subtype marked by the expression of SOX6\_ATGR1 genes (SRY-Box Transcription Factor 6 and Angiotensin II Receptor Type 1) was highly susceptible to PD. Several canonical cell stress pathways, including TP53 and NR2F2 genes, were implicated in transcriptional changes within SOX6\_AGTR1 cells in PD patients, as well as molecular processes associated with degeneration. In particular, TP53 has been implicated in motor neuron death, and NR2F2 has previously been shown to promote mitochondrial dysfunction in several disease models, including PD [49]. These findings further support the idea that genetic influences are inherent to the cells involved PD-associated neurodegeneration. [49].

### 1.1.2.1 PD and $\alpha$ -Syn

The first and most characterized PD-linked gene is the SNCA encoding for  $\alpha$ -Syn. Numerous studies have demonstrated that SNCA mutations lead to a higher propensity for misfolding and aggregation mechanisms compared to the wild-type form. Aberrant  $\alpha$ -Syn encourages pathological post-translational modifications, including phosphorylation, truncation, and oxidation [50]. Toxicity resulting from dysregulated cellular processes are among the mechanisms implied in the  $\alpha$ -Syn mediated neurotoxicity, representing another hallmark of the pathology. Indeed, PD is also characterized by the accumulation of  $\alpha$ -Syn protein aggregates within cytoplasmic inclusions called Lewy bodies, and dystrophic neurites (called Lewy neurites), localized within both nigral and extranigral neurons [51]. At the ultrastructural level, Lewy bodies represent densely packed granular accumulations of filaments measuring approximately 10-15 nm in diameter. More specifically,  $\alpha$ -Syn adopts a  $\beta$ -sheet-rich amyloid-like structure that is prone to aggregate, generating intracellular inclusions. Normally,  $\alpha$ -Syn is found in presynaptic terminals, where it plays a role in synaptic vesicle release and maintenance by assisting the SNARE complex and maintaining synaptic homeostasis [52]. However, the oligomeric intermediates of this aggregation process are toxic and induce both alteration of mitochondrial, lysosomal and proteasomal functions, and membrane and cytoskeleton damage, finally disrupting the synaptic functions and contributing also to neuronal degeneration (**Figure 3**) [53]. Recently, new immunopathological lesions of  $\alpha$ - and  $\gamma$ -synuclein have been found in the human brain, (including unfolded monomers, soluble oligomers, protofibrils, and high molecular weight insoluble fibrils), suggesting the possibility that oxidation and/or protein aggregation may play a role in the etiology of various NDs, including PD [54].

Moreover, considering that  $\alpha$ -Syn can spread both between neurons and between neurons and glia, it has been proposed an alternative spreading mechanism mediated by extracellular vesicles (EVs, see **Section 1.3**). This pathway seems to be mostly associated with the harmful form of aggregated  $\alpha$ -Syn, potentially hastening the progression of PD [55]. Recent findings indicate that, although  $\alpha$ -Syn can be secreted independently or actively transported within EVs, it is primarily within EVs that this protein tends to assume a toxic oligomeric state. Moreover, oligomeric  $\alpha$ -Syn, safeguarded within EVs, is more readily taken up by recipient cells, including glial cells [55].

However, besides the numerous evidences about the critical role of  $\alpha$ -Syn aggregation in spreading the pathology, nowadays this view is challenged, considering the failures of the

two clinical trials "*SPARK*" and "*PASADENA*" [56]. *SPARK* (Study of Parkinson's Efficacy of Nilotinib) was a Phase II clinical trial (NCT03205488) investigating the use of the repurposed cancer drug nilotinib [57], to reduce  $\alpha$ -Syn levels in individuals with moderately advanced PD [58]. However, although they observed satisfactory safety and tolerability to nilotinib, the limited penetration into the cerebrospinal fluid, and the negative trend in efficacy data suggested that further testing of nilotinib in PD should not be pursued and the trial was discontinued [58]. On the other hand, *PASADENA* (Phase 2 Study of Prasinezumab in Early Parkinson's Disease) was a Phase II clinical trial (NCT03100149) evaluating the safety and efficacy of prasinezumab, an antibody targeting  $\alpha$ -Syn, in early-stage PD [59]. Results from a previous Phase 1 study (NCT02157714) indicated that this investigational treatment had the potential to reduce  $\alpha$ -Syn levels in the blood of individuals with PD. However, Prasinezumab therapy showed no significant advancements in PD patients [60].

While much attention has been given to the toxic  $\alpha$ -Syn aggregates, there is also evidence that normal  $\alpha$ -Syn loss of function may contribute to PD pathogenesis. This "loss-of-function" hypothesis suggests that the accumulation of abnormal  $\alpha$ -Syn aggregates interferes with its normal physiological roles, as occurs in PD and in other synucleinopathies. As a result, the normal functions of synapses and, accordingly, neurotransmission are compromised. This synaptic function disruption may potentially contribute to the motor and cognitive deficits observed in these diseases [61], [62]. As shown by several studies, animal models with reduced levels of  $\alpha$ -Syn exhibited synaptic dysfunction and impairments in motor function. Additionally, genetic mutations that lead to a complete loss of  $\alpha$ -Syn function have been associated with rare cases of familial PD [63]. Therapies aimed at restoring normal  $\alpha$ -Syn function or mitigating the effects of its loss are being explored as potential treatments for PD and related disorders [64]. Ongoing research seeks to better elucidate the complex interplay between  $\alpha$ -Syn's normal function, its aggregation, and the pathology of NDs like PD [64].

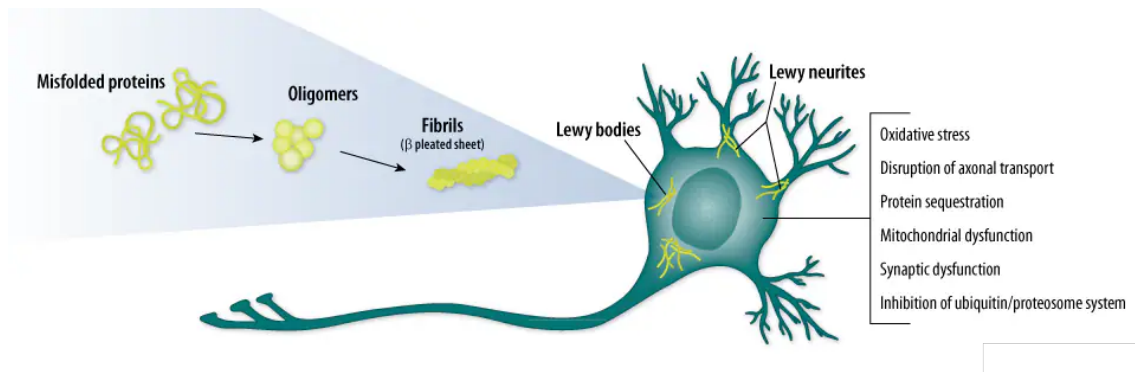


**Figure 3.**  $\alpha$ -Syn aggregation and its impact in PD. Misfolded  $\alpha$ -Syn proteins undergo a transformation into pathological oligomers and more complex aggregates, which ultimately give rise to the formation of fibrils. These fibrils then accumulate within Lewy bodies and Lewy neurites found in neurons affected by PD. Several implications stemming from the presence of these fibrillar  $\alpha$ -Syn deposits including: oxidative stress, disruption of axonal transport, protein sequestration, mitochondrial dysfunction, synaptic dysfunction, inhibition of ubiquitin/proteasome system. (Source <https://www.rndsystems.com/resources/articles/alpha-synuclein-based-model-studying-parkinsons-disease-pathology>).

### 1.1.2.2 PD and Mitochondrial dysfunction

In both idiopathic and familial PD, mitochondrial dysfunction is crucial. As said before, mutations on DJ-1, PINK1 and Parkin genes have been linked to mitochondrial pathways. The first evidence about the direct link between mitochondrial dysfunction and PD was reported in the SNpc of postmortem PD brains in 1990, where a deficiency of the mitochondrial complex I, a component of the electron transport chain, was found [65]. This finding was further supported, in 1983, by the discovery of the neurotoxin MPTP which induces permanent Parkinsonian symptoms. This chemical, which is now frequently used to mimic PD in animal models (see **Section 1.1.1** and **1.4**), inhibits the complex I, which results in abnormal mitochondrial respiration and increased Reactive Oxygen Species (ROS) production, both of which contribute to the degeneration of DAergic neurons [66]. Moreover, as we recently demonstrated by High Resolution Respirometry (HRR), MPP<sup>+</sup> also induces extensive mitochondrial damage at the inner membrane level, as evidenced by heightened LEAK respiration, and significantly reduces the oxygen flow dedicated to ADP phosphorylation in respirometry measurements (see **Section 3.1**) [26].

Several mutations in PD-associated genes have been connected to mitochondrial dysfunctions. For instance, PINK1 and parkin are essential elements involved in the system that controls the elimination of damaged mitochondria, i.e., mitophagy [67]. Mitophagy is part of four-stage system known as Mitochondrial Quality Control (MQC), which includes also mitochondrial biosynthesis, fusion, and fission. Considering that all

mitochondrial dynamics are carefully controlled to maintain the homeostasis of the organelle, any impairments in one of these steps could lead to mitochondrial dysfunction. Finally, PD patients have also been shown to have mitochondrial DNA mutations, deletions, or rearrangements [68], [69]. However, while it's clear that mitochondria play an important role in PD pathology, the exact mechanisms by which they contribute to the disease and whether mitochondrial dysfunction is a primary cause or a consequence of other PD-related processes are still areas of active investigation. Understanding these connections may lead to new potential therapeutic strategies for treating PD [70].

### **1.1.2.3 PD and Neuroinflammation**

Another hallmark of PD pathophysiology is neuroinflammation. The evidence of neuroinflammation in PD dates back to 1988 when McGeer observed an increase in major histocompatibility complex (MHC) molecules and b2-microglobulin in the brains of postmortem PD patients. Subsequent findings revealed the accumulation of ROS, NO, TNF- $\alpha$ , IL-1 $\beta$ , IFN- $\gamma$ , and cyclooxygenase-2 (COX-2) products, further supporting the role of inflammation in the disease context [71], [72].

In this context, glial cells, particularly reactive astrocytes and microglial cells, play a pivotal role in the onset and progression of the disease [73]. Remarkably, glia can have either a "beneficial" or a "detrimental" phenotype depending on the type of signal molecules released in the microenvironment, which may have important implications for DAergic neuronal survival (see **Section 1.2.3** for more details) [74]. Dysfunctions of the astroglial cell compartment, in which both astrocyte and microglia activation execute key activities, is acknowledged to have a substantial role in PD, even though it is unclear whether neuroinflammation begins DAergic neurodegeneration or it is a correlated consequence [75]. Indeed, the neuronal loss is accompanied by important changes in astrocytes and microglia compartment. Microglia exhibit signs of activation, while astrocytes become enlarged and accumulate the intermediate filament protein known as glial fibrillary acidic protein (GFAP) [52]. The glial compartment normally exerts a positive and neurotrophic influence on neuronal populations under normal conditions. However, chronic disturbances in glial homeostasis can potentially shift their behavior toward a neurotoxic state, ultimately leading to neuronal death [76]. Although inflammation is a tightly regulated mechanism, necessary for maintaining tissue homeostasis and responding to injuries or infections, the disruption of this balance can



trigger an uncontrolled escalation of inflammation-derived conditions, worsening neuronal damage and potentially leading to chronicization [77].

The prolonged exposure of microglia to acute stimuli results in morphological and gene expression changes, leading to an activated state that produces various pro-inflammatory mediators, such as cytokines (tumor necrosis factor-alpha (TNF- $\alpha$ ), interleukin-1 beta (IL-1 $\beta$ ), and interferon-gamma (IFN- $\gamma$ ), etc.), chemokines (CCL2, CCL3, etc.), eicosanoids, and reactive free radicals like ROS, nitric oxide (NO), etc.). These molecules further damage neurons, intensifying the inflammatory response. Over time, these events compromise the integrity of the BBB, allowing immune cells and inflammatory molecules from outside the CNS to enter the brain, exacerbating chronic inflammation with detrimental consequences [71]. Aging also contributes to structural deterioration in astroglial cells, reduced expression of neurotrophic factors, impaired phagocytic activity, and an increase in pro-inflammatory molecules, resulting in a loss of their neuroprotective function [78]. In summary, all these elements contribute to this inflammatory cascade typical of PD (**Figure 4**).

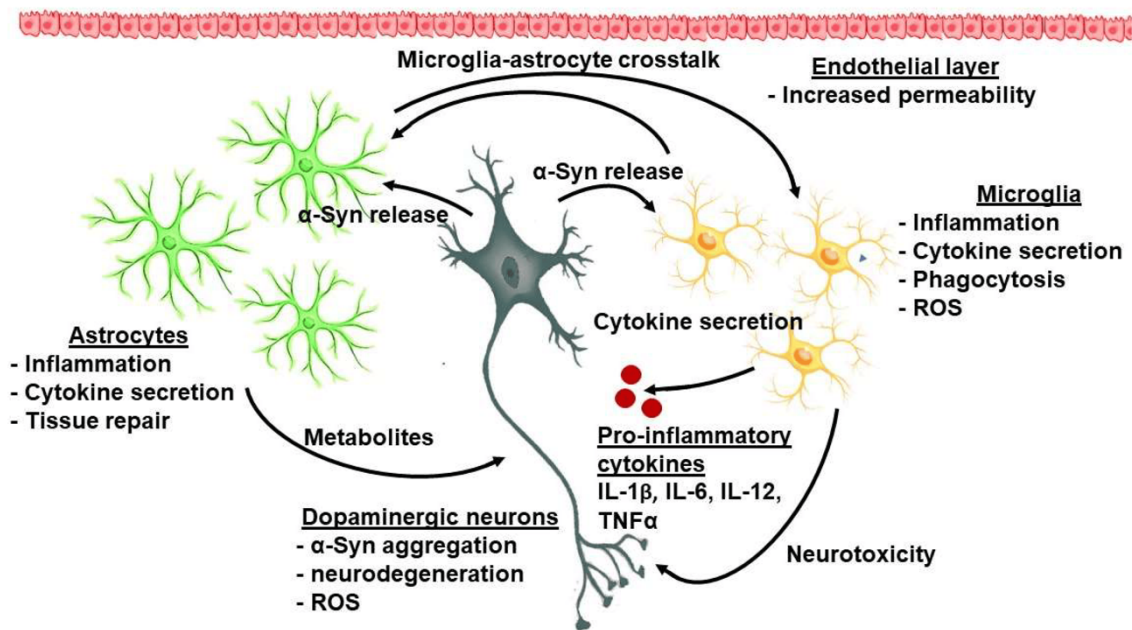


**Figure 4.** Inflammation plays a pivotal role in the progression and outcome of PD. In normal condition, inflammation is tightly regulated and has a crucial role in maintaining the integrity of the CNS. However, when this regulation is altered, the immune response can become excessive and detrimental (through the release of release a wide array of inflammatory molecules, including cytokines, eicosanoids, chemokines, and reactive free radicals), evolving into chronic and persistent inflammation that fuels the process of progressive neurodegeneration. (Source <https://doi.org/10.3390/ijms232314997>).

#### 1.1.2.4 PD and Gut microbiota

Recently, also the composition of the gut microbiota has been linked to PD [10]. The gut microbiota plays a significant role in the development of various health issues, such as cancer, inflammation, and NDs [10]. It has been proposed that the microbial population within the gastrointestinal system could exert a pivotal influence on the brain through a bidirectional interaction involving the neural, neuroendocrine, and immune systems, within a network referred to as the “*gut-brain axis*” [79]. Several studies have shown significant differences in the gut microbial population between PD patients and healthy individuals, involving species like Lactobacilli and Fecalibacteria [80]. Additionally, also *Helicobacter Pylori*, a stomach-infecting pathogen, has also been associated with PD by affecting the absorption of L-Dopa, leading to motor fluctuations in PD patients [81]. Imbalances in the gut microbiota, a condition known as dysbiosis, and specifically, an excessive growth of bacteria in the small intestine, can potentially be linked to gastrointestinal symptoms and motor function problems in individuals with PD [80]. Moreover, alterations in intestinal permeability could facilitate the action of toxins, thus resulting in an enhanced inflammatory response within the Enteric Nervous System (ENS) [82]. Ultimately, this could trigger an exacerbated immune response both in the intestines and in the CNS [83]. All these findings seem to support the Braak’s model, which propose that the onset of the disease occurs when an exogenous agent enters the CNS, likely through the gastrointestinal system, and then spreads via the vagal nerve to the brain [84]. This is supported also by new data, that define two different subtypes of PD. The one called “*body-first PD*” starts in the body and involves the gut and heart before affecting the brain, while the second type of progression is called “*brain-first PD*”, since the pathology starts in the brain's nigrostriatal system, and possibly induced by genetic factors [85].

In the end, although strong data clearly indicates a connection between genes and different environmental variables – including age, neurotoxic exposure, and inflammation – the “origins” of DAergic neuron degeneration are still unknown. Moreover, in most cases, PD is diagnosed when approximately 50-60% of DAergic neurons in the SNpc have already degenerated, and 70-80% of dopamine depletion occurred in the STR, making unavailing any type of intervention [86]–[89].

### 1.1.3 Clinical features and diagnosis

Starting from the late 20<sup>th</sup> century to the present day, many scientific advancements have been made about the knowledge of PD mechanisms and novel additional therapeutic options have been taken into consideration. As said, PD is part of the "*Movement Disorders*", with a slow but progressive degeneration of the brain areas mainly involved in motor control. Generally, people affected by PD exhibit the cardinal motor symptoms, such as resting tremor, rigidity, hypokinesia, bradykinesia, and postural instability. Other motor features include gait disturbances, micrographia, speech disturbances, hypomimia, and abnormal blinking and eye movements [90]. However, although the clinical diagnosis is based on the presence of motor features, PD is also associated with non-motor symptoms, with mechanisms not completely understood. Non-motor symptoms range from dysphagia to sleep, gastrointestinal, sensory, cognitive and neuropsychiatric disorders (**Figure 5**). Typically, these symptoms are underestimated, but they can impact on the patient's disease-related quality of life and disability [90]. Importantly, different PD phenotypes can be seen as non-motor symptoms during PD progression. This is why "*The International Parkinson and Movement Disorder Society*" created a number of criteria to detect and classify PD, which were supported by numerous clinical investigations [39], [91]–[93].

# PARKINSON'S DISEASE

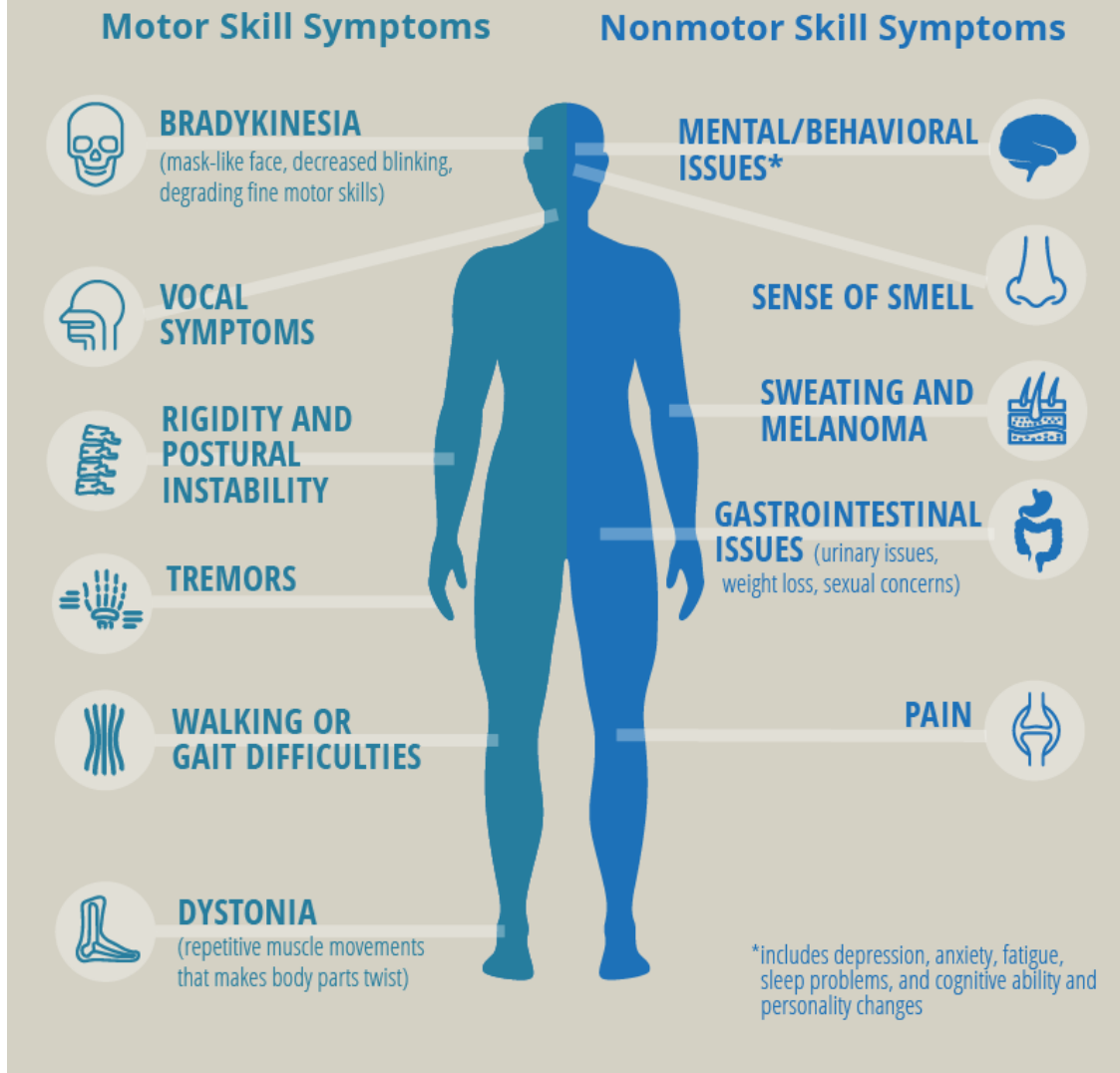


**Figure 5.** This schematic representation provides an illustrative overview of the classical symptoms associated with PD. The symptoms are categorized into two main groups: motor and non-motor symptoms. The most common motor symptoms are: bradykinesia, rigidity, postural instability, tremors, vocal symptoms, walking or gait difficulties and dystonia. Among the non-motor symptoms there are: mental and behavioral issues, sense of smell, gastrointestinal issues, pain, sweating and melanoma. (Source: <https://www.drprepillay.org/brain/parkinsons-disease/>).

Usually, the disease is diagnosed by evaluating the patient's medical history and performing a neurological examination. The patient's positive reaction to L-Dopa or other specialized drugs for PD is another fundamental and essential indicator for a proper diagnosis. Many disorders, such as multiple system atrophy and dementia with Lewy bodies, display symptoms similar to those of PD, and are called with the term of parkinsonism [93]. Although these disorders may initially be misdiagnosed as PD,

specific medical tests, as well as the evaluation of the response to drug treatments, can help to better assess the cause and to make an accurate diagnosis [93]. Indeed, although these other pathologies have similar characteristics, they require specific treatments, different from those used for PD. Interestingly, Siderowf and coworkers, earlier this year, were responsible for a groundbreaking development in the field, unveiling a new tool to identify people with PD during the early stages or even before symptoms begin [94]. This tool, known as the  $\alpha$ -Syn seeding amplification assay ( $\alpha$ Syn-SAA), has the ability to detect the key hallmark of the pathology, i.e., abnormal  $\alpha$ -Syn. As said, the key aspect of  $\alpha$ Syn-SAA is the remarkable capability to identify abnormal  $\alpha$ -Syn also in those individuals who have not yet been diagnosed or exhibited clinical symptoms but are at a high risk of developing the disease. The  $\alpha$ Syn-SAA leverages a characteristic of pathologic  $\alpha$ -Syn: it induces normal  $\alpha$ -Syn to misfold and clump. Previously, the presence of these clumps could only be confirmed through postmortem analysis. This assay works by introducing normal  $\alpha$ -Syn into spinal fluid samples that are prepared with a fluorescent dye. If abnormal  $\alpha$ -Syn is present, clumps form, causing the dye to fluoresce [94], [95]. This discovery marks a significant shift in our understanding of PD, since it has transformed the disease from one primarily diagnosed and measured through subjective clinical assessments to an objectively biologically defined disease [94], [95].

Notably, also in terms of positron emission tomography (PET) tracers, there have been important advancements. In their study, Xiang and collaborators, used PET with specific radiopharmaceuticals (called [18F]-F0502B) which specifically bind to  $\alpha$ -Syn deposits [96]. This tracer exhibits a strong affinity and selectivity for  $\alpha$ -Syn, avoiding to bind A $\beta$  or Tau fibrils, and it preferentially interact with  $\alpha$ -Syn aggregates within brain tissue. The results demonstrated that [18F]-F0502B successfully images  $\alpha$ -Syn deposits in the brains of both mouse models and non-human primates with PD [96], further supporting the feasibility of this technique for PD diagnosis. In the end, both strategies, have the potential to greatly improve the earlier diagnosis, targeted treatments, and more efficient drug development.

#### **1.1.4 Therapeutic approaches for the treatment of PD**

Unfortunately, to date there are no treatments able to stop or reverse the course of the pathology, since the pharmacological treatments currently available can only alleviate the symptoms [97]. The major goals of PD treatments are based on the replacement of

dopamine levels in the brain using: (i) L-Dopa; (ii) dopamine receptor agonists; (iii) dopamine metabolism inhibitors; and (iv) by boosting dopamine release.

L-Dopa is the gold standard for the treatment of PD and it is the most effective drug for the treatment of motor symptoms [98]. Unlike dopamine, L-Dopa crosses the BBB and is converted into dopamine by decarboxylation in the presynaptic terminals of DAergic neurons of the SNpc [99]. This reaction is catalyzed by an enzyme called aromatic L-amino acid decarboxylase (AADC), also known as DOPA decarboxylase [98], [99]. After the release, it is transported back into the dopaminergic terminals or is metabolized either by catechol-O-methyltransferase (COMT) or by MAO-B [100], [101]. Although L-Dopa provides significant improvements of the motor symptoms, it displays several side effects such as nausea, hypotension, somnolence, hallucinations, and impulse control disturbances [102]. It induces also motor complications (motor fluctuations, dyskinesias, dystonia), probably due to the discontinuous stimulation of striatal dopamine receptors, as opposed to the physiological supply of dopamine [103]. Moreover, the repeated use of this drug leads to diminished levels of AADC over time, with consequently loss of efficacy of L-Dopa. To avoid this problem, in a phase I study, the putaminal administration of an experimental adeno-associated virus serotype-2 vector designed to deliver the AADC gene, enhanced motor function, and diminished the need for antiparkinsonian medications in individuals with advanced PD [101].

For all these reasons, L-Dopa is mainly used in older patients with severe motor symptoms, while younger patients with mild symptoms, are treated with dopamine agonists, which directly stimulate the postsynaptic dopamine receptors in the STR bypassing the need for dopamine production by damaged neurons [103]. There are several dopamine agonists available, and they can be categorized into two main classes: “*ergot-derived dopamine agonists*” and “*non-ergot dopamine agonists*”. The older ergot-derived dopamine agonists, including bromocriptine, cabergoline, lisuride, and pergolide, are currently less used due to a higher risk of side effects and complications, such as valvular and lung fibrosis [104]. In contrast, the newer non-ergot dopamine agonists, such as pramipexole, ropinirole, rotigotine, apomorphine, and piribedil, are more commonly used today. Pramipexole and ropinirole are the most frequently prescribed dopamine agonists in the United States [104].

Other treatments include the use of dopamine metabolism inhibitors. These drugs work by blocking the breakdown of dopamine or by inhibiting enzymes responsible for dopamine metabolism [105]. By doing so, they help increase the availability of dopamine

in the brain, which can alleviate some of the motor symptoms associated with PD. The most used are MAO-B and COMT inhibitors [105]. Like dopamine agonists, MAO-B inhibitors (such as azilect or zelapar) are widely used in the treatment of mild and early forms of PD, as they offer symptomatic improvement with fewer complications than L-Dopa [106]. On the contrary, COMT inhibitors (such as Comtan, or Tasmar) are used to prolong the effect of L-Dopa. Therefore, when L-Dopa starts to lose its efficacy, COMT inhibitors are administered to PD patients together with L-Dopa, increasing its bioavailability with consequent improvement of motor fluctuations (**Table 2**) [107].

When the drug treatments fail, DBS is a possible alternative [28]. DBS involves the implantation of electrodes in specific brain areas (e.g., subthalamic nucleus, the internal globus pallidus or the thalamus), connected to a small electrical device which provides a steady, high-frequency electric current [28]. In particular, DBS acts on the cells and fibers closest to the implanted electrode, changing the firing rate of individual basal ganglia neurons [28]. Moreover, the electric current also affects the synapses, leading to calcium release by astrocytes and promoting the local release of neurotransmitters, such as adenosine and glutamate [108]. Thus, DBS induces both electrical and chemical effects, which together provide an effective therapeutic option for the treatment of motor and non-motor symptoms related to PD [108]. However, this procedure shows several limitations such as the invasiveness because it requires surgical implantation of electrodes into specific brain regions, the electrode misplacement which is a critical point for the success of DBS, device-related complications, psychosocial impact and finally the cost and accessibility, because it is an expensive procedure [109]. Despite these limitations, DBS remains a valuable and often life-changing treatment option for many individuals with PD.

**Table 2.** Summary of all the possible pharmaceutical approaches for the treatment of PD. (Source: <https://practicalneurology.com/articles/2018-may/pharmaceutical-treatment-of-parkinsons-disease#table>).

ACTION	DRUGS	AVAILABLE FORMULATIONS	COMMON SIDE EFFECTS
Dopamine precursor with metabolic inhibitor	Levodopa/carbidopa	Tablets (IR, ER) Dissolving tablets	Nausea, vomiting, orthostatic hypotension, vivid dreams, hallucinations, delusions
MAO inhibitors reduce levodopa and dopamine degradation	Rasagiline	Tablets	Hypertension, orthostatic hypotension, potentiation of levodopa-related side effects
	Selegiline	Tablets, capsules, orally disintegrating tablets	
	Safinamide	Tablets	
COMT inhibitors reduce levodopa and dopamine degradation	Entacapone	Tablets	Potentiation of levodopa-related side effects, diarrhea, orange color of urine
	Tolcapone	Tablets	Potentiation of levodopa-related side effects, hepatotoxicity,
Dopamine receptor agonists	Pramipexole	Tablets, ER tablets	Nausea, vomiting, orthostatic hypotension, hallucinations, psychosis, impulse control disorders, peripheral edema
	Ropinirole	Tablets, ER tablets	
	Rotigotine	Transdermal patches	
	Apomorphine	Subcutaneous injection	
Other/Unknown	Anticholinergics (trihexyphenidyl, benztropine)	Tablets	Dry mouth, dry eyes, confusion, hallucinations, constipation, urinary retention
	Amantadine	Tablets, capsules, ER tablets	Dry mouth, dry eyes, livedo reticularis, confusion, hallucinations, constipation, urinary retention, peripheral edema
Abbreviations: COMT, catechol- <i>o</i> -methyltransferase; ER, extended release; IR, immediate release; MAO, monoamine oxidase.			

As said, these therapies are not able to block the progression of the disease, and this has prompted researchers to invest in regenerative cell therapies aimed at restoring DAergic functionality. For example, advances in stem cell biology have enabled the development of cell replacement therapies, which include the use of human pluripotent stem cells (hPSCs), neural stem cells (NSCs), and mesenchymal stem cells (MSCs) [110]. hPSCs, which include human embryonic stem cells (hESCs) and induced pluripotent stem cells (iPSCs), have the remarkable ability to differentiate into various cell types, including DAergic neurons [111]. In 1998, ESCs were the pioneering choice for transplantation [112]. However, their application was constrained due to adverse immune responses and ethical concerns [113]. Nevertheless, there is currently an active phase I/II clinical trial (NCT03119636) assessing the safety and efficacy of intracranial transplantation of human ESC-derived neural precursor cells in PD patients. This trial is based on promising results observed in primate PD models [114].



Next, protocols have been developed to properly differentiate iPSCs into DAergic neurons, representing a significant advantage over other cell sources. Importantly, iPSCs can be generated from a patient's own cells, such as skin (fibroblasts) or blood cells. This personalized approach reduces the risk of immune rejection, as the cells are a genetic match to the patient [115]–[117]. Furthermore, these cells possess neurotrophic and immunomodulatory properties, enabling them to mitigate inflammation and suppress apoptosis in damaged tissues. Different studies demonstrated that when transplanted in primate PD models, iPSC not only survive but also could produce a significant number of functional DAergic neurons [118]–[120]. However, there are still challenges to address, including the safety and the functionality of the generated neurons, immune compatibility issues, and the risk of tumorigenesis [121].

MSCs represent another potential candidate for PD cell therapy. These cells exhibit remarkable plasticity and readily integrate into host tissues, as evidenced in various conditions, including NDs, autoimmune diseases, and diabetes [122], [123]. Multiple studies have highlighted their capacity for trans-differentiation into DAergic neuronal phenotypes [124]. Currently, two ongoing clinical trials are assessing the safety and efficacy of umbilical cord-derived MSCs, either undifferentiated (administered intravenously, NCT03550183) or differentiated into NSCs (administered intrathecally, NCT03684122), in PD patients. However, despite the symptomatic improvement observed with MSC transplantation in PD, these trophic effects are often transient [125], [126]. Furthermore, systemic injection of these cells has sometimes led to severe side effects, such as pulmonary thrombosis, while intracranial transplantation, as an alternative, is a highly invasive procedure [127].

Another strategy for restoring damaged DAergic neurons includes the use of NSCs, which can potentially be used for transplantation in PD. In 2015, an Australian phase I clinical trial was launched to evaluate the safety and efficacy of human parthenogenetic-derived neural stem cells (ISC-hpNSC) as a potential therapeutic intervention for PD. These stem cells were surgically implanted into both the striatum and SNpc of individuals with moderate to severe PD (NCT02452723) [128], [129]. Consistent with these discoveries, there is currently an ongoing clinical trial exploring the safety and effectiveness of intranasal delivery of human fetal NSCs in patients with PD (NCT03128450).

Interestingly, the primary function of astrocytes in transforming the challenging microenvironment within and around the neurogenic niches became evident when adult subventricular zone (SVZ) NSCs were transplanted into the aged MPTP PD mouse

model. Indeed, when L'Episcopo and coworkers transplanted NSCs into SNpc of aged mice previously exposed to MPTP, about one-third of these transplanted cells differentiated into astrocytic cells. Then, in conjunction with the resident astrocytes, they initiated the Wnt/ $\beta$ -catenin signaling pathway within SNpc DAergic neurons. This ultimately resulted in the rescue of neurons and modulation of the immune system [130]. Indeed, the use of astrocytes assumes a pivotal role in reshaping the hostile microenvironment. Alongside DAergic neurons, astrocytes provide a more trophic environment for the neurons, potentially enhancing their survival and function (see **Section 1.2**). The use of astrocytes in transplantation therapy for PD is still at the experimental stage, and research is ongoing to better understand their therapeutic potential and the specific mechanisms by which they may benefit PD patients [131]. Therefore, astrocytes alone played a pivotal role in promoting the survival, repair, and regeneration of DAergic neurons. In addition, as demonstrated by Serapide and coworkers, grafting astrocytes from VMB into the SNpc of aged mice with MPTP-induced motor impairment resulted in beneficial antioxidant and anti-inflammatory effects. This underscores the significance of astrocyte-derived factors and mechanisms as essential components for achieving successful therapeutic outcomes in PD [132].

Although cell therapies show encouraging effects for the treatment of many pathologies, including PD, adverse effects ranging from immune reactions to potential tumorigenesis after transplantation, have prompted researchers to consider other solutions – like the use of EVs (see **Section 1.3**) – as alternative regenerative strategies (cell-free therapy).

## 1.2 Glial cells: a turning point in the therapeutic strategy of PD

The CNS is composed of two main cell types, neurons and glial cells. The latter are further divided into microglia, and macroglia which includes astrocytes, oligodendrocytes (along with NG2 cells), ependymal cells and radial glia cells (RGCs) (**Figure 6**) [133].

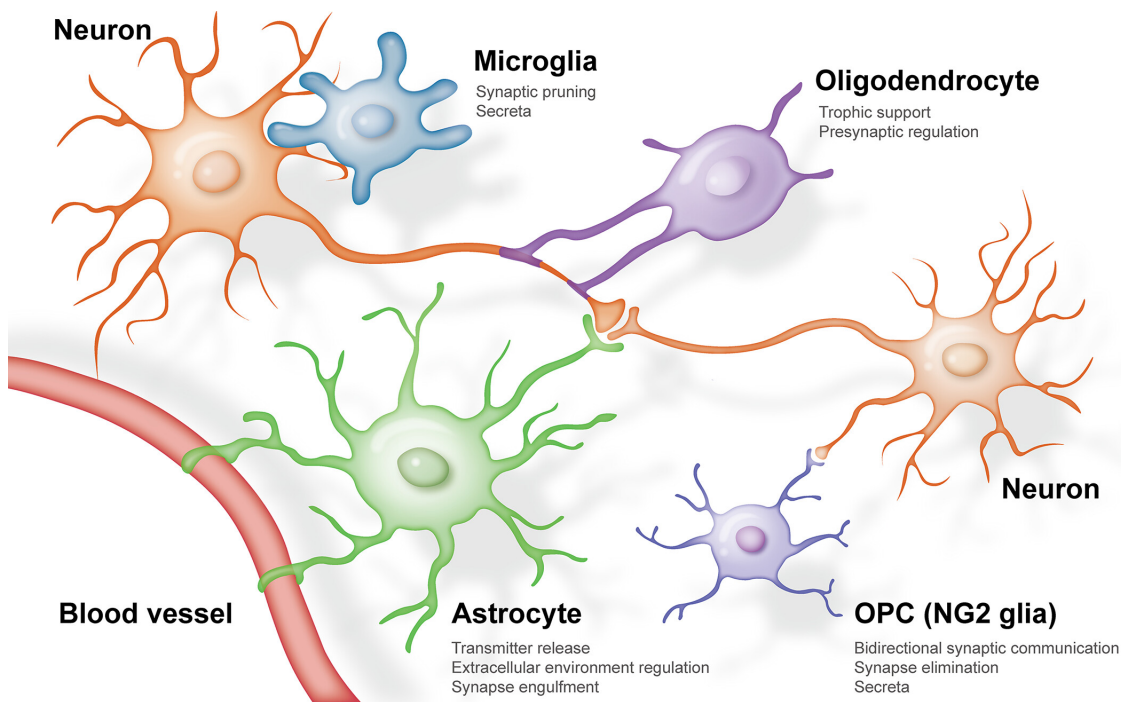


**Figure 6.** Neural cells components in the adult brain: neurons and glial cells. The traditional classification of glial cells includes astrocytes, microglia, oligodendrocytes, and oligodendrocyte precursor cells (OPCs, also known as NG2 glia). (Source: <https://doi.org/10.1002/glia.24343>).

In terms of size and structure, glial cells strongly differ from neurons. Neurons are composed of a cell body, a long axon and several dendrites, useful for the transfer of electrical signals [134]. Glial cells do not have axons and dendrites like neurons, but they have complex processes extending from their cell bodies. As a result, glial cells are usually smaller than neurons (the dimensions depending on the type) and represent a relevant cellular population, constituting about 33-66% of the total brain mass [135]. However, as said before, while they have distinct functions, they are extremely heterogeneous [136], [137]. Heterogeneity is a key feature of both neurons and glial cells in the nervous system. It refers to the presence of various spatial positioning subtypes with distinct structural, functional, and molecular characteristics, useful to perform specialized roles in different regions and circuits [138], [139]. The regional diversity of

neurons and glial cells reflects the specialization and adaptation of the nervous system to perform a wide range of functions. Different brain regions and parts of the nervous system require unique cellular compositions and functions to support sensory perception, motor control, higher cognitive functions, and autonomic processes [136]–[139].

### 1.2.1 Glia history

The history of glia, also called “*neuroglia*” or simply “*glial cells*”, is a fascinating journey of scientific discovery and evolving understanding of the brain and nervous system. Glial cells are a vital component of the nervous system, working in conjunction with neurons to support their functions [140]. The early observations of glial cells began in the early 19<sup>th</sup> century. The study of the cells within the CNS in that period was limited to morphological observations using rudimentary microscopes, which primarily revealed cell bodies. The two primary cell types were in the process of being characterized, although at the time, the lack of adequate techniques did not allow to discriminate their “glial” or “neuronal” nature. Neuroscientists firstly focused on neurons, the electrically excitable cells of the nervous system, while the glial cells were often overlooked or misinterpreted [141]. In the 1850s, the pathologist Rudolf Virchow coined the term “*glia*” (Greek for “glue”), suggesting that glial cells served as merely supportive structures to hold neurons together (connective tissue). Moreover, he also introduced the term “myelin”, which in his description reminded the bone marrow [142]. Later, between 1870 and 1872, the cellular nature of glia was deeply studied and defined by Camillo Golgi [143]. He was the first to give the precise depictions of glial cells, described as “*round cells with long and delicate processes, many of which extended toward blood vessels*” [143]. Golgi's work led to the identification of two distinct types of glial cells, namely fibrous and protoplasmic cells, and he achieved the initial comprehensive visualization of radial glial cells in 1885 [144]. The development of more advanced microscopes in the late 19<sup>th</sup> century allowed scientists to better study the structure of nervous tissue. In 1894, the Spanish histologist Santiago Ramón y Cajal made significant contributions to our current understanding of neurons and glia, providing the first direct histological evidence of the structural individuality of both neurons and glial cells [145]. However, it was not until the early 20<sup>th</sup> century that information about the subtypes and functions of glial cells in the central nervous system became known. Indeed, Cajal together with Rí o-Hortega

and Penfield, began to identify and classify various types of glial cells, including astrocytes, oligodendrocytes, and microglia [145]. Next, thanks to the employment of more sophisticated techniques and tools, such as electron microscopy and immunohistochemistry, scientists were able to go deeper into the functions and diversity of glial cells. Therefore, contrary to common belief, it was discovered that glial cells are not simply “silent” cells, with the only function to support neurons, but they have multiple important roles. Indeed, it was found that glial cells are involved in: i) the formation of astrocytic networks via gap junctions, together with neurons and blood vessels, supporting the BBB; ii) brain plasticity and neurotransmission, as highlighted by the “*tripartite synapse*” concept, by which the synapse should be considered as a functional unit consisting of presynaptic and postsynaptic neuron, and the astrocyte; iii) monitoring sleep and wakefulness states; iv) the expression of neurotransmitter receptors, along with the release of neurotransmitters like glutamate and GABA [146]–[148]. Moreover, glia has been recognized to play an integral role in various NDs, such as multiple sclerosis (MS), AD, and PD, making them a target for potential therapeutic interventions [149], [150]. Nowadays, the research in this field continues to unveil new aspects of glial cell functions, including their role in neuroinflammation, neuroprotection, and synaptic plasticity.

### **1.2.2 Microglia**

The resident immune cells of the brain are known as microglia, highly flexible and dynamic cells that play pivotal roles in the healthy CNS during development [146]. Indeed, they represent the immunocompetent and phagocytic cells of the CNS. With their dynamic cellular processes and the development of a highly branched morphology, microglia have been predominantly examined in vertebrates, with few references in some Annelids and Mollusks, while they are notably absent in *Drosophila* [151], [152]. Unlike astrocytes and oligodendrocytes (which derive from RGCs and OPCs respectively), microglia cells derive from yolk sac erythromyeloid progenitor cells, which shortly colonize the brain after neural precursors begin differentiating [146], [153]. They are smaller than astrocytes and oligodendrocytes (hence the name microglia), and have variable shapes and oblong nuclei [154], [155]. As brain parenchyma's resident macrophages, microglia actively engage in numerous essential CNS functions, like gliogenesis, vasculogenesis, and neurogenesis, as well as they contribute to synaptic

maturation and myelination through their dynamic process motility, secretion of soluble factors, and proficient phagocytosis capabilities [156], [157]. Moreover, these cells responses to pathological conditions that can have both beneficial and detrimental effects, some of which may directly contribute to disease [158]. For all these reasons, the terms “resting” and “activated” microglia were employed to describe, from a morphological perspective, cells in physiological conditions (resting) versus pathological conditions (activated). This nomenclature was extensively used in the 1980s-1990s [158]. Another alternative terminology was borrowed, in the early 2000s, from the field of immunology, with macrophages defined as M1 and M2, based on their different activated phenotype, established through *in vitro* studies. This classification introduced the concept of M1 and M2 phenotype also for microglia [159]. M1 was closely linked to the concept of “activated” microglia, and represented the classical activation, which was considered pro-inflammatory and neurotoxic. The second one, was relative to an alternative activation, characterized by anti-inflammatory and neuroprotective properties [160]. These terms gained widespread usage in microglial research during the 2010s, with an increasing number of studies phenotyping macrophages and microglia into detrimental M1 and beneficial M2, categories based on the expression of specific markers associated with these conditions [159].

However, it soon became clear that microglial responses were more intricate than this simple classification [161]. Interestingly, an important study dating to 2005, challenged these concepts, since it was discovered that microglia are remarkably dynamic also in the absence of pathological challenges [162]. This discovery was made possible through non-invasive two-photon *in vivo* imaging, revealing that microglia continuously survey the brain parenchyma with their highly mobile processes. These results have led to the current view of microglia as the most dynamically active cells in the healthy mature brain [151], [163], and therefore never truly at rest. Indeed, microglial cells do not shift from a “resting” to an “activated” state in response to trauma, injury, infection, disease, or other challenges. Instead, they are continuously active, and change their physiology to adapt to the stages of life, CNS regions, species, sex, and the health or disease state. Consequently, although still widely used, the dichotomy “resting/activated” and “M1/M2” microglia need to be reconsidered [153], [164].

Currently, we know that microglia exist in a variety of dynamic and multifaceted states, which mainly depend on the context, including the disease stage, genetic background, and the microenvironment where they located. Therefore, altered states of microglia have

been observed in the diseased human brain and in animal models of different pathological conditions [152]. The changes are related to their morphology, phagocytic capabilities, and inflammatory signaling properties, which collectively contribute significantly to the neuroinflammatory response in pathological scenarios [165], [166]. The signals microglia encounter can vary significantly during the course of disease progression, encompassing stimuli from apoptotic cells, extracellular debris, toxic proteins (e.g.,  $\beta$ -amyloid and  $\alpha$ -Syn), as well as signals resulting from disruptions in the BBB and alterations in the functionality of neurons and other glial cells (e.g., the release of inflammatory factors) (see **Section 1.2.3**) [152], [165], [166].

For instance, recent studies strongly support the role of microglial pro-inflammatory signaling in the pathogenesis of PD, particularly in the context of the microglial NOD-like receptor family pyrin domain containing 3 (NLRP3) inflammasome. The activation of the NLRP3 inflammasome pathway can be instigated by fibrillary  $\alpha$ -Syn or DAergic cell death, even in the absence of  $\alpha$ -Syn aggregates [167], [168]. On the other hand, there are growing evidences about the protective roles played by microglia under neurodegenerative conditions. For instance, microglia were found involved in the reduction of toxic accumulation of  $\beta$ -amyloid in the context of AD [169]. Also, following the activation of Triggering Receptor Expressed on Myeloid Cells 2 (TREM2), microglia enhanced their phagocytic ability reducing therefore neuroinflammation in PD mouse models [170], [171]. Ultimately, these discoveries reinforce the concept of heterogeneity, suggesting that the same microglial states, which may be beneficial in specific contexts, can prove detrimental in others. The outcome depends entirely on the intricate interactions between microglia and their microenvironment.

### **1.2.3 Macrogia**

As said before, among the neuroglia, the macroglia are the most abundant cell types, which includes RGCs, oligodendrocytes, ependymal cells and astrocytes.

#### **1.2.3.1 RGCs, oligodendrocytes and ependymal cells**

RGCs are recognized as a type of NSCs, capable of self-renewal and generate various types of neural cells, including neurons and other glial cells. Indeed, they play a pivotal role during the embryonic development of the brain [172]. RGCs are named for their long,

radial processes that extend from the inner (ventricular) surface of the developing brain to the outer (pial) surface. Their extended long fibers act as a scaffold, guiding immature neurons towards their proper positions. As neurons migrate, RGCs often differentiate into specialized glial cells, such as astrocytes or oligodendrocytes [173]. Moreover, while RGCs have traditionally been associated with embryonic brain development, some studies suggest that a subset of these cells may persist in the adult brain and continue to have a role in processes like neurogenesis and brain repair [174].

Some RGCs, as they mature, differentiate into OPCs, which in turn differentiate into oligodendrocytes. Although OPCs are multipotent, meaning they can differentiate into various cell types, they mainly develop into mature oligodendrocytes [173]. However, these cells are not simply a transitional stage in the development of oligodendrocytes and in the myelination process [175]. Indeed, in addition to their self-renewing function, OPCs create a complex and extensive network that works as neuronal activity sensors, immune-responsive cells, and vascular regulators [176]. From a clinical point of view, OPCs have gained much interest due to their ability to proliferate in adulthood. In fact, these are involved in the re-myelination processes following brain acute or chronic lesions in pathology like multiple sclerosis, the most common demyelinating disease [177].

Oligodendrocytes, in turn, play a fundamental role in supporting and insulating nerve fibers to ensure efficient and rapid transmission of nerve impulses, as the Schwann cells does at the level of the peripheral nervous system [175]. Indeed, oligodendrocytes are able to extend their processes, forming the myelin sheath which surrounds the axons of more than 50 neurons [178].

While the role of oligodendrocytes in PD was not extensively studied, there are emerging evidences suggesting their involvement in the disease. For instance, Devika Agarwal and colleagues, through a single-nuclei transcriptomic atlas of the SNpc in humans, have been recently demonstrated that there is an association between PD genetic risk factors and specific gene expression patterns in oligodendrocytes. These patterns encompass genes related to mitochondrial function, protein folding, and ubiquitination pathways [179].

A subset of RGCs undergo differentiation to become ependymal cells. They compose the delicate membrane that lines both the central canal of the spinal cord and the ventricles within the brain, known as ependyma [174]. They have a dual function: i) generating cerebrospinal fluid, and ii) playing a significant role in preserving the integrity of the BBB [180]. These cells are small and closely align to construct this membrane, with cilia that facilitate the continuous circulation of cerebrospinal fluid [180].



### 1.2.3.2 Astrocytes

Astrocytes represent the most abundant type of glial cells in the CNS [181]. These cells were first observed by Jaques Dutrochet in the early 19th century, though he did not use the term "astrocytes." It was not until the late 19th century that the term "astrocyte" was coined by von Lenhossék, a Hungarian neuropathologist, who described their distinctive morphology [181]. Indeed, their name, from the Greek *Ástron* (star) and *Kútos* (cavity), describes their star-like morphology with numerous processes that surround the neuronal synapses. They originate from neural progenitor cells (NPCs) within the SVZ, and migrate along radial glial processes to disperse throughout the CNS [182]. Astrocytes were initially categorized into two fundamental morphological subtypes: protoplasmic and fibrous. Protoplasmic astrocytes are commonly found in the grey matter, while fibrous astrocytes predominate in the white matter of the CNS [183]. However, with the advancements of high-throughput single-cell RNA sequencing, became increasingly evident the astrocyte heterogeneity and its relevance in both health and disease. Indeed, astrocyte functions are closely linked to the brain region, and eventually to the type of brain injury, as well as to the age and the sex of the individual [184], [185]. More in detail, single-cell RNA sequencing studies revealed that the heterogeneity originates from two primary sources: astrocyte subsets driven by developmental programs, referred to as developmentally induced astrocyte (DIA) subsets, and astrocyte subsets induced in response to external stimuli, known as stimulus-induced astrocyte (SIA) subsets [184], [185].

Under physiological conditions, astrocytes are functionally indispensable for normal brain activities as they play a crucial function in brain homeostasis [186]. In addition to the "mechanical" and metabolic support to the neuronal counterpart, they perform several functions such as: i) contribution to axonal growth and BBB formation, thanks to their processes around the endothelial cells of the blood vessel; ii) regulation of synapse formation and plasticity of neurons, through their participation in tripartite synapses; and iii) neuroprotective function through the release of growth and neurotropic factors, anti-inflammatory, and anti-oxidant molecules, via a bidirectional astrocyte-neuron crosstalk [187]–[189].

In these regards, by reacting to signals within their microenvironment, astrocytes possess the capacity to either exacerbate or stop inflammation and neurodegeneration, actively participating in several neurological conditions, such as MS, Huntington's disease, AD, PD and also behavioral neuropsychiatric disorders [190]. The morphological and

functional changes astrocytes undergo in these conditions, are commonly referred to as “astrogliosis” or “astrocyte reactivity” [191]. Regarding reactive astrocytes, Liddelov and colleagues in 2017 proposed two distinct phenotypes, the detrimental A1 and the protective one A2, mimicking the M1/M2 dichotomy. A1 astrocytes were described to play a role in many NDs, including PD, and exhibit negative and neurotoxic behaviors that are in turn brought on by activated microglia. On the other hand, A2 astrocytes released neurotrophic molecules and expressed receptors for neurotransmitters, cytokines, chemokines and hormones – in association with those produced by microglia – in order to maintain the homeostasis in the brain and in the cerebral microenvironment [192]. However, recent findings revealed the co-existence of A1 and A2 phenotypes. Indeed, as for microglia cells, the classification of A1/A2 astrocytes cannot be rigid, as their behavior and physiology are subjected to several variations based on the specific context of the brain's microenvironment. This context-dependent nature makes it challenging to definitively categorize them as purely protective or detrimental ones [193]–[195].

Certainly, reactive astrocytes have pro-inflammatory roles, by the release of a plethora of molecules that facilitate the invasion of immune cells into the CNS [196], [197]. More in detail, as neurodegeneration advances, astrocytes undergo changes in calcium homeostasis and alterations in gene expression, leading to modifications in their synaptic homeostatic role with consequent impaired neuronal activity [198]. Finally, at the later neurodegenerative stages, astrocytes upregulate pathways associated with a pro-inflammatory milieu and subsequent neuronal harm [198]. For example, in the case of amyotrophic lateral sclerosis (ALS), some studies have shown how astrocytes expressing a mutated form of the superoxide dismutase (SOD) enzyme, encoded by SOD1 gene, had a direct effect on the survival of motor neurons, causing their rapid degeneration in co-culture experiments [188]. In the case of AD, astrocytes exhibited an increased expression of genes encoding serine protease inhibitor A3N (Serpina3n) and the lysosomal cysteine protease cathepsin B (Ctsb), both of which are involved in amyloid processing [199].

Several functions and consequences of this “activation” have been identified also in PD, revealing astrocytes as important contributors to PD onset and progression through both gain- and loss-of-function mechanisms [200]. Significantly, in the SNpc, microglia and reactive astrocytes serve as the primary “cellular-hub” handling crucial cellular processes, including oxidative and endoplasmic reticulum stress, mitochondrial, lysosomal, proteasomal, autophagic activities,  $\alpha$ -Syn aggregation and spreading, all leading to

DAergic neurons' death. Interestingly, several evidences supported also their positive roles deriving from the release of molecules such as neurotrophin-3 and BDNF, that support axon regeneration [201], [202]. Also, astrocytes from the VMB release a variety of pro-survival and neuroprotective factors, such as the glial-derived neurotrophic factor (GDNF) and the basic fibroblast growth factor (bFGF), that are crucial for the development of DAergic neurons, the same which degenerate in PD patients [203]. Identifying the molecular mechanisms governing astrocyte subsets and their functions holds promise for the development of innovative therapies for neurological disorders.

#### **1.2.4 The “bad” and the “good” side of glial cells in the context of PD**

During the last 20 years of research the pivotal role of glia-neuron crosstalk in the development and progression of NDs, including PD, was uncovered [204]. Astrocytes and microglia are able to produce a plethora of molecules, such as neurotransmitters, neuromodulators, neuropeptides, hormones and neuroimmune regulatory molecules, with beneficial or detrimental effects [205]. Indeed, the so-called “activated” glial state is thought to represent a susceptibility factor in the delicate balance between anti-inflammatory and pro-inflammatory factors. This could potentially lead to a detrimental loop of amplified inflammation between neurons and glial cells, ultimately contributing to the neurodegenerative process (**Figure 7**). However, while many studies have initially focused on the detrimental responses of astrocyte and microglia to PD injuries, an increasing body of evidence unequivocally have demonstrated the ability of astrocytes and microglia to play pivotal roles in protecting and repairing neurons. However, the mechanisms that trigger the glial “beneficial” phenotype are currently under active investigation [205].

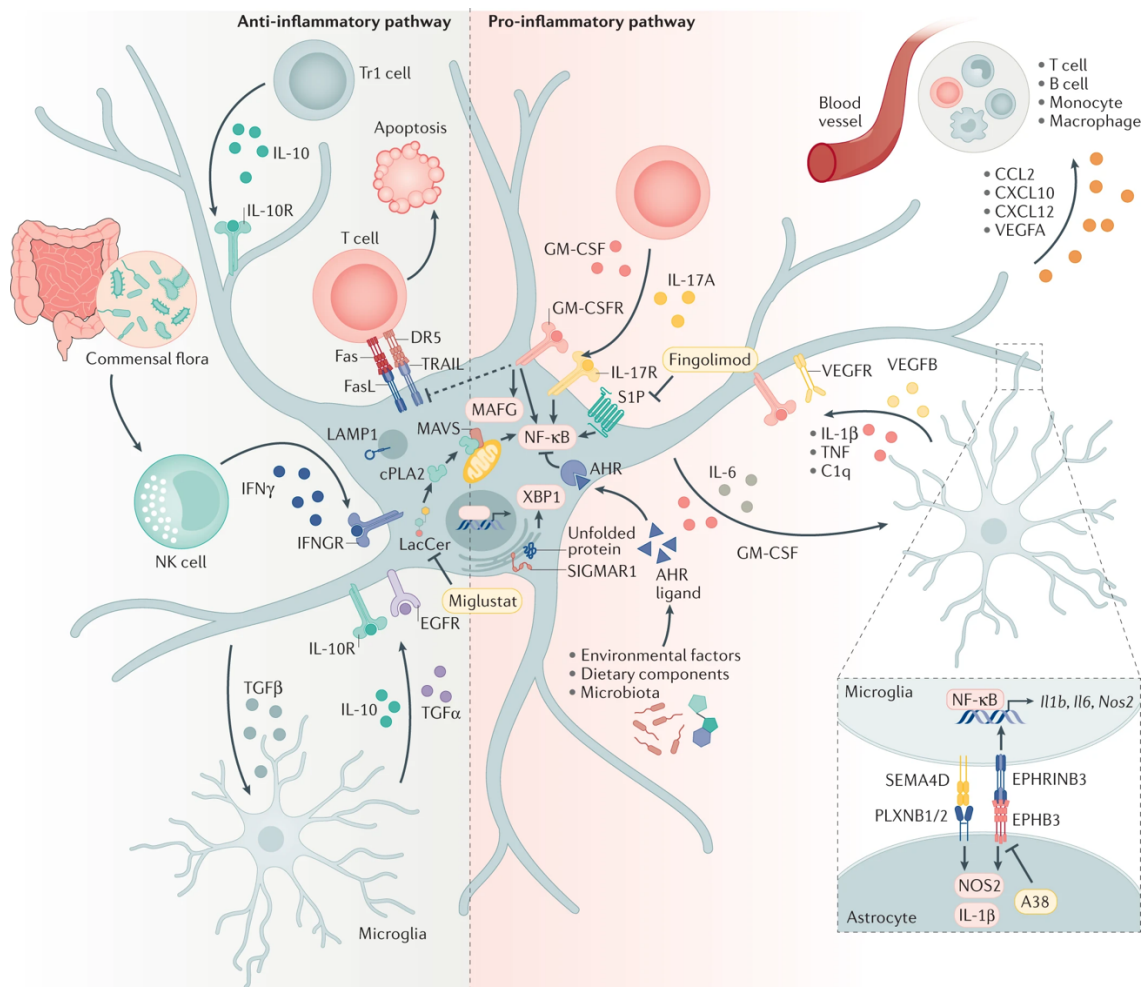


**Figure 7.** Multifaced roles of astrocytes in the context of CNS inflammation. Astrocytes actively participate in CNS inflammation, exhibiting both pro-inflammatory and anti-inflammatory functions. Their interactions with various cells and molecules within the CNS lead to the secretion of pro-inflammatory mediators, including cytokines and chemokines, along with the production of elevated levels of ROS and nitrogen species. This leads to a vicious cycle of inflammation and DAergic degeneration. However, glial cells have neuroprotective properties, which promote neuroprotection and the healing of damaged neurons. (Source: <https://doi.org/10.1038/s41573-022-00390-x>).

Among the plethora of pro-inflammatory molecules released by activated glial cells during PD progression it is worth to mention the nuclear factor  $\kappa$ B (NF- $\kappa$ B), which signals inflammasome induction, cytokines such as TNF- $\alpha$ , IL-1 $\beta$ , IL-6, and reactive compounds like ROS and NO [74], [206], [207]. This cycle of chronic glia activation and degeneration of DAergic neurons influences, in a preponderant way, the degree of the lesion and the overall adverse consequences on SNpc neurons [208], [209]. For instance, during the early stages of degeneration, aggregated  $\alpha$ -Syn released from dysfunctional DAergic neurons can trigger glial cells to release pro-inflammatory factors in the SNpc microenvironment, leading to further microglia activation and neuronal cell death. In turn, glial activation may contribute to the overall degeneration process through the prion-like propagation of misfolded  $\alpha$ -Syn [210], [211]. Moreover, astrocytes and microglia have a

prominent role in mediating the harmful effects of aging, regulating gene expression and the response to detrimental environmental factors with the effect to counteract nigrostriatal self-repair [212].

In this scenario, astrocytes play a decisive role. Indeed, while they can work with microglia to exacerbate neurotoxicity, they can also mitigate microglia activation and promote neuroprotection and neurorepair [213]. Both astrocytes and microglia exhibit numerous neuroprotective and pro-neurogenic properties. They release anti-inflammatory cytokines (e.g., IL-4 and IL-10), neurotrophic factors (e.g., BDNF and insuline-like growth factor, IGF-1) and extracellular matrix proteins (e.g., fibronectin) [73], [214]–[216]. Additionally, they play a crucial role in clearing the excess of glutamate from neuronal synapses and possess receptors for anti-inflammatory molecules [217]. Notably, following moderate neuronal damage, reactive astrocytes contribute to neuron survival and synaptic recovery through a signaling pathway mediated by STAT3 [218], [219]. This bidirectional relationship between reactive astrocytes and microglia allows astrocytes to modulate the extent of the inflammatory response [218], [219]. However, as demonstrated in a PD rat model (i.e., 6-OHDA-induced nigrostriatal lesions), when astrocyte dysfunction and persistent microglia activation occur, the severity of SNpc neurodegeneration accelerates due to the inhibition of glial-dependent compensatory mechanisms of neuronal repair [220].

It is still unclear how astrocytes and microglia are able to specifically deliver “bad” or “good” cargoes to the dysfunctional DAergic neurons [205]. Therefore, in the intricate pathogenesis of PD, the glial compartment takes a pivotal role when it comes to neuroinflammation, and the communication between the glial compartment and neurons result to be fundamental [72], [221]. In all the various pathways of intercellular communication, such as neuron-to-neuron, glia-to-glia, neuron-to-glia, or glia-to-neuron, EVs offer an efficient means to precisely transport biomolecular messengers, including cytokines, enzymes, mRNAs and non-coding RNAs (including microRNAs) [222]. This raises an intriguing question: can astrocyte-derived EVs (AS-EVs) contribute to the pivotal glial-neuronal communication network in the context of PD? Understanding the role of AS-EVs in this intricate dialogue may hold the key to unlock new insights into the disease's mechanisms and potential treatment strategies (see **Section 1.3** and **1.3.7**).

### 1.2.5 The role of CCL3 chemokine in astrocyte stimulation

Chemokines, also known as chemotactic cytokines, belong to the family of small cytokines (8-10 KDa) [223]. They are signaling proteins secreted by cells which induce leukocytes or other cell types (such as endothelium and epithelial cells) to migrate in a specific direction [224]. Some chemokines are thought to be pro-inflammatory, and during an immunological response, their release is stimulated in order to draw immune system cells to the infection site [223]. On the other hand, some of them are thought to be homeostatic, playing a role in the regulation of cell migration during standard physiological processes and tissue development [225]. Chemokines display four cysteine residues in conserved positions, which are essential for maintaining their three-dimensional shape and their functions [223]. In particular, these proteins interact with G protein-associated transmembrane receptors (on the surface of target cells), to produce a biological effect. There are four main subfamilies of chemokines: CXC, CC, CX3C and C [223].

The CC chemokine family includes Chemokine (C-C motif) ligand 3 (CCL3), also known as macrophage inflammatory protein 1- $\alpha$ , which has two contiguous cysteines close to the N-terminal [226]. It was first identified by Lord and colleagues in 1976 as a bone marrow-based inhibitor of stem cell proliferation [227]. Through its binding to the main receptors – CCR1, CCR4 and CCR5 – CCL3 plays a significant role in the recruitment and activation of polymorphonuclear leukocytes during acute inflammation [228]. In the peripheral immune system, various immune cells produce CCL3, primarily monocytes, macrophages, dendritic cells and T cells. Its main function is to act as a chemoattractant and modulator of immune responses, participating in cell-mediated immunity [229]. In the brain, CCL3 is secreted by glial cells during an inflammatory response, modulating the immune response and contributing to the regulation of neuroinflammatory processes [230]. In this regard, an increased expression of pro-inflammatory chemokines (i.e., CCL3, CXCL10 and CXCL11) was observed in MPTP-based mouse model of basal ganglia injury, during both nigrostriatal degeneration and self-recovery [231]. Moreover, *in vitro* studies revealed that CCL3-treated astrocytes promote powerful neuroprotective effects in MPP<sup>+</sup>-injured neurons and neurogenic effects in NSCs, thus supporting the essential role of astrocytes for the survival, restoration, and regeneration of DAergic neurons [232]. Together these studies highlighted the importance of the astrocyte-neuron communication for the regulation of neuroprotective mechanisms in the parkinsonian

brain, suggesting also a relevant contribution of the chemokine CCL3 [233]. However, the molecular details of this complex cross-talk are not fully understood yet. For this reason, it seems reasonable to anticipate a possible involvement of the EVs – naturally released from all cells type – to mediate the transport of bioactive molecules (in a time- and space-controlled manner) from glia to DAergic neurons.

### 1.3 Extracellular Vesicles (EVs)

Cell-to-cell communication is a fundamental process that allows cells to interact, coordinate, and respond to various signals and cues. This communication is essential for the proper functioning of tissues, organs, and organ systems, enabling them to work together efficiently and maintain homeostasis [234]. The selective packaging of signaling molecules for secretion has long posed a fundamental question in the field of membrane trafficking. In particular, during the last 20 years, alongside the classic pathways of cellular communication, such as cell-to-cell contacts, paracrine and endocrine signaling, a new modality of intercellular communication mediated by EVs has been proposed [235]. EVs are complex lipid nanostructures released by both prokaryotic and eukaryotic cells into the extracellular space, which contain cytosolic and membrane proteins, nucleic acids (DNA/RNA), metabolites etc. (**Figure 8**) [236].

The study of EVs began in 1946, when Chargaff and West, following high-speed centrifugation, identified for the first time in plasma the presence of platelet-derived procoagulant particles [237]. In the following decades, EVs have been isolated from various tissues, but it was initially thought to act only as “waste carriers”, eliminating non-functional/unneeded components from the cells [238]. Only in the 1990s EVs were recognized as an additional mechanism of cell-to-cell communication, thanks to their ability to exchange “information” between cells, both in homeostatic and pathological conditions. For all these reasons they have gained growing interest in the scientific community [238]. The secretion of EVs is conserved throughout evolution, from prokaryotes to more complex eukaryotes [239]. Indeed, both Gram positive and negative bacteria release EVs responsible of bacterial virulence, host immunomodulation and communication with other cells [240].

In human, all the cells of the body are virtually able to secrete EVs in the extracellular environment, both *in vitro* and *in vivo* [241], [242]. As a result, they can be isolated from many biological fluids, such as urine, saliva, blood, plasma, amniotic fluid, breast milk, cerebrospinal fluid, etc. [243], [244]. Moreover, it is known that their molecular cargoes can change in response to different stimuli and in different physio-pathological conditions (see **Section 1.3.3**). For all these reasons, EVs can be used for the non-invasive research of new biomarkers of health and disease [245]. Additionally, thanks to their ability to cross the BBB, their stability in circulation and their low immunogenicity, EVs can be opportunely engineered and used as advanced nanotherapeutic agents and drug delivery



system for different molecules (e.g., siRNAs, chemotherapeutic agents and immunomodulators etc), offering numerous advantages compared to their synthetic counterpart (e.g., liposomes, see **Section 1.3.6**) [246].

Therefore, the potential of EVs is twofold, both for fundamental and translational research: (i) for the identification of novel disease mechanisms; and (ii) as diagnostic/prognostic and therapeutic tools for the treatment of various diseases, including cancer and NDs, such as AD and PD. During these years, increasingly efforts in establishing guidelines, standard methodologies and nomenclatures in EV research have been done. This cooperative approach has yielded notable progress in various aspects of EV biology, including EV biogenesis and, to some extent, EV uptake [247]. However, our understanding of how EVs work within living organisms, and the mechanisms that control cargo sorting and delivery remains incomplete, highlighting the need for more focused investigation [248]. Furthermore, the detailed comprehension of the specific contribution of each EV-associated molecule in orchestrating the final outcome in target cells still needs to be fully clarified [248]. To address these knowledge gaps effectively, it is crucial to develop enhanced tools and *in vivo* models for EV research. Therefore, the interdisciplinary collaboration between researchers from different fields and expertise, including basic cell biology, clinical research, biotechnology and computer science, will be helpful to drive the field forward [247].

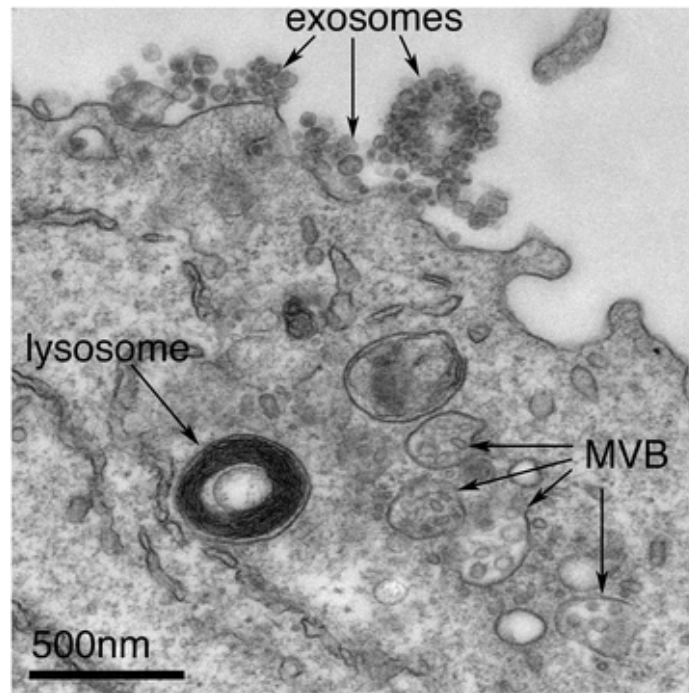


**Figure 8.** TEM micrograph of exosomes released from an Epstein-Barr virus-transformed B cell. The image depicts multivesicular bodies (MVB), which have the capability to transport their contents for degradation within lysosomes or merge with the cell's surface. Once merged with the plasma membrane, they release intraluminal vesicles as exosomes, as indicated by the arrows at the top of the picture. (Source: <https://doi.org/10.1186/s12915-016-0268-z>).

### 1.3.1 Historical background

The origins of EV research arguably date back to studies on coagulation before the 1980s and 1990s, when numerous investigations hinted at potential structures that would later be described as EVs [249]. As previously mentioned, the first study was conducted in the 1940s by Chargaff and West with experiments about coagulation [237]. More precisely, in 1946, they observed that the coagulation time was significantly shortened when the high-velocity sediment (particulate fraction) was added to the supernatant of human plasma [237]. However, only 17 years later, in 1967, Wolf documented the presence of a particulate substance, which could be separated by high-speed centrifugation, originating from platelets but different to them. This material, now recognized as EV fraction, was captured in electron microscopy images and it was referred to as “*Platelet dust*” [250]. In 1974, Nunez and collaborators described for the first time the presence of EVs in the bat thyroid gland, and introduced the concept of “multivesicular bodies” (MVBs) [251]. Moreover, other reports described the presence of these secreted vesicular structures in other organisms different from mammals, such as flagellated alga [252], the yeast

*Candida tropicalis* [253], and bacteria such as *Corynebacterium* [254] and *Escherichia coli*, with the latter producing EVs containing lipopolysaccharide complexes [255].

However, the crucial experiments in which EVs were specifically recognized as functional entities took place between the 1980s and the 1990s. In 1983, EVs were described as key mediators in the process of erythrocytes maturation. In particular, the secretion of EVs was found to mediate the removal of the transferrin receptor – responsible of iron uptake – ensuring the maturation of erythrocytes in specialized oxygen-carrying cells [256]. Subsequently, in 1996, the capability of B cells to release EVs transporting antigens to T lymphocytes was unveiled, emphasizing the involvement of EVs also in immune-related processes [11]. Notably, it was discovered that cytokines could be shed via EVs [257], and EVs derived from immune cells were identified as key players in the immune system's function [258].

These findings stimulated the publication of a huge number of EV-related studies [259]. Worthy of note, for example, is the important study from 1998, where the use of dendritic cells derived-EVs as potential “cell free” anti-tumor vaccine was described [260]. From 2000, the attention was further focused on the nature of these vesicles, with a particular interest for the proteomic and lipidomic payloads [261]. Starting from 2004, EVs were isolated from different biological fluids, including urine, suggesting their potential as biomarkers [262]. Another turning point was in 2007, when Valadi and collaborators demonstrated the ability of EVs to transport nucleic acids, particularly RNAs, that retained functional activity when delivered to target cells (**Figure 9**) [263].

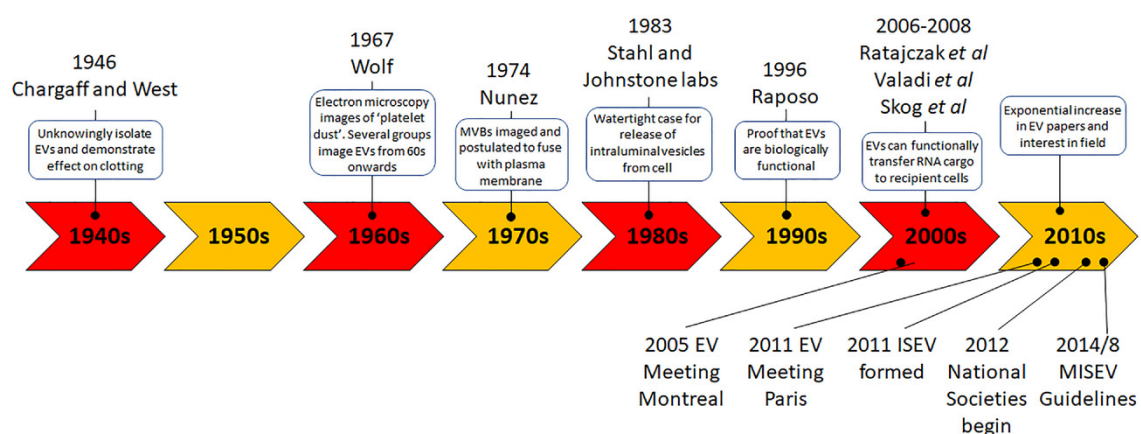


**Figure 9.** Timeline of main milestones in EV research from 1940 to 2010. In the 2000s: 2005 marked the inaugural EV meeting in Montreal, followed by the 2011 EV meeting in Paris. The year 2011 saw the establishment of the International Society for Extracellular Vesicles (ISEV), while in 2012, National Societies dedicated to EV research began to take shape. The pivotal year of 2014 witnessed the inception of the MISEV (Minimal Information for Studies of Extracellular Vesicles) guidelines (Source: <https://doi.org/10.1002/jev2.12144>).

Since 2010, research in the EV field has grown significantly, in relation to the increase of funding opportunities, with the consequent development of several companies, patents and clinical trials. Indeed, many biotechnology companies focused on the development of EV-based diagnostic tools and drug delivery systems [249]. Also, the number of patents utilizing EVs as diagnostic indicators and therapeutic delivery carriers has increased during these decade. The United States witnessed the filing of more than 500 patents encompassing various terms associated with EVs [259]. Moreover, to illustrate their practical applications, more than 30 clinical trials specifically integrated the use of EVs, either for diagnostic purposes or as therapeutic agents, with a predominant focus on cancer biology [259]. Clinical trials are crucial for determining the potential of EV-based interventions and represent a significant step toward realizing their therapeutic applications (see **Section 1.3.6**). Over the next few years, the positive trend in EV research is expected to continue, leading to increased advances in understanding EV biology and resulting translational benefits.

### **1.3.2 EV biogenesis**

Although all secreted membrane vesicles are now collectively referred to as “EVs”, they are indeed highly heterogeneous, making challenging to characterize their specific properties and functions [264]. EVs represent a group of circulating nanostructures produced by virtually all cells. They are delimited by a phospholipid bilayer with a size ranging from 30 to >1000 nm [265]. Their biogenesis, content and delivery mechanisms characterize each type of vesicles [266]. Indeed, EV classification is constantly evolving, with new classes continuously emerging during the years [242]. Nevertheless, based on the current knowledge of their biogenesis, EVs can be grouped into three major subtypes: exosomes, shedding vesicles (also known as microvesicles or ectosomes) and apoptotic bodies (**Figure 10**).

- Exosomes include vesicles with a size ranging from 30 to 150 nm with an endosomal origin [267]. They derive from the invagination process of the late endosome membrane, which results in the formation of MVBs, containing intraluminal vesicles (ILVs). The MVBs may undergo a double fate: they can fuse with the lysosomes with the consequent digestion of the content; or they can fuse with the plasma membrane, releasing the ILVs into the extracellular space, which will take the name of exosomes [268]. In this context,

the Endosomal Sorting Complexes Required for Transport (ESCRT) machinery plays a pivotal role for the sorting of cargoes to ILVs in the MVBs, and thus for the exosome formation. However, ESCRT and ESCRT-accessory proteins (i.e., Alix, TSG101, HSC70, and HSP90) are also involved in the outward budding of the plasma membrane, both for microvesicles and virus release [269], [270].

ESCRT pathway involves the coordinated action of four ESCRT complexes (ESCRT-0, ESCRT-I, ESCRT-II, and ESCRT-III), in addition to disassembly and deubiquitylating enzymes on the endosome membrane. ESCRT-I and ESCRT-II complexes contribute to the bending of the endosomal membrane to form an ILV [271]. Then, ESCRT-II induces the formation of ESCRT-III filaments, which in turn induce the nascent ILV to detach from the endosomal membrane [272]. This process may also be facilitated by ALIX, an ESCRT accessory protein, that binds lysobisphosphatidic acid on the MVB membrane [273]. To cap off the process, the AAA ATPase VPS4 disassembles the ESCRT-III filaments from the membrane, resetting the ESCRT system and potentially aiding in vesicle fission [274].

Interestingly, when the ESCRT machinery is compromised or inhibited, the secretion of exosomes is not completely abolished [275]. Indeed, together with the ESCRT machinery, there are evidences indicating the release of exosomes into the extracellular space via alternative ESCRT-independent mechanisms [276]. First of all, researcher have pinpointed a distinct variation of the ESCRT pathway known as the syndecan–syntenin–ALIX pathway, which exhibits particular vulnerability when the genes responsible for ESCRT and ESCRT-accessory proteins are knocked down [277], [278]. Syndecan 1, a transmembrane heparan sulfate proteoglycan, oligomerizes and facilitates signaling by binding to growth factors and chemokines. Syndecan 1 interacts with the scaffold protein of syntenin and ALIX on endosomes, linking the scaffold itself to CD63 (see below) [277], [278]. Another variation of the ESCRT pathway involves accessory ESCRT-III proteins (CHMP1, CHMP5) and increased sodium tolerance protein 1 (IST1), crucial for forming a unique class of exosomes under conditions of glutamine deprivation and/or mTOR-Akt inhibition [279]. These exosomes are produced within RAB11-positive recycling endosomes, suggesting that accessory ESCRT-III proteins have a role in stress-induced EV biogenesis [279].

Other mechanisms of exosome biogenesis via ESCRT-independent pathway, include the involvement of lipids in the exosome biogenesis. Indeed, lipids influence various aspects of endosome biology, such as the regulation of endosome positioning through cholesterol

[280], control of endosome size [281] and the formation of ILVs mediated by ceramide [282]. Therefore, it is thought that certain cone-shaped lipids, such as ceramide and phosphatidic acid, possess the ability to induce spontaneous negative curvature of the membrane, leading to invagination into the endosome membrane when present on the outer leaflet [282], [283]. In support of this concept, the generation of exosomes depends on the hydrolysis of sphingomyelin by neutral sphingomyelinase 2 (nSMase2) to produce ceramide, which causes the membrane of endosomal multivesicular bodies to bud inward [282]. Moreover, distinctive raft-associated lipids may play a role in promoting the formation of ILVs [284]. In addition to nSMase2 activity, the ceramide itself positively regulates exosome biogenesis. The ceramide transporter (CERT) and the receptor-mediated signaling at the level of MVBs by the ceramide metabolite SIP may also have implications for the biogenesis of ectosomes (see below) at sites where the endoplasmic reticulum interfaces with the plasma membrane [285]–[288].

It has been demonstrated that also members of the tetraspanin family (CD9, CD63 and CD81) can act as ESCRT-independent pathway [289]. Like ceramide, tetraspanins have a wedge-like structure, suggesting that both molecular classes may possibly share the same biophysical mechanism to induce membrane curvature and consequently exosome biogenesis [290], [291]. However, the exact mechanisms through which tetraspanins exert their influence on vesicle sorting and release are an area of ongoing research, with conflicting results [289]. Indeed, there are reports indicating that the knockout of CD63 is associated with a reduction of the ILVs number in melanoma, breast cancer and HEK293 cells [289], [292]–[294]. On the contrary, in other studies, there is either no discernible impact [278], or even an increase in the total secreted exosomes in other cell types [295]. A potential explanation for these disparities is the presence of multiple tetraspanins within the same tetraspanin-enriched microdomains. Depending on the specific tetraspanin involved, there would be different effects on EV biogenesis [294].

In the end, the involvement of alternative pathways in exosome release suggests a complex and adaptable system for their secretion, allowing cells to respond to various physiological and pathological conditions [296].

- Shedding vesicles (or microvesicles or ectosomes) are produced directly by the budding of the plasma membrane, which protrudes outwards until their release in the extracellular environment. The vesicles size ranges from 30 nm to >1  $\mu$ m (up to 10  $\mu$ m in the case of large oncosomes) [297]. Their differences in size, are reflected in differences on the biogenesis mechanisms. As far as the small ectosomes or microvesicles are concerned,

their biogenesis is very similar to the exosomes, involving both ESCRT-dependent and -independent pathways. Indeed, TSG101 is recruited to the plasma membrane through its interaction with arrestin domain-containing protein 1 (ARRDC1), leading to the formation of microvesicles [269]. Instead, little is known about large oncosome biogenesis. It remains uncertain whether early ESCRT machinery or tetraspanins are involved, as observed in exosome or small ectosome biogenesis. On the contrary, the process appears to be driven by rearrangements of the actin cytoskeleton, leading to plasma membrane blebbing and scission for their subsequent release [298].

- Apoptotic bodies/blebs are released by apoptotic cells and have a dimension between 50 nm and 5  $\mu\text{m}$  [299]. The process involves caspase 3 substrates, particularly critical contributors like ROCK1. The role of ROCK1 is to trigger actomyosin contractility, leading to membrane blebbing, which can originate either from the plasma membrane itself or from the tips of surface protrusions known as apoptopodia [300], [301].

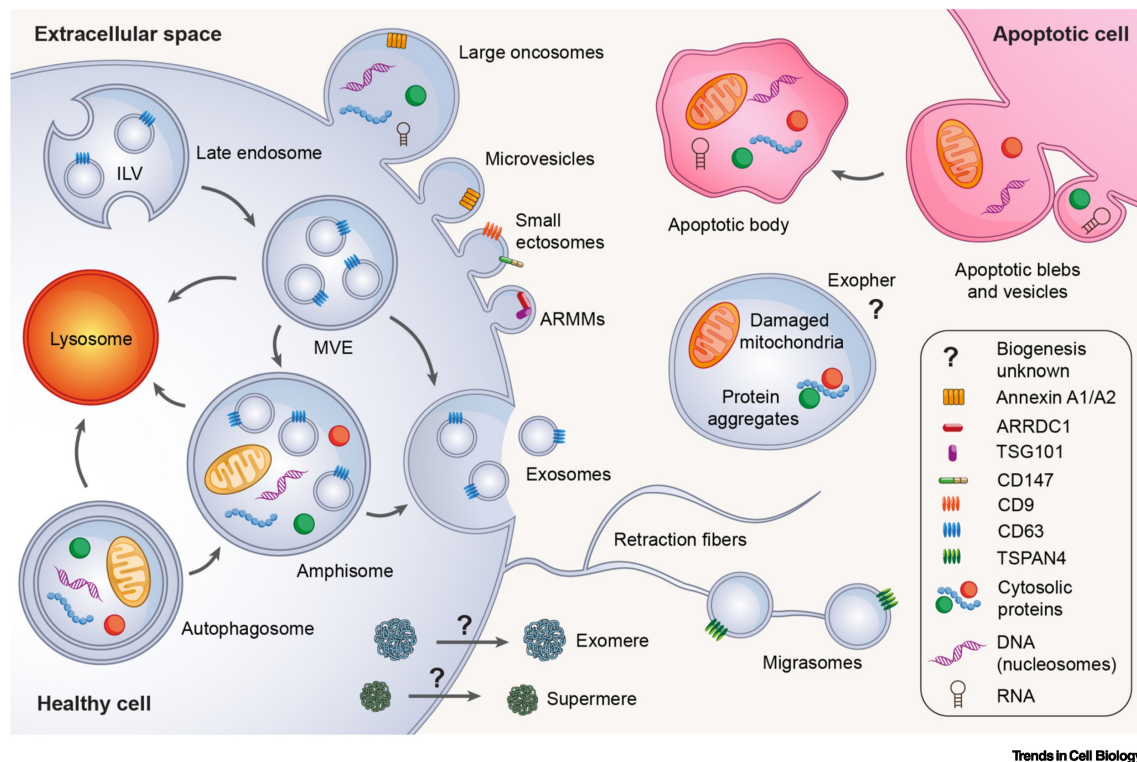


**Figure 10.** Schematic representation of EV subtypes and biogenesis in eukaryotic cells. Shedding vesicles, which include microvesicles, large and tiny ectosomes, arrestin domain-containing protein 1-mediated microvesicles (ARMMs), are generated by the outward budding of the plasma membrane and the subsequent release of vesicles into the extracellular space. They range in size from 30 nm to 10  $\mu\text{m}$  and they differ also in molecular make-up, and release mechanisms. ILVs are produced by the inward budding of the limiting membranes of late endosomes, which results in the production of MBVs. MBVs may move to the lysosomes for destruction or to the cell surface to fuse with the plasma membrane, where ILVs are released into the extracellular environment as 30-150 nm exosomes. Also, MBVs and autophagosomes may combine to form an organelle known as an amphisome, either directed towards lysosomes or routed to the plasma membrane for the release of their contents. In the figure are represented also: apoptotic bodies/blebs,



migrasomes (large EVs that are released from migrating cells' retraction fibers), exophers (large EVs that appear to be produced under stress to preserve tissue homeostasis), exomeres and supermeres (non-vesicular extracellular nanoparticles, which can be found in the circulation, secreted by both healthy and cancerous cells). (Source: <https://doi.org/10.1016/j.tcb.2023.01.002>).

However, the presence of numerous overlapping pathways and molecules, coupled with the previously mentioned lack of complete understanding of the biogenesis process, results in the absence of specific markers for distinguishing different vesicle subclasses. Indeed, there are several issues contributing to the difficulties in the EV classification: i) the same cell can produce simultaneously different types of EVs; ii) in many cases, EV subgroups overlap in size, density and morphology, leading to great obstacles in purifying single classes of EVs without contamination by the other subtypes; and iii) the use of different protocols for EV isolation results in the recovery of different types of EVs [302]. Thus, the necessity to develop standardized protocols for the isolation and the characterization of different populations of EVs.

### **1.3.2.1 EV purification methods**

Classical methods used for EV isolation include: differential ultracentrifugation (dUC), filtration and precipitation. dUC relies on high-speed centrifugation to separate EVs from large particles and may be associated with density gradient ultracentrifugation to further separate EVs based on their density. It is also common a modification of traditional ultracentrifugation, named density cushion ultracentrifugation, which isolate EVs with a density gradient cushion, reducing the risk of pelleting cellular debris [303]. Even if dUC is still the most used technique, it is time-consuming, requires specialized and expensive equipment and may co-isolate contaminants [304].

Filtration methods separate EVs by size, but they lack specificity and can result in EV loss [305]. Chemical precipitation methods, like polyethylene glycol, are user-friendly but co-precipitate contaminants. Moreover, the presence of residual polymers may interfere with downstream EV applications [306].

Nowadays, besides the classical methods of EV isolation, new isolation methods facilitate the exploration of EV heterogeneity, allowing researchers to better understand the distinct functions and characteristics of different EV subtypes [307], [308]. Between them it is worth to mention: size-based isolation via size exclusion chromatography (SEC) and tangential flow filtration (TFF), which allow to separate EVs minimizing the co-isolation of contaminants [309]; immunoaffinity purification, to isolate EVs expressing specific



antigens [310]; microfluidic methods, which enhances reproducibility for their low sample volume requirements and the automation [311]; asymmetric field flow fractionation (AF4), which separates EVs based on their hydrodynamic size [312] (**Figure 11**).

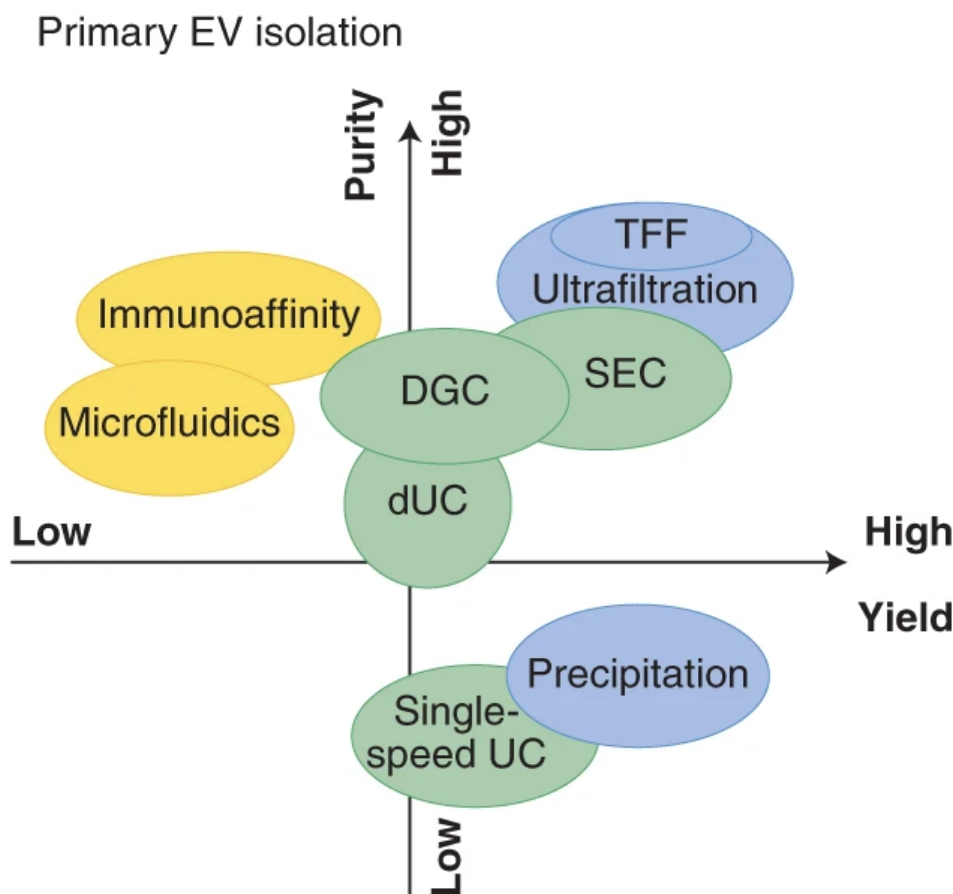


**Figure 11.** Categorizing the most common methods for EV isolation based on their purity and recovery. These methods include dUC (Differential Ultracentrifugation), DGC (Density Gradient Centrifugation), SEC (size exclusion chromatography), TFF (tangential flow filtration), Ultrafiltration, Immunoaffinity, Microfluidics, Precipitation. Source: <https://www.nature.com/articles/s41565-021-00931-2>.

To date, following the guidelines of the "Minimal Information for Studies of Extracellular Vesicles" (MISEV) of 2018 and 2021 [313], [314], EVs are better distinguished on the basis of measurable physical characteristics, that can be used to develop standardized protocols of purification. Therefore, the EVs are separated according to their size into: small vesicles (sEVs), < 200 nm (the most studied), and medium/large vesicles > 200 nm. Given the rapid expansion in the field of EVs, these MISEV recommendations represent a helpful road map to help the standardization (in terms of nomenclature, methods and results), the transparency of the publications. Also, interdisciplinary collaborations are

encouraged between researchers from different fields (biology, medicine, material science etc.) to further enhance our understanding of EVs [247]. However, there are certain issues associated with the MISEV guidelines, that limit their broader adoption. For instance, the rapid and continuous evolving knowledge in the field makes difficult to fit in rigid classifications and requirements. Indeed, while the guidelines are widely recognized and supported by the scientific community, they are not easily applicable in all the facets of EV research. It is key to avoid a dogmatic view to finally help advance the field [315].

### 1.3.3 EV cargoes

EVs play an important role in cell-to-cell communication since, once released into the extracellular environment, they can reach different target cells and trigger a specific biological response (see **Section 1.3.5**), determined by the molecules transported. Indeed, EVs contain a payload (lipids, proteins, nucleic acids, metabolites etc.), which reflect the content and thus the physio/pathological conditions of the donor cells [316]. Notably, the vesicle membranes protect the EV content from the degradation operated by the external proteases and nucleases [316]. The EV membrane composition differs from that of the plasma membrane of donor cell, probably due to the recruitment of specific lipids and proteins (i.e., lipid raft) at the membrane level during EV biogenesis (see **Section 1.3.4**) [235].

Regarding the vesicle cargoes, multi-omics characterization (e.g., RNA-seq, mass-spectrometry) of EVs derived from primary cell cultures, cell lines, tissue cultures or isolated from biofluids, revealed an heterogenous compositions in terms of nucleic acids, proteins, lipids etc. (**Figure 12**). All the information derived from these studies are collected in specific databases, such as “*Vesiclepedia*”, “*EVpedia*”, “*Exocarta*”, with the aim to help the scientific community working on this field. These databases are constantly updated with information deriving from novel studies [317].

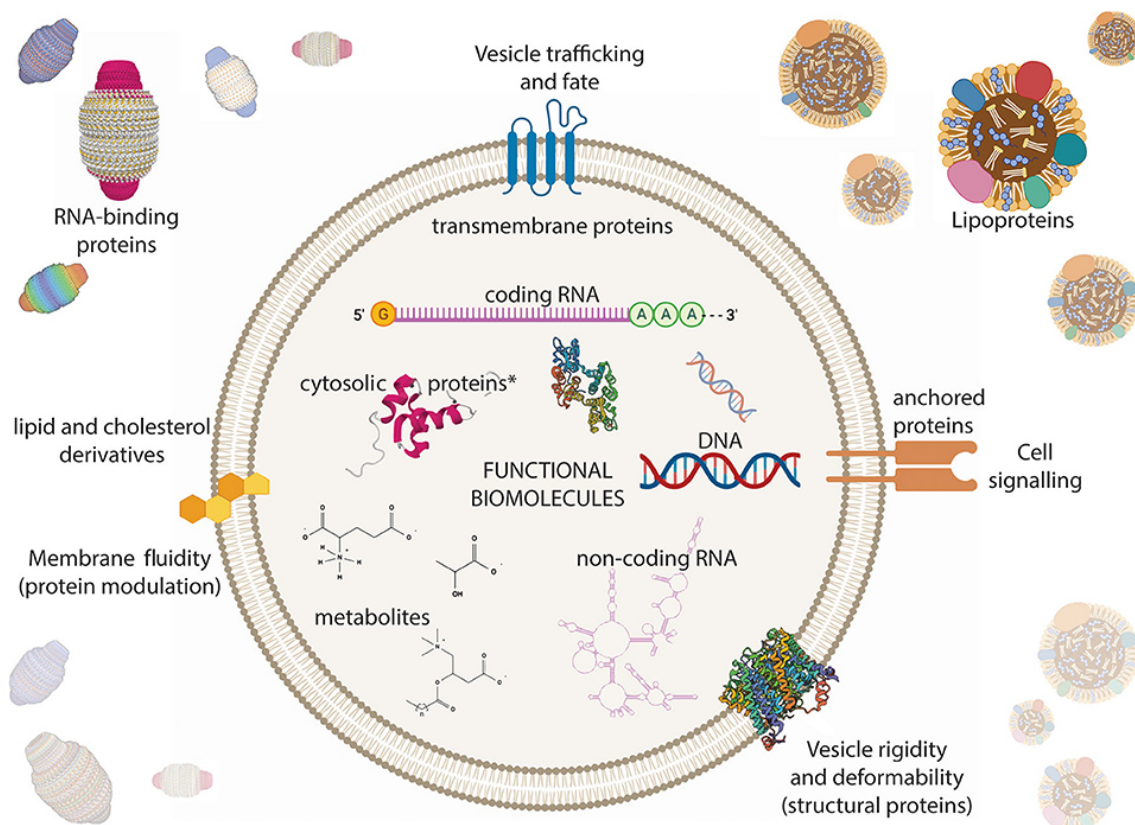


**Figure 12.** EVs carry a comprehensive array of biomolecule categories associated with cellular processes. They encapsulate DNA, various types of RNAs (both coding and non-coding), and proteins in diverse forms, including freely soluble, membrane-associated, membrane-anchored, and transmembrane configurations. Additionally, EVs contain metabolites and other small molecules. (Source: <https://doi.org/10.3389/fgene.2020.00700>).

The EV-associated proteins and their post-translational modifications (e.g., ubiquitylation, cleavage, palmitoylation) reflect the cellular origin, the environmental factors, the stimuli to which the donor cell is subjected to and in some way also the biogenesis mechanism [238]. As previously described (see **Section 1.3.2**), there are numerous mechanisms which govern biogenesis processes, including the ESCRT machinery, the syndecan–syntenin–ALIX pathway, tetraspanins, lipids and ARRDC1. These sorting mechanisms selectively load specific protein cargoes into EVs [247]. During the years, the researchers have focused their attention preferentially on membrane protein cargoes that are on the EV surface. This focus arises from the close association of these cargoes with membranous structures, making them more suitable for labeling and available for a wide range of analytical methods [247]. The most represented are plasma membrane proteins and the proteins involved in vesicular trafficking [264]. They include

the tetraspanin family such as CD9, CD63 and CD81. These transmembrane proteins, together with other proteins associated with the plasma membrane, are commonly identified in EV samples and are enriched in the vesicle lysates compared to the donor cells [318]. Other vesicular trafficking proteins, such as ESCRT accessory factors (i.e., Alix, TSG101, HSC70 and HSP90) are present in exosomes regardless of the donor cell type, and often used as general markers of EVs [319]. On the other hand, the incorporation of specific array of cytosolic proteins into ILVs has primarily been elucidated within the context of autophagy, where it is known as the microautophagy process [320]. This intricate interplay between sorting mechanisms and cargoes necessitates careful consideration, as it can result in the generation of distinct EV subtypes with varying compositions and, consequently, potentially diverse function [321]. Thus, while the tetraspanins are used as general EV markers, proteins linked to cytoplasm (e.g.,  $\beta$ -Actin and  $\beta$ -Tubulin) and organelles like mitochondria, Golgi and endoplasmic reticulum (e.g., succinate dehydrogenase complex flavoprotein subunit A (SHDA) and Tom20, Golga, Calnexin etc.) are generally used as non-vesicular markers, to evaluate (for instance by western blotting) any possible cellular contamination deriving from the isolation and purification methods used [322]. However, these proteins may also be actively included inside the EVs, considering the intricate inter-organelle trafficking between the mitochondria and the endosomal system [323] [324]. According to these results, EVs are shown to contain both mtDNA and fully active mitochondrial proteins (ATP synthase, cytochrome c oxidase subunits, etc.), although the exact molecular mechanisms by which these proteins may play a functional role in recipient cells is not fully elucidated, yet [325]. Other findings suggest the possibility that mitochondrial-derived vesicles (MDVs) – involved in the mitochondrial quality control (MQC) system – may be rearranged within the MBVs and released in the extracellular microenvironment as exosomes [68].

In PD, mitochondrial dysfunction is known to be a key factor contributing to the degeneration of DAergic neurons (see **Section 1.1.2.2**). Since MDVs are involved in maintaining mitochondrial health, researchers have hypothesized that changes in the content or in the characteristics of circulating MDV could reflect mitochondrial dysfunction and cellular stress associated with PD, representing another source of promising biomarkers [326].

In addition, EV-associated proteins are involved in their uptake (see **Section 1.3.5**), and they are also essential to perform EV function. For instance, Chun and collaborators demonstrated that human astrocyte-derived EVs could improve the electrophysiological

function and anti-apoptotic behavior of hiPSC-derived cortical neurons [327]. Proteomic analysis of these EVs revealed the presence of various neuroprotective proteins, such as HSP, lipoprotein receptor-related protein 1 (LRP1) and apolipoprotein E (APOE) [327]. Proteins promoting neuronal excitability and synaptic development, such as potassium channel tetramerization domain containing 12 (KCTD12), glucose-6-phosphate dehydrogenase (G6PD), kinesin family member 5B (KIF5B), and spectrin-alpha non-erythrocytic1 (SPTAN1), have been also found [327]. In a similar way, Montecchi and coworkers found that astrocyte-derived EVs contained a set of proteins associated with the regulation of oligodendrocyte differentiation, myelination, nitrogen metabolism and oxidative stress [328]. In the context of NDs, You and coworkers discovered that integrin- $\beta$ 1 (ITGB1) is found to be enriched in astrocyte-EVs from total brain of AD patients, and correlated with brain  $\beta$ -amyloid and tau levels in independent cohorts [329].

All these findings suggest that studying the protein content of EVs contributes to the understanding of the pathology and opens up the way for innovative medical interventions [265].

While it is well-established that transmembrane proteins and ESCRT components play a crucial role in protein cargo selection, the mechanism(s) governing the incorporation of RNAs (eventually bound to RNA-binding proteins) into EVs are far less understood. Several studies have shown that EVs, especially small EVs, are notably enriched in specific RNAs compared to the donor cell, implying the existence of selective sorting mechanisms [330]–[332]. Moreover, the RNA content in small EVs differs from that in large EVs, with a notable abundance of specific RNA subtypes [330]–[332]. These include long non-coding RNA (lncRNA), microRNA (miRNA), tRNA-derived fragments (tRFs) and circular RNA (circRNA) [333], [334]. In 2007 Valadi and his collaborators identified the capability of EVs to deliver functional mRNA and miRNAs to recipient cells [263]. In particular, they observed the presence of mouse-specific proteins in human cell cultures when treated with mouse-EVs depleted of proteins, indicating the functional role of the mRNA content [263]. Since then, EVs have been considered as important carriers of genetic information able to alter gene expression in the target cells. Thanks to next generation sequencing (NGS) techniques, the collection of genetic material associated with EVs is increasingly growing. The RNA loading within EVs is context-specific, for example it plays a regulatory role in synaptic plasticity within the CNS [335]. As demonstrated by Chaudhuri and colleagues, inflammation may be responsible for an altered loading of neuroinflammatory proteins and miRNA in astrocyte-derived EVs (see

**Section 1.3.7).** These components have been observed to inhibit neurite outgrowth, dampen neuronal firing, and encourage neuronal apoptosis [336].

Over the years, while the protein and RNA content carried by EVs have been extensively studied, the DNA within EVs has received less attention [337]. Indeed, DNA may be found in the blood circulation either as cell-free molecules or may be found in association with the EVs [338]. In the bloodstream, it has been traditionally believed that a substantial portion of the DNA found within EVs comes from apoptotic bodies. However, ongoing research is actively challenging this assumption, especially as a growing number of EVs that do not originate from apoptosis have been observed to carry DNA [337]. EVs are associated with various types of DNA (dsDNA, ssDNA, mtDNA), that can be found at the EV surface or within the vesicular lumen, where it is protected from the external environment [339]. Many studies support the idea that EV-DNAs can have an impact on the target cells, with possible implication on homeostasis maintenance, inflammatory responses and horizontal gene transfer [340]–[342]. However, the EV-DNA functions need to be further investigated.

#### **1.3.4 EV secretion**

The secretion of EVs, including exosomes and shedding vesicles, is a tightly regulated process that can be influenced by various cellular and environmental factors. As previously said, the exosome release into the extracellular environment involves several steps to finally obtain the fusion of MVBs with the plasma membrane [343]. On the contrary, shedding vesicles are directly released by the plasma membrane budding. Their release is expected to be faster, as their cargoes reside close to the plasma membrane and are ready to be incorporated within the vesicles, resulting in the immediate release following their formation [343]. Therefore, it is possible to appreciate a temporal gap between exosome biogenesis and their subsequent release [238] (**Figure 13**).

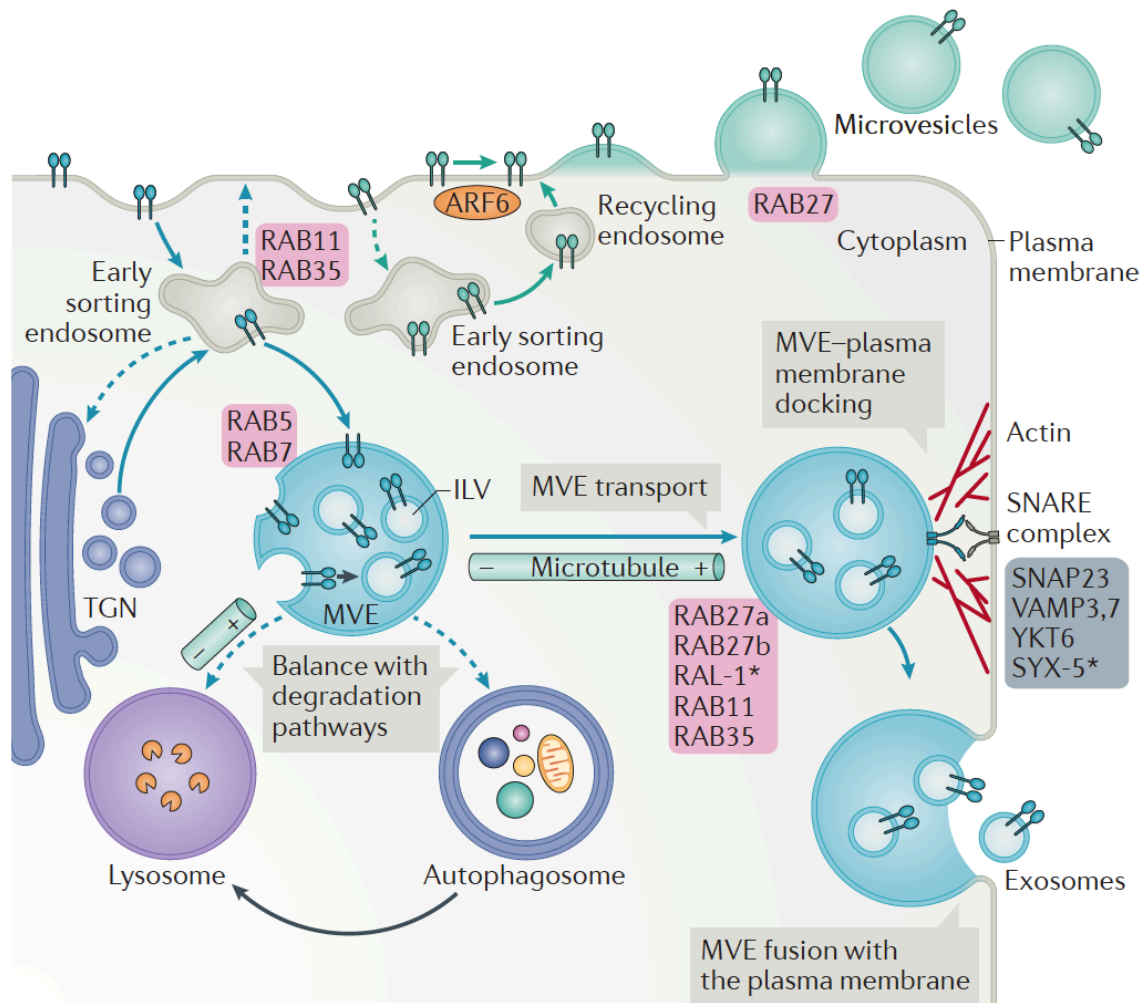


**Figure 13.** The production of exosomes and shedding vesicles requires the precise orchestration of multiple intracellular trafficking steps. These steps (blue arrows for exosomes and green arrows for shedding vesicles), determine how cargo is delivered to the site where EVs are formed. In the case of exosomes, they also determine the fate of the MVB. Cargo destined for MVBs can originate from endocytosis at the plasma membrane, or early sorting endosomes through the biosynthetic pathway originating from the trans-Golgi network (TGN). Retrograde transport, leading either back to the TGN or back to the plasma membrane, can redirect cargo away from their intended destination within the MVBs (represented by dashed arrows). These sorting processes are under the control of RAS-related protein (RAB) GTPases. Once matured, MVBs not destined for lysosomal or autophagosomal degradation, are transported along microtubules to the plasma membrane. The final step of exosome release involves docking and fusion, with RABs, actin and SNARE proteins playing key roles in these processes. In the case of shedding vesicles formation, endocytic uptake and recycling can respectively decrease and increase the incorporation of membrane and membrane-bound cargoes into shedding vesicles. (Source: <https://doi.org/10.1038/nrm.2017.125>).

More in detail, considering that MVBs are typically associated with late endosomes, whose primary fate is to fuse with lysosomes for degradation of their contents, exosome secretion has been linked to impaired lysosomal degradation [344]. Indeed, when the endolysosomal system becomes congested, it might prompt MVBs to find alternative pathways such as secretion [247], [345]. However, the exact mechanisms regulating the balance between the MVBs degradative and secretory capacity remain largely unexplored, although it strongly impacts on cell functions [247]. This equilibrium is, at

least in part, governed by the cargoes sorting mechanisms within MVBs [346]. The acquisition of their fusogenic capacity could depend on the recruitment of specific molecular machinery during ILV biogenesis, with both ESCRT-dependent and ESCRT-independent pathways, specifically associated with either degradation or secretion of MVBs [346]. For instance, it has been demonstrated that TSG101, which can be subjected to ISGylation (addition of ISG15), led to lysosomal degradation and consequently impaired exosome secretion [347]. In summary, these machineries, by inducing inward budding of microdomains, can alter the composition of the limiting membrane of MVBs, recruiting or excluding additional components which regulates lysosomal fusion (e.g., TSPAN6), MVB transport (e.g., ORP1L), docking (e.g., RAB27), or fusion (e.g., SNAREs). The accumulation or depletion of membrane cargoes on MVBs, either due to recycling or other factors related to cellular trafficking dynamics, and the overall cellular environment, can impact these processes and, consequently, exosome secretion [346].

MVB transport to lysosomes occurs through retrograde movement on microtubules, facilitated by the RAB-GTPase RAB7, its associated proteins and dynein [348]. Remarkably, RAB7 is also necessary for exosome release, with the ubiquitylation status of RAB7 influencing the preference for lysosomal targeting over exosome secretion [348]. Moreover, the fate of MVBs is influenced also by their cholesterol content. Indeed, cholesterol-enriched MVBs usually result in exosome secretion. Consequently, also changes in the lipid composition of the MVB membrane regulate the fate of MVBs themselves [349], [350]. Furthermore, other essential components for exosome secretion are RAB27A and RAB27B, along with their effectors (synaptotagmin-like protein 4 and exophilin 5), which play a crucial role in regulating the motility and docking of MVBs to the plasma membrane [348]. The final step which leads to the release of ILVs in the extracellular environments, following the fusion with the plasma membrane, is mediated by SNARE proteins and members of the synaptotagmin family [351]. However, while certain SNARE complexes are involved in exosome secretion, their roles can vary among different cell types [351]. Moreover, exosome secretion is also regulated by the levels of  $Ca^{2+}$ , which might activate the SNARE complexes [352].

Another crucial point to consider is the balance between exosome secretion and macroautophagy [353]. Specifically, the fusion of MVBs with autophagosomes can hinder exosome secretion. In this context, it has been observed that the prion protein (PrP) promotes exosome secretion by inhibiting autophagosome formation [353]. This effect is mediated by the interaction with the caveolin and the modulation of caveolin's inhibitory



influence on autophagosome formation (see **Section 1.3.5**), suggesting that the capacity of MVBs to release exosomes is counterbalanced by their fusion with autophagosomes [354].

As far as shedding vesicle secretion is concerned, this is supported by different mechanisms that act on plasma membrane microdomains [355]. Typically, these mechanisms demand less energy because they rely on membrane protrusions like filopodia or microvilli, or they involve retraction and scission through nanotubes and retraction fibers [356]. These processes are regulated by molecular factors such as the actin cytoskeleton, (i.e., actin-associated regulatory proteins that shape these protrusions), lipid microdomain organizers (again tetraspanins, such as tetraspanin-4 and CD9), sugar-rich molecules forming the glycocalyx, and proteins capable of bending bilayers like BAR domain proteins [357]. More in details, shedding vesicle release requires their fission from the plasma membrane through actin-myosin interaction, and involves also small GTP-binding proteins like ARF6 and ARF1, that play a role in the contraction process [358], [359]. However, the release of cellular material in the extracellular space, as in the case of large ectosomes, raises questions about how cells manage their membrane resources while maintaining a balance between membrane loss and EV secretion. One method to supply membranes for budding sites involves vesicular transport, where the plasma membrane contributes membranes to the endosomal pathway and vice-versa, suggesting a potential link between exosome formation at the level of the endosomes and the plasma membrane [247]. Moreover, cargoes that play a role in recruiting budding machinery for EV formation continually move between endosomes and the plasma membrane. Those that recycle through retrograde transport or return to the plasma membrane become less abundant at exosome biogenesis sites but are likely more concentrated at shedding vesicle biogenesis sites [296]. However, there is currently a gap in comprehensive studies that investigate the regulation of EV secretion due to the lack of data that systematically compares different cell types [296].

All these concepts define EV secretion not as a constitutive event that occurs randomly or in response to endosomal congestion, but as an inducible process that cells engage in response to different conditions. Different triggers, such as physical contact with neighboring cells for shedding vesicle generation, cytokines and calcium signaling cascades, can indeed induce an increase in EV secretion [360].

### 1.3.5 Mechanisms of EV signaling with target cells

After being released into the extracellular space, EVs can signal to target cells through different mechanisms, mainly based on protein interactions. These dynamic processes can change depending on the status of the donor cell and the surrounding microenvironment [361]. In this context, the composition of the EV membrane plays a pivotal role by selectively targeting specific recipient cell types. Indeed, there are evidences *in vivo* where EVs – with different compositions – can effectively target specific organs, leading to precise changes in the local microenvironment [362]. However, there are also substantial data indicating that recipient cells can be promiscuous, engaging in interactions with EVs through mechanisms that lack specificity. For instance, a non-selective targeting mechanism involves the presence of phosphatidylserine at the outer membranes of EVs, that facilitates cell attachment and entry [363]. Moreover, there is an emerging recognition of the role of a surface EV “corona” in the interaction with target cells [364]. EVs have the potential to engage with various soluble components, resulting in the formation of a corona, a layer of biomolecules that adheres to the surface of the EVs. The corona formation is a commonly observed phenomenon in different biofluids, and its composition is reflective of the originating cell type, the cellular milieu and the conditions during EV production [365]. The process of corona formation is the result of electrostatic interactions and protein aggregation [364]. In addition to the nonspecific adsorption of proteins onto the EV surface, specific interactions between receptors and ligands can also occur. For all these reasons, the corona can significantly affect the interaction between EVs and target cells or tissues [366].

The EV uptake has been investigated starting from the already known cellular mechanisms used to incorporate external material. The mechanisms of EV internalization involve several molecules, such as tetraspanins, heparan sulfate proteoglycans, integrin receptors, tetherin and others [367], [368]. This diversity allows a single group of vesicles to engage with various cell types. Assessing the relative contribution of these specific uptake methods, and how they impact on target cell signaling and entry, represent an important challenge for the field [367], [368]. Following the contact to the surface of recipient cells, EVs may directly trigger a signaling pathway or may be internalized using different uptake mechanisms (e.g., endocytosis and direct fusion) [369] (**Figure 14**).

EVs can initiate intracellular signaling pathways through direct interactions with the surface receptors or ligands of target cells. EV signaling can exert an impact on the

cellular phenotype through membrane-bound morphogens like Wnt [370], and the Notch ligand DII4 [371]. This signaling can also influence the motility, migration, and invasiveness of cancer cells.

On the other hand, endocytosis stands out as the prevalent route for EVs to convey signals and occurs through different pathways, such as clathrin-dependent, caveolin-mediated, macropinocytosis, phagocytosis and lipid raft-mediated internalization [372], [373]. Clathrin-mediated endocytosis requires the assembly of clathrin-coated vesicles containing a multitude of receptors and their ligands [374]. Similarly, caveolin-1 plays a pivotal role in the caveolae-dependent pathway, with the oligomerization of caveolins affecting the formation of caveolin-rich rafts in the plasma membrane. Increased activity of caveolin scaffolding domains promotes the caveolae-dependent pathway [375]. The macropinocytosis is a non-specific, large-scale form of endocytosis where cells engulf a volume of extracellular fluid, along with any suspended particles, including eventually the EVs, within that fluid [376]. In the same way, phagocytosis involves the engulfment of EVs typically by specialized phagocytic cells, such as macrophages or dendritic cells. It is more common for larger vesicles like microvesicles [377]. As already said, the lipid composition of both EV and target cell membranes significantly influences the uptake mechanism, with lipid rafts playing a substantial role in the EV internalization [280]. Lipid rafts are membrane microdomains enriched in cholesterol, glycosphingolipids and glycosyl-phosphatidylinositol-anchored proteins [378]. These rafts serve as platforms for the clustering of specific proteins and facilitate the recognition and binding of EVs to target cell membranes [379]. Usually, they are associated with various types of endocytosis, including caveolin-dependent endocytosis and micropinocytosis [379], [380].

Besides endocytosis mechanisms there is also the fusion process, which represents a more direct mechanism of EV uptake. This is another avenue of internalization, where the EV membrane directly merges with the cell plasma membrane [381]. Indeed, some EVs, particularly small-EVs, can directly fuse with the plasma membrane of the recipient cell, releasing their contents into the cytoplasm [382]. Another potential pathway for EVs to enter the cell cytoplasm, where their cargoes can exert functional effects, is through fusion with the membrane of endosomes [383], [384]. This mechanism, known as “back fusion”, allows EVs, particularly those with an intra-endosomal origin (ILVs), to potentially escape the acidic pH and proteases within the endo-lysosome pathway. The back fusion

process may be facilitated by changes in charge and conformation of proteins and lipids, driven by the acidic pH, which could enhance the fusion [383], [384].

In some cases, cells can form tunneling nanotubes (TNTs), essential for rapid communication between distant cells. TNTs are long, filamentous structures that establish physical connections between cells, allowing direct transfer of cellular components [385]. Notably, EVs can travel through TNTs, enhancing their ability to reach target cells and deliver cargoes [386].

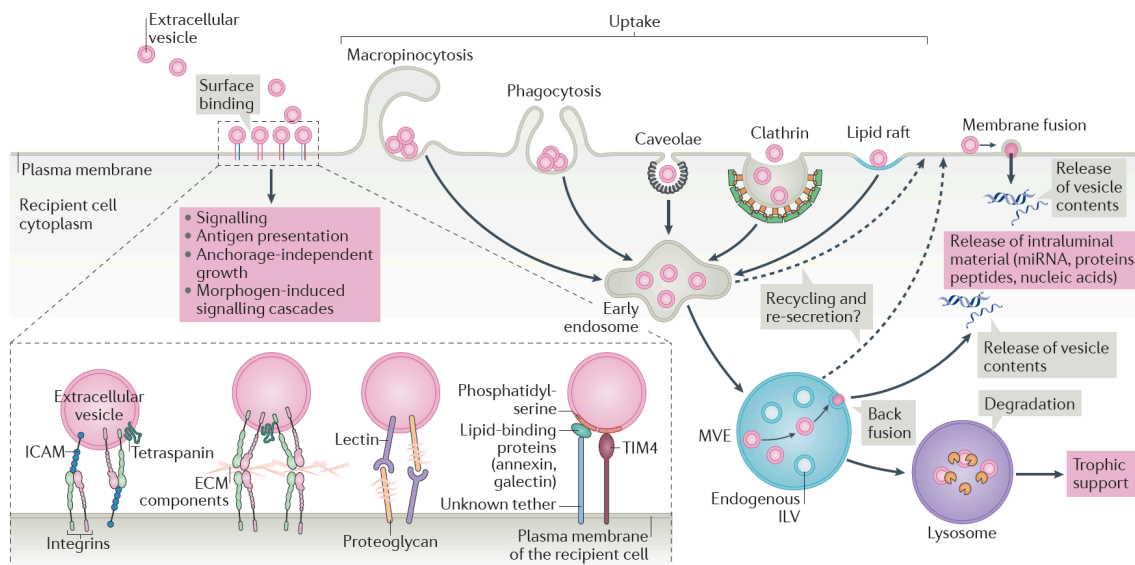


**Figure 14.** Schematic representation of EV signaling with eukaryotic target cells. Once released in the extracellular space, EVs will interact with the cell surface of the recipient cell, with different fates. Depending on the cell type, multiple pathways can lead to the internalization of EVs. They can remain bound to the surface of the target cells and initiate an intracellular signaling (antigen presentation, anchorage-independent growth, morphogen-induced signaling cascades). Another mechanism includes the release of intraluminal contents into the cytoplasm of the target cell by membrane fusion. Finally, the uptake mechanisms include clathrin-dependent and clathrin-independent endocytosis, such as micropinocytosis and phagocytosis, as well as endocytosis via lipid raft and caveolae. (Source: <https://doi.org/10.1038/nrm.2017.125>).

However, it is important to note that EV uptake may transpire through either a combination of pathways or alternative mechanisms, if the preferred pathway is obstructed [145]. The complexity and redundancy of cellular uptake mechanisms reflect the remarkable adaptability and resilience of cells. They have evolved intricate pathways for the internalization of various materials, allowing them to respond to changing conditions and needs. The possibility of relying on different mechanisms ensures cells can continue functioning even when one pathway is compromised. This provides a robust defense against pathogens, a mean to regulate nutrient intake, and the capacity to finely

respond to external stimuli. This complexity can make it challenging to dissect the internalization mechanism using specific uptake inhibitors [147]. Indeed, achieving an efficient pharmacological treatment for long-term inhibition or the selective targeting of specific uptake pathways in *in vitro* experiments remains a formidable task [387]. The inhibition of certain EV uptake pathways might affect the uptake of other essential molecules, leading to undesirable side effects [387]. Moreover, the use of specific dyes (e.g., PKH26, CellVue, etc.) or genetic approaches to label EVs, for the visualization and the measurement of EV uptake, is hindered by the recycling of internalized material by recipient cells, making challenging an accurate quantification. These difficulties intensify when investigating different EV-based drug administration protocols that involve various dosages and durations. In response to these complexities, a theoretical evaluation may help the experimental design, to optimize the use of precious resources necessary to produce and to purify EVs [387].

Several models predicting the uptake of several molecules have been proposed in the literature. For instance, Wattis and collaborators, proposed a mathematical model of low-density lipoprotein (LDL) endocytosis, consisting of a system of ordinary differential equations. The model is validated using *in vitro* experimental data and is employed to investigate differences in system behavior when cells are supplied with a single bolus of extracellular LDL versus a continuous supply of LDL particles, which better reflects *in vivo* conditions [388]. More recently, Gandham and coworkers developed three mathematical models to gain insights into the intricate dynamics of miRNA transfer in the tumor microenvironment. The first model uses ordinary differential equations to describe the rate-limiting steps in miRNA transfer [389]. In the second model, experiments are conducted to establish the concentration-effect relationship of miRNA Let-7b on High-mobility group AT-hook 2 mRNA levels [389]. The third model integrates the parameters from the first two models to predict the kinetics and effect relationship of EV-mediated Let-7b in recipient cells and determine the minimum miRNA copies required to induce functional effects [389]. However, these models often focus on specific uptake mechanisms and are useful for designing selective uptake experiments. In contrast as already said, cells employ diverse and complex pathways for EV internalization. Hence, the necessity of a more generalized analytical model for EV uptake [388], [390] (see **Section 3.3.3**). In the end, the creation of innovative *in vitro* and *in vivo* systems for modeling EV transfer and cargo release, represent an important goal for the field. This will help not only to understand the EV behavior, but also to design

vesicles able to escape the lysosomal pathway, and therefore fully functional inside the cells.

### 1.3.6 Therapeutic potential of EVs

EVs can carry multiple molecules, allowing to characterize them at various levels: genomics, transcriptomics and proteomics [391]. Due to this aspect, they offer translational opportunities both as source of biomarkers, and also as potential nanotherapeutic agents [203]. There are several reasons to consider EVs as valuable tools for biomarker discovery. First of all, they reflect accurately the pathophysiological status of the donor cell. Additionally, the lipid bilayer protects their cargoes from degradation, therefore they are easily recoverable and identifiable. Moreover, they are highly stable and able to transport their cargoes across the biological barriers (e.g., the BBB) into the systemic circulation, making them accessible for isolation and subsequent analysis [392]. Indeed, EVs can be isolated from many biological fluids, such as blood, cerebrospinal fluid, urine and others. Also, for their nature, EVs provide different classes of molecules at once (both the external layer made of lipids, proteins etc., and the internal lumen with the soluble components) as source of novel biomarkers. This, in turn, can give new and comprehensive insights about different pathological conditions (**Figure 15**).

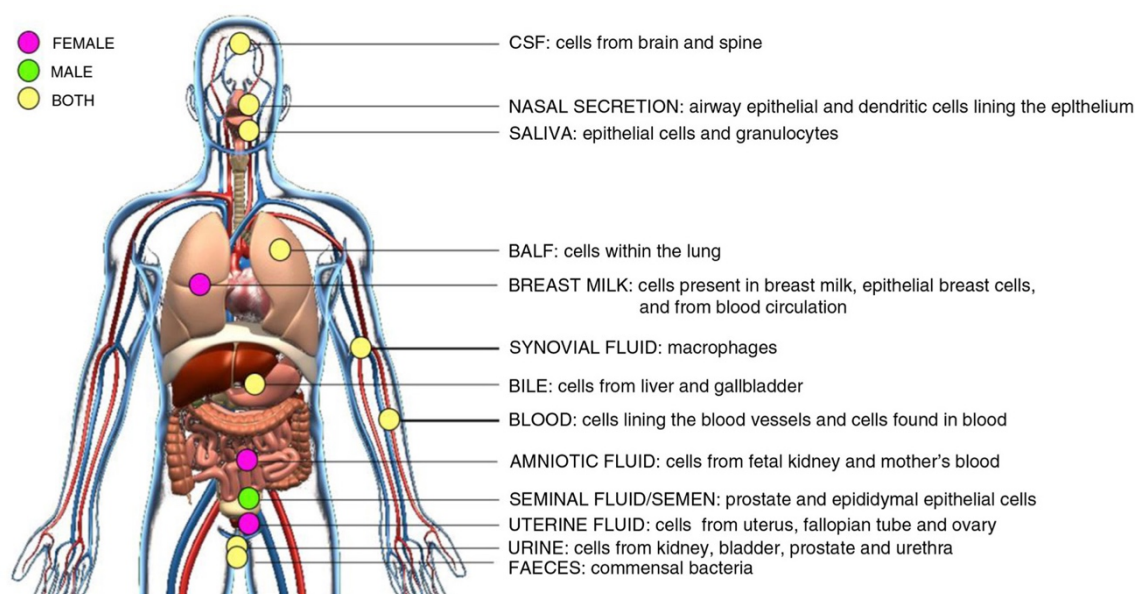


**Figure 15.** The diagram highlights the body fluids where EVs have been identified and it indicates their potential cellular origins. Pink markers denote body fluids exclusive to females, green markers signify body fluids unique to males, and yellow markers represent body fluids found in both females and males.

Abbreviations: CSF = cerebrospinal fluid; BALF = bronchoalveolar lavage fluid. (Source: <https://doi.org/10.3402/jev.v4.27066>).

In particular, there are two different ways to use EVs as biomarkers: i) as diagnostic markers, to establish a particular disease in the acute/progressive phase; ii) as prognostic markers, to determine the course of a disease, or the responsiveness of a patient to a therapy [393], [394]. The first evidence of EVs as biomarkers, dates back to 2004, when Pisitkun and his colleagues identified the presence of aquaporin 2 in the urine-derived exosomes. Aquaporin 2 is a protein responsible to facilitate water movement from the luminal membrane into the bloodstream, and when it is present in the urine it suggests potential kidney problems [395]. Overall, this discovery paved the attention on the potential diagnostic applications of EVs [396]. Indeed, there are several evidences showing how the pathological conditions can modify the content of vesicles, suggesting they may be used as a diagnostic tool for the early detection of NDs, including PD [397]. In this context, biomolecules like proteins and miRNAs transported via EVs from neurons or glial cells seem to be really promising. As the presence of  $\alpha$ -Syn aggregates in LB is a typical hallmark of PD, to date there is a substantial body of research examining  $\alpha$ -Syn levels within EVs in different biological fluids. For instance,  $\alpha$ -Syn is consistently elevated in PD patients' plasma samples compared to healthy controls. This supports the idea that  $\alpha$ -Syn within neuronal plasma EVs could serve as a predictive marker for the progression of the disease [397]. Indeed, in a longitudinal study involving PD patients, Niu and colleagues established a direct association between vesicular  $\alpha$ -Syn levels and the severity of the disease [398]. Moreover, also the assessment of initial  $\alpha$ -Syn aggregates, specifically oligomers (o- $\alpha$ -Syn), could offer an advantage in the early detection of PD. For instance, despite numerous studies indicating a marked reduction in the total  $\alpha$ -Syn (t- $\alpha$ -Syn) levels in the cerebrospinal fluid of PD patients, it has been demonstrated that the o- $\alpha$ -syn/t- $\alpha$ -syn ratio stands out as the most sensitive and specific parameter for distinguishing PD from control subjects [56], [399]. Therefore, despite the inherent limitations arising from the different protocols for EV isolation,  $\alpha$ -Syn within EVs emerges as a potential biomarker for PD. In addition to  $\alpha$ -Syn, there are also many evidences about other EV-carried PD protein such as LRRK2, DJ-1, apolipoproteins, PrP<sup>C</sup> and other candidate biomarkers. These additional protein candidates offer promising avenues for understanding and diagnosing the disease [394].



Other studies on EVs recovered from blood, serum or cerebrospinal fluid of PD patients revealed the presence of specific miRNAs that are either more abundant or less abundant in relation to the onset of PD [400]. Notably, the analyses from various sequencing-based investigations have indicated an enrichment of miR-195, miR-24, miR-153, miR-409-3p, miR-10a-5p, let-7-c-3p, and miR-331-5p, and a reduction of miR-19b, miR-1, and miR-505 in blood-derived EVs from PD patients compared to EVs from control subjects [401], [402]. Several protocols are currently under development to isolate EVs from specific cell types (and thus body regions), given that also peripheral cells can release vesicles into biological fluids. For instance, several reports have suggested the utilization of the L1CAM antibody for the selective isolation of neuronal-derived vesicles from whole blood [403]. However, this is currently matter of intense investigation [404], [405].

On the other hand, for the already mentioned properties (i.e., the ability to transport bioactive cargo, overcome biological barriers, their stability in circulation), and also their low immunogenicity, both naturally-occurring and engineered EVs can serve as nanotherapeutic carriers [406]. Indeed, they have the potential to selectively reach the desired target site, and subsequently release their cargoes (see **Section 1.3.5**). Unlike their artificial counterpart (e.g., liposomes) naturally occurring vesicles offer the advantage of greater compatibility with cellular membranes (due to sharing a similar membrane structure and composition). Moreover, EVs exhibit a greater capacity and a broader spectrum for delivering molecules compared to liposome cargoes, even though their production on a larger scale is challenging [407] (**Figure 16**).

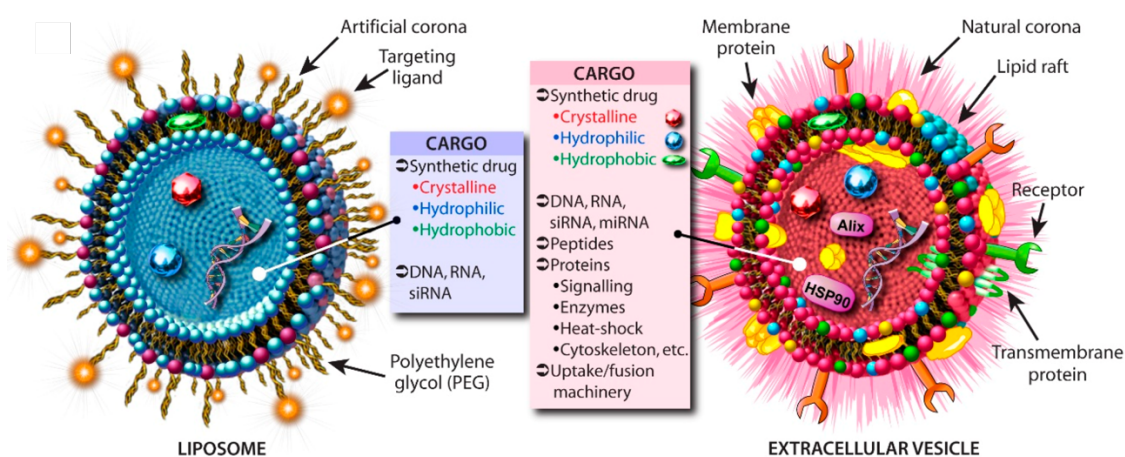


**Figure 16.** Illustrated representation of lipid-based vesicular carriers: liposomes vs EVs. It is noteworthy that in contrast to liposomes, EV membranes encompass a diverse array of lipid classes and additionally incorporate transmembrane and membrane-associated proteins, receptors, adhesion molecules, and a natural corona. Liposomes need to be intentionally engineered to achieve these characteristics. (Source: <https://doi.org/10.3390/ijms17020172>).



In the context of CNS, during the last decade, natural or modified EVs have been proposed as different strategies to treat PD [392]. This can be achieved by utilizing producer cells such as macrophages, stem cells, neurons or glia. These cells can produce and package various bioactive molecules, such as miRNAs, mRNA and proteins, within EVs to ameliorate PD symptoms or hinder its progression [203]. For example, stem cell-derived EVs from dental pulp have neurogenic properties, as evidenced by their ability to rescue human DAergic neurons from apoptosis induced by 6-OHDA [408]. When administered intranasally in a mouse PD model, these stem cell-derived EVs improved motor symptoms and normalize Tyrosine hydroxylase (TH) expression in both SNpc and striatum [409]. Additionally, human mesenchymal stem cells, engineered to produce exosomes carrying therapeutic catalase mRNA, and implanted in PD mice's brains, resulted in the attenuation of neurotoxicity and neuroinflammation [410].

Interestingly, also the administration of AS-EVs, holds promising potential for the treatment of NDs, including PD [411]. For instance, when EVs are released by astrocytes activated by the treatment with specific chemokines, they may result in the inhibition of DAergic neuron loss, the suppression of neuroinflammation, the promotion of neurogenesis and angiogenesis, and the enhancement of overall brain functions (see **Section 1.2.3** and **3.2**) [412]. These advancements provide encouraging prospects for the development of novel therapeutic strategies in the context of NDs by the use of natural-occurring EVs.

On the other hand, as anticipated, EVs can be engineered to express beneficial molecules aimed at promoting neurorepair and inhibiting neuroinflammation [246], [381]. EVs can be manipulated to deliver: (i) anti-oxidant agents (e.g., curcumin, catalase or ApoD) which protect neurons from oxidative stress [413], [414]; (ii) growth factors (e.g., GDNF) to stimulate proliferation of DAergic neurons [415]; (iii) dopamine to ameliorate behavioral parameters [416], [417]; (iv) siRNAs silencing the expression of SNCA gene to decrease  $\alpha$ -Syn levels [418]. Overall, these findings, although in the preclinical stage, hold great promise for the advancement of PD treatment, offering novel potential therapeutic options.

The interest in the field of EVs as nanotherapeutics has constantly increased, as witnessed by their application in several clinical trials [246], [419]. The first study used loaded EVs to create a vaccine for a lung tumor [420], [421]. More in details, patient dendritic cell-derived EVs were loaded with tumor-derived peptides, boosting therefore the patient immune response to lung cancer cells, in both phase I and phase II/III studies [420], [421].

Since then, other studies have been conducted to examine the potential of different type of EVs (including autologous EVs and plant-derived EVs), in treating disorders like cancer, stroke and also NDs [246], [392], [422] (**Table 3**).

**Table 3.** Ongoing clinical trials with EVs: stem cells-derived EVs, allogenic and autologous EVs, other cells sources of EVs and drug-loaded-EVs. (Source: <https://doi.org/10.1038/s41565-021-00931-2>).

No.	Name <sup>a</sup>	Status	Condition	Type of EV <sup>b</sup>	Location	NCT number
<b>Stem-cell-derived EVs</b>						
1	A Clinical Study of Mesenchymal Progenitor Cell Exosomes Nebulizer for the Treatment of Pulmonary Infections	Recruiting; phase 1/2	Drug-resistant infections	MSC-/progenitor-cell-derived exosomes	Shanghai, China	NCT04544215
2	Effect of Microvesicles and Exosomes Therapy on $\beta$ -Cell Mass in Type I Diabetes Mellitus (T1DM)	Unknown status	Diabetes mellitus type 1	MSC-derived exosomes	Sahel, Egypt	NCT02138331
3	Evaluation of Safety and Efficiency of Exosome Inhalation in SARS-CoV-2 Associated Pneumonia	Enrolling by invitation; phase 1/2	SARS-CoV-2 pneumonia	MSC-derived exosomes	Samara, Russia	NCT04491240
4	A Pilot Clinical Study on Inhalation of Mesenchymal Stem Cells Exosomes for the Treatment of Severe Novel Coronavirus Pneumonia	Completed; phase 1	SARS-CoV-2 pneumonia	MSC-derived exosomes	Shanghai, China	NCT04276987
5	Safety and Efficiency of Method of Exosome Inhalation in COVID-19 Associated Pneumonia	Enrolling by invitation; phase 2	SARS-CoV-2 pneumonia	MSC-derived exosomes	Samara, Russia	NCT04602442
6	Effect of UMCSs Derived Exosomes on Dry Eye in Patients With cGVHD	Recruiting; phase 1/2	Dry eye	Umbilical MSC-derived exosomes	Guangzhou, China	NCT04213248
7	MSC-Exos Promote Healing of MHs	Recruiting; early phase 1	Macular holes	MSC-derived exosomes	Tianjin, China	NCT03437759
8	A Tolerance Clinical Study on Aerosol Inhalation of Mesenchymal Stem Cells Exosomes in Healthy Volunteers	Recruiting; phase 1	Safety and tolerance studies	MSC-derived exosomes	Shanghai, China	NCT04313647
9	Allogenic Mesenchymal Stem Cell Derived Exosome in Patients with Acute Ischemic Stroke	Completed; phase 1/2	Cerebrovascular disorders	Mesenchymal-stromal-cell-derived exosomes	Tehran, Iran	NCT03384433
10	Evaluation of Adipose Derived Stem Cells Exosomes in Treatment of Periodontitis	Recruiting; early phase 1	Periodontitis	Adipose-derived stem-cell-derived exosomes	Cairo, Egypt	NCT04270006
<b>Allogenic and autologous EVs</b>						
11	Safety and Efficacy Evaluation of Allogenic Adipose MSC-Exosomes in Patients with Alzheimer's Disease	Recruiting; phase 1/2	Alzheimer's disease	Allogenic adipose MSC-derived exosomes	Shanghai, China	NCT04388982
12	A Clinical Study of Mesenchymal Stem Cell Exosomes Nebulizer for the Treatment of ARDS	Not yet recruiting; phase 1/2	Acute respiratory distress syndrome	Allogenic human MSC-derived exosomes	Ruijin, China	NCT04602104
13	MSC Extracellular Vesicles in Dystrophic Epidermolysis Bullosa	Not yet recruiting; phase 1	Dystrophic epidermolysis bullosa	Allogenic MSC-derived EVs	Aegle Therapeutics	NCT04173650
14	Effect of Plasma Derived Exosomes on Cutaneous Wound Healing	Enrolling by invitation; early phase 1	Ulcer	Autologous exosome-rich plasma	Kumamoto, Japan	NCT02565264
<b>Other cells or EV sources</b>						
15	COVID-19 Specific T Cell Derived Exosomes	Active; phase 1	SARS-CoV-2 pneumonia	T-cell-derived exosomes	Kayseri, Turkey	NCT04389385
16	Extracellular Vesicle Infusion Therapy for Severe COVID-19	Not yet recruiting; phase 2	SARS-CoV-2 pneumonia, acute respiratory distress syndrome	Bone-marrow-derived EVs	Direct Biologics	NCT04493242
17	Edible Plant Exosome Ability to Prevent Oral Mucositis Associated with Chemoradiation Treatment of Head and Neck Cancer	Active; phase 1	Head and neck cancer, oral mucositis	Grape exosomes and fentanyl patch	Louisville, USA	NCT01668849
<b>Drug-loaded EVs</b>						
18	iExosomes in Treating Participants with Metastatic Pancreas Cancer with KrasG12D Mutation	Recruiting; phase 1	Metastatic pancreatic adenocarcinoma, pancreatic ductal adenocarcinoma	Mesenchymal-stromal-cell-derived exosomes loaded with siRNA against KrasG12D	Houston, USA	NCT03608631
19	Study Investigating the Ability of Plant Exosomes to Deliver Curcumin to Normal and Colon Cancer Tissue	Active; phase 1	Colon cancer	Plant exosomes loaded with curcumin	Louisville, USA	NCT01294072
20	Trial of a Vaccination with Tumor Antigen-loaded Dendritic Cell-derived Exosomes	Completed; phase 2	Non-small-cell lung cancer	Dendritic-cell-derived exosomes loaded with antigen	Villejuif, France	NCT01159288

In this context, different routes of administration (e.g., intranasal, intravenous, subcutaneous) may also improve the delivery of EVs and, therefore, facilitate the desired effects [246], [423]. Researchers are exploring various strategies to optimize EV delivery methods for different medical applications, aiming to harness the potential of EVs in regenerative medicine and drug delivery, for the treatment of various diseases, including PD [246]. While several challenges remain to be solved (large-scale isolation and characterization, drug loading and functionalization, evaluation of immunogenicity and biodistribution models, formulation and storage, choice of liposomal comparators, etc.), the diagnostic and therapeutic potential of EVs has grown exponentially, with great expectations for the translational application of EVs [246], [424].

In conclusion, naturally occurring EVs, which require no or limited *in vitro* manipulation, could have an inherent neuroprotective potential. In particular, EVs derived from specific cell types, such as astrocytes (AS-EVs), exhibit a therapeutic effectiveness when compared to the direct administration of the corresponding donor cells, thus providing an alternative to cell transplantation for PD treatment (see **next Section**).

### **1.3.7 Dual role of astrocyte-derived EVs in PD**

The intricate involvement of EVs in intercellular signaling is still an open field of investigation which aims to fully comprehend their contributions in both physiological and pathological contexts. Some studies have shed light on the multifaceted EV roles in physiological processes (such as the immune response modulation), while others have uncovered their participation in several pathological processes, including NDs [425]. However, EVs may play a dual role: either as triggers of disease or as protective players (**Figure 17**).

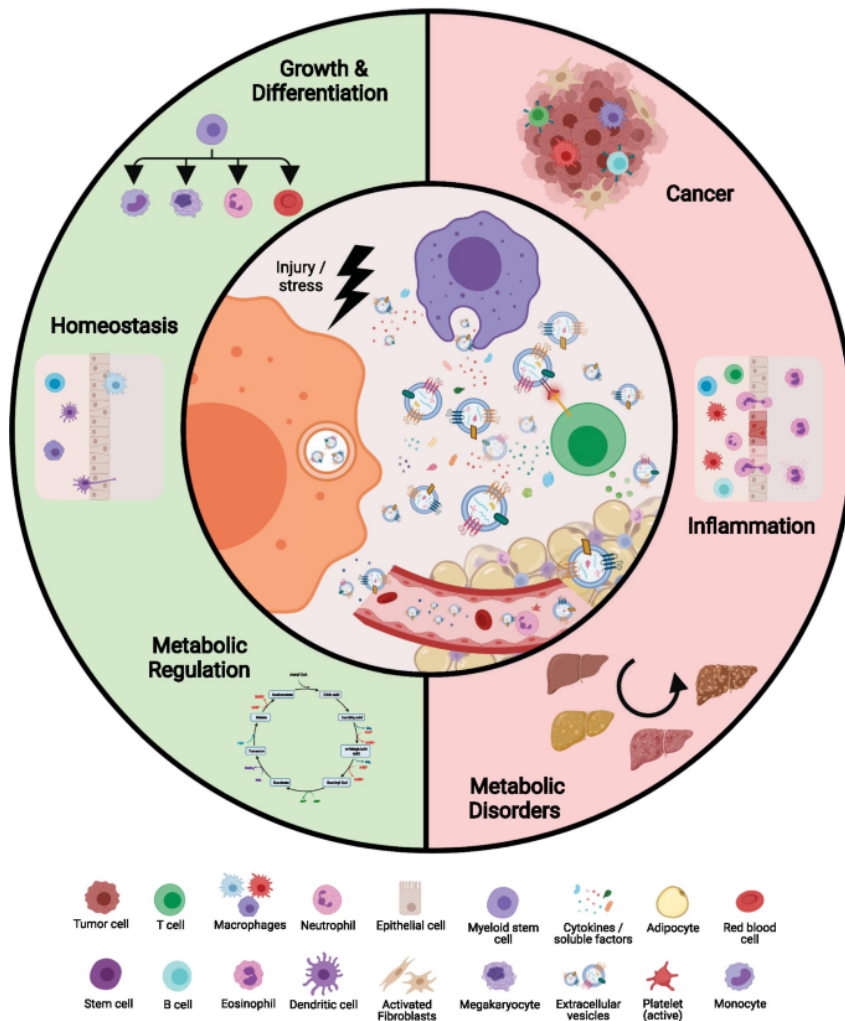


**Figure 17.** Many potential roles of EVs in physio- and pathological contexts. Intercellular communication via EVs plays a pivotal role in maintaining physiological processes and tissue homeostasis. However, injury and stress can disrupt these communication patterns within the tissue microenvironment. If these disruptions persist, interactions facilitated by EVs among stromal, immune, and parenchymal cells can contribute to the onset of various diseases. (Source: <https://doi.org/10.1186/s12964-021-00787-y>).

In the context of NDs, EVs were primarily characterized as carriers for misfolded or dysfunctional mutant proteins, such as  $\beta$ -amyloid oligomers in AD, SOD1 in amyotrophic lateral sclerosis, or  $\alpha$ -Syn in PD [426]. Moreover, also the EV quantity and composition are directly influenced by external environmental risk factors associated with PD [427]. This transfer mediated by EVs was shown to cause neurodegeneration in recipient cells (both neuron-to-neuron and glia-to-neuron EV propagation) [428], [429]. More in detail, on one hand,  $\alpha$ -Syn-EVs can spread between cells, contributing to the spatial and temporal progression of DAergic neuron degeneration. On the other hand,  $\alpha$ -Syn-EVs may target glial cells, particularly microglia [430]. When exposed to  $\alpha$ -Syn-EVs, microglia may adopt pro-inflammatory phenotype, leading to the further dissemination of EVs containing pro-inflammatory cytokines and the toxic, aggregated form of  $\alpha$ -Syn

to the surrounding glial and neuronal environment. This, in turn, sets in motion a self-reinforcing cycle of neuroinflammation-driven degeneration [430]. Moreover, EVs involved in PD pathogenesis carry a range of cargoes beyond toxic  $\alpha$ -Syn aggregates and cytokines. For instance, recent findings indicate that miRNAs can actively move between cells via EV-mediated transport, contributing to the progression of PD in the affected brain [431], [432]. As far as AS-EVs are concerned, a study by Datta-Chaudhuri and colleagues in 2018 revealed that the stimulation of primary cortical rat astrocytes with pro-inflammatory cytokines, like IL-1 $\beta$  or TNF $\alpha$ , led to the release of EVs enriched with two miRNAs, miR-125a-5p and miR-16-5p [336]. Subsequently, the treatment of primary hippocampal and cortical neurons with these AS-EVs resulted in the downregulation of neurotrophin receptor K3 (NTRK3) and its downstream effector Bcl-2 through the transferred miRNAs. This downregulation, in turn, impeded the dendritic growth of developing neurons, reduced dendritic complexity in mature neurons, and lowered neuronal excitability [336]. Also, in a recent study by Rus Jacquet and colleagues, the impact of the LRRK2 G2019S mutation on AS-EVs generated from patient-derived iPSCs was investigated [433]. This mutation led to substantial changes in the production and content of AS-EVs, resulting in abnormal accumulations of proteins associated with PD. Notably, the study found that DAergic neurons can uptake AS-EVs, but these vesicles fail to provide the complete neurotrophic support necessary for the survival and well-being of dopaminergic neurons [433]. This suggests that the disrupted communication between astrocytes and neurons, influenced by altered EV properties, may contribute to the progression of PD [433].

All these findings strongly support the idea that astrocytes are influenced by the specific microenvironment or stimuli to which they are subjected (see **Section 1.2.3**). Consequently, the selective release of glial-derived EVs, particularly AS-EVs, enriched with harmful mRNA/miRNA cargoes, likely plays a critical role in determining the negative fate of neurons [434].

On the other hands, over the past decades, emerging evidences further demonstrated that EVs can fulfill significant neuroprotective roles in various degenerative conditions, including PD [406]. For instance, AS-EVs have been shown to be able of shielding neighboring cells from oxidative stress by transferring vital antioxidant molecules, including Apolipoprotein D (ApoD) or peroxiredoxins, both *in vitro* and *in vivo* [414]. Indeed, the pivotal roles of EVs in modulating the response to oxidative stress, have supported them as important messengers in the context of NDs [414], [435]. Recent

evidences have brought to light a profound way of communication between astrocytes and neurons, predominantly facilitated through the release of EVs [434], [436]. These vesicles exhibit neurotrophic and neuroprotective properties, particularly when released by astrocytes under normal physiological conditions (see **Section 1.2.4**). They contain an array of neurotrophic compounds, including fibroblast growth factor-2 (FGF-2), vascular-endothelial growth factor (VEGF), and heat shock proteins (HSPs), thereby promoting neurogenesis, angiogenesis, synaptic plasticity, and cognitive functions [437]–[439]. Moreover, when released by activated astrocytes, for instance under sustained conditions of oxidative stress or neuronal hyperactivity, EVs promote beneficial effects through the release of molecules, such as synapsin-1 and glutamate transporters, which are crucial in neuroprotection, neurite outgrowth, synapse formation, neurotransmitter regulation and glutamate reuptake [440], [441].

Nowadays, increasing evidences are accumulating about the role of AS-EVs in neuroprotection, when exposed to harmful stimuli. For instance, the study conducted by Taylor and colleagues revealed that astrocytes exposed to hypothermic conditions release EVs enriched in Hsp70, with anti-oxidant and neuroprotective activity [442]. Similarly, it has been demonstrated that “stressed” astrocytes secrete EVs containing glycoproteins like synapsin I, which promote neuronal survival [440]. More recently, Maestro and collaborators found that even non-stimulated astrocytes can release EVs enriched with ApoD. These ApoD-loaded EVs are efficiently internalized by SH-SY5Y cells subjected to paraquat, as PD model [414]. Interestingly, AS-EVs are able to enhance neuronal survival, suggesting the potential of ApoD-loaded EVs as a treatment option for PD [414]. In a similar way, it has been demonstrated that astrocyte derived from the adult rat cerebral cortex release EVs that target cortical neurons in an *ex vivo/in vitro* co-culture [434]. These AS-EVs contained the neuroprotective protein neuroglobin, suggesting a possible astrocyte-dependent mechanism for maintaining cortical neuron survival [434]. Further support to astrocyte-mediated neuroprotection was provided by Shakespear and colleagues [443]. They showed that AS-EVs significantly reduce cell death in SH-SY5Y cells and primary mesencephalic DAergic neurons subjected to MPP<sup>+</sup> toxicity [443]. However, there are some limitations in these studies, due to the use of AS-EVs derived from general brain regions, such as the cortex, or the whole brain. These limitations primarily reside in the region specificity of astrocytes. Indeed, astrocytes from different brain regions may have distinct roles in supporting neurons, and approaches that do not take into account this heterogeneity may lack functional details of the EV neuroprotective

mechanisms (see **Section 1.2.3.2**). For all these reasons, the use of astrocytes from specific brain region involved in PD, such as the VMB (harboring DAergic cell bodies) and the STR (where dopamine is released), may be helpful to understand how astrocytes in the nigrostriatal regions contribute to EV production and consequently to define their specific function in terms of neuroprotection vs. neurodegeneration (see **Section 3.2**) [444].

In conclusion, AS-EVs can have both detrimental and neuroprotective effects, depending on the specific physiological conditions. The main challenge is to understand when, where and how the fate of AS-EVs is established in various pathophysiological contexts. This knowledge may help the development of innovative EV-based therapies, to enhance neuroprotection in PD [411].

## 1.4 PD experimental model

In order to improve our current understanding of PD pathophysiology and develop novel therapies for a better symptom management, PD-relevant experimental disease models are needed. The classical animal PD models, which have been used since the 1960s, are obtained by local or systemic administration of toxins responsible for the destruction of nigrostriatal DAergic neurons. In such *in vivo* models, the more used neurotoxins are MPTP, 6-hydroxydopamine (6-OHDA), rotenone and paraquat [445]. These toxin-based models have proven valuable for identifying and evaluating treatments for the primary motor symptoms of PD. Consequently, they have contributed to the development of dopamine agonists and DBS, serving as important tools to address L-Dopa-induced dyskinesia. However, these models have not succeeded in predicting the clinical success of neuroprotective strategies, as they are not able to fully recapitulate the underlying pathophysiological mechanisms of the disease, highlighting the need of more precise models [446].

Considering the multifaced aspects of this disorder, the identification of rare genetic variants contributed to our comprehension of sporadic PD. Consequently, genetic models assume considerable significance in the validation of hypotheses and in the evaluation of neuroprotective therapies [447]. Transgenic animals that overexpress mutant forms of genes like  $\alpha$ -Syn, Parkin, or LRRK2 – associated with familial PD – can develop symptoms resembling the disease [448]. Moreover, also viral vectors can be used to introduce specific genes or gene mutations into the brains of animals [448]. These



approaches allow researchers to investigate the role of specific genes or proteins in the development of PD pathology [448]. A wide array of animal models has been used to this aim. For instance, easy to handle and adaptable model organisms like *Caenorhabditis Elegans* and *Drosophila Melanogaster*, have been useful in unraveling PD genetic interactions and mechanisms [445]. On the other hand, mammalian models, including mouse (*Mus musculus*), and rat (*Rattus norvegicus*), as well as non-human primates such as monkeys, are essential for replicating alterations at the circuit level [445].

Although animal models are considered the gold standard for disease studies, *in vitro* models are rapider, cheaper and do not require any ethical approval compared to the *in vivo* counterpart [449]. One of the most common *in vitro* systems is represented by primary cell cultures – isolated from animal models – of neurons or glia cells (such as astrocytes) [449]. Also, the use of stem cell lines, such as ESCs, iPSCs, and NSCs, which can be reprogrammed and induced towards an astrocyte or neuronal phenotype, are frequently used [450].

As far as the neurons are concerned, one of the most reliable cellular models is represented by primary cell cultures of DAergic neurons from the SNpc [451], [452]. However, there are several problems linked to the use of these cells. Indeed, whatever method is used to obtain “pure” primary mesencephalic DAergic neurons from embryonic brains, there is a significant rate of variability among independent cell preparations. This is mainly due to the methods used by different authors to culture them [451], [452]. Moreover, TH neurons account only for approximately 1-5% of the total number of neurons, thus making this approach prone to criticisms about the specificity of TH neuron response [453], [454].

An alternative PD model is represented by the human neuroblastoma cell line SH-SY5Y [455]. This cell line is often used in neuroscience research due to its human origin, catecholaminergic properties and ease of handling. It is a subclone of the SK-N-SH cell line, established in 1970 from a bone marrow biopsy of a 4-year-old patient's metastatic neuroblastoma [455]. Undifferentiated SH-SY5Y cells show biochemical properties of catecholaminergic neurons and express immature neuronal markers, such as Nestin [456]. For this reason, they are often used following differentiation towards a DAergic-like neuronal phenotype, more useful as a PD cell model [456]. Conditions like gradual serum deprivation and treatments with differentiation-inducing agents, such as the vitamin A derivative all-trans retinoic acid (RA), brain-derived neurotrophic factor (BDNF), nerve growth factor (NGF), cholesterol, oestradiol, etc., allow cells to become morphologically

similar to mature primary neurons, with elongated neurites. Once differentiated, SH-SY5Y cells express mature neuronal markers such as TH, microtubule-associated protein 2 (MAP2), neuronal nuclei (NeuN) etc. [457]. Then, they are subjected to pharmacological treatments and/or genetic manipulation to mimic PD conditions. As said before, the compounds mostly used in pharmacological approaches are MPP<sup>+</sup>, a derivative of the MPTP (see **Section 1.1.1**), 6-OHDA, rotenone and hydrogen peroxide (H<sub>2</sub>O<sub>2</sub>), responsible for oxidative stress and mitochondrial dysfunction typical of the pathology (see **Section 3**) [458]. In particular, MPP<sup>+</sup> is typically administered to the cells in culture and is actively taken up by DAT on the surface of neurons. This uptake is similar to what happens *in vivo* [27]. Once inside neurons, MPP<sup>+</sup> accumulates within mitochondria (via the transporter called the mitochondrial membrane potential-dependent organic cation transporter), where it inhibits the activity of NADH-ubiquinone oxidoreductase (complex I) within the mitochondrial electron transport system (ETS) [459]. This blockade leads to ATP depletion and the generation of ROS [460]. Furthermore, prolonged exposure to this toxin significantly hampers the synthesis of respiratory subunits encoded by mtDNA [460]. Over time, the cumulative effects of ATP depletion, oxidative stress and mitochondrial dysfunction can trigger apoptotic or necrotic cell death pathways, ultimately leading to the death of DAergic neurons [27].

As mentioned for animal models, in addition to neurotoxin-based strategies, genetic approaches (knock out or overexpression of mutated genes involved in familial cases of PD) have also been adopted to induce a PD-like phenotype [461]. However, even though the genetic models can mimic specific genetic mutations seen in PD, providing insights into the underlying molecular mechanisms of the disease, they may not fully recapitulate the complexity of PD [461]. Indeed, the combination of both neurotoxin exposure and genetic models provides a more comprehensive understanding of PD [461].

As far as the primary astrocyte cultures are concerned, they represent a valuable *in vitro* model to study glia role in PD. In particular, considering that astrocytes display an extreme heterogeneity closely linked to the brain region, the use of astrocytes isolated from the regions mainly involved in PD (i.e., VMB and STR), may be more appropriate to investigate how they are linked to PD pathogenesis. Indeed, astrocytes cultured from affected brain regions in PD patients can provide insights into the microenvironment closely mimicking the pathological conditions [462]. On the other side, they play an important role in investigating therapeutic potential in mitigating PD-related pathology [463]. Additionally, insights into the interaction between astrocytes, genetic mutations,

and BBB integrity offer a more comprehensive understanding of the complex mechanisms underlying PD pathology [462], [464]. Moreover, as discussed in the **Section 1.2.3.2** and **3.2**, the involvement of astrocytes in PD context plays a pivotal role thanks to their cross-talk with neurons [462]. Indeed, under neurodegenerative conditions, they can contribute to neuroinflammation or neuroprotection by the release of pro- or anti-inflammatory molecules (e.g., cytokines, chemokines, neurotrophic and neurogenic factors) (see **Section 1.2.3**). In particular, the release of EVs, which in turn reflect the status of the donor astrocytes, may contribute to this glia-to-neuron communication (see **Section 3.2**) [444].

## 2. Aims of the study and methods

From a clinical and social perspective, NDs – including PD – represent an emergency for our society [41]. In particular, PD is a neurodegenerative process that affects neuronal cell bodies within the VMB, and their axons which project in the STR. This results in the reduction of dopamine, the neurotransmitter involved in the motor control (see **Section 1.1**) [2].

In this context, a critical role is played by the glial compartment, as astrocytes and microglia can respond to the cerebral injury in a dual manner, by inducing detrimental effects, with the release of cytotoxic and proinflammatory factors, or by mediating neuroprotection (see **Section 1.2.4**) [462]. The communication between the glial compartment and neurons is implicated in all the events occurring during PD. Hence, research has striven to define those factors able to push this delicate balance toward the “good side” of glial cells. However, it is still unknown which are the mechanisms underlying the intricate glia-neuron crosstalk.

Therefore, EVs, especially those released by astrocytes (AS-EVs), have been proposed to be involved in the signaling mechanism within the inflamed environment [203], [465]. EVs are a heterogeneous class of vesicles continuously released by cells in both physiological conditions [236]. Notably, EV content can change depending on the donor cell status and in response to different stimuli, providing both detrimental and neuroprotective effects, depending on the context (see **Section 1.3.7**) [263].

In this context, my PhD project aimed at characterizing the contribution of EVs, in particular small-EVs (e.g., exosomes), to the neuroprotective effects mediated by astrocytes and, possibly, to define the molecular details of such a complex intercellular signaling between astrocytes and target DAergic neurons.

For this reason, the first step was to establish a suitable PD model. By using high-resolution respirometry (HRR), we measured the oxygen (O<sub>2</sub>) consumption related to each respiratory state, in differentiated SH-SY5Y cells, which we have chosen as target DAergic-like neurons, exposed to the MPP<sup>+</sup> neurotoxin, to obtain an *in vitro* PD model (see **Section 1.4** and **3.1**). Once discovered the molecular details of the mitochondrial toxicity mediated by MPP<sup>+</sup>, we focused on:

(i) The characterization of the EV donor cells (i.e., primary murine cultures of astrocytes from the VMB and STR, the main regions involved in PD) in terms of purity,

morphology, proliferation and viability. This analysis was performed both in basal and following astrocyte activation induced by the treatment with the chemokine CCL3. This chemokine was chosen both as it has been found overexpressed under PD conditions, and as it stimulates astrocytes to exert a robust neuroprotection both in cellular and pre-clinical PD models [231] (see **Section 1.2.4** and **3.2**).

(ii) The study of VMB- and STR-AS-EVs, in terms of morphology, size and concentration, in both basal and CCL3-activated conditions. In particular, we were interested in understanding whether the brain region of origin and/or the CCL3 treatment could impact on the EV secretion, in terms of quality and quantity (see **Section 3.2**).

(iii) The investigation of the functional interactions between AS-EVs and target neurons (differentiated SH-SY5Y), under neurodegenerative conditions. In particular, we tested the AS-EV neuroprotective potential against oxidative stress, induced by H<sub>2</sub>O<sub>2</sub>, and mitochondrial toxicity induced by MPP<sup>+</sup> (see **Section 3.2**).

(iv) The investigation of AS-EVs uptake mechanisms by differentiated SH-SY5Y cells and the integration of these data into an analytical model. For this purpose, we conducted an internalization study at several time-points, with different concentrations of vesicles. Then we performed a comparative analysis between biological experiments and mathematical model solutions to ascertain the characteristic values of unknown parameters. Finally, we provided examples of how this model can be applied to predict experimental outcomes and guide the design of new experiments (see **Section 3.3**).

All these strategies, coupled with the results from proteomics and RNA-seq analyses (ongoing in our lab), will allow the identification of the EV-associated biomolecules potentially involved in the complex astrocyte-neuron cross-talk in the context of PD. In conclusion, the possibility of characterizing EVs and understanding their neuroprotective potential, may pave the way for the development of innovative nanotherapeutic approaches to tackle PD.

## 3. Results

### 3.1 MPP<sup>+</sup> neurotoxin induces mitochondrial toxicity on RA-differentiated SH-SY5Y cell line

*Sources:*

Risiglione, P., Leggio, L., Cubisino, S.A.M., Reina, S., **Paternò, G.**, Marchetti, B., Magrì, A., Iraci, N., Messina, A. *High-Resolution Respirometry Reveals MPP<sup>+</sup> Mitochondrial Toxicity Mechanism in a Cellular Model of Parkinson's Disease. Int. J. Mol. Sci.* 2020, 21, 7809. <https://doi.org/10.3390/ijms21217809>

Along with protein aggregation, neuroinflammation and oxidative stress, mitochondrial dysfunction is a significant hallmark of PD. The MPP<sup>+</sup> neurotoxin, a lipophilic cation, is widely used to mimic the PD phenotype in many *in vitro* models, including the RA-differentiated SH-SY5Y cell line (see **Section 1.1.3**). In particular, this neurotoxin is able to reach the mitochondria inside the cells, and inhibits the electron flow from complex I to coenzyme Q, contributing to ATP depletion and ROS increase. Understanding the precise alterations in mitochondrial respiration caused by the MPP<sup>+</sup> treatment is therefore critical.

To investigate the mitochondrial parameters affected by MPP<sup>+</sup>, we used the HRR technology. First, we confirmed the suitability of our differentiation protocol, based on RA supplementation and gradual serum deprivation over 8 days, to obtain DAergic-like neurons. Compared to undifferentiated cells, RA-differentiated SH-SY5Y cells exhibited morphological alterations, with slender and branching neurites. Additionally, immunofluorescence analysis of RA-differentiated SH-SY5Y revealed a reduced expression of the Nestin marker, associated with undifferentiated proliferating cells, and an increased expression of TH, a key enzyme in dopamine synthesis. Once established the DAergic model with the differentiation protocol, we evaluated the MPP<sup>+</sup> toxicity on differentiated SH-SY5Y cells by cell viability assay, upon 24 h exposure. We found that the cell viability decreased in a dose-dependent manner, so we were able to select the MPP<sup>+</sup> concentration for the subsequent experiments. In particular, we have chosen the lowest MPP<sup>+</sup> concentration (i.e., 1 mM), that induced only ~10% cell death, compared to untreated cells. In this condition, we assumed that any mitochondrial impairment was more likely due to the neurotoxin itself, instead of significant cell death (see **Figure 1** of the paper).

Then, we analyzed O<sub>2</sub> consumption profile of RA-differentiated SH-SY5Y cells by HRR, using specific Substrate-Uncoupler-Inhibitor Titration (SUIT) protocol. This protocol enables the exploration of various respiratory states, utilizing both naturally occurring and externally introduced substrates, that reach the mitochondria after permeabilization of the cell membranes. To briefly summarize, the ROUTINE state represents the normal physiological O<sub>2</sub> consumption in intact cells. After membrane permeabilization, all the endogenous substrates (including ADP) leave the cells, resulting in O<sub>2</sub> consumption related to the non-phosphorylating or LEAK state. The OXPHOS state, denoting O<sub>2</sub> flow sustained by the mitochondrial respiratory chain, is obtained with the addition of exogenous substrates, mainly pyruvate, malate, glutamate, succinate and saturating concentrations of ADP. Subsequently, the maximal respiratory capacity (ETS) is determined using the optimal uncoupler concentration. Finally, specific inhibition of complex I and III with rotenone and antimycin, respectively, facilitate the determination of the residual respiration, referred to as ROX. Interestingly, we observed that MPP<sup>+</sup> drastically reduced O<sub>2</sub> consumption (up to 70%) associated with the ROUTINE, OXPHOS and ETS states. These findings suggested that MPP<sup>+</sup> has a profound impact on the mitochondrial functionality, and this is correlated to different variables, including electron transport system activity, mitochondrial mass and biogenesis, all of which are affected by MPP<sup>+</sup> exposure (see **Figure 2** of the paper).

In the same way, the flux control ratio was calculated. This depicts the various respiratory states independently of mitochondrial content, by normalizing each flux to the maximum flux. Surprisingly, MPP<sup>+</sup> treatment specifically affected the LEAK state, resulting in a significant increase of 63%, without differences in the ROUTINE and OXPHOS states among the samples. This suggested the presence of injury at the inner mitochondrial membrane level, affecting proton gradient maintenance and, consequently, ATP production (see **Figure 3** of the paper).

Another crucial parameter for assessing the impact of MPP<sup>+</sup> on mitochondrial respiration is the coupling efficiency. It is referred as the ratio of O<sub>2</sub> flux that is linked to ADP phosphorylation within a particular respiratory state. In particular, we found that, while in the untreated cells ~63% of O<sub>2</sub> consumption was linked with the phosphorylation process, in MPP<sup>+</sup> treated cells only 28% of the flux was coupled. In the same way, the coupling efficiency of both OXPHOS and ETS states, was notably reduced following exposure to the neurotoxin, albeit to a lesser extent (a decrease of ~15%) (see **Figure 4** of the paper).

In general, the decrease in coupling efficiency across all respiratory states underscored the significant influence of MPP<sup>+</sup> on the previously mentioned phosphorylation flows. Finally, HRR was employed to assess the contribution of the complex I to OXPHOS respiration. As with the other respiratory states, the O<sub>2</sub> level sustained by complex I in OXPHOS was substantially reduced upon the addition of MPP<sup>+</sup> (a decrease of ~60%). Consequently, also the coupling efficiency supported by complex I exhibited a significant decrease, shifting from 69% in control to 53% in MPP<sup>+</sup>-treated cells. After that, complex I was inhibited by rotenone, allowing us to determinate the contribution of the complex II to ETS. Interestingly, we observed a significant increase of flux control ratio (+81%) in MPP<sup>+</sup>-treated cells compared to the control. This suggested the existence of compensatory mechanisms initiated by succinate dehydrogenase in response to complex I inhibition (see **Figure 5** of the paper).

To go deeper into this aspect, we used an alternative HRR protocol specifically designed to gauge electron flow into the Q-junction, independently of complex I. Then, we assessed the O<sub>2</sub> flows linked to complex II for both control and MPP<sup>+</sup>-treated cells, and we did not find any differences between the samples (see **Figure 6** of the paper). These findings suggested that the previously observed enhancement of complex II activity in MPP<sup>+</sup>-treated cells likely arose from the inhibition of complex I activity rather than from the toxin itself. For a more in-depth understanding of the results presented in the figures, including sample size (N) and the statistical tests, referring to the publication is recommended. In conclusion, in this work we brought to light the bioenergetics defects occurring in mitochondria of MPP<sup>+</sup> treated DAergic neurons, taking advantage from the use of RA-differentiated SH-SY5Y cells and HRR analysis. We saw that the mechanism of MPP<sup>+</sup> toxicity involves the impairment of complex I activity by increasing ROS production. As a result, a compensatory response by complex II is observed through a significant increase of its activity. Collectively, these findings illustrate the presence of a protective mechanism initiated by complex II in response to various triggers, such as toxins and protein aggregates, which impact the complex I activity. Moreover, we observed that these effects can only be attributed to the direct impairment of complex I, rather than the MPP<sup>+</sup> itself. In summary, this study offers a comprehensive view of the bioenergetic defects in the presence of MPP<sup>+</sup>. All these findings hold significant relevance for our research, as they establish a comprehensive PD model, in which we can assess the neuroprotective potential of EVs released by nigrostriatal astrocytes (see **next Section**).



## 3.2 EVs released by nigrostriatal astrocytes preserve cell death and mitochondrial function in a cellular model of PD

Sources:

Leggio, L., L'Episcopo, F., Magrì, A., Ulloa-Navas, M. J., **Paternò, G.**, Vivarelli, S., Bastos, C. A. P., Tirolo, C., Testa, N., Caniglia, S., Risiglione, P., Pappalardo, F., Serra, A., García-Tárraga, P., Faria, N., Powell, J. J., Peruzzotti-Jametti, L., Pluchino, S., García-Verdugo, J. M., Messina, A., Marchetti, B., Iraci, N. *Small Extracellular Vesicles Secreted by Nigrostriatal Astrocytes Rescue Cell Death and Preserve Mitochondrial Function in Parkinson's Disease.* *Adv. Healthcare Mater.* 2022, 11, 2201203. <https://doi.org/10.1002/adhm.202201203>

The previous findings were of significant relevance to our research, as they unveiled the molecular details of the mitochondrial toxicity mediated by MPP<sup>+</sup>, thus allowing us to establish the experimental conditions to model and study PD. Starting from this point, we were able to assess the potential neuroprotective effects of astrocytes-derived EVs (AS-EVs). Recent advances in neuroscience research have shed light on the pivotal role of EVs in facilitating intercellular communication within the brain, under both physiological conditions and during disease states. In the context of PD – characterized by selective DAergic neuron degeneration within the VMB, and their terminals in the STR – astrocytes exert dual harmful/protective functions, with mechanisms not fully elucidated, yet. In fact, the intricate glia-neuron crosstalk mechanisms remain elusive, and it is plausible that EVs released by astrocytes play a role in this context. Therefore, the understanding of their involvement in communication between injured DAergic neurons and nigrostriatal astrocytes could unravel fundamental aspects of PD pathology.

First of all, to uncover potential differences in AS-EVs derived from the two brain regions mainly affected in PD, we established murine astrocyte primary culture from the VMB and STR. In addition, as a control group external to the nigrostriatal system, we used astrocytes from whole brains depleted of these regions, denoted as  $\Delta$ VS-AS. Astrocyte characterization was performed in both basal and CCL3 treated conditions, in order to evaluate also the effect of this chemokine on the AS-EV secretion and function (see **Section 1.2.5**). The results showed highly pure astrocyte primary cultures ( $\geq 98\%$  GFAP positive cells), without any differences in the proliferation rates following CCL3 treatment. Furthermore, to evaluate the overall health of astrocytes at the time of EV isolation, we measured both the cell viability and the cell death, and no significant differences were found among experimental groups (see **Figure S1** of the paper). This

demonstrated that the production of AS-EVs from different brain regions would not be affected by any of the previous mentioned factors.

Subsequently, we isolated EVs from astrocytes supernatants by differential ultracentrifugation and characterized them in terms of dimensions, concentration, and the presence of specific markers, via different techniques. More in detail, by nanoparticle tracking analysis (NTA) and transmission electron microscopy (TEM), we observed that astrocytes secreted small-EVs (~100 nm) with a rate defined by the brain area of origin. Specifically, in basal conditions astrocytes from the VMB (VMB-AS) released more EVs than STR and  $\Delta$ VS astrocytes (STR-,  $\Delta$ VS-AS). In addition, the treatment with CCL3 stimulated VMB-AS to secrete a greater number of EVs compared to the other two regions, which did not exhibit any significant change in the secretion rate (see **Figure 1** of the paper). To confirm that astrocytes from all regions were able to respond to the CCL3 treatment, we assessed the expression of the primary CCL3 receptors, Ccr1 and Ccr5, by qPCR. Interestingly, our gene expression analysis revealed a specific potential for the nigrostriatal system – namely VMB and STR – to respond to the chemokine. Indeed, VMB and STR-AS displayed comparable levels of Ccr1 and Ccr5 mRNAs, while they were significantly lower in  $\Delta$ VS-AS (see **Figure S2** of the paper). Therefore, given the limited responsiveness of  $\Delta$ VS-AS to our stimulation protocol, we concentrated our further investigations only on the nigrostriatal system, finding that while VMB-AS increased the EV secretion in response to CCL3, STR-AS produced more membrane protrusions (see **Figure S2** of the paper).

Next, we performed both immunogold-labelling transmission electron microscopy (IG-TEM) and western blot (WB) analyses to profile the AS-EVs from the nigrostriatal system. Interestingly, we observed the presence of both CD63 and CD9, as well as Pcdcd6ip (Alix) in all EV samples. On the contrary, cellular markers (see **Section 1.3.3**), such as Golga2, calnexin, SDHA and actin are predominantly retained within the cells. All these findings confirmed the enrichment in small-EVs in our vesicular preparations and their high purity, without any relevant contamination deriving from other cellular components (see **Figure 2** of the paper).

Having comprehensively characterized both primary astrocyte cultures and their EVs, we employed nigrostriatal AS-EVs to explore their specific functional effects when transferred to both RA-differentiated and undifferentiated SH-SY5Y cells. First of all, we verified the EV uptake by target cells. Via immunofluorescence and confocal analyses, we observed that PKH26-labelled AS-EVs were efficiently internalized by RA-

differentiated SH-SY5Y cells after 6 h of incubation, and partially co-localized with TH, a typical DAergic neuron marker. Moreover, in order to quantify this uptake process, we employed the Imaging Flow Cytometry (IFC). Interestingly we observed that the fluorescence intensity increased in a time-dependent manner (2 h, 6 h, 24 h), with the 6 h time-point as the minimum incubation time to get a significant increase (from 1.4- to 1.7-fold) in the fluorescence intensity compared to untreated cells. The same IFC analyses were applied also to the undifferentiated SH-SY5Y, used as a control cell line to evaluate both the EV uptake and neuroprotective effects. The results revealed a similar kinetics for both VMB- and STR-AS-EVs, suggesting that the subsequent functional experiments would not have been affected by a different EV entry rate in the target cells (see **Figure 3** and **S3** of the paper).

However, despite this uniformity, we uncovered profound functional disparities regarding the AS-EV neuroprotective potential. In particular, we tested AS-EVs against oxidative stress induced by H<sub>2</sub>O<sub>2</sub>, (used as a general source of ROS to model PD *in vitro*), and mitochondrial toxicity induced by MPP<sup>+</sup> (as previously characterized in **Section 3.1**). First of all, we conducted preliminary experiments to determine the optimal concentration of H<sub>2</sub>O<sub>2</sub> (35 μM) and MPP<sup>+</sup> (1 mM) able to induce ~40% and ~10% reductions in cell viability, respectively, avoiding therefore to slip into a massive cell death. Moreover, given the internalization data, the target cells were pre-incubated with AS-EVs at a 5:1 ratio (i.e., EVs secreted by 5 donor astrocytes and given to 1 target neuron) 6 h prior to H<sub>2</sub>O<sub>2</sub> or MPP<sup>+</sup> challenge, allowing a substantial preventive vesicle uptake. Immunofluorescence analysis revealed that H<sub>2</sub>O<sub>2</sub> induced an increased production of cleaved caspase-3, while both VMB- and STR-AS-EVs independently counteracted H<sub>2</sub>O<sub>2</sub> induced cell death. Interestingly, EVs originating from astrocytes treated with CCL3 displayed a heightened efficacy in preventing the activation of caspase-3 in RA-differentiated SH-SY5Y cells, using mechanisms that warrant further investigation. Crucially, direct treatment of target neurons with CCL3 *per se* did not replicate the neuroprotective effects of AS-EVs. This novel discovery sheds light on the mechanism of chemokine-mediated neuroprotection previously documented for nigrostriatal astrocytes (see **Section 1.2.5**). Moreover, it underscores the significant role played by the inflammatory microenvironment in amplifying the “beneficial” neuroprotection provided by astrocytes (see **Figure 4** and **S4** of the paper).

On the other hand, taking advantage of MPP<sup>+</sup> neurotoxin to mimic PD *in vitro*, and thanks to the use of HRR (see **Section 3.1**), we investigated the ability of AS-EVs to target

mitochondrial functions. First, we confirmed the effects of MPP<sup>+</sup> on complex I that, as expected, resulted in a significant reduction (up to ~53%) of its activity. Interestingly, when pre-treated with all AS-EVs (i.e., VMB -/+ CCL3 and STR -/+ CCL3) the complex I functions were fully preserved. As a control experiments, we performed the same HRR analyses with both the astrocyte conditioned media (ACM), or the same media depleted of EVs, obtained after ultracentrifugation (supernatant, SNT). In both cases, we did not observe any recover in MPP<sup>+</sup>-injured cells, confirming that only intact and concentrated AS-EVs were able to rescue MPP<sup>+</sup>-induced complex I inhibition (see **Figure 5** and **S5** of the paper). Collectively, these findings demonstrate the capacity of nigrostriatal AS-EVs to efficiently preserve complex I activity.

Moreover, MPP<sup>+</sup> was also responsible for the dramatic reduction of the O<sub>2</sub> fluxes devoted to ATP production, known as net fluxes. In particular, compared to the control group, the MPP<sup>+</sup>-injured cells presented a reduction up to ~75%, in both ROUTINE and OXPHOS states. Remarkably, only the pre-treatment with VMB-AS-EVs, but not STR-AS-EVs, significantly restored the ATP production in MPP<sup>+</sup>-injured SH-SY5Y cells, without any difference between basal and CCL3 conditions. These results were also confirmed by the degree of coupling between oxidative phosphorylation and electron flows (coupling efficiency), which was fully restore specifically by VMB-AS-EV pre-treatment. Again, no significant variations in net fluxes or coupling efficiency were observed when ACM/SNT were used (see **Figure 5** and **S5** of the paper). These findings suggest a regional specificity of VMB-AS-EVs compared to STR-AS-EVs to fully rescue the mitochondrial functions of MPP<sup>+</sup>-injured neurons.

To go deeper with the characterization of the neuroprotective potential of AS-EVs in the context of PD, we performed the previous functional experiments using the undifferentiated SH-SY5Y cells as an alternative cell line. In particular, we tested AS-EVs in the presence of both H<sub>2</sub>O<sub>2</sub> and MPP<sup>+</sup> but we did not observe neither any recover of H<sub>2</sub>O<sub>2</sub>-induced cell death (see **Figure 4** and **S4** of the paper), nor any rescue of mitochondrial functionality (see **Figure 5** and **S5** of the paper). These results supported the hypothesis that nigrostriatal astrocyte-derived EVs are able to be neuroprotective specifically towards DAergic neuron confirming, again, the relevance of the surrounding regional microenvironment for the astrocyte-mediated neuroprotection in the context of PD. For a more in-depth understanding of the results presented in the figures, including sample size (N) and the statistical tests, referring to the publication is recommended.

In conclusion, this study offers a comprehensive analysis of the phenotypic and functional properties of nigrostriatal AS-EVs in the context of PD. In particular we found a novel role for AS-EVs in facilitating intercellular signaling, in a region-specific and context-dependent way, with neuroprotective implications for PD. However, more experiments are needed to further dissect the potential molecular mechanism(s) involved in the EV-mediated neuroprotection (see **next Sections**). In the future, the results stemming from this study could lead to the design of personalized AS-EV therapies to hinder disease progression and facilitate neurological recovery.

### 3.3 An analytical model for quantifying EV uptake mechanism by differentiated SH-SY5Y cell line

Sources:

Iraci, N., Leggio, L., Lombardo, A., Panarello, C., Pappalardo, F., **Paternò, G.** *An Analytical Model for the Inference of the EV Reception Process Parameters in Cell-to-Cell Communication. In Proceedings of ACM Conference (Conference'17), 2023.* <https://doi.org/10.1145/3576781.3608716>

Once demonstrated the capability of nigrostriatal AS-EVs to have protective effects under neurodegenerative conditions, the subsequent phase of our investigation was to further understand the mechanisms involved in this process. As a first line of research, we explored the AS-EV uptake into target neurons. In collaboration with Prof. A. Lombardo group (Dept. of Electrical, Electronic and Computer Engineering), we developed an analytical model to predict the rate of EV uptake, aiming to optimize the design of EV biological experiments, reducing cost and time. Indeed, working with EVs requires to face several technical challenges, especially in the study of EV uptake processes. Despite fluorescent dye labeling allows visualization and measurement of the internalization process, there are several issues related to single EV resolution over time and the recycling of internalized material, hindering precise quantitative measures of the number or concentration of internalized EVs. Moreover, the complexity and time-consuming nature of these experiments, particularly in terms of EV production and instrument expenses, make detailed time analysis impractical. In the literature, several models of EV uptake have been proposed, but they often focus on specific uptake mechanisms. However, as previously described in the **Section 1.3.5**, cells employ a wide array of intricate pathways for EV internalization. Moreover, these processes are also used for the internalization of other molecules and the physiological recycling of membranes, not just EV uptake. This makes challenging the prolonged use of uptake inhibitors for the dissection of the EV entry route within target neurons.

Therefore, we introduced an analytical model of a generic EV uptake process by target cells. First of all, based on laboratory data, we estimated the unknown parameters of the model. More in detail, we took advantage of fluorescent EV labeling, which allowed us to visualize and measure the internalization process in RA-differentiated SH-SY5Y cells, in order to compare the mathematical model solutions with the *in vitro* data. We performed a time-point internalization study (6 h, 24 h, 48 h, and 72 h), with two different

concentrations of vesicles, 1:2 and 5:1 (astrocyte:neuron ratio). Interestingly, we observed that AS-EV uptake is a dynamic process, proportional to the number of vesicles. Moreover, EVs continued to enter even after 24 h of incubation, reaching a plateau after 48 h. Doing so, our model, based on a mathematical inverse process, enabled us to infer specific parameters of the EV uptake. These parameters included the rates associated with chemical reactions involved in the EV binding and internalization, as well as the disassociation and recycling of EVs. Specifically, we monitored the temporal changes in the concentrations of external ( $V_e$ ), bound ( $V_b$ ), and internalized ( $V_i$ ) EVs, while considering constant the binding ( $rb$ ) and the internalization rate ( $ri$ ). Furthermore, recognizing that some EV-cell interactions may disassociate before internalization and accounting for potential recycling processes, we incorporated the bond disassociation rate ( $rd$ ) and recycling rate constant ( $rr$ ) into our model. Then, to quantify EV internalization at the single-cell level, we employed both IFC and a plate reader (PR). More in detail, we detected EV uptake at the single-cell level by IFC, in terms of mean fluorescence intensity. However, to convert this measure into the number of internalized EVs, the fluorescence of a single EV should be known. Since the IFC instrument magnification does not permit the detection of single EV fluorescence, we conducted a parallel set of experiments, involving the use of PR. The EV treatment followed the same strategy as for the IFC analysis, and we were able to measure EV-derived fluorescence. After that, by comparing and integrating data from IFC and PR, while assuming linearity, we determined the fluorescence emitted by a single EV and tracked the number of EVs internalized by target cells over time (see **Figure 1** of the paper). Subsequently we applied the model to predict the outcomes of a follow-up experiment, where the initial quantity of EVs was altered. Of note, the model demonstrated its effectiveness in forecasting results, underscoring its practical utility in the design of novel biological experiments tailored to achieve specific desired objectives (see **Figure 1** of the paper).

In conclusion, we described the experimental setup used to refine and evaluate the model, followed by a detailed characterization of the dynamics regulating EV uptake in wet experiments using the model. Our goal is to offer a versatile tool applicable across various scenarios, including inferring unknown biological parameters, designing experiments, and analyzing repeated EV administrations for therapeutic use over time.

## 4. Conclusions and future perspectives

PD is a complex neurodegenerative condition, affecting 1% of people over the age of 65. As the global population ages, the prevalence of PD is expected to increase, which will place a growing burden on healthcare systems and caregivers [1]. The pathology is characterized by motor symptoms such as tremors, postural instability, bradykinesia, and rigidity, as well as non-motor symptoms like cognitive impairments and sleep disorders [466]. These manifestations are the result of the progressive degeneration of DAergic neurons in the SNpc, in the VMB, and their axons projecting to the STR, leading to a reduction in dopamine levels [43], [44]. Unfortunately, to date, the causes and mechanisms responsible for DAergic neuron degeneration remain unknown, and there are currently no therapies available to stop or reverse the progression of this condition [467]. Hence, more research is needed for developing effective therapeutic strategies, ultimately improving the quality of life for those affected by PD [468]. While the exact causes and mechanisms behind the development of PD are not fully understood, researchers have identified several factors that may contribute to its onset, like genetic and environmental factors, ageing, inflammation and exposure to neurotoxins [468]. However, an important turning point in the development of novel therapeutic approaches for PD, may lie within the glial compartment, through the bidirectional signaling with neurons. Indeed, the communication between the glial compartment and neurons is at the center of all events occurring during PD [189]. In particular, both astrocytes and microglia respond to brain damage by releasing a spectrum of pro-inflammatory and anti-inflammatory molecules, as well as neuroprotective and neurotoxic mediators. The delicate balance of these responses determines whether the outcome leans toward recovery or neuronal degeneration [189]. In this context, research strives to define the factors able to push the beneficial effects of glia cells, while mitigating or even eliminating their potentially harmful aspects. However, the exact mechanisms underlying the complex communication between astrocytes and neurons remain elusive.

EVs are emerging as a new modality of cell-to-cell communication, thus potentially representing the ideal candidates involved in this intricate cross-talk [235], [406], [425]. Indeed, EVs serve as powerful vehicles for the transfer of bioactive molecules (e.g., lipids, nucleic acids, protein etc.) between astrocytes and neurons [238]. Considering the above, the main objective of this doctoral project was to investigate the potential



neuroprotective effects of nigrostriatal AS-EVs (namely VMB- and STR-AS-EVs) in the context of PD.

First of all, we established a model of DAergic neurons useful to study PD pathology and evaluate the potential neuroprotective effects of AS-EVs. More in detail, our study reveals a comprehensive understanding of the mechanistic intricacies underlying mitochondrial toxicity induced by MPP<sup>+</sup>, through the HRR technique. MPP<sup>+</sup> – widely used as *in vitro* and *in vivo* PD models – has the unique ability to accumulate within mitochondria and specifically inhibit the complex I. It is worth to mention that a deficiency of the mitochondrial complex I within the SNpc is well-documented in sporadic PD patients [469], [470]. This deficiency plays a significant role in neuronal loss, underscoring its importance in the pathology. As expected, MPP<sup>+</sup> causes extensive damage to the IMM, leading to an increase in ROS production. In particular we showed that this damage impairs the activity of complex I, redirecting electrons to alternative substrates and decreasing ATP synthesis, particularly during routine and OXPHOS respiration. In response to these challenges, complex II activity increases during ETS respiration, suggesting a compensatory mechanism. These findings highlight a protective response initiated by complex II when complex I is impaired, such as in the presence of toxins or protein aggregates. Furthermore, with the introduction of an alternative SUIIT protocol, we demonstrated that these effects are specifically attributed to the direct impairment of complex I rather than the MPP<sup>+</sup> compound itself. Overall, this knowledge has significant implications for the establishment of standardized methodologies in studies utilizing this neurotoxin as a PD model [26]. In particular, we have been able to develop an *in vitro* PD model to interrogate the potential neuroprotective impact of AS-EVs.

Next, we strived to perform a comprehensive exploration of the phenotypic and functional characteristics of AS-EVs derived from the main brain regions affected in PD. First of all, we showed that astrocytes from the nigrostriatal system secrete small-EVs (~100 nm), released with specific rates. Then, we demonstrated that these EVs have different neuroprotective functions, based on their brain region of origin and the stimuli which the donor cells are subjected to.

About the phenotypic characterization, VMB-AS release a higher number of vesicles compared to STR-AS, and astrocytes from brain regions depleted of VMB and STR ( $\Delta$ VS-AS). Moreover, CCL3 – a well-known chemokine with powerful neuroprotective and neurogenic effects [232], [233] – plays a pivotal role in regulating EV production, specifically for VMB-AS, which respond by releasing more vesicles. This contrasting

intrinsic and extrinsic responsiveness observed in VMB-AS and STR-AS reflects the well-documented heterogeneity of astrocytes within the CNS [471]. Even though, the regulatory mechanisms governing this heterogeneity, whether related to transcriptional or epigenetic programs, remain still as an outstanding open question for the field. Additionally, these results underscore the need for a deeper understanding of the functional implications of such region-specific responses to microenvironmental cues between the VMB (where DAergic neurons reside) and the STR (where they project) for PD pathogenesis and the development of new therapeutic approaches.

Indeed, while numerous studies have identified harmful factors associated with astrocytes, little is known about the mechanisms driving the induction of pro-reparative states and their cellular/molecular effectors. Originally seen as a potential “Trojan horse” for neurodegeneration, AS-EVs have recently emerged as significant carriers of “beneficial messages” to target neurons. However, regional disparities have not been adequately addressed, as AS-EV preparations have predominantly originated from the cerebral cortex, whole brain, or immortalized glioma cells.

Therefore, as far concern as the functional study, here we used nigrostriatal AS-EVs to investigate their specific impact when transferred to RA-differentiated vs. undifferentiated SH-SY5Y cells. In particular, we found that AS-EV uptake by both types of target cells is similar, regardless the regional origin or treatment of the donor astrocytes. However, despite this homogeneity, they show significant differences in their neuroprotective potential. More in detail, RA-differentiated SH-SY5Y cells were exposed to two distinct sources of toxicity, simulating oxidative stress ( $H_2O_2$ ) and mitochondrial dysfunction relevant to PD ( $MPP^+$ , as previously characterized). Interestingly, we revealed that AS-EVs differentially mediate neuroprotection depending on the specific challenge. In particular, all AS-EVs, especially those derived from CCL3 treated astrocytes, are able to counteract cell death induced by  $H_2O_2$ . It is worth noting that directly treating target neurons with CCL3 do not reproduce the same neuroprotective effects of AS-EVs. Also, we uncovered that preventive treatment with both VMB- and STR-AS-EVs efficiently restores CI activity in neurons affected by  $MPP^+$ . However, only VMB-AS-EVs fully preserve mitochondrial functionality, particularly the  $O_2$  flows devoted to ATP synthesis.

Several factors may contribute to this distinct effect of VMB-AS-EVs compared to STR-AS-EVs, such as the different vulnerability and function of neurons in these brain regions. Additionally, regional differences in sensitivity to mitochondrial inhibitors, metabolic

impairments, protein aggregation and mitochondrial instability could explain the lack of a full beneficial response with STR-AS-EVs. However, further studies are needed to determine whether the heterogeneity of AS-EVs between VMB and STR results from intrinsic regional differences or is influenced by external factors in the microenvironment. Notably, the positive effects of AS-EVs are not observed when we used ACM (even though ACM itself contains EVs, at a lower concentration) or ACM depleted of EVs (SNT). Although we cannot exclude the possibility that other molecules might be co-purified with EVs, these findings indicate that the AS-EV functions are likely attributable to the vesicles themselves (when used highly concentrated), and also show that the ultracentrifugation process does not damage the vesicles, releasing in the supernatant eventual protective molecules.

Furthermore, when the same vesicles are applied on injured undifferentiated SH-SY5Y cells, AS-EVs are not able to exert the same neuroprotective effects. This specificity in AS-EV responsiveness points to a higher protective activity toward the dopamine neuronal phenotype, emphasizing the importance of astrocytes regional characteristics in modulating vulnerability specifically in DAergic neurons [444]. Therefore, these findings support the pivotal role of EVs in the communication between astrocytes and neurons in a region-specific and context-dependent manner.

Nevertheless, further efforts are necessary to understand the potential molecular mechanism(s) involved in the EV-mediated neuroprotection. Hence, the subsequent phase of our investigation aimed to dissect how AS-EVs interact and are uptake by target neurons. Investigating this uptake process often involves inhibiting specific pathways to discern their relative contributions to EV signaling. However, pharmacological inhibitors lack specificity and may disrupt multiple pathways, which often overlap with those used for other cellular processes like membrane recycling. This complexity poses challenges for validating specific mechanisms experimentally, necessitating a focus on common features shared by all uptake mechanisms. To date, the direct visualization of EV uptake over time, and the estimation of the parameters involved in such process remains a formidable challenge. In particular, the whole cellular membrane dynamics make difficult to have a precise quantitative measurement of the number of internalized EVs over time, and their relationship to the observed effects. Moreover, time-dependent analyses in this context require multiple replicates, increasing the resources needed for experiments with EVs. Therefore, in collaboration with Prof. A. Lombardo group (Dept. of Electrical, Electronic and Computer Engineering, University of Catania), we developed a

mathematical model to: i) aid the inference of elusive biological parameters that are yet to be fully understood; ii) provide a useful tool for designing tailored experiments with EVs, reducing cost and time. We showed that labeled AS-EV uptake by RA-differentiated SH-SY5Y cells is a dynamic process, which reaches a plateau after 48 h, and with a direct correlation to the number of vesicles. Moreover, through a comparative analysis between wet experiments and mathematical model solutions, we revealed previously unknown parameters related to the chemical reactions of EV binding, internalization, disassociation and recycling. This prompts us to quantify the fluorescence emitted by a single EV and quantify the number of EVs internalized by the target cells over time. Subsequently, we used the model to predict the outcomes of a follow-up experiment, with a different concentration of EVs. Of note, the model effectively predicts the outcomes, showcasing its practical value in designing experiments for specific objectives [472]. Interestingly, the presented model and methodology are adaptable to various vesicle-cell interactions, provided new data is available for the specific EV-cell pair. In the end, the model can support the development of therapeutic strategies by guiding the design of EV administration patterns based on known relationships between EV uptake phases and functional effects on target cells. This mechanistic understanding of EV signaling holds promise for advancing innovative and personalized treatments. By employing this analytical model, researchers can optimize their experimental designs and make informed decisions, leading to resource savings while advancing the boundaries of scientific exploration. These findings show once more how the interdisciplinarity may bridge the gap between fundamental scientific discoveries and translational potential.

Finally, to further investigate about the potential molecular mechanism(s) involved in the EV neuroprotection, also the identification of specific molecular cargoes will be useful. As said before, EVs contain a wide array of molecules (DNA, RNAs, proteins, lipids, metabolites) whose abundance depends on donor cell identity and stimuli. The presence of specific ncRNAs and proteins within AS-EVs adds another layer of complexity to the intricate communication between astrocytes and neurons [235]. Indeed, the previous findings suggest the presence of astrocytic molecular mechanisms that orchestrate the selective sorting of specific proteins/ncRNAs for secretion via EVs, which will be further elucidated [235]. Also, the transferred cargoes may possess distinct functions upon reaching target cells, opening the way for the possible use of AS-EVs in brain repair and regeneration. Consequently, our current focus lies in a comprehensive multi-omics profiling of AS-EVs to identify the key molecular player(s) responsible for

neuroprotection in terms of proteins (via LC/MS) and small ncRNAs (via RNA-seq). Understanding the specific molecular cargoes within AS-EVs from different brain regions, can shed light on their distinct regulatory effects on mitochondrial pathways in target neurons. Moreover, the identification of the molecules responsible for this neuroprotective effect will eventually allow to the production of modified EVs with a great translational potential. However, discerning the relative contributions of these potential candidates remains a challenging task for the field, and the road ahead is still long. Indeed, as once the potential molecular candidate has been identified, the additional steps will be: i) applying EVs to primary relevant target cells, such as VMB neurons and NSCs, and evaluating their effects; ii) assessing the effect of EV treatment in an *in vivo* model of PD. This is of paramount importance because, firstly, the use of neuroblastoma cell lines as a model system does not fully replicate the complexity of interactions between astrocytes and neurons in the brain. Moreover, while *in vitro* methodologies provide valuable insights into cellular mechanisms, they may not entirely capture the dynamic and multifaceted nature of NDs like PD. Future studies could explore complementary approaches such as *in vivo* imaging or post-mortem analyses to corroborate *in vitro* findings and provide a more comprehensive understanding of EV-mediated neuroprotection. Finally, it's crucial to outline potential strategies for further elucidating the mechanisms underlying EV-mediated neuroprotection. This could involve integrating multidisciplinary approaches, such as molecular biology, bioinformatics, and systems biology, to unravel complex signaling networks and identify key molecular effectors.

The concept that EVs could play a role in astrocyte-neuron communication, with region-specific and context-dependent variations, represents a fascinating vision. Indeed, this could provide insights into the underlying mechanisms of the disease, offer new avenues for treating the pathology. Indeed, in the long term, knowledge stemming from this study may lead to the design of novel therapies based on the use of EVs as innovative nano-drugs for the treatment of PD. However, further research is needed to determine the extent to which AS-EVs contribute to the neuroprotective effects observed in experimental models of PD.

## 5. References

- [1] D. K. Simon, C. M. Tanner, and P. Brundin, “Parkinson Disease Epidemiology, Pathology, Genetics, and Pathophysiology,” *Clin Geriatr Med*, vol. 36, no. 1, pp. 1–12, 2020, doi: 10.1016/j.cger.2019.08.002.
- [2] W. Poewe *et al.*, “Parkinson disease,” *Nat Rev Dis Primers*, vol. 3, no. 1, p. 17013, Mar. 2017, doi: 10.1038/nrdp.2017.13.
- [3] L. Philipe de Souza Ferreira *et al.*, “Sex differences in Parkinson’s Disease: An emerging health question,” *Clinics*, vol. 77, p. 100121, Jan. 2022, doi: 10.1016/j.clinsp.2022.100121.
- [4] R. de la Fuente-Fernández *et al.*, “Age-specific progression of nigrostriatal dysfunction in Parkinson’s disease,” *Ann Neurol*, vol. 69, no. 5, pp. 803–810, May 2011, doi: 10.1002/ana.22284.
- [5] H. Deng, P. Wang, and J. Jankovic, “The genetics of Parkinson disease,” *Ageing Res Rev*, vol. 42, pp. 72–85, Mar. 2018, doi: 10.1016/j.arr.2017.12.007.
- [6] L. Streubel-Gallasch *et al.*, “Parkinson’s Disease–Associated LRRK2 Interferes with Astrocyte-Mediated Alpha-Synuclein Clearance,” *Mol Neurobiol*, vol. 58, no. 7, pp. 3119–3140, Jul. 2021, doi: 10.1007/s12035-021-02327-8.
- [7] N. Dzamko, C. L. Geczy, and G. M. Halliday, “Inflammation is genetically implicated in Parkinson’s disease,” *Neuroscience*, vol. 302, pp. 89–102, Aug. 2015, doi: 10.1016/j.neuroscience.2014.10.028.
- [8] L.-Y. Zhao *et al.*, “Role of the gut microbiota in anticancer therapy: from molecular mechanisms to clinical applications,” *Signal Transduct Target Ther*, vol. 8, no. 1, p. 201, May 2023, doi: 10.1038/s41392-023-01406-7.
- [9] H. Zhang *et al.*, “Implications of Gut Microbiota in Neurodegenerative Diseases,” *Front Immunol*, vol. 13, Feb. 2022, doi: 10.3389/fimmu.2022.785644.
- [10] S. Hirschberg, B. Gisevius, A. Duscha, and A. Haghikia, “Implications of Diet and The Gut Microbiome in Neuroinflammatory and Neurodegenerative Diseases,” *Int J Mol Sci*, vol. 20, no. 12, p. 3109, Jun. 2019, doi: 10.3390/ijms20123109.
- [11] J. Parkinson, “An Essay on the Shaking Palsy,” *J Neuropsychiatry Clin Neurosci*, vol. 14, no. 2, pp. 223–236, May 2002, doi: 10.1176/jnp.14.2.223.
- [12] P. A. Kempster, B. Hurwitz, and A. J. Lees, “A new look at James Parkinson’s Essay on the Shaking Palsy,” *Neurology*, vol. 69, no. 5, pp. 482–485, Jul. 2007, doi: 10.1212/01.wnl.0000266639.50620.d1.
- [13] S. Hostiuc, E. Drima, and O. Buda, “Shake the Disease. Georges Marinesco, Paul Blocq and the Pathogenesis of Parkinsonism, 1893,” *Front Neuroanat*, vol. 10, Jun. 2016, doi: 10.3389/fnana.2016.00074.
- [14] J. H. LYOYD, “LEÇONS SUR LES MALADIES NERVEUSES,” *J Nerv Ment Dis*, vol. 26, no. 12, pp. 772–773, 1899.
- [15] R. Moriyasu, “Zur pathologischen Anatomie der Paralysis agitans,” *Arch Psychiatr Nervenkr*, vol. 44, no. 2, pp. 789–814, Jul. 1908, doi: 10.1007/BF01821569.

- [16] A. J. Lees, M. Selikhova, L. A. Andrade, and C. Duyckaerts, "The black stuff and Konstantin Nikolaevich Tretiakoff," *Movement Disorders*, vol. 23, no. 6, pp. 777–783, Apr. 2008, doi: 10.1002/mds.21855.
- [17] C. G. Goetz, "The History of Parkinson's Disease: Early Clinical Descriptions and Neurological Therapies," *Cold Spring Harb Perspect Med*, vol. 1, no. 1, pp. a008862–a008862, Sep. 2011, doi: 10.1101/cshperspect.a008862.
- [18] A. CARLSSON, M. LINDQVIST, T. MAGNUSSON, and B. WALDECK, "On the Presence of 3-Hydroxytyramine in Brain," *Science (1979)*, vol. 127, no. 3296, pp. 471–471, Feb. 1958, doi: 10.1126/science.127.3296.471.
- [19] H. Ehringer and O. Hornykiewicz, "Verteilung Von Noradrenalin Und Dopamin (3-Hydroxytyramin) Im Gehirn Des Menschen Und Ihr Verhalten Bei Erkrankungen Des Extrapyramidalen Systems," *Klin Wochenschr*, vol. 38, no. 24, pp. 1236–1239, Dec. 1960, doi: 10.1007/BF01485901.
- [20] W. BIRKMAYER and O. HORNYKIEWICZ, "[The L-3,4-dioxyphenylalanine (DOPA)-effect in Parkinson-akinesia].," *Wien Klin Wochenschr*, vol. 73, pp. 787–8, Nov. 1961.
- [21] G. C. Cotzias, M. H. Van Woert, and L. M. Schiffer, "Aromatic Amino Acids and Modification of Parkinsonism," *New England Journal of Medicine*, vol. 276, no. 7, pp. 374–379, Feb. 1967, doi: 10.1056/NEJM196702162760703.
- [22] M. M. Hoehn and M. D. Yahr, "Parkinsonism: onset, progression, and mortality," *Neurology*, vol. 17, no. 5, pp. 427–427, May 1967, doi: 10.1212/WNL.17.5.427.
- [23] Y. Smith, T. Wichmann, S. A. Factor, and M. R. DeLong, "Parkinson's Disease Therapeutics: New Developments and Challenges Since the Introduction of Levodopa," *Neuropsychopharmacology*, vol. 37, no. 1, pp. 213–246, Jan. 2012, doi: 10.1038/npp.2011.212.
- [24] J. Langston, P. Ballard, J. Tetrud, and I. Irwin, "Chronic Parkinsonism in humans due to a product of meperidine-analog synthesis," *Science (1979)*, 1983, doi: 10.1126/science.6823561.
- [25] J. W. Langston, I. Irwin, E. B. Langston, and L. S. Forno, "1-Methyl-4-phenylpyridinium ion (MPP<sup>+</sup>): Identification of a metabolite of MPTP, a toxin selective to the substantia nigra," *Neurosci Lett*, vol. 48, no. 1, pp. 87–92, Jul. 1984, doi: 10.1016/0304-3940(84)90293-3.
- [26] P. Risiglione *et al.*, "High-Resolution Respirometry Reveals MPP<sup>+</sup> Mitochondrial Toxicity Mechanism in a Cellular Model of Parkinson's Disease," *Int J Mol Sci*, vol. 21, no. 21, p. 7809, Oct. 2020, doi: 10.3390/ijms21217809.
- [27] J. W. Langston, "The MPTP story," *Journal of Parkinson's Disease*. 2017. doi: 10.3233/JPD-179006.
- [28] J. Frey *et al.*, "Past, Present, and Future of Deep Brain Stimulation: Hardware, Software, Imaging, Physiology and Novel Approaches," *Front Neurol*, vol. 13, Mar. 2022, doi: 10.3389/fneur.2022.825178.
- [29] C. Pont-Sunyer *et al.*, "The prodromal phase of leucine-rich repeat kinase 2-associated Parkinson disease: Clinical and imaging Studies," *Movement Disorders*, vol. 32, no. 5, pp. 726–738, May 2017, doi: 10.1002/mds.26964.

- [30] M. G. Spillantini, R. A. Crowther, R. Jakes, M. Hasegawa, and M. Goedert, “ $\alpha$ -Synuclein in filamentous inclusions of Lewy bodies from Parkinson’s disease and dementia with Lewy bodies,” *Proceedings of the National Academy of Sciences*, vol. 95, no. 11, pp. 6469–6473, May 1998, doi: 10.1073/pnas.95.11.6469.
- [31] H. Braak, K. Del Tredici, U. Rüb, R. A. I. de Vos, E. N. H. Jansen Steur, and E. Braak, “Staging of brain pathology related to sporadic Parkinson’s disease,” *Neurobiol Aging*, vol. 24, no. 2, pp. 197–211, Mar. 2003, doi: 10.1016/S0197-4580(02)00065-9.
- [32] I. Trigo-Damas, N. L.-G. del Rey, and J. Blesa, “Novel models for Parkinson’s disease and their impact on future drug discovery,” *Expert Opin Drug Discov*, vol. 13, no. 3, pp. 229–239, Mar. 2018, doi: 10.1080/17460441.2018.1428556.
- [33] J. Blesa, S. Phani, V. Jackson-Lewis, and S. Przedborski, “Classic and New Animal Models of Parkinson’s Disease,” *J Biomed Biotechnol*, vol. 2012, pp. 1–10, 2012, doi: 10.1155/2012/845618.
- [34] E. Dolgin, “First therapy targeting Parkinson’s proteins enters clinical trials,” *Nat Med*, vol. 18, no. 7, pp. 992–993, Jul. 2012, doi: 10.1038/nm0712-992b.
- [35] AFFiRiS, “AFFiRiS Announces Top Line Results of First-in-Human Clinical Study Using AFFITOPE® PD03A, Confirming Immunogenicity and Safety Profile in Parkinson’s Disease Patients,” 2017.
- [36] T. R. Sampson *et al.*, “Gut Microbiota Regulate Motor Deficits and Neuroinflammation in a Model of Parkinson’s Disease,” *Cell*, vol. 167, no. 6, pp. 1469–1480.e12, 2016, doi: 10.1016/j.cell.2016.11.018.
- [37] J. Blesa, I. Trigo-Damas, M. Dileone, N. L.-G. del Rey, L. F. Hernandez, and J. A. Obeso, “Compensatory mechanisms in Parkinson’s disease: Circuits adaptations and role in disease modification,” *Exp Neurol*, vol. 298, pp. 148–161, Dec. 2017, doi: 10.1016/j.expneurol.2017.10.002.
- [38] R. Martínez-Fernández *et al.*, “Focused ultrasound subthalamotomy in patients with asymmetric Parkinson’s disease: a pilot study,” *Lancet Neurol*, vol. 17, no. 1, pp. 54–63, Jan. 2018, doi: 10.1016/S1474-4422(17)30403-9.
- [39] T. F. Outeiro *et al.*, “Defining the Riddle in Order to Solve It: There Is More Than One ‘Parkinson’s Disease,’” *Movement Disorders*, vol. 38, no. 7, pp. 1127–1142, Jul. 2023, doi: 10.1002/mds.29419.
- [40] S. H. Shahmoradian *et al.*, “Lewy pathology in Parkinson’s disease consists of crowded organelles and lipid membranes,” *Nat Neurosci*, 2019, doi: 10.1038/s41593-019-0423-2.
- [41] D. M. Wilson, M. R. Cookson, L. Van Den Bosch, H. Zetterberg, D. M. Holtzman, and I. Dewachter, “Hallmarks of neurodegenerative diseases,” *Cell*, vol. 186, no. 4, pp. 693–714, Feb. 2023, doi: 10.1016/j.cell.2022.12.032.
- [42] W. Dauer and S. Przedborski, “Parkinson’s Disease,” *Neuron*, vol. 39, no. 6, pp. 889–909, Sep. 2003, doi: 10.1016/S0896-6273(03)00568-3.
- [43] O. Garritsen, E. Y. van Battum, L. M. Grossouw, and R. J. Pasterkamp, “Development, wiring and function of dopamine neuron subtypes,” *Nat Rev Neurosci*, vol. 24, no. 3, pp. 134–152, Mar. 2023, doi: 10.1038/s41583-022-00669-3.
- [44] D. Aarsland, M. K. Beyer, and M. W. Kurz, “Dementia in Parkinson’s disease,” *Curr Opin Neurol*, vol. 21, no. 6, pp. 676–682, Dec. 2008, doi: 10.1097/WCO.0b013e3283168df0.



- [45] B. R. Bloem, M. S. Okun, and C. Klein, "Parkinson's disease," *The Lancet*, vol. 397, no. 10291, pp. 2284–2303, Jun. 2021, doi: 10.1016/S0140-6736(21)00218-X.
- [46] J. O. Aasly, "Long-Term Outcomes of Genetic Parkinson's Disease," *J Mov Disord*, vol. 13, no. 2, pp. 81–96, May 2020, doi: 10.14802/jmd.19080.
- [47] J. Tran, H. Anastacio, and C. Bardy, "Genetic predispositions of Parkinson's disease revealed in patient-derived brain cells," *NPJ Parkinsons Dis*, vol. 6, no. 1, p. 8, Apr. 2020, doi: 10.1038/s41531-020-0110-8.
- [48] C. Blauwendraat, M. A. Nalls, and A. B. Singleton, "The genetic architecture of Parkinson's disease," *Lancet Neurol*, vol. 19, no. 2, pp. 170–178, Feb. 2020, doi: 10.1016/S1474-4422(19)30287-X.
- [49] T. Kamath *et al.*, "Single-cell genomic profiling of human dopamine neurons identifies a population that selectively degenerates in Parkinson's disease," *Nat Neurosci*, vol. 25, no. 5, pp. 588–595, May 2022, doi: 10.1038/s41593-022-01061-1.
- [50] R. Balestrino and A. H. V. Schapira, "Parkinson disease," *Eur J Neurol*, vol. 27, no. 1, pp. 27–42, Jan. 2020, doi: 10.1111/ene.14108.
- [51] C. W. Shults, "Lewy bodies," *Proceedings of the National Academy of Sciences*, vol. 103, no. 6, pp. 1661–1668, Feb. 2006, doi: 10.1073/pnas.0509567103.
- [52] D. W. Dickson, "Parkinson's Disease and Parkinsonism: Neuropathology," *Cold Spring Harb Perspect Med*, vol. 2, no. 8, pp. a009258–a009258, Aug. 2012, doi: 10.1101/cshperspect.a009258.
- [53] L. V. Kalia, S. K. Kalia, P. J. McLean, A. M. Lozano, and A. E. Lang, "α-Synuclein oligomers and clinical implications for Parkinson disease," *Ann Neurol*, vol. 73, no. 2, pp. 155–169, Feb. 2013, doi: 10.1002/ana.23746.
- [54] I. Surgucheva, K. L. Newell, J. Burns, and A. Surguchov, "New α- and γ-synuclein immunopathological lesions in human brain," *Acta Neuropathol Commun*, vol. 2, no. 1, p. 132, Dec. 2014, doi: 10.1186/s40478-014-0132-8.
- [55] G. Gustafsson *et al.*, "Secretion and Uptake of α-Synuclein Via Extracellular Vesicles in Cultured Cells," *Cell Mol Neurobiol*, 2018, doi: 10.1007/s10571-018-0622-5.
- [56] P. Calabresi, A. Mechelli, G. Natale, L. Volpicelli-Daley, G. Di Lazzaro, and V. Ghiglieri, "Alpha-synuclein in Parkinson's disease and other synucleinopathies: from overt neurodegeneration back to early synaptic dysfunction," *Cell Death Dis*, vol. 14, no. 3, p. 176, Mar. 2023, doi: 10.1038/s41419-023-05672-9.
- [57] T. Sacha and G. Saglio, "Nilotinib in the treatment of chronic myeloid leukemia," *Future Oncology*, vol. 15, no. 9, pp. 953–965, Mar. 2019, doi: 10.2217/fon-2018-0468.
- [58] T. Simuni *et al.*, "Efficacy of Nilotinib in Patients With Moderately Advanced Parkinson Disease," *JAMA Neurol*, vol. 78, no. 3, p. 312, Mar. 2021, doi: 10.1001/jamaneurol.2020.4725.
- [59] G. Pagano *et al.*, "A Phase II Study to Evaluate the Safety and Efficacy of Prasinezumab in Early Parkinson's Disease (PASADENA): Rationale, Design, and Baseline Data," *Front Neurol*, vol. 12, Oct. 2021, doi: 10.3389/fneur.2021.705407.

- [60] G. Pagano *et al.*, “Trial of Prasinezumab in Early-Stage Parkinson’s Disease,” *New England Journal of Medicine*, vol. 387, no. 5, pp. 421–432, Aug. 2022, doi: 10.1056/NEJMoa2202867.
- [61] P. Calabresi, G. Di Lazzaro, G. Marino, F. Campanelli, and V. Ghiglieri, “Advances in understanding the function of alpha-synuclein: implications for Parkinson’s disease,” *Brain*, vol. 146, no. 9, pp. 3587–3597, Sep. 2023, doi: 10.1093/brain/awad150.
- [62] P. Lyra, V. Machado, S. Rota, K. R. Chaudhuri, J. Botelho, and J. J. Mendes, “Revisiting Alpha-Synuclein Pathways to Inflammation,” *Int J Mol Sci*, vol. 24, no. 8, p. 7137, Apr. 2023, doi: 10.3390/ijms24087137.
- [63] C. Zhang *et al.*, “Progress in Parkinson’s disease animal models of genetic defects: Characteristics and application,” *Biomedicine & Pharmacotherapy*, vol. 155, p. 113768, Nov. 2022, doi: 10.1016/j.biopha.2022.113768.
- [64] A. J. Espay *et al.*, “Revisiting protein aggregation as pathogenic in sporadic Parkinson and Alzheimer diseases,” *Neurology*, vol. 92, no. 7, pp. 329–337, Feb. 2019, doi: 10.1212/WNL.0000000000006926.
- [65] A. H. V. Schapira, J. M. Cooper, D. Dexter, J. B. Clark, P. Jenner, and C. D. Marsden, “Mitochondrial Complex I Deficiency in Parkinson’s Disease,” *J Neurochem*, vol. 54, no. 3, pp. 823–827, Mar. 1990, doi: 10.1111/j.1471-4159.1990.tb02325.x.
- [66] J. W. Langston, L. S. Forno, J. Tetrud, A. G. Reeves, J. A. Kaplan, and D. Karluk, “Evidence of active nerve cell degeneration in the substantia nigra of humans years after 1-methyl-4-phenyl-1,2,3,6-tetrahydropyridine exposure.,” *Ann Neurol*, vol. 46, no. 4, pp. 598–605, Oct. 1999, doi: 10.1002/1531-8249(199910)46:4<598::aid-ana7>3.0.co;2-f.
- [67] A. M. Pickrell and R. J. Youle, “The Roles of PINK1, Parkin, and Mitochondrial Fidelity in Parkinson’s Disease,” *Neuron*, vol. 85, no. 2, pp. 257–273, Jan. 2015, doi: 10.1016/j.neuron.2014.12.007.
- [68] A. Picca *et al.*, “Mitochondrial Dysfunction and Aging: Insights from the Analysis of Extracellular Vesicles,” *Int J Mol Sci*, vol. 20, no. 4, p. 805, Feb. 2019, doi: 10.3390/ijms20040805.
- [69] A. Picca *et al.*, “Mitochondrial Signatures in Circulating Extracellular Vesicles of Older Adults with Parkinson’s Disease: Results from the EXosomes in PARKinson’s Disease (EXPAND) Study,” *J Clin Med*, vol. 9, no. 2, p. 504, Feb. 2020, doi: 10.3390/jcm9020504.
- [70] J. A. Korecka *et al.*, “Phenotypic Characterization of Retinoic Acid Differentiated SH-SY5Y Cells by Transcriptional Profiling,” *PLoS One*, vol. 8, no. 5, p. e63862, May 2013, doi: 10.1371/journal.pone.0063862.
- [71] F. L’Episcopo *et al.*, “Microglia polarization, gene-environment interactions and wnt/ $\beta$ -catenin signaling: Emerging roles of glia-neuron and glia-stem/neuroprogenitor crosstalk for dopaminergic neurorestoration in aged Parkinsonian brain,” *Frontiers in Aging Neuroscience*. 2018. doi: 10.3389/fnagi.2018.00012.
- [72] H.-M. Gao and J.-S. Hong, “Why neurodegenerative diseases are progressive: uncontrolled inflammation drives disease progression,” *Trends Immunol*, vol. 29, no. 8, pp. 357–365, Aug. 2008, doi: 10.1016/j.it.2008.05.002.

- [73] H. S. Kwon and S.-H. Koh, “Neuroinflammation in neurodegenerative disorders: the roles of microglia and astrocytes,” *Transl Neurodegener*, vol. 9, no. 1, p. 42, Dec. 2020, doi: 10.1186/s40035-020-00221-2.
- [74] M. G. Tansey and M. S. Goldberg, “Neuroinflammation in Parkinson’s disease: Its role in neuronal death and implications for therapeutic intervention,” *Neurobiol Dis*, vol. 37, no. 3, pp. 510–518, Mar. 2010, doi: 10.1016/j.nbd.2009.11.004.
- [75] A. Grotemeyer, R. L. McFleder, J. Wu, J. Wischhusen, and C. W. Ip, “Neuroinflammation in Parkinson’s Disease – Putative Pathomechanisms and Targets for Disease-Modification,” *Front Immunol*, vol. 13, May 2022, doi: 10.3389/fimmu.2022.878771.
- [76] M. P. Abbracchio and C. Verderio, “Pathophysiological roles of P2 receptors in glial cells,” *Novartis Found Symp*, vol. 276, pp. 91–103; discussion 103-12, 275–81, 2006.
- [77] M. L. Monje, H. Toda, and T. D. Palmer, “Inflammatory Blockade Restores Adult Hippocampal Neurogenesis,” *Science (1979)*, vol. 302, no. 5651, pp. 1760–1765, Dec. 2003, doi: 10.1126/science.1088417.
- [78] W. J. Streit, “Microglia and neuroprotection: implications for Alzheimer’s disease,” *Brain Res Rev*, vol. 48, no. 2, pp. 234–239, Apr. 2005, doi: 10.1016/j.brainresrev.2004.12.013.
- [79] M. Elfil, S. Kamel, M. Kandil, B. B. Koo, and S. M. Schaefer, “Implications of the Gut Microbiome in Parkinson’s Disease,” *Movement Disorders*, pp. 1–14, 2020, doi: 10.1002/mds.28004.
- [80] A. Fasano *et al.*, “The role of small intestinal bacterial overgrowth in Parkinson’s disease,” *Movement Disorders*, vol. 28, no. 9, pp. 1241–1249, 2013, doi: 10.1002/mds.25522.
- [81] D. Nyholm and P. M. Hellström, “Effects of *Helicobacter pylori* on Levodopa Pharmacokinetics,” *J Parkinsons Dis*, vol. 11, no. 1, pp. 61–69, Feb. 2021, doi: 10.3233/JPD-202298.
- [82] S. Kim *et al.*, “Transneuronal Propagation of Pathologic  $\alpha$ -Synuclein from the Gut to the Brain Models Parkinson’s Disease,” *Neuron*, vol. 103, no. 4, pp. 627-641.e7, 2019, doi: 10.1016/j.neuron.2019.05.035.
- [83] D. Devos *et al.*, “Colonic inflammation in Parkinson’s disease,” *Neurobiol Dis*, vol. 50, no. 1, pp. 42–48, 2013, doi: 10.1016/j.nbd.2012.09.007.
- [84] A. B. Singleton, J. A. Hardy, and T. Gasser, “The Birth of the Modern Era of Parkinson’s Disease Genetics,” *J Parkinsons Dis*, vol. 7, no. s1, pp. S87–S93, Mar. 2017, doi: 10.3233/JPD-179009.
- [85] J. Horsager *et al.*, “Brain-first versus body-first Parkinson’s disease: a multimodal imaging case-control study,” *Brain*, vol. 143, no. 10, pp. 3077–3088, Oct. 2020, doi: 10.1093/brain/awaa238.
- [86] C. D. Marsden, “Parkinson’s disease,” *The Lancet*, vol. 335, no. 8695, pp. 948–949, Apr. 1990, doi: 10.1016/0140-6736(90)91006-V.
- [87] N. Heng *et al.*, “Striatal Dopamine Loss in Early Parkinson’s Disease: Systematic Review and Novel Analysis of Dopamine Transporter Imaging,” *Mov Disord Clin Pract*, vol. 10, no. 4, pp. 539–546, Apr. 2023, doi: 10.1002/mdc3.13687.

- [88] Y. A. Sidorova, K. P. Volcho, and N. F. Salakhutdinov, “Neuroregeneration in Parkinson’s Disease: From Proteins to Small Molecules,” *Curr Neuropharmacol*, vol. 17, no. 3, pp. 268–287, Feb. 2019, doi: 10.2174/1570159X16666180905094123.
- [89] A. Slézia *et al.*, “Behavioral, neural and ultrastructural alterations in a graded-dose 6-OHDA mouse model of early-stage Parkinson’s disease,” *Sci Rep*, vol. 13, no. 1, p. 19478, Nov. 2023, doi: 10.1038/s41598-023-46576-0.
- [90] B. Müller, J. Assmus, K. Herlofson, J. P. Larsen, and O.-B. Tysnes, “Importance of motor vs. non-motor symptoms for health-related quality of life in early Parkinson’s disease,” *Parkinsonism Relat Disord*, vol. 19, no. 11, pp. 1027–1032, Nov. 2013, doi: 10.1016/j.parkreldis.2013.07.010.
- [91] D. Berg *et al.*, “Movement disorder society criteria for clinically established early Parkinson’s disease,” *Movement Disorders*, vol. 33, no. 10, pp. 1643–1646, Oct. 2018, doi: 10.1002/mds.27431.
- [92] R. B. Postuma *et al.*, “MDS clinical diagnostic criteria for Parkinson’s disease,” *Movement Disorders*, vol. 30, no. 12, pp. 1591–1601, Oct. 2015, doi: 10.1002/mds.26424.
- [93] E. Tolosa, A. Garrido, S. W. Scholz, and W. Poewe, “Challenges in the diagnosis of Parkinson’s disease,” *Lancet Neurol*, vol. 20, no. 5, pp. 385–397, May 2021, doi: 10.1016/S1474-4422(21)00030-2.
- [94] A. Siderowf *et al.*, “Assessment of heterogeneity among participants in the Parkinson’s Progression Markers Initiative cohort using  $\alpha$ -synuclein seed amplification: a cross-sectional study,” *Lancet Neurol*, vol. 22, no. 5, pp. 407–417, May 2023, doi: 10.1016/S1474-4422(23)00109-6.
- [95] Y. Han, D. Wu, Y. Wang, J. Xie, and Z. Zhang, “Skin alpha-synuclein deposit patterns: A predictor of Parkinson’s disease subtypes,” *EBioMedicine*, vol. 80, p. 104076, Jun. 2022, doi: 10.1016/j.ebiom.2022.104076.
- [96] J. Xiang *et al.*, “Development of an  $\alpha$ -synuclein positron emission tomography tracer for imaging synucleinopathies,” *Cell*, vol. 186, no. 16, pp. 3350–3367.e19, Aug. 2023, doi: 10.1016/j.cell.2023.06.004.
- [97] T. Pardo-Moreno *et al.*, “Current Treatments and New, Tentative Therapies for Parkinson’s Disease,” *Pharmaceutics*, vol. 15, no. 3, p. 770, Feb. 2023, doi: 10.3390/pharmaceutics15030770.
- [98] S. Ovallath and B. Sulthana, “Levodopa: History and therapeutic applications,” *Ann Indian Acad Neurol*, vol. 20, no. 3, p. 185, 2017, doi: 10.4103/aian.AIAN\_241\_17.
- [99] A. Abbott, “Levodopa: the story so far,” *Nature*, vol. 466, no. 7310, pp. S6–S7, Aug. 2010, doi: 10.1038/466S6a.
- [100] K. R. Gandhi and A. Saadabadi, *Levodopa (L-Dopa)*. 2023.
- [101] H. Wood, “Gene therapy boosts response to levodopa in patients with Parkinson disease,” *Nat Rev Neurol*, vol. 16, no. 5, pp. 242–242, May 2020, doi: 10.1038/s41582-020-0351-5.
- [102] I. Beaulieu-Boire and A. E. Lang, “Behavioral effects of levodopa,” *Movement Disorders*, vol. 30, no. 1, pp. 90–102, Jan. 2015, doi: 10.1002/mds.26121.

- [103] C. W. Olanow, J. A. Obeso, and F. Stocchi, “Continuous dopamine-receptor treatment of Parkinson’s disease: scientific rationale and clinical implications,” *Lancet Neurol*, vol. 5, no. 8, pp. 677–687, Aug. 2006, doi: 10.1016/S1474-4422(06)70521-X.
- [104] J. Choi and K. A. Horner, *Dopamine Agonists*. 2023.
- [105] S. Ramesh and A. S. P. M. Arachchige, “Depletion of dopamine in Parkinson’s disease and relevant therapeutic options: A review of the literature,” *AIMS Neurosci*, vol. 10, no. 3, pp. 200–231, 2023, doi: 10.3934/Neuroscience.2023017.
- [106] D. Robakis and S. Fahn, “Defining the Role of the Monoamine Oxidase-B Inhibitors for Parkinson’s Disease,” *CNS Drugs*, vol. 29, no. 6, pp. 433–441, Jun. 2015, doi: 10.1007/s40263-015-0249-8.
- [107] T. Müller, “Catechol-O-Methyltransferase Inhibitors in Parkinson’s Disease,” *Drugs*, vol. 75, no. 2, pp. 157–174, Feb. 2015, doi: 10.1007/s40265-014-0343-0.
- [108] A. C. P. Campos *et al.*, “Unraveling the Role of Astrocytes in Subthalamic Nucleus Deep Brain Stimulation in a Parkinson’s Disease Rat Model,” *Cell Mol Neurobiol*, vol. 40, no. 6, pp. 939–954, Aug. 2020, doi: 10.1007/s10571-019-00784-3.
- [109] A. R. Charmley, T. Kimber, N. Mahant, and A. Lehn, “Driving restrictions following deep brain stimulation surgery,” *BMJ Neurol Open*, vol. 3, no. 2, p. e000210, Dec. 2021, doi: 10.1136/bmjno-2021-000210.
- [110] M. Parmar, S. Grealish, and C. Henchcliffe, “The future of stem cell therapies for Parkinson disease,” *Nat Rev Neurosci*, vol. 21, no. 2, pp. 103–115, Feb. 2020, doi: 10.1038/s41583-019-0257-7.
- [111] Z. Zhu and D. Huangfu, “Human pluripotent stem cells: an emerging model in developmental biology,” *Development*, vol. 140, no. 4, pp. 705–717, Feb. 2013, doi: 10.1242/dev.086165.
- [112] J. A. Thomson, “Embryonic Stem Cell Lines Derived from Human Blastocysts,” *Science (1979)*, vol. 282, no. 5391, pp. 1145–1147, Nov. 1998, doi: 10.1126/science.282.5391.1145.
- [113] W. Chen, Q. Huang, S. Ma, and M. Li, “Progress in Dopaminergic Cell Replacement and Regenerative Strategies for Parkinson’s Disease.,” *ACS Chem Neurosci*, vol. 10, no. 2, pp. 839–851, 2019, doi: 10.1021/acchemneuro.8b00389.
- [114] Y.-K. Wang *et al.*, “Human Clinical-Grade Parthenogenetic ESC-Derived Dopaminergic Neurons Recover Locomotive Defects of Nonhuman Primate Models of Parkinson’s Disease,” *Stem Cell Reports*, vol. 11, no. 1, pp. 171–182, Jul. 2018, doi: 10.1016/j.stemcr.2018.05.010.
- [115] D. Doi *et al.*, “Pre-clinical study of induced pluripotent stem cell-derived dopaminergic progenitor cells for Parkinson’s disease,” *Nat Commun*, vol. 11, no. 1, p. 3369, Jul. 2020, doi: 10.1038/s41467-020-17165-w.
- [116] G. Bonaventura *et al.*, “iPSCs: A Preclinical Drug Research Tool for Neurological Disorders,” *Int J Mol Sci*, vol. 22, no. 9, p. 4596, Apr. 2021, doi: 10.3390/ijms22094596.
- [117] A. Morizane, “Cell therapy for Parkinson’s disease with induced pluripotent stem cells,” *Inflamm Regen*, vol. 43, no. 1, p. 16, Feb. 2023, doi: 10.1186/s41232-023-00269-3.

- [118] T. Kikuchi *et al.*, “Survival of Human Induced Pluripotent Stem Cell–Derived Midbrain Dopaminergic Neurons in the Brain of a Primate Model of Parkinson’s Disease,” *J Parkinsons Dis*, vol. 1, no. 4, pp. 395–412, 2011, doi: 10.3233/JPD-2011-11070.
- [119] T. Kikuchi *et al.*, “Human iPS cell-derived dopaminergic neurons function in a primate Parkinson’s disease model,” *Nature*, vol. 548, no. 7669, pp. 592–596, Aug. 2017, doi: 10.1038/nature23664.
- [120] J. Takahashi, “Preparing for first human trial of induced pluripotent stem cell-derived cells for Parkinson’s disease: an interview with Jun Takahashi,” *Regenerative Med*, vol. 14, no. 2, pp. 93–95, Feb. 2019, doi: 10.2217/rme-2018-0158.
- [121] X. Liu, W. Li, X. Fu, and Y. Xu, “The immunogenicity and immune tolerance of pluripotent stem cell derivatives,” *Frontiers in Immunology*. 2017. doi: 10.3389/fimmu.2017.00645.
- [122] V. K. Harris *et al.*, “Phase I Trial of Intrathecal Mesenchymal Stem Cell-derived Neural Progenitors in Progressive Multiple Sclerosis,” *EBioMedicine*, 2018, doi: 10.1016/j.ebiom.2018.02.002.
- [123] A. F. Evangelista *et al.*, “Bone marrow-derived mesenchymal stem/stromal cells reverse the sensorial diabetic neuropathy via modulation of spinal neuroinflammatory cascades,” *J Neuroinflammation*, vol. 15, no. 1, p. 189, Dec. 2018, doi: 10.1186/s12974-018-1224-3.
- [124] E. Mezey, “Turning Blood into Brain: Cells Bearing Neuronal Antigens Generated in Vivo from Bone Marrow,” *Science (1979)*, vol. 290, no. 5497, pp. 1779–1782, Dec. 2000, doi: 10.1126/science.290.5497.1779.
- [125] N. P. Staff, D. T. Jones, and W. Singer, “Mesenchymal Stromal Cell Therapies for Neurodegenerative Diseases,” *Mayo Clinic Proceedings*. 2019. doi: 10.1016/j.mayocp.2019.01.001.
- [126] M. Kitada and M. Dezawa, “Parkinson’s disease and mesenchymal stem cells: Potential for cell-based therapy,” *Parkinson’s Disease*. 2012. doi: 10.1155/2012/873706.
- [127] N. K. Venkataramana *et al.*, “Open-labeled study of unilateral autologous bone-marrow-derived mesenchymal stem cell transplantation in Parkinson’s disease,” *Translational Research*, 2010, doi: 10.1016/j.trsl.2009.07.006.
- [128] N. Iraci *et al.*, “Extracellular vesicles are independent metabolic units with asparaginase activity,” *Nat Chem Biol*, 2017, doi: 10.1038/nchembio.2422.
- [129] C. Cossetti *et al.*, “Extracellular vesicles from neural stem cells transfer IFN- $\gamma$  via Ifngr1 to activate Stat1 signaling in target cells,” *Mol Cell*, 2014, doi: 10.1016/j.molcel.2014.08.020.
- [130] F. L’Episcopo *et al.*, “Neural Stem Cell Grafts Promote Astroglia-driven Neurorestoration in the Aged Parkinsonian Brain via Wnt/ $\beta$ -catenin Signalling,” *Stem Cells*, 2018, doi: 10.1002/stem.2827.
- [131] T. Wang, Y. Sun, and U. Dettmer, “Astrocytes in Parkinson’s Disease: From Role to Possible Intervention,” *Cells*, vol. 12, no. 19, p. 2336, Sep. 2023, doi: 10.3390/cells12192336.
- [132] M. F. Serapide *et al.*, “Boosting Antioxidant Self-defenses by Grafting Astrocytes Rejuvenates the Aged Microenvironment and Mitigates Nigrostriatal Toxicity in

- Parkinsonian Brain via an Nrf2-Driven Wnt/ $\beta$ -Catenin Prosurvival Axis.,” *Front Aging Neurosci*, vol. 12, p. 24, 2020, doi: 10.3389/fnagi.2020.00024.
- [133] J. W. Bigbee, “Cells of the Central Nervous System: An Overview of Their Structure and Function,” 2023, pp. 41–64. doi: 10.1007/978-3-031-12390-0\_2.
- [134] P. E. Ludwig, V. Reddy, and M. Varacallo, *Neuroanatomy, Neurons*. 2023.
- [135] F. A. C. Azevedo *et al.*, “Equal numbers of neuronal and nonneuronal cells make the human brain an isometrically scaled-up primate brain,” *J Comp Neurol*, vol. 513, no. 5, pp. 532–541, Apr. 2009, doi: 10.1002/cne.21974.
- [136] F. Baroni and A. Mazzoni, “Heterogeneity of heterogeneities in neuronal networks,” *Front Comput Neurosci*, vol. 8, Dec. 2014, doi: 10.3389/fncom.2014.00161.
- [137] P. Bezzi, V. Magnaghi, R. C. Paolicelli, and J.-P. Hornung, “Editorial: Glial heterogeneity: impact on neuronal function and dysfunction,” *Front Neuroanat*, vol. 17, Jul. 2023, doi: 10.3389/fnana.2023.1249919.
- [138] N. Perez-Nieves, V. C. H. Leung, P. L. Dragotti, and D. F. M. Goodman, “Neural heterogeneity promotes robust learning,” *Nat Commun*, vol. 12, no. 1, p. 5791, Oct. 2021, doi: 10.1038/s41467-021-26022-3.
- [139] C. Chhatbar and M. Prinz, “From shape to contents: heterogeneity of CNS glial cells,” *Acta Neuropathol*, vol. 143, no. 2, pp. 123–124, Feb. 2022, doi: 10.1007/s00401-021-02398-w.
- [140] A. Verkhratsky, M. S. Ho, and V. Parpura, “Evolution of Neuroglia,” 2019, pp. 15–44. doi: 10.1007/978-981-13-9913-8\_2.
- [141] X. Fan and Y. Agid, “At the Origin of the History of Glia,” *Neuroscience*, vol. 385, pp. 255–271, Aug. 2018, doi: 10.1016/j.neuroscience.2018.05.050.
- [142] V. Parpura and A. Verkhratsky, “Neuroglia at the Crossroads of Homeostasis, Metabolism and Signalling: Evolution of the Concept,” *ASN Neuro*, vol. 4, no. 4, p. AN20120019, Apr. 2012, doi: 10.1042/AN20120019.
- [143] M. Bentivoglio *et al.*, “The Original Histological Slides of Camillo Golgi and His Discoveries on Neuronal Structure,” *Front Neuroanat*, vol. 13, Feb. 2019, doi: 10.3389/fnana.2019.00003.
- [144] V. Cani and P. Mazzarello, “Golgi and Ranvier: from the black reaction to a theory of referred pain.,” *Funct Neurol*, vol. 30, no. 1, pp. 73–7, 2015.
- [145] R. Yuste, “The discovery of dendritic spines by Cajal,” *Front Neuroanat*, vol. 9, Apr. 2015, doi: 10.3389/fnana.2015.00018.
- [146] R. C. Paolicelli *et al.*, “Microglia states and nomenclature: A field at its crossroads,” *Neuron*, vol. 110, no. 21, pp. 3458–3483, Nov. 2022, doi: 10.1016/j.neuron.2022.10.020.
- [147] R. de Ceglia *et al.*, “Specialized astrocytes mediate glutamatergic gliotransmission in the CNS,” *Nature*, vol. 622, no. 7981, pp. 120–129, Oct. 2023, doi: 10.1038/s41586-023-06502-w.
- [148] I. Farhy-Tselnicker and N. J. Allen, “Astrocytes, neurons, synapses: a tripartite view on cortical circuit development,” *Neural Dev*, vol. 13, no. 1, p. 7, Dec. 2018, doi: 10.1186/s13064-018-0104-y.

- [149] R. Stevenson, E. Samokhina, I. Rossetti, J. W. Morley, and Y. Buskila, “Neuromodulation of Glial Function During Neurodegeneration,” *Front Cell Neurosci*, vol. 14, Aug. 2020, doi: 10.3389/fncel.2020.00278.
- [150] A. J. Gleichman and S. T. Carmichael, “Glia in neurodegeneration: Drivers of disease or along for the ride?,” *Neurobiol Dis*, vol. 142, p. 104957, Aug. 2020, doi: 10.1016/j.nbd.2020.104957.
- [151] A. Nimmerjahn, F. Kirchhoff, and F. Helmchen, “Resting microglial cells are highly dynamic surveillants of brain parenchyma in vivo.,” *Science*, vol. 308, no. 5726, pp. 1314–8, May 2005, doi: 10.1126/science.1110647.
- [152] H. Kettenmann, U.-K. Hanisch, M. Noda, and A. Verkhratsky, “Physiology of Microglia,” *Physiol Rev*, vol. 91, no. 2, pp. 461–553, Apr. 2011, doi: 10.1152/physrev.00011.2010.
- [153] A. Sierra, M.-À. Tremblay, and H. Wake, “Never-resting microglia: physiological roles in the healthy brain and pathological implications,” *Front Cell Neurosci*, vol. 8, Aug. 2014, doi: 10.3389/fncel.2014.00240.
- [154] L. Muzio, A. Viotti, and G. Martino, “Microglia in Neuroinflammation and Neurodegeneration: From Understanding to Therapy,” *Front Neurosci*, vol. 15, Sep. 2021, doi: 10.3389/fnins.2021.742065.
- [155] Y.-L. Tan, Y. Yuan, and L. Tian, “Microglial regional heterogeneity and its role in the brain,” *Mol Psychiatry*, vol. 25, no. 2, pp. 351–367, Feb. 2020, doi: 10.1038/s41380-019-0609-8.
- [156] Q. Li and B. A. Barres, “Microglia and macrophages in brain homeostasis and disease,” *Nat Rev Immunol*, vol. 18, no. 4, pp. 225–242, Apr. 2018, doi: 10.1038/nri.2017.125.
- [157] R. C. Paolicelli and M. T. Ferretti, “Function and Dysfunction of Microglia during Brain Development: Consequences for Synapses and Neural Circuits,” *Front Synaptic Neurosci*, vol. 9, May 2017, doi: 10.3389/fnsyn.2017.00009.
- [158] W. J. Streit, M. B. Graeber, and G. W. Kreutzberg, “Functional plasticity of microglia: A review,” *Glia*, vol. 1, no. 5, pp. 301–307, 1988, doi: 10.1002/glia.440010502.
- [159] C. D. Mills, K. Kincaid, J. M. Alt, M. J. Heilman, and A. M. Hill, “M-1/M-2 Macrophages and the Th1/Th2 Paradigm,” *The Journal of Immunology*, vol. 164, no. 12, pp. 6166–6173, Jun. 2000, doi: 10.4049/jimmunol.164.12.6166.
- [160] F. O. Martinez and S. Gordon, “The M1 and M2 paradigm of macrophage activation: time for reassessment,” *F1000Prime Rep*, vol. 6, Mar. 2014, doi: 10.12703/P6-13.
- [161] R. M. Ransohoff, “A polarizing question: do M1 and M2 microglia exist?,” *Nat Neurosci*, vol. 19, no. 8, pp. 987–991, Aug. 2016, doi: 10.1038/nn.4338.
- [162] M.-È. Tremblay, C. Lecours, L. Samson, V. Sánchez-Zafra, and A. Sierra, “From the Cajal alumni Achúcarro and Río-Hortega to the rediscovery of never-resting microglia,” *Front Neuroanat*, vol. 9, Apr. 2015, doi: 10.3389/fnana.2015.00045.
- [163] D. Davalos *et al.*, “ATP mediates rapid microglial response to local brain injury in vivo,” *Nat Neurosci*, 2005, doi: 10.1038/nn1472.
- [164] U.-K. Hanisch and H. Kettenmann, “Microglia: active sensor and versatile effector cells in the normal and pathologic brain,” *Nat Neurosci*, vol. 10, no. 11, pp. 1387–1394, Nov. 2007, doi: 10.1038/nn1997.



- [165] Y. Wu, L. Dissing-Olesen, B. A. MacVicar, and B. Stevens, “Microglia: Dynamic Mediators of Synapse Development and Plasticity,” *Trends Immunol*, vol. 36, no. 10, pp. 605–613, Oct. 2015, doi: 10.1016/j.it.2015.08.008.
- [166] M. Colonna and O. Butovsky, “Microglia Function in the Central Nervous System During Health and Neurodegeneration,” *Annu Rev Immunol*, vol. 35, no. 1, pp. 441–468, Apr. 2017, doi: 10.1146/annurev-immunol-051116-052358.
- [167] H. Scheiblich *et al.*, “Microglial NLRP3 Inflammasome Activation upon TLR2 and TLR5 Ligation by Distinct  $\alpha$ -Synuclein Assemblies,” *The Journal of Immunology*, vol. 207, no. 8, pp. 2143–2154, Oct. 2021, doi: 10.4049/jimmunol.2100035.
- [168] S. Jewell, A. M. Herath, and R. Gordon, “Inflammasome Activation in Parkinson’s Disease,” *J Parkinsons Dis*, vol. 12, no. s1, pp. S113–S128, Sep. 2022, doi: 10.3233/JPD-223338.
- [169] S. Mandrekar, Q. Jiang, C. Y. D. Lee, J. Koenigsnecht-Talboo, D. M. Holtzman, and G. E. Landreth, “Microglia Mediate the Clearance of Soluble A $\beta$  through Fluid Phase Macropinocytosis,” *The Journal of Neuroscience*, vol. 29, no. 13, pp. 4252–4262, Apr. 2009, doi: 10.1523/JNEUROSCI.5572-08.2009.
- [170] M. Ren *et al.*, “TREM2 overexpression attenuates neuroinflammation and protects dopaminergic neurons in experimental models of Parkinson’s disease,” *Exp Neurol*, vol. 302, pp. 205–213, Apr. 2018, doi: 10.1016/j.expneurol.2018.01.016.
- [171] N. Stefanova, “Microglia in Parkinson’s Disease,” *J Parkinsons Dis*, vol. 12, no. s1, pp. S105–S112, Sep. 2022, doi: 10.3233/JPD-223237.
- [172] H. Jinnou *et al.*, “Radial Glial Fibers Promote Neuronal Migration and Functional Recovery after Neonatal Brain Injury,” *Cell Stem Cell*, vol. 22, no. 1, pp. 128–137.e9, Jan. 2018, doi: 10.1016/j.stem.2017.11.005.
- [173] R. Tognatta and R. H. Miller, “Contribution of the oligodendrocyte lineage to CNS repair and neurodegenerative pathologies,” *Neuropharmacology*, vol. 110, pp. 539–547, Nov. 2016, doi: 10.1016/j.neuropharm.2016.04.026.
- [174] Y. Miranda-Negrón and J. E. García-Arrarás, “Radial glia and radial glia-like cells: Their role in neurogenesis and regeneration,” *Front Neurosci*, vol. 16, Nov. 2022, doi: 10.3389/fnins.2022.1006037.
- [175] D. E. Bergles and W. D. Richardson, “Oligodendrocyte Development and Plasticity,” *Cold Spring Harb Perspect Biol*, vol. 8, no. 2, p. a020453, Feb. 2016, doi: 10.1101/cshperspect.a020453.
- [176] L. A. Akay, A. H. Effenberger, and L.-H. Tsai, “Cell of all trades: oligodendrocyte precursor cells in synaptic, vascular, and immune function,” *Genes Dev*, vol. 35, no. 3–4, pp. 180–198, Feb. 2021, doi: 10.1101/gad.344218.120.
- [177] M. Zawadzka *et al.*, “CNS-Resident Glial Progenitor/Stem Cells Produce Schwann Cells as well as Oligodendrocytes during Repair of CNS Demyelination,” *Cell Stem Cell*, vol. 6, no. 6, pp. 578–590, Jun. 2010, doi: 10.1016/j.stem.2010.04.002.
- [178] N. Baumann and D. Pham-Dinh, “Biology of Oligodendrocyte and Myelin in the Mammalian Central Nervous System,” *Physiol Rev*, vol. 81, no. 2, pp. 871–927, Apr. 2001, doi: 10.1152/physrev.2001.81.2.871.

- [179] D. Agarwal *et al.*, “A single-cell atlas of the human substantia nigra reveals cell-specific pathways associated with neurological disorders,” *Nat Commun*, vol. 11, no. 1, p. 4183, Aug. 2020, doi: 10.1038/s41467-020-17876-0.
- [180] A. MacDonald *et al.*, “Single Cell Transcriptomics of Ependymal Cells Across Age, Region and Species Reveals Cilia-Related and Metal Ion Regulatory Roles as Major Conserved Ependymal Cell Functions,” *Front Cell Neurosci*, vol. 15, Jul. 2021, doi: 10.3389/fncel.2021.703951.
- [181] S. Jäkel and L. Dimou, “Glial Cells and Their Function in the Adult Brain: A Journey through the History of Their Ablation,” *Front Cell Neurosci*, vol. 11, Feb. 2017, doi: 10.3389/fncel.2017.00024.
- [182] A. V. Molofsky and B. Deneen, “Astrocyte development: A Guide for the Perplexed,” *Glia*, vol. 63, no. 8, pp. 1320–1329, Aug. 2015, doi: 10.1002/glia.22836.
- [183] W. L. Andriezen, “The Neuroglia Elements in the Human Brain,” *BMJ*, vol. 2, no. 1700, pp. 227–230, Jul. 1893, doi: 10.1136/bmj.2.1700.227.
- [184] H.-H. Tsai *et al.*, “Regional Astrocyte Allocation Regulates CNS Synaptogenesis and Repair,” *Science (1979)*, vol. 337, no. 6092, pp. 358–362, Jul. 2012, doi: 10.1126/science.1222381.
- [185] B. S. Khakh and B. Deneen, “The Emerging Nature of Astrocyte Diversity,” *Annu Rev Neurosci*, vol. 42, no. 1, pp. 187–207, Jul. 2019, doi: 10.1146/annurev-neuro-070918-050443.
- [186] V. Hartenstein and A. Giangrande, “Connecting the nervous and the immune systems in evolution,” *Commun Biol*, vol. 1, no. 1, p. 64, Jun. 2018, doi: 10.1038/s42003-018-0070-2.
- [187] K. R. Jessen, “Glial cells,” *Int J Biochem Cell Biol*, vol. 36, no. 10, pp. 1861–1867, Oct. 2004, doi: 10.1016/j.biocel.2004.02.023.
- [188] F. P. Di Giorgio, M. A. Carrasco, M. C. Siao, T. Maniatis, and K. Eggan, “Non-cell autonomous effect of glia on motor neurons in an embryonic stem cell-based ALS model,” *Nat Neurosci*, vol. 10, no. 5, pp. 608–614, May 2007, doi: 10.1038/nn1885.
- [189] H.-G. Lee, M. A. Wheeler, and F. J. Quintana, “Function and therapeutic value of astrocytes in neurological diseases,” *Nat Rev Drug Discov*, vol. 21, no. 5, pp. 339–358, May 2022, doi: 10.1038/s41573-022-00390-x.
- [190] M. A. Wheeler *et al.*, “MAFG-driven astrocytes promote CNS inflammation,” *Nature*, vol. 578, no. 7796, pp. 593–599, Feb. 2020, doi: 10.1038/s41586-020-1999-0.
- [191] S. A. Liddelow and B. A. Barres, “Reactive Astrocytes: Production, Function, and Therapeutic Potential,” *Immunity*, vol. 46, no. 6, pp. 957–967, Jun. 2017, doi: 10.1016/j.immuni.2017.06.006.
- [192] S. A. Liddelow *et al.*, “Neurotoxic reactive astrocytes are induced by activated microglia,” *Nature*, vol. 541, no. 7638, pp. 481–487, Jan. 2017, doi: 10.1038/nature21029.
- [193] K. Li, J. Li, J. Zheng, and S. Qin, “Reactive Astrocytes in Neurodegenerative Diseases,” *Aging Dis*, vol. 10, no. 3, p. 664, 2019, doi: 10.14336/AD.2018.0720.

- [194] J. T. Hinkle, V. L. Dawson, and T. M. Dawson, “The A1 astrocyte paradigm: New avenues for pharmacological intervention in neurodegeneration,” *Movement Disorders*, vol. 34, no. 7, pp. 959–969, Jul. 2019, doi: 10.1002/mds.27718.
- [195] M. V. Sofroniew, “Astrocyte Reactivity: Subtypes, States, and Functions in CNS Innate Immunity,” *Trends Immunol*, vol. 41, no. 9, pp. 758–770, Sep. 2020, doi: 10.1016/j.it.2020.07.004.
- [196] M. V. Sofroniew, “Astrocyte barriers to neurotoxic inflammation,” *Nat Rev Neurosci*, vol. 16, no. 5, pp. 249–263, May 2015, doi: 10.1038/nrn3898.
- [197] V. Rothhammer and F. J. Quintana, “Control of autoimmune CNS inflammation by astrocytes,” *Semin Immunopathol*, vol. 37, no. 6, pp. 625–638, Nov. 2015, doi: 10.1007/s00281-015-0515-3.
- [198] C. Escartin *et al.*, “Reactive astrocyte nomenclature, definitions, and future directions,” *Nat Neurosci*, vol. 24, no. 3, pp. 312–325, Mar. 2021, doi: 10.1038/s41593-020-00783-4.
- [199] N. Habib *et al.*, “Disease-associated astrocytes in Alzheimer’s disease and aging,” *Nat Neurosci*, vol. 23, no. 6, pp. 701–706, Jun. 2020, doi: 10.1038/s41593-020-0624-8.
- [200] M. A. Mohamed *et al.*, “Astrogliosis in aging and Parkinson’s disease dementia: a new clinical study with 11C-BU99008 PET,” *Brain Commun*, vol. 4, no. 5, Sep. 2022, doi: 10.1093/braincomms/fcac199.
- [201] M. A. Anderson *et al.*, “Required growth facilitators propel axon regeneration across complete spinal cord injury,” *Nature*, vol. 561, no. 7723, pp. 396–400, Sep. 2018, doi: 10.1038/s41586-018-0467-6.
- [202] M. A. Anderson *et al.*, “Astrocyte scar formation aids central nervous system axon regeneration,” *Nature*, vol. 532, no. 7598, pp. 195–200, Apr. 2016, doi: 10.1038/nature17623.
- [203] B. Marchetti *et al.*, “Glia-Derived Extracellular Vesicles in Parkinson’s Disease,” *J Clin Med*, vol. 9, no. 6, p. 1941, Jun. 2020, doi: 10.3390/jcm9061941.
- [204] F. L’Episcopo, C. Tirolò, N. Testa, S. Caniglia, M. Concetta Morale, and B. Marchetti, “Glia as a Turning Point in the Therapeutic Strategy of Parkinsons Disease,” *CNS Neurol Disord Drug Targets*, vol. 9, no. 3, pp. 349–372, Jul. 2010, doi: 10.2174/187152710791292639.
- [205] B. Marchetti and M. P. Abbracchio, “To be or not to be (inflamed) – is that the question in anti-inflammatory drug therapy of neurodegenerative disorders?,” *Trends Pharmacol Sci*, vol. 26, no. 10, pp. 517–525, Oct. 2005, doi: 10.1016/j.tips.2005.08.007.
- [206] L. Qin *et al.*, “Systemic LPS causes chronic neuroinflammation and progressive neurodegeneration,” *Glia*, vol. 55, no. 5, pp. 453–462, Apr. 2007, doi: 10.1002/glia.20467.
- [207] X. Su, K. A. Maguire-Zeiss, R. Giuliano, L. Prifti, K. Venkatesh, and H. J. Federoff, “Synuclein activates microglia in a model of Parkinson’s disease,” *Neurobiol Aging*, vol. 29, no. 11, pp. 1690–1701, Nov. 2008, doi: 10.1016/j.neurobiolaging.2007.04.006.
- [208] F. L’Episcopo *et al.*, “Switching the Microglial Harmful Phenotype Promotes Lifelong Restoration of Substantia Nigra Dopaminergic Neurons from Inflammatory Neurodegeneration in Aged Mice,” *Rejuvenation Res*, vol. 14, no. 4, pp. 411–424, Aug. 2011, doi: 10.1089/rej.2010.1134.

- [209] F. Episcopo, C. Tirolo, N. Testa, S. Caniglia, M. Morale, and B. Marchetti, “Reactive Astrocytes Are Key Players in Nigrostriatal Dopaminergic Neurorepair in the Mptp Mouse Model of Parkinson’s Disease: Focus on Endogenous Neurorestoration,” *Curr Aging Sci*, vol. 6, no. 1, pp. 45–55, Jul. 2013, doi: 10.2174/1874609811306010007.
- [210] E. C. Hirsch and S. Hunot, “Neuroinflammation in Parkinson’s disease: a target for neuroprotection?,” *Lancet Neurol*, vol. 8, no. 4, pp. 382–397, Apr. 2009, doi: 10.1016/S1474-4422(09)70062-6.
- [211] G. Codolo *et al.*, “Triggering of Inflammasome by Aggregated  $\alpha$ -Synuclein, an Inflammatory Response in Synucleinopathies,” *PLoS One*, 2013, doi: 10.1371/journal.pone.0055375.
- [212] T. J. Collier, N. M. Kanaan, and J. H. Kordower, “Aging and Parkinson’s disease: Different sides of the same coin?,” *Movement Disorders*, vol. 32, no. 7, pp. 983–990, 2017, doi: 10.1002/mds.27037.
- [213] H. Franklin, B. E. Clarke, and R. Patani, “Astrocytes and microglia in neurodegenerative diseases: Lessons from human in vitro models,” *Prog Neurobiol*, vol. 200, p. 101973, May 2021, doi: 10.1016/j.pneurobio.2020.101973.
- [214] D. Singh, “Astrocytic and microglial cells as the modulators of neuroinflammation in Alzheimer’s disease,” *J Neuroinflammation*, vol. 19, no. 1, p. 206, Aug. 2022, doi: 10.1186/s12974-022-02565-0.
- [215] E. F. Garland, I. J. Hartnell, and D. Boche, “Microglia and Astrocyte Function and Communication: What Do We Know in Humans?,” *Front Neurosci*, vol. 16, Feb. 2022, doi: 10.3389/fnins.2022.824888.
- [216] M. Linnerbauer, M. A. Wheeler, and F. J. Quintana, “Astrocyte Crosstalk in CNS Inflammation,” *Neuron*, vol. 108, no. 4, pp. 608–622, Nov. 2020, doi: 10.1016/j.neuron.2020.08.012.
- [217] S. R. Subramaniam and H. J. Federoff, “Targeting Microglial Activation States as a Therapeutic Avenue in Parkinson’s Disease,” *Front Aging Neurosci*, vol. 9, Jun. 2017, doi: 10.3389/fnagi.2017.00176.
- [218] J. M. Lawrence, K. Schardien, B. Wigdahl, and M. R. Nonnemacher, “Roles of neuropathology-associated reactive astrocytes: a systematic review,” *Acta Neuropathol Commun*, vol. 11, no. 1, p. 42, Mar. 2023, doi: 10.1186/s40478-023-01526-9.
- [219] G. E. Tyzack *et al.*, “Astrocyte response to motor neuron injury promotes structural synaptic plasticity via STAT3-regulated TSP-1 expression,” *Nat Commun*, 2014, doi: 10.1038/ncomms5294.
- [220] K. Kuter, Ł. Olech, and U. Głowacka, “Prolonged Dysfunction of Astrocytes and Activation of Microglia Accelerate Degeneration of Dopaminergic Neurons in the Rat Substantia Nigra and Block Compensation of Early Motor Dysfunction Induced by 6-OHDA,” *Mol Neurobiol*, 2018, doi: 10.1007/s12035-017-0529-z.
- [221] F. L’Episcopo *et al.*, “Microglia Polarization, Gene-Environment Interactions and Wnt/ $\beta$ -Catenin Signaling: Emerging Roles of Glia-Neuron and Glia-Stem/Neuroprogenitor Crosstalk for Dopaminergic Neurorestoration in Aged Parkinsonian Brain,” *Front Aging Neurosci*, vol. 10, Feb. 2018, doi: 10.3389/fnagi.2018.00012.

- [222] M. Pascual, F. Ibáñez, and C. Guerri, “Exosomes as mediators of neuron-glia communication in neuroinflammation,” *Neural Regen Res*, vol. 15, no. 5, p. 796, 2020, doi: 10.4103/1673-5374.268893.
- [223] C. E. Hughes and R. J. B. Nibbs, “A guide to chemokines and their receptors,” *FEBS J*, vol. 285, no. 16, pp. 2944–2971, Aug. 2018, doi: 10.1111/febs.14466.
- [224] H. Xu *et al.*, “New genetic and epigenetic insights into the chemokine system: the latest discoveries aiding progression toward precision medicine,” *Cell Mol Immunol*, vol. 20, no. 7, pp. 739–776, May 2023, doi: 10.1038/s41423-023-01032-x.
- [225] D. Raman, T. Sobolik-Delmaire, and A. Richmond, “Chemokines in health and disease,” *Exp Cell Res*, vol. 317, no. 5, pp. 575–589, Mar. 2011, doi: 10.1016/j.yexcr.2011.01.005.
- [226] R. Bonecchi, “Chemokines and chemokine receptors: an overview,” *Frontiers in Bioscience*, vol. Volume, no. 14, p. 540, 2009, doi: 10.2741/3261.
- [227] B. I. LORD, K. J. MORI, E. G. WRIGHT, and L. G. LAJTHA, “An Inhibitor of Stem Cell Proliferation in Normal Bone Marrow,” *Br J Haematol*, vol. 34, no. 3, pp. 441–445, Nov. 1976, doi: 10.1111/j.1365-2141.1976.tb03590.x.
- [228] B. Sherry *et al.*, “Resolution of the two components of macrophage inflammatory protein 1, and cloning and characterization of one of those components, macrophage inflammatory protein 1 beta.,” *Journal of Experimental Medicine*, vol. 168, no. 6, pp. 2251–2259, Dec. 1988, doi: 10.1084/jem.168.6.2251.
- [229] T. H. Schaller, K. A. Batich, C. M. Suryadevara, R. Desai, and J. H. Sampson, “Chemokines as adjuvants for immunotherapy: implications for immune activation with CCL3.,” *Expert Rev Clin Immunol*, vol. 13, no. 11, pp. 1049–1060, Nov. 2017, doi: 10.1080/1744666X.2017.1384313.
- [230] R. Chui and K. Dorovini-Zis, “Regulation of CCL2 and CCL3 expression in human brain endothelial cells by cytokines and lipopolysaccharide,” *J Neuroinflammation*, vol. 7, no. 1, p. 1, 2010, doi: 10.1186/1742-2094-7-1.
- [231] F. L’Episcopo *et al.*, “Reactive astrocytes and Wnt/ $\beta$ -catenin signaling link nigrostriatal injury to repair in 1-methyl-4-phenyl-1,2,3,6-tetrahydropyridine model of Parkinson’s disease,” *Neurobiol Dis*, vol. 41, no. 2, pp. 508–527, Feb. 2011, doi: 10.1016/j.nbd.2010.10.023.
- [232] B. Marchetti *et al.*, “Parkinson’s disease, aging and adult neurogenesis: Wnt/ $\beta$ -catenin signalling as the key to unlock the mystery of endogenous brain repair,” *Aging Cell*, vol. 19, no. 3, Mar. 2020, doi: 10.1111/acel.13101.
- [233] B. Marchetti, “Nrf2/Wnt resilience orchestrates rejuvenation of glia-neuron dialogue in Parkinson’s disease,” *Redox Biol*, vol. 36, p. 101664, Sep. 2020, doi: 10.1016/j.redox.2020.101664.
- [234] E. Armingol, A. Officer, O. Harismendy, and N. E. Lewis, “Deciphering cell–cell interactions and communication from gene expression,” *Nat Rev Genet*, vol. 22, no. 2, pp. 71–88, Feb. 2021, doi: 10.1038/s41576-020-00292-x.
- [235] A. C. Dixon, T. R. Dawson, D. Di Vizio, and A. M. Weaver, “Context-specific regulation of extracellular vesicle biogenesis and cargo selection,” *Nat Rev Mol Cell Biol*, vol. 24, no. 7, pp. 454–476, Jul. 2023, doi: 10.1038/s41580-023-00576-0.

- [236] M. Tkach and C. Théry, “Communication by Extracellular Vesicles: Where We Are and Where We Need to Go,” *Cell*, vol. 164, no. 6, pp. 1226–1232, Mar. 2016, doi: 10.1016/j.cell.2016.01.043.
- [237] E. Chargaff and R. West, “The Biological Significance of The Thromboplastic Proteins of Blood,” *J Biol Chem*, no. 7, 1946.
- [238] G. van Niel, G. D’Angelo, and G. Raposo, “Shedding light on the cell biology of extracellular vesicles,” *Nat Rev Mol Cell Biol*, vol. 19, no. 4, pp. 213–228, Apr. 2018, doi: 10.1038/nrm.2017.125.
- [239] B. L. Deatheragea and B. T. Cooksona, “Membrane vesicle release in bacteria, eukaryotes, and archaea: A conserved yet underappreciated aspect of microbial life,” *Infection and Immunity*. 2012. doi: 10.1128/IAI.06014-11.
- [240] R. A. Ñahui Palomino, C. Vanpouille, P. E. Costantini, and L. Margolis, “Microbiota–host communications: Bacterial extracellular vesicles as a common language,” *PLoS Pathog*, vol. 17, no. 5, p. e1009508, May 2021, doi: 10.1371/journal.ppat.1009508.
- [241] F. J. Verweij *et al.*, “The power of imaging to understand extracellular vesicle biology in vivo,” *Nat Methods*, vol. 18, no. 9, pp. 1013–1026, Sep. 2021, doi: 10.1038/s41592-021-01206-3.
- [242] M. Tkach, J. Kowal, and C. Théry, “Why the need and how to approach the functional diversity of extracellular vesicles,” *Philosophical Transactions of the Royal Society B: Biological Sciences*, vol. 373, no. 1737, p. 20160479, Jan. 2018, doi: 10.1098/rstb.2016.0479.
- [243] J. Saint-Pol, F. Gosselet, S. Duban-Deweere, G. Pottiez, and Y. Karamanos, “Targeting and Crossing the Blood-Brain Barrier with Extracellular Vesicles,” *Cells*, vol. 9, no. 4, p. 851, Apr. 2020, doi: 10.3390/cells9040851.
- [244] A. Yoshimura *et al.*, “Generation of a novel transgenic rat model for tracing extracellular vesicles in body fluids,” *Sci Rep*, vol. 6, no. 1, p. 31172, Aug. 2016, doi: 10.1038/srep31172.
- [245] B. Pang *et al.*, “Extracellular vesicles: the next generation of biomarkers for liquid biopsy-based prostate cancer diagnosis,” *Theranostics*, vol. 10, no. 5, pp. 2309–2326, 2020, doi: 10.7150/thno.39486.
- [246] I. K. Herrmann, M. J. A. Wood, and G. Fuhrmann, “Extracellular vesicles as a next-generation drug delivery platform,” *Nat Nanotechnol*, vol. 16, no. 7, pp. 748–759, Jul. 2021, doi: 10.1038/s41565-021-00931-2.
- [247] G. van Niel, D. R. F. Carter, A. Clayton, D. W. Lambert, G. Raposo, and P. Vader, “Challenges and directions in studying cell–cell communication by extracellular vesicles,” *Nat Rev Mol Cell Biol*, vol. 23, no. 5, pp. 369–382, May 2022, doi: 10.1038/s41580-022-00460-3.
- [248] A. Ghodasara, A. Raza, J. Wolfram, C. Salomon, and A. Popat, “Clinical Translation of Extracellular Vesicles,” *Adv Healthc Mater*, vol. 12, no. 28, Nov. 2023, doi: 10.1002/adhm.202301010.
- [249] Y. Couch *et al.*, “A brief history of nearly EV-erything – The rise and rise of extracellular vesicles,” *J Extracell Vesicles*, vol. 10, no. 14, 2021, doi: 10.1002/jev2.12144.

- [250] P. Wolf, "The Nature and Significance of Platelet Products in Human Plasma," *Br J Haematol*, vol. 13, no. 3, pp. 269–288, May 1967, doi: 10.1111/j.1365-2141.1967.tb08741.x.
- [251] E. A. Nunez, J. Wallis, and M. D. Gershon, "Secretory processes in follicular cells of the bat thyroid. III. The occurrence of extracellular vesicles and colloid droplets during arousal from hibernation," *American Journal of Anatomy*, vol. 141, no. 2, pp. 179–201, Oct. 1974, doi: 10.1002/aja.1001410203.
- [252] S. Aaronson, U. Behrens, R. Orner, and T. H. Haines, "Ultrastructure of intracellular and extracellular vesicles, membranes, and myelin figures produced by *Ochromonas danica*," *J Ultrastruct Res*, vol. 35, no. 5–6, pp. 418–430, Jun. 1971, doi: 10.1016/S0022-5320(71)80003-5.
- [253] A. G. Chigaleičhik, L. A. Belova, V. M. Grishchenko, and S. S. Rylkin, "[Several properties of the extracellular vesicles of *Candida tropicalis* yeasts grown on n-alkanes].," *Mikrobiologiya*, vol. 46, no. 3, pp. 467–71, 1977.
- [254] V. V Vysotskiĭ, I. K. Mazurova, and E. A. Shmeleva, "[Extracellular material of some representatives of the genus *Corynebacterium* (the electron microscopic aspect)].," *Zh Mikrobiol Epidemiol Immunobiol*, no. 8, pp. 90–5, Aug. 1977.
- [255] O. Käppeli and W. R. Finnerty, "Partition of alkane by an extracellular vesicle derived from hexadecane-grown *Acinetobacter*," *J Bacteriol*, vol. 140, no. 2, pp. 707–712, Nov. 1979, doi: 10.1128/jb.140.2.707-712.1979.
- [256] B.-T. Pan and R. M. Johnstone, "Fate of the transferrin receptor during maturation of sheep reticulocytes in vitro: Selective externalization of the receptor," *Cell*, vol. 33, no. 3, pp. 967–978, Jul. 1983, doi: 10.1016/0092-8674(83)90040-5.
- [257] A. MacKenzie, H. L. Wilson, E. Kiss-Toth, S. K. Dower, R. A. North, and A. Surprenant, "Rapid Secretion of Interleukin-1 $\beta$  by Microvesicle Shedding," *Immunity*, vol. 15, no. 5, pp. 825–835, Nov. 2001, doi: 10.1016/S1074-7613(01)00229-1.
- [258] G. Van Niel, "Intestinal epithelial exosomes carry MHC class II/peptides able to inform the immune system in mice," *Gut*, vol. 52, no. 12, pp. 1690–1697, Dec. 2003, doi: 10.1136/gut.52.12.1690.
- [259] S. Roy, F. H. Hochberg, and P. S. Jones, "Extracellular vesicles: the growth as diagnostics and therapeutics; a survey," *J Extracell Vesicles*, vol. 7, no. 1, Dec. 2018, doi: 10.1080/20013078.2018.1438720.
- [260] L. Zitvogel *et al.*, "Eradication of established murine tumors using a novel cell-free vaccine: dendritic cell derived exosomes," *Nat Med*, vol. 4, no. 5, pp. 594–600, May 1998, doi: 10.1038/nm0598-594.
- [261] R. Tenchov, J. M. Sasso, X. Wang, W.-S. Liaw, C.-A. Chen, and Q. A. Zhou, "Exosomes—Nature’s Lipid Nanoparticles, a Rising Star in Drug Delivery and Diagnostics," *ACS Nano*, vol. 16, no. 11, pp. 17802–17846, Nov. 2022, doi: 10.1021/acsnano.2c08774.
- [262] J. M. Street *et al.*, "Identification and proteomic profiling of exosomes in human cerebrospinal fluid," *J Transl Med*, vol. 10, no. 1, p. 5, Dec. 2012, doi: 10.1186/1479-5876-10-5.

- [263] H. Valadi, K. Ekström, A. Bossios, M. Sjöstrand, J. J. Lee, and J. O. Lötvall, “Exosome-mediated transfer of mRNAs and microRNAs is a novel mechanism of genetic exchange between cells,” *Nat Cell Biol*, vol. 9, no. 6, pp. 654–659, Jun. 2007, doi: 10.1038/ncb1596.
- [264] G. Raposo and W. Stoorvogel, “Extracellular vesicles: Exosomes, microvesicles, and friends,” *Journal of Cell Biology*, vol. 200, no. 4, pp. 373–383, Feb. 2013, doi: 10.1083/jcb.201211138.
- [265] M. Yáñez-Mó *et al.*, “Biological properties of extracellular vesicles and their physiological functions,” *J Extracell Vesicles*, vol. 4, no. 1, p. 27066, Jan. 2015, doi: 10.3402/jev.v4.27066.
- [266] C. Théry, S. Amigorena, G. Raposo, and A. Clayton, “Isolation and Characterization of Exosomes from Cell Culture Supernatants and Biological Fluids,” *Curr Protoc Cell Biol*, vol. 30, no. 1, Mar. 2006, doi: 10.1002/0471143030.cb0322s30.
- [267] S. L. N. Maas, X. O. Breakefield, and A. M. Weaver, “Extracellular Vesicles: Unique Intercellular Delivery Vehicles,” *Trends Cell Biol*, vol. 27, no. 3, pp. 172–188, Mar. 2017, doi: 10.1016/j.tcb.2016.11.003.
- [268] R. Kalluri and V. S. LeBleu, “The biology , function , and biomedical applications of exosomes,” *Science (1979)*, vol. 367, no. 6478, Feb. 2020, doi: 10.1126/science.aau6977.
- [269] J. F. Nabhan, R. Hu, R. S. Oh, S. N. Cohen, and Q. Lu, “Formation and release of arrestin domain-containing protein 1-mediated microvesicles (ARMMs) at plasma membrane by recruitment of TSG101 protein,” *Proceedings of the National Academy of Sciences*, vol. 109, no. 11, pp. 4146–4151, Mar. 2012, doi: 10.1073/pnas.1200448109.
- [270] J. E. Garrus *et al.*, “Tsg101 and the Vacuolar Protein Sorting Pathway Are Essential for HIV-1 Budding,” *Cell*, vol. 107, no. 1, pp. 55–65, Oct. 2001, doi: 10.1016/S0092-8674(01)00506-2.
- [271] W. M. Henne, N. J. Buchkovich, and S. D. Emr, “The ESCRT Pathway,” *Dev Cell*, vol. 21, no. 1, pp. 77–91, Jul. 2011, doi: 10.1016/j.devcel.2011.05.015.
- [272] J. H. Hurley and P. I. Hanson, “Membrane budding and scission by the ESCRT machinery: it’s all in the neck,” *Nat Rev Mol Cell Biol*, vol. 11, no. 8, pp. 556–566, Aug. 2010, doi: 10.1038/nrm2937.
- [273] J. Larios, V. Mercier, A. Roux, and J. Gruenberg, “ALIX- and ESCRT-III–dependent sorting of tetraspanins to exosomes,” *Journal of Cell Biology*, vol. 219, no. 3, Mar. 2020, doi: 10.1083/jcb.201904113.
- [274] M. A. Y. Adell *et al.*, “Recruitment dynamics of ESCRT-III and Vps4 to endosomes and implications for reverse membrane budding,” *Elife*, vol. 6, Oct. 2017, doi: 10.7554/eLife.31652.
- [275] M. Colombo *et al.*, “Analysis of ESCRT functions in exosome biogenesis, composition and secretion highlights the heterogeneity of extracellular vesicles,” *J Cell Sci*, Jan. 2013, doi: 10.1242/jcs.128868.
- [276] J. Donoso-Quezada, S. Ayala-Mar, and J. González-Valdez, “The role of lipids in exosome biology and intercellular communication: Function, analytics and applications,” *Traffic*, vol. 22, no. 7, pp. 204–220, Jul. 2021, doi: 10.1111/tra.12803.



- [277] M. A. Stepp, S. Pal-Ghosh, G. Tadvalkar, and A. Pajoohesh-Ganji, “Syndecan-1 and Its Expanding List of Contacts,” *Adv Wound Care (New Rochelle)*, vol. 4, no. 4, pp. 235–249, Apr. 2015, doi: 10.1089/wound.2014.0555.
- [278] M. F. Baietti *et al.*, “Syndecan–syntenin–ALIX regulates the biogenesis of exosomes,” *Nat Cell Biol*, vol. 14, no. 7, pp. 677–685, Jul. 2012, doi: 10.1038/ncb2502.
- [279] S. Fan *et al.*, “Glutamine deprivation alters the origin and function of cancer cell exosomes,” *EMBO J*, vol. 39, no. 16, Aug. 2020, doi: 10.15252/embj.2019103009.
- [280] N. Rocha *et al.*, “Cholesterol sensor ORP1L contacts the ER protein VAP to control Rab7–RILP–p150Glued and late endosome positioning,” *Journal of Cell Biology*, vol. 185, no. 7, pp. 1209–1225, Jun. 2009, doi: 10.1083/jcb.200811005.
- [281] K. Sobo *et al.*, “Late Endosomal Cholesterol Accumulation Leads to Impaired Intra-Endosomal Trafficking,” *PLoS One*, vol. 2, no. 9, p. e851, Sep. 2007, doi: 10.1371/journal.pone.0000851.
- [282] K. Trajkovic *et al.*, “Ceramide Triggers Budding of Exosome Vesicles into Multivesicular Endosomes,” *Science (1979)*, vol. 319, no. 5867, pp. 1244–1247, Feb. 2008, doi: 10.1126/science.1153124.
- [283] H. Matsuo *et al.*, “Role of LBPA and Alix in Multivesicular Liposome Formation and Endosome Organization,” *Science (1979)*, vol. 303, no. 5657, pp. 531–534, Jan. 2004, doi: 10.1126/science.1092425.
- [284] G. P. Otto and B. J. Nichols, “The roles of flotillin microdomains – endocytosis and beyond,” *J Cell Sci*, vol. 124, no. 23, pp. 3933–3940, Dec. 2011, doi: 10.1242/jcs.092015.
- [285] T. Kajimoto *et al.*, “Involvement of G $\beta\gamma$  subunits of Gi protein coupled with S1P receptor on multivesicular endosomes in F-actin formation and cargo sorting into exosomes,” *Journal of Biological Chemistry*, vol. 293, no. 1, pp. 245–253, Jan. 2018, doi: 10.1074/jbc.M117.808733.
- [286] S. M. Crivelli *et al.*, “Function of ceramide transfer protein for biogenesis and sphingolipid composition of extracellular vesicles,” *J Extracell Vesicles*, vol. 11, no. 6, Jun. 2022, doi: 10.1002/jev2.12233.
- [287] B. Barman *et al.*, “VAP-A and its binding partner CERT drive biogenesis of RNA-containing extracellular vesicles at ER membrane contact sites,” *Dev Cell*, vol. 57, no. 8, pp. 974–994.e8, Apr. 2022, doi: 10.1016/j.devcel.2022.03.012.
- [288] M. Fukushima, D. Dasgupta, A. S. Mauer, E. Kakazu, K. Nakao, and H. Malhi, “StAR-related lipid transfer domain 11 (STARD11)–mediated ceramide transport mediates extracellular vesicle biogenesis,” *Journal of Biological Chemistry*, vol. 293, no. 39, pp. 15277–15289, Sep. 2018, doi: 10.1074/jbc.RA118.002587.
- [289] G. van Niel *et al.*, “The Tetraspanin CD63 Regulates ESCRT-Independent and -Dependent Endosomal Sorting during Melanogenesis,” *Dev Cell*, vol. 21, no. 4, pp. 708–721, Oct. 2011, doi: 10.1016/j.devcel.2011.08.019.
- [290] B. Zimmerman *et al.*, “Crystal Structure of a Full-Length Human Tetraspanin Reveals a Cholesterol-Binding Pocket,” *Cell*, vol. 167, no. 4, pp. 1041–1051.e11, Nov. 2016, doi: 10.1016/j.cell.2016.09.056.
- [291] H. T. McMahon and E. Boucrot, “Membrane curvature at a glance,” *J Cell Sci*, vol. 128, no. 6, pp. 1065–1070, Mar. 2015, doi: 10.1242/jcs.114454.

- [292] S. N. Hurwitz, M. M. Conlon, M. A. Rider, N. C. Brownstein, and D. G. Meckes, “Nanoparticle analysis sheds budding insights into genetic drivers of extracellular vesicle biogenesis,” *J Extracell Vesicles*, vol. 5, no. 1, Jan. 2016, doi: 10.3402/jev.v5.31295.
- [293] N. Rabas *et al.*, “PINK1 drives production of mtDNA-containing extracellular vesicles to promote invasiveness,” *Journal of Cell Biology*, vol. 220, no. 12, Dec. 2021, doi: 10.1083/jcb.202006049.
- [294] M. L. Tognoli *et al.*, “Lack of involvement of CD63 and CD9 tetraspanins in the extracellular vesicle content delivery process,” *Commun Biol*, vol. 6, no. 1, p. 532, May 2023, doi: 10.1038/s42003-023-04911-1.
- [295] S. H. Petersen, E. Odintsova, T. A. Haigh, A. B. Rickinson, G. S. Taylor, and F. Berditchevski, “The role of tetraspanin CD63 in antigen presentation via MHC class II,” *Eur J Immunol*, vol. 41, no. 9, pp. 2556–2561, Sep. 2011, doi: 10.1002/eji.201141438.
- [296] S. Gurung, D. Perocheau, L. Touramanidou, and J. Baruteau, “The exosome journey: from biogenesis to uptake and intracellular signalling,” *Cell Communication and Signaling*, vol. 19, no. 1, p. 47, Apr. 2021, doi: 10.1186/s12964-021-00730-1.
- [297] E. Cocucci, G. Racchetti, and J. Meldolesi, “Shedding microvesicles: artefacts no more,” *Trends Cell Biol*, vol. 19, no. 2, pp. 43–51, Feb. 2009, doi: 10.1016/j.tcb.2008.11.003.
- [298] D. Di Vizio *et al.*, “Oncosome Formation in Prostate Cancer: Association with a Region of Frequent Chromosomal Deletion in Metastatic Disease,” *Cancer Res*, vol. 69, no. 13, pp. 5601–5609, Jul. 2009, doi: 10.1158/0008-5472.CAN-08-3860.
- [299] M. Battistelli and E. Falcieri, “Apoptotic Bodies: Particular Extracellular Vesicles Involved in Intercellular Communication,” *Biology (Basel)*, vol. 9, no. 1, p. 21, Jan. 2020, doi: 10.3390/biology9010021.
- [300] I. K. H. Poon *et al.*, “Unexpected link between an antibiotic, pannexin channels and apoptosis,” *Nature*, vol. 507, no. 7492, pp. 329–334, Mar. 2014, doi: 10.1038/nature13147.
- [301] G. K. Atkin-Smith *et al.*, “A novel mechanism of generating extracellular vesicles during apoptosis via a beads-on-a-string membrane structure,” *Nat Commun*, vol. 6, no. 1, p. 7439, Jun. 2015, doi: 10.1038/ncomms8439.
- [302] K. W. Witwer *et al.*, “Standardization of sample collection, isolation and analysis methods in extracellular vesicle research,” *J Extracell Vesicles*, vol. 2, no. 1, p. 20360, Jan. 2013, doi: 10.3402/jev.v2i0.20360.
- [303] P. Duong, A. Chung, L. Bouchareychas, and R. L. Raffai, “Cushioned-Density Gradient Ultracentrifugation (C-DGUC) improves the isolation efficiency of extracellular vesicles,” *PLoS One*, vol. 14, no. 4, p. e0215324, Apr. 2019, doi: 10.1371/journal.pone.0215324.
- [304] M. A. Livshits *et al.*, “Isolation of exosomes by differential centrifugation: Theoretical analysis of a commonly used protocol,” *Sci Rep*, vol. 5, no. 1, p. 17319, Nov. 2015, doi: 10.1038/srep17319.
- [305] M. L. Heinemann and J. Vykoukal, “Sequential Filtration: A Gentle Method for the Isolation of Functional Extracellular Vesicles,” 2017, pp. 33–41. doi: 10.1007/978-1-4939-7253-1\_4.

- [306] M. A. Rider, S. N. Hurwitz, and D. G. Meckes, “ExtraPEG: A Polyethylene Glycol-Based Method for Enrichment of Extracellular Vesicles,” *Sci Rep*, vol. 6, no. 1, p. 23978, Apr. 2016, doi: 10.1038/srep23978.
- [307] E. Willms, C. Cabañas, I. Mäger, M. J. A. Wood, and P. Vader, “Extracellular Vesicle Heterogeneity: Subpopulations, Isolation Techniques, and Diverse Functions in Cancer Progression,” *Front Immunol*, vol. 9, Apr. 2018, doi: 10.3389/fimmu.2018.00738.
- [308] A. Akbar, F. Malekian, N. Baghban, S. P. Kodam, and M. Ullah, “Methodologies to Isolate and Purify Clinical Grade Extracellular Vesicles for Medical Applications,” *Cells*, vol. 11, no. 2, p. 186, Jan. 2022, doi: 10.3390/cells11020186.
- [309] G. Corso *et al.*, “Reproducible and scalable purification of extracellular vesicles using combined bind-elute and size exclusion chromatography,” *Sci Rep*, vol. 7, no. 1, p. 11561, Sep. 2017, doi: 10.1038/s41598-017-10646-x.
- [310] L. Filipović *et al.*, “Affinity-based isolation of extracellular vesicles by means of single-domain antibodies bound to macroporous methacrylate-based copolymer,” *N Biotechnol*, vol. 69, pp. 36–48, Jul. 2022, doi: 10.1016/j.nbt.2022.03.001.
- [311] L. Leggio *et al.*, “Label-free approaches for extracellular vesicle detection,” *iScience*, vol. 26, no. 11, p. 108105, Nov. 2023, doi: 10.1016/j.isci.2023.108105.
- [312] H. Zhang and D. Lyden, “Asymmetric-flow field-flow fractionation technology for exomere and small extracellular vesicle separation and characterization,” *Nat Protoc*, vol. 14, no. 4, pp. 1027–1053, Apr. 2019, doi: 10.1038/s41596-019-0126-x.
- [313] C. Théry *et al.*, “Minimal information for studies of extracellular vesicles 2018 (MISEV2018): a position statement of the International Society for Extracellular Vesicles and update of the MISEV2014 guidelines,” *J Extracell Vesicles*, vol. 7, no. 1, p. 1535750, Dec. 2018, doi: 10.1080/20013078.2018.1535750.
- [314] K. W. Witwer *et al.*, “Updating MISEV: Evolving the minimal requirements for studies of extracellular vesicles,” *J Extracell Vesicles*, vol. 10, no. 14, Dec. 2021, doi: 10.1002/jev2.12182.
- [315] R. Poupardin, M. Wolf, and D. Strunk, “Adherence to minimal experimental requirements for defining extracellular vesicles and their functions,” *Adv Drug Deliv Rev*, vol. 176, p. 113872, Sep. 2021, doi: 10.1016/j.addr.2021.113872.
- [316] T. Skotland, K. Sagini, K. Sandvig, and A. Llorente, “An emerging focus on lipids in extracellular vesicles,” *Adv Drug Deliv Rev*, vol. 159, pp. 308–321, 2020, doi: 10.1016/j.addr.2020.03.002.
- [317] E. R. Abels and X. O. Breakefield, “Introduction to Extracellular Vesicles: Biogenesis, RNA Cargo Selection, Content, Release, and Uptake,” *Cell Mol Neurobiol*, vol. 36, no. 3, pp. 301–312, Apr. 2016, doi: 10.1007/s10571-016-0366-z.
- [318] J. Jankovičová, P. Sečová, K. Michalková, and J. Antalíková, “Tetraspanins, More than Markers of Extracellular Vesicles in Reproduction,” *Int J Mol Sci*, vol. 21, no. 20, p. 7568, Oct. 2020, doi: 10.3390/ijms21207568.
- [319] H. W. Choi *et al.*, “Perivascular dendritic cells elicit anaphylaxis by relaying allergens to mast cells via microvesicles,” *Science (1979)*, vol. 362, no. 6415, Nov. 2018, doi: 10.1126/science.aao0666.

- [320] L. Salimi *et al.*, “Synergies in exosomes and autophagy pathways for cellular homeostasis and metastasis of tumor cells,” *Cell Biosci*, vol. 10, no. 1, p. 64, Dec. 2020, doi: 10.1186/s13578-020-00426-y.
- [321] S. Gurunathan, M.-H. Kang, M. Qasim, K. Khan, and J.-H. Kim, “Biogenesis, Membrane Trafficking, Functions, and Next Generation Nanotherapeutics Medicine of Extracellular Vesicles,” *Int J Nanomedicine*, vol. Volume 16, pp. 3357–3383, May 2021, doi: 10.2147/IJN.S310357.
- [322] J. Kowal *et al.*, “Proteomic comparison defines novel markers to characterize heterogeneous populations of extracellular vesicle subtypes,” *Proceedings of the National Academy of Sciences*, vol. 113, no. 8, Feb. 2016, doi: 10.1073/pnas.1521230113.
- [323] G. Soto-Herederó, F. Baixauli, and M. Mittelbrunn, “Interorganelle Communication between Mitochondria and the Endolysosomal System,” *Front Cell Dev Biol*, vol. 5, Nov. 2017, doi: 10.3389/fcell.2017.00095.
- [324] D. Torralba, F. Baixauli, and F. Sánchez-Madrid, “Mitochondria Know No Boundaries: Mechanisms and Functions of Intercellular Mitochondrial Transfer,” *Front Cell Dev Biol*, vol. 4, Sep. 2016, doi: 10.3389/fcell.2016.00107.
- [325] D. Liu, Z. Dong, J. Wang, Y. Tao, X. Sun, and X. Yao, “The existence and function of mitochondrial component in extracellular vesicles,” *Mitochondrion*, vol. 54, pp. 122–127, Sep. 2020, doi: 10.1016/j.mito.2020.08.005.
- [326] L. Popov, “Mitochondrial-derived vesicles: Recent insights,” *J Cell Mol Med*, vol. 26, no. 12, pp. 3323–3328, Jun. 2022, doi: 10.1111/jcmm.17391.
- [327] C. Chun *et al.*, “Astrocyte-derived extracellular vesicles enhance the survival and electrophysiological function of human cortical neurons in vitro,” *Biomaterials*, vol. 271, p. 120700, Apr. 2021, doi: 10.1016/j.biomaterials.2021.120700.
- [328] T. Montecchi *et al.*, “Differential Proteomic Analysis of Astrocytes and Astrocytes-Derived Extracellular Vesicles from Control and Rai Knockout Mice: Insights into the Mechanisms of Neuroprotection,” *Int J Mol Sci*, vol. 22, no. 15, p. 7933, Jul. 2021, doi: 10.3390/ijms22157933.
- [329] Y. You *et al.*, “Human neural cell type-specific extracellular vesicle proteome defines disease-related molecules associated with activated astrocytes in Alzheimer’s disease brain,” *J Extracell Vesicles*, vol. 11, no. 1, Jan. 2022, doi: 10.1002/jev2.12183.
- [330] H. Lee, C. Li, Y. Zhang, D. Zhang, L. E. Otterbein, and Y. Jin, “Caveolin-1 selectively regulates microRNA sorting into microvesicles after noxious stimuli,” *Journal of Experimental Medicine*, vol. 216, no. 9, pp. 2202–2220, Sep. 2019, doi: 10.1084/jem.20182313.
- [331] X.-M. Liu, L. Ma, and R. Schekman, “Selective sorting of microRNAs into exosomes by phase-separated YBX1 condensates,” *Elife*, vol. 10, Nov. 2021, doi: 10.7554/eLife.71982.
- [332] R. Garcia-Martin *et al.*, “MicroRNA sequence codes for small extracellular vesicle release and cellular retention,” *Nature*, vol. 601, no. 7893, pp. 446–451, Jan. 2022, doi: 10.1038/s41586-021-04234-3.
- [333] K. M. Kim, K. Abdelmohsen, M. Mustapic, D. Kapogiannis, and M. Gorospe, “RNA in extracellular vesicles,” *Wiley Interdiscip Rev RNA*, vol. 8, no. 4, p. e1413, Jul. 2017, doi: 10.1002/wrna.1413.

- [334] E. R. Dellar, C. Hill, G. E. Melling, D. R. F. Carter, and L. A. Baena-Lopez, “Unpacking extracellular vesicles: RNA cargo loading and function,” *Journal of Extracellular Biology*, vol. 1, no. 5, May 2022, doi: 10.1002/jex2.40.
- [335] A. Datta Chaudhuri, R. M. Dasgheyb, L. R. DeVine, H. Bi, R. N. Cole, and N. J. Haughey, “Stimulus-dependent modifications in astrocyte-derived extracellular vesicle cargo regulate neuronal excitability,” *Glia*, vol. 68, no. 1, pp. 128–144, Jan. 2020, doi: 10.1002/glia.23708.
- [336] A. D. Chaudhuri *et al.*, “TNF $\alpha$  and IL-1 $\beta$  modify the miRNA cargo of astrocyte shed extracellular vesicles to regulate neurotrophic signaling in neurons article,” *Cell Death Dis*, vol. 9, no. 3, 2018, doi: 10.1038/s41419-018-0369-4.
- [337] S. Grabuschnig *et al.*, “Putative Origins of Cell-Free DNA in Humans: A Review of Active and Passive Nucleic Acid Release Mechanisms,” *Int J Mol Sci*, vol. 21, no. 21, p. 8062, Oct. 2020, doi: 10.3390/ijms21218062.
- [338] J. Elzanowska, C. Semira, and B. Costa-Silva, “DNA in extracellular vesicles: biological and clinical aspects,” *Mol Oncol*, vol. 15, no. 6, pp. 1701–1714, Jun. 2021, doi: 10.1002/1878-0261.12777.
- [339] B. K. Thakur *et al.*, “Double-stranded DNA in exosomes: a novel biomarker in cancer detection,” *Cell Res*, vol. 24, no. 6, pp. 766–769, Jun. 2014, doi: 10.1038/cr.2014.44.
- [340] A. Takahashi *et al.*, “Exosomes maintain cellular homeostasis by excreting harmful DNA from cells,” *Nat Commun*, vol. 8, no. 1, p. 15287, May 2017, doi: 10.1038/ncomms15287.
- [341] S. Fischer *et al.*, “Indication of Horizontal DNA Gene Transfer by Extracellular Vesicles,” *PLoS One*, vol. 11, no. 9, p. e0163665, Sep. 2016, doi: 10.1371/journal.pone.0163665.
- [342] A. Anel, A. Gallego-Lleyda, D. de Miguel, J. Naval, and L. Martínez-Lostao, “Role of Exosomes in the Regulation of T-cell Mediated Immune Responses and in Autoimmune Disease,” *Cells*, vol. 8, no. 2, p. 154, Feb. 2019, doi: 10.3390/cells8020154.
- [343] M. Colombo, G. Raposo, and C. Théry, “Biogenesis, Secretion, and Intercellular Interactions of Exosomes and Other Extracellular Vesicles,” *Annu Rev Cell Dev Biol*, 2014, doi: 10.1146/annurev-cellbio-101512-122326.
- [344] E. Eitan, C. Suire, S. Zhang, and M. P. Mattson, “Impact of lysosome status on extracellular vesicle content and release,” *Ageing Research Reviews*. 2016. doi: 10.1016/j.arr.2016.05.001.
- [345] A. Bécot, C. Volgers, and G. van Niel, “Transmissible Endosomal Intoxication: A Balance between Exosomes and Lysosomes at the Basis of Intercellular Amyloid Propagation,” *Biomedicines*, vol. 8, no. 8, p. 272, Aug. 2020, doi: 10.3390/biomedicines8080272.
- [346] R. Palmulli and G. van Niel, “To be or not to be... secreted as exosomes, a balance finely tuned by the mechanisms of biogenesis,” *Essays Biochem*, vol. 62, no. 2, pp. 177–191, May 2018, doi: 10.1042/EBC20170076.
- [347] C. Villarroya-Beltri *et al.*, “ISGylation controls exosome secretion by promoting lysosomal degradation of MVB proteins,” *Nat Commun*, vol. 7, no. 1, p. 13588, Nov. 2016, doi: 10.1038/ncomms13588.
- [348] M. Ostrowski *et al.*, “Rab27a and Rab27b control different steps of the exosome secretion pathway,” *Nat Cell Biol*, vol. 12, no. 1, pp. 19–30, Jan. 2010, doi: 10.1038/ncb2000.

- [349] F. W. Pfrieger and N. Vitale, “Thematic Review Series: Exosomes and Microvesicles: Lipids as Key Components of their Biogenesis and Functions, Cholesterol and the journey of extracellular vesicles,” *J Lipid Res*, vol. 59, no. 12, pp. 2255–2261, Dec. 2018, doi: 10.1194/jlr.R084210.
- [350] W. Möbius *et al.*, “Recycling Compartments and the Internal Vesicles of Multivesicular Bodies Harbor Most of the Cholesterol Found in the Endocytic Pathway,” *Traffic*, vol. 4, no. 4, pp. 222–231, Apr. 2003, doi: 10.1034/j.1600-0854.2003.00072.x.
- [351] R. Jahn and R. H. Scheller, “SNAREs — engines for membrane fusion,” *Nat Rev Mol Cell Biol*, vol. 7, no. 9, pp. 631–643, Sep. 2006, doi: 10.1038/nrm2002.
- [352] A. Savina, M. Furlán, M. Vidal, and M. I. Colombo, “Exosome Release Is Regulated by a Calcium-dependent Mechanism in K562 Cells,” *Journal of Biological Chemistry*, vol. 278, no. 22, pp. 20083–20090, May 2003, doi: 10.1074/jbc.M301642200.
- [353] F. Baixauli, C. L<sup>3</sup>pez-Ot<sup>3</sup>n, and M. Mittelbrunn, “Exosomes and Autophagy: Coordinated Mechanisms for the Maintenance of Cellular Fitness,” *Front Immunol*, vol. 5, Aug. 2014, doi: 10.3389/fimmu.2014.00403.
- [354] M. V. S. Dias *et al.*, “PRNP/prion protein regulates the secretion of exosomes modulating CAV1/caveolin-1-suppressed autophagy,” *Autophagy*, vol. 12, no. 11, pp. 2113–2128, Nov. 2016, doi: 10.1080/15548627.2016.1226735.
- [355] Y. Zhang, Y. Liu, H. Liu, and W. H. Tang, “Exosomes: biogenesis, biologic function and clinical potential,” *Cell Biosci*, vol. 9, no. 1, p. 19, Dec. 2019, doi: 10.1186/s13578-019-0282-2.
- [356] K. Rilla, “Diverse plasma membrane protrusions act as platforms for extracellular vesicle shedding,” *J Extracell Vesicles*, vol. 10, no. 11, Sep. 2021, doi: 10.1002/jev2.12148.
- [357] D. M. Leite, D. Matias, and G. Battaglia, “The Role of BAR Proteins and the Glycocalyx in Brain Endothelium Transcytosis,” *Cells*, vol. 9, no. 12, p. 2685, Dec. 2020, doi: 10.3390/cells9122685.
- [358] S. Schlienger, S. Campbell, and A. Claing, “ARF1 regulates the Rho/MLC pathway to control EGF-dependent breast cancer cell invasion,” *Mol Biol Cell*, vol. 25, no. 1, pp. 17–29, Jan. 2014, doi: 10.1091/mbc.e13-06-0335.
- [359] A. E. Sedgwick, J. W. Clancy, M. Olivia Balmert, and C. D’Souza-Schorey, “Extracellular microvesicles and invadopodia mediate non-overlapping modes of tumor cell invasion,” *Sci Rep*, vol. 5, no. 1, p. 14748, Oct. 2015, doi: 10.1038/srep14748.
- [360] M. Mathieu, L. Martin-Jaular, G. Lavieu, and C. Théry, “Specificities of secretion and uptake of exosomes and other extracellular vesicles for cell-to-cell communication,” *Nat Cell Biol*, vol. 21, no. 1, pp. 9–17, Jan. 2019, doi: 10.1038/s41556-018-0250-9.
- [361] D. Wu *et al.*, “Profiling surface proteins on individual exosomes using a proximity barcoding assay,” *Nat Commun*, vol. 10, no. 1, p. 3854, Aug. 2019, doi: 10.1038/s41467-019-11486-1.
- [362] A. Hoshino *et al.*, “Tumour exosome integrins determine organotropic metastasis,” *Nature*, vol. 527, no. 7578, pp. 329–335, Nov. 2015, doi: 10.1038/nature15756.
- [363] G. I. Perez *et al.*, “Phosphatidylserine-Exposing Annexin A1-Positive Extracellular Vesicles: Potential Cancer Biomarkers,” *Vaccines (Basel)*, vol. 11, no. 3, p. 639, Mar. 2023, doi: 10.3390/vaccines11030639.

- [364] M. Heidarzadeh, A. Zarebkohan, R. Rahbarghazi, and E. Sokullu, “Protein corona and exosomes: new challenges and prospects,” *Cell Communication and Signaling*, vol. 21, no. 1, p. 64, Mar. 2023, doi: 10.1186/s12964-023-01089-1.
- [365] M. Wolf *et al.*, “A functional corona around extracellular vesicles enhances angiogenesis, skin regeneration and immunomodulation,” *J Extracell Vesicles*, vol. 11, no. 4, Apr. 2022, doi: 10.1002/jev2.12207.
- [366] E. I. Buzas, “Opportunities and challenges in studying the extracellular vesicle corona,” *Nat Cell Biol*, vol. 24, no. 9, pp. 1322–1325, Sep. 2022, doi: 10.1038/s41556-022-00983-z.
- [367] A. E. Morelli *et al.*, “Endocytosis, intracellular sorting, and processing of exosomes by dendritic cells,” *Blood*, vol. 104, no. 10, pp. 3257–3266, Nov. 2004, doi: 10.1182/blood-2004-03-0824.
- [368] E. I. Buzás, E. Á. Tóth, B. W. Sódar, and K. É. Szabó-Taylor, “Molecular interactions at the surface of extracellular vesicles,” *Semin Immunopathol*, vol. 40, no. 5, pp. 453–464, Sep. 2018, doi: 10.1007/s00281-018-0682-0.
- [369] S. Tabak, S. Schreiber-Avissar, and E. Beit-Yannai, “Influence of Anti-Glaucoma Drugs on Uptake of Extracellular Vesicles by Trabecular Meshwork Cells,” *Int J Nanomedicine*, vol. Volume 16, pp. 1067–1081, Feb. 2021, doi: 10.2147/IJN.S283164.
- [370] V. Luga *et al.*, “Exosomes Mediate Stromal Mobilization of Autocrine Wnt-PCP Signaling in Breast Cancer Cell Migration,” *Cell*, vol. 151, no. 7, pp. 1542–1556, Dec. 2012, doi: 10.1016/j.cell.2012.11.024.
- [371] S. Yamamoto, E. Azuma, M. Muramatsu, T. Hamashima, Y. Ishii, and M. Sasahara, “Significance of Extracellular Vesicles: Pathobiological Roles in Disease,” *Cell Struct Funct*, vol. 41, no. 2, pp. 137–143, 2016, doi: 10.1247/csf.16014.
- [372] K. J. McKelvey, K. L. Powell, A. W. Ashton, J. M. Morris, and S. A. McCracken, “Exosomes: Mechanisms of Uptake,” *J Circ Biomark*, vol. 4, p. 7, Nov. 2015, doi: 10.5772/61186.
- [373] K. O’Brien, S. Ughetto, S. Mahjoun, A. V. Nair, and X. O. Breakefield, “Uptake, functionality, and re-release of extracellular vesicle-encapsulated cargo,” *Cell Rep*, vol. 39, no. 2, p. 110651, Apr. 2022, doi: 10.1016/j.celrep.2022.110651.
- [374] T. Tian *et al.*, “Exosome Uptake through Clathrin-mediated Endocytosis and Macropinocytosis and Mediating miR-21 Delivery,” *Journal of Biological Chemistry*, vol. 289, no. 32, pp. 22258–22267, Aug. 2014, doi: 10.1074/jbc.M114.588046.
- [375] G. J. Doherty and H. T. McMahon, “Mechanisms of Endocytosis,” *Annu Rev Biochem*, vol. 78, no. 1, pp. 857–902, Jun. 2009, doi: 10.1146/annurev.biochem.78.081307.110540.
- [376] I. Nakase, N. B. Kobayashi, T. Takatani-Nakase, and T. Yoshida, “Active macropinocytosis induction by stimulation of epidermal growth factor receptor and oncogenic Ras expression potentiates cellular uptake efficacy of exosomes,” *Sci Rep*, vol. 5, no. 1, p. 10300, Jun. 2015, doi: 10.1038/srep10300.
- [377] D. Feng *et al.*, “Cellular Internalization of Exosomes Occurs Through Phagocytosis,” *Traffic*, vol. 11, no. 5, pp. 675–687, May 2010, doi: 10.1111/j.1600-0854.2010.01041.x.
- [378] K. Sapoń, R. Mańka, T. Janas, and T. Janas, “The role of lipid rafts in vesicle formation,” *J Cell Sci*, vol. 136, no. 9, May 2023, doi: 10.1242/jcs.260887.

- [379] L. A. Mulcahy, R. C. Pink, and D. R. F. Carter, “Routes and mechanisms of extracellular vesicle uptake.,” *J Extracell Vesicles*, vol. 3, 2014, doi: 10.3402/jev.v3.24641.
- [380] H. Wei, J.-D. M. Malcor, and M. T. Harper, “Lipid rafts are essential for release of phosphatidylserine-exposing extracellular vesicles from platelets,” *Sci Rep*, vol. 8, no. 1, p. 9987, Jul. 2018, doi: 10.1038/s41598-018-28363-4.
- [381] D. E. Murphy *et al.*, “Extracellular vesicle-based therapeutics: natural versus engineered targeting and trafficking,” *Exp Mol Med*, vol. 51, no. 3, p. 32, Mar. 2019, doi: 10.1038/s12276-019-0223-5.
- [382] A. E. Russell *et al.*, “Biological membranes in EV biogenesis, stability, uptake, and cargo transfer: an ISEV position paper arising from the ISEV membranes and EVs workshop,” *J Extracell Vesicles*, vol. 8, no. 1, p. 1684862, Dec. 2019, doi: 10.1080/20013078.2019.1684862.
- [383] M. Karmacharya, S. Kumar, and Y.-K. Cho, “Tuning the Extracellular Vesicles Membrane through Fusion for Biomedical Applications,” *J Funct Biomater*, vol. 14, no. 2, p. 117, Feb. 2023, doi: 10.3390/jfb14020117.
- [384] B. S. Joshi, M. A. de Beer, B. N. G. Giepmans, and I. S. Zuhorn, “Endocytosis of Extracellular Vesicles and Release of Their Cargo from Endosomes,” *ACS Nano*, vol. 14, no. 4, pp. 4444–4455, Apr. 2020, doi: 10.1021/acsnano.9b10033.
- [385] S. Dagar and S. Subramaniam, “Tunneling Nanotube: An Enticing Cell–Cell Communication in the Nervous System,” *Biology (Basel)*, vol. 12, no. 10, p. 1288, Sep. 2023, doi: 10.3390/biology12101288.
- [386] C. Zurzolo, “Tunneling nanotubes: Reshaping connectivity,” *Curr Opin Cell Biol*, vol. 71, pp. 139–147, Aug. 2021, doi: 10.1016/j.ceb.2021.03.003.
- [387] M. Catalano and L. O’Driscoll, “Inhibiting extracellular vesicles formation and release: a review of EV inhibitors,” *J Extracell Vesicles*, vol. 9, no. 1, Sep. 2020, doi: 10.1080/20013078.2019.1703244.
- [388] J. A. D. Wattis *et al.*, “Mathematical Model for Low Density Lipoprotein (LDL) Endocytosis by Hepatocytes,” *Bull Math Biol*, vol. 70, no. 8, pp. 2303–2333, Nov. 2008, doi: 10.1007/s11538-008-9347-9.
- [389] S. K. Gandham, H. Z. Attarwala, and M. M. Amiji, “Mathematical Modeling and Experimental Validation of Extracellular Vesicle-Mediated Tumor Suppressor MicroRNA Delivery and Propagation in Ovarian Cancer Cells,” *Mol Pharm*, vol. 19, no. 11, pp. 4067–4079, Nov. 2022, doi: 10.1021/acs.molpharmaceut.2c00525.
- [390] A. Lombardo, G. Morabito, C. Panarello, and F. Pappalardo, “Modeling biological receivers,” in *Proceedings of the 9th ACM International Conference on Nanoscale Computing and Communication*, New York, NY, USA: ACM, Oct. 2022, pp. 1–6. doi: 10.1145/3558583.3558847.
- [391] E. Shaba *et al.*, “Multi-Omics Integrative Approach of Extracellular Vesicles: A Future Challenging Milestone,” *Proteomes*, vol. 10, no. 2, p. 12, Apr. 2022, doi: 10.3390/proteomes10020012.
- [392] O. P. B. Wiklander, M. Brennan, J. Lötvall, X. O. Breakefield, and S. E. L. Andaloussi, “Advances in therapeutic applications of extracellular vesicles,” *Science Translational Medicine*. 2019. doi: 10.1126/scitranslmed.aav8521.



- [393] J. McKiernan *et al.*, “A Prospective Adaptive Utility Trial to Validate Performance of a Novel Urine Exosome Gene Expression Assay to Predict High-grade Prostate Cancer in Patients with Prostate-specific Antigen 2–10 ng/ml at Initial Biopsy,” *Eur Urol*, vol. 74, no. 6, pp. 731–738, Dec. 2018, doi: 10.1016/j.eururo.2018.08.019.
- [394] L. Leggio *et al.*, “Extracellular Vesicles as Novel Diagnostic and Prognostic Biomarkers for Parkinson’s Disease,” *Aging Dis*, vol. 12, no. 6, p. 1494, 2021, doi: 10.14336/AD.2021.0527.
- [395] A. K. Azad, T. Raihan, J. Ahmed, A. Hakim, T. H. Emon, and P. A. Chowdhury, “Human Aquaporins: Functional Diversity and Potential Roles in Infectious and Non-infectious Diseases,” *Front Genet*, vol. 12, Mar. 2021, doi: 10.3389/fgene.2021.654865.
- [396] T. Pisitkun, R.-F. Shen, and M. A. Knepper, “Identification and proteomic profiling of exosomes in human urine,” *Proceedings of the National Academy of Sciences*, vol. 101, no. 36, pp. 13368–13373, Sep. 2004, doi: 10.1073/pnas.0403453101.
- [397] G. Zhang *et al.*, “New Perspectives on Roles of Alpha-Synuclein in Parkinson’s Disease,” *Front Aging Neurosci*, 2018, doi: 10.3389/fnagi.2018.00370.
- [398] M. Niu *et al.*, “A longitudinal study on  $\alpha$ -synuclein in plasma neuronal exosomes as a biomarker for Parkinson’s disease development and progression,” *Eur J Neurol*, 2020, doi: 10.1111/ene.14208.
- [399] L. Parnetti *et al.*, “CSF and blood biomarkers for Parkinson’s disease,” *Lancet Neurol*, vol. 18, no. 6, pp. 573–586, Jun. 2019, doi: 10.1016/S1474-4422(19)30024-9.
- [400] L. Wang and L. Zhang, “Circulating Exosomal miRNA as Diagnostic Biomarkers of Neurodegenerative Diseases,” *Front Mol Neurosci*, vol. 13, Apr. 2020, doi: 10.3389/fnmol.2020.00053.
- [401] J. A. Saugstad *et al.*, “Analysis of extracellular RNA in cerebrospinal fluid,” *J Extracell Vesicles*, vol. 6, no. 1, p. 1317577, Dec. 2017, doi: 10.1080/20013078.2017.1317577.
- [402] X. Y. Cao *et al.*, “MicroRNA biomarkers of Parkinson’s disease in serum exosome-like microvesicles,” *Neurosci Lett*, 2017, doi: 10.1016/j.neulet.2017.02.045.
- [403] E. J. Goetzl *et al.*, “Altered lysosomal proteins in neural-derived plasma exosomes in preclinical Alzheimer disease,” *Neurology*, 2015, doi: 10.1212/WNL.0000000000001702.
- [404] Y. You *et al.*, “ATP1A3 as a target for isolating neuron-specific extracellular vesicles from human brain and biofluids,” *Sci Adv*, vol. 9, no. 37, Sep. 2023, doi: 10.1126/sciadv.adi3647.
- [405] D. E. Gomes and K. W. Witwer, “L1CAM-associated extracellular vesicles: A systematic review of nomenclature, sources, separation, and characterization,” *Journal of Extracellular Biology*, vol. 1, no. 3, Mar. 2022, doi: 10.1002/jex2.35.
- [406] L. Leggio *et al.*, “Extracellular Vesicles as Nanotherapeutics for Parkinson’s Disease,” *Biomolecules*, vol. 10, no. 9, p. 1327, Sep. 2020, doi: 10.3390/biom10091327.
- [407] S. Ohno, G. Drummen, and M. Kuroda, “Focus on Extracellular Vesicles: Development of Extracellular Vesicle-Based Therapeutic Systems,” *Int J Mol Sci*, vol. 17, no. 2, p. 172, Feb. 2016, doi: 10.3390/ijms17020172.

- [408] A. Jarmalaviciute and A. Pivoriunas, “Neuroprotective properties of extracellular vesicles derived from mesenchymal stem cells,” *Neural Regen Res*, vol. 11, no. 6, p. 904, 2016, doi: 10.4103/1673-5374.184480.
- [409] K. Narbutė *et al.*, “Intranasal Administration of Extracellular Vesicles Derived from Human Teeth Stem Cells Improves Motor Symptoms and Normalizes Tyrosine Hydroxylase Expression in the Substantia Nigra and Striatum of the 6-Hydroxydopamine-Treated Rats,” *Stem Cells Transl Med*, 2019, doi: 10.1002/sctm.18-0162.
- [410] R. Kojima *et al.*, “Designer exosomes produced by implanted cells intracerebrally deliver therapeutic cargo for Parkinson’s disease treatment,” *Nat Commun*, vol. 9, no. 1, 2018, doi: 10.1038/s41467-018-03733-8.
- [411] X. Xia, Y. Wang, and J. C. Zheng, “Extracellular vesicles, from the pathogenesis to the therapy of neurodegenerative diseases,” *Transl Neurodegener*, vol. 11, no. 1, p. 53, Dec. 2022, doi: 10.1186/s40035-022-00330-0.
- [412] W. Zhang, D. Xiao, Q. Mao, and H. Xia, “Role of neuroinflammation in neurodegeneration development,” *Signal Transduct Target Ther*, vol. 8, no. 1, p. 267, Jul. 2023, doi: 10.1038/s41392-023-01486-5.
- [413] X. Zhuang *et al.*, “Treatment of brain inflammatory diseases by delivering exosome encapsulated anti-inflammatory drugs from the nasal region to the brain,” *Molecular Therapy*, 2011, doi: 10.1038/mt.2011.164.
- [414] R. Pascua-Maestro, E. González, C. Lillo, M. D. Ganformina, J. M. Falcón-Pérez, and D. Sanchez, “Extracellular Vesicles Secreted by Astroglial Cells Transport Apolipoprotein D to Neurons and Mediate Neuronal Survival Upon Oxidative Stress,” *Front Cell Neurosci*, vol. 12, Jan. 2019, doi: 10.3389/fncel.2018.00526.
- [415] Y. Zhao *et al.*, “GDNF-transfected macrophages produce potent neuroprotective effects in Parkinson’s disease mouse model,” *PLoS One*, vol. 9, no. 9, p. e106867, 2014, doi: 10.1371/journal.pone.0106867.
- [416] R. Pahuja *et al.*, “Trans-blood brain barrier delivery of dopamine-loaded nanoparticles reverses functional deficits in parkinsonian rats,” *ACS Nano*, 2015, doi: 10.1021/nm506408v.
- [417] L. Alvarez-Erviti, Y. Seow, H. Yin, C. Betts, S. Lakhal, and M. J. A. Wood, “Delivery of siRNA to the mouse brain by systemic injection of targeted exosomes,” *Nat Biotechnol*, vol. 29, no. 4, pp. 341–345, 2011, doi: 10.1038/nbt.1807.
- [418] X. Wu, T. Zheng, and B. Zhang, “Exosomes in Parkinson’s Disease,” *Neurosci Bull*, vol. 33, no. 3, pp. 331–338, Jun. 2017, doi: 10.1007/s12264-016-0092-z.
- [419] J. Sanz-Ros, C. Mas-Bargues, N. Romero-García, J. Huete-Acevedo, M. Dromant, and C. Borrás, “Extracellular Vesicles as Therapeutic Resources in the Clinical Environment,” *Int J Mol Sci*, vol. 24, no. 3, p. 2344, Jan. 2023, doi: 10.3390/ijms24032344.
- [420] J. M. Pitt *et al.*, “Dendritic cell-derived exosomes for cancer therapy,” *Journal of Clinical Investigation*, vol. 126, no. 4, pp. 1224–1232, Apr. 2016, doi: 10.1172/JCI81137.
- [421] B. Escudier *et al.*, “Vaccination of metastatic melanoma patients with autologous dendritic cell (DC) derived-exosomes: results of the first phase I clinical trial,” *J Transl Med*, vol. 3, no. 1, p. 10, 2005, doi: 10.1186/1479-5876-3-10.

- [422] K. W. Witwer and C. Théry, “Extracellular vesicles or exosomes? On primacy, precision, and popularity influencing a choice of nomenclature,” *J Extracell Vesicles*, vol. 8, no. 1, p. 1648167, Dec. 2019, doi: 10.1080/20013078.2019.1648167.
- [423] “Erratum for Pharmacokinetics and biodistribution of extracellular vesicles administered intravenously and intranasally to *Macaca nemestrina*,” *Journal of Extracellular Biology*, vol. 1, no. 12, Dec. 2022, doi: 10.1002/jex2.67.
- [424] L. Leggio *et al.*, “Mastering the Tools: Natural versus Artificial Vesicles in Nanomedicine,” *Adv Healthc Mater*, vol. 9, no. 18, p. 2000731, Sep. 2020, doi: 10.1002/adhm.202000731.
- [425] L. R. Lizarraga-Valderrama and G. K. Sheridan, “Extracellular vesicles and intercellular communication in the central nervous system,” *FEBS Lett*, vol. 595, no. 10, pp. 1391–1410, May 2021, doi: 10.1002/1873-3468.14074.
- [426] S. Liu *et al.*, “Highly efficient intercellular spreading of protein misfolding mediated by viral ligand-receptor interactions,” *Nat Commun*, vol. 12, no. 1, p. 5739, Oct. 2021, doi: 10.1038/s41467-021-25855-2.
- [427] M. Tsalenchuk, S. M. Gentleman, and S. J. Marzi, “Linking environmental risk factors with epigenetic mechanisms in Parkinson’s disease,” *NPJ Parkinsons Dis*, vol. 9, no. 1, p. 123, Aug. 2023, doi: 10.1038/s41531-023-00568-z.
- [428] E. Emmanouilidou *et al.*, “Cell-Produced  $\alpha$ -Synuclein Is Secreted in a Calcium-Dependent Manner by Exosomes and Impacts Neuronal Survival,” *The Journal of Neuroscience*, vol. 30, no. 20, pp. 6838–6851, May 2010, doi: 10.1523/JNEUROSCI.5699-09.2010.
- [429] H. Asai *et al.*, “Depletion of microglia and inhibition of exosome synthesis halt tau propagation,” *Nat Neurosci*, vol. 18, no. 11, pp. 1584–1593, Nov. 2015, doi: 10.1038/nn.4132.
- [430] S. Bido *et al.*, “Microglia-specific overexpression of  $\alpha$ -synuclein leads to severe dopaminergic neurodegeneration by phagocytic exhaustion and oxidative toxicity,” *Nat Commun*, vol. 12, no. 1, p. 6237, Oct. 2021, doi: 10.1038/s41467-021-26519-x.
- [431] S. Asikainen *et al.*, “Global microRNA Expression Profiling of *Caenorhabditis elegans* Parkinson’s Disease Models,” *Journal of Molecular Neuroscience*, vol. 41, no. 1, pp. 210–218, May 2010, doi: 10.1007/s12031-009-9325-1.
- [432] C. W. Winkler, K. G. Taylor, and K. E. Peterson, “Location is everything: let-7b microRNA and TLR7 signaling results in a painful TRP,” *Science Signaling*. 2014. doi: 10.1126/scisignal.2005407.
- [433] A. de Rus Jacquet, J. L. Tancredi, A. L. Lemire, M. C. DeSantis, W.-P. Li, and E. K. O’Shea, “The LRRK2 G2019S mutation alters astrocyte-to-neuron communication via extracellular vesicles and induces neuron atrophy in a human iPSC-derived model of Parkinson’s disease,” *Elife*, vol. 10, Sep. 2021, doi: 10.7554/eLife.73062.
- [434] A. Venturini *et al.*, “Exosomes from astrocyte processes: Signaling to neurons,” *Front Pharmacol*, 2019, doi: 10.3389/fphar.2019.01452.
- [435] I. Colvett, H. Saternos, C. Coughlan, A. Vielle, and A. Ledreux, “Extracellular vesicles from the CNS play pivotal roles in neuroprotection and neurodegeneration: lessons from in vitro experiments,” *Extracell Vesicles Circ Nucl Acids*, vol. 4, no. 1, pp. 89–106, 2023, doi: 10.20517/evcna.2023.07.

- [436] D. R. Graykowski, Y.-Z. Wang, A. Upadhyay, and J. N. Savas, “The Dichotomous Role of Extracellular Vesicles in the Central Nervous System,” *iScience*, vol. 23, no. 9, p. 101456, Sep. 2020, doi: 10.1016/j.isci.2020.101456.
- [437] P. Proia *et al.*, “Astrocytes shed extracellular vesicles that contain fibroblast growth factor-2 and vascular endothelial growth factor,” *Int J Mol Med*, Jan. 2008, doi: 10.3892/ijmm.21.1.63.
- [438] C. Hering and A. K. Shetty, “Extracellular Vesicles Derived From Neural Stem Cells, Astrocytes, and Microglia as Therapeutics for Easing TBI-Induced Brain Dysfunction,” *Stem Cells Transl Med*, vol. 12, no. 3, pp. 140–153, Mar. 2023, doi: 10.1093/stcltm/szad004.
- [439] F. Delgado-Peraza *et al.*, “Neuron-derived extracellular vesicles in blood reveal effects of exercise in Alzheimer’s disease,” *Alzheimers Res Ther*, vol. 15, no. 1, p. 156, Sep. 2023, doi: 10.1186/s13195-023-01303-9.
- [440] S. Wang *et al.*, “Synapsin I Is an Oligomannose-Carrying Glycoprotein, Acts As an Oligomannose-Binding Lectin, and Promotes Neurite Outgrowth and Neuronal Survival When Released via Glia-Derived Exosomes,” *The Journal of Neuroscience*, vol. 31, no. 20, pp. 7275–7290, May 2011, doi: 10.1523/JNEUROSCI.6476-10.2011.
- [441] R.-D. Gosselin, P. Meylan, and I. Decosterd, “Extracellular microvesicles from astrocytes contain functional glutamate transporters: regulation by protein kinase C and cell activation,” *Front Cell Neurosci*, vol. 7, 2013, doi: 10.3389/fncel.2013.00251.
- [442] A. R. Taylor, M. B. Robinson, D. J. Gifondorwa, M. Tytell, and C. E. Milligan, “Regulation of heat shock protein 70 release in astrocytes: Role of signaling kinases,” *Dev Neurobiol*, 2007, doi: 10.1002/dneu.20559.
- [443] N. Shakespear, M. Ogura, J. Yamaki, and Y. Homma, “Astrocyte-Derived Exosomal microRNA miR-200a-3p Prevents MPP<sup>+</sup>-Induced Apoptotic Cell Death Through Down-Regulation of MKK4,” *Neurochem Res*, vol. 45, no. 5, pp. 1020–1033, May 2020, doi: 10.1007/s11064-020-02977-5.
- [444] L. Leggio *et al.*, “Small Extracellular Vesicles Secreted by Nigrostriatal Astrocytes Rescue Cell Death and Preserve Mitochondrial Function in Parkinson’s Disease,” *Adv Healthc Mater*, p. 2201203, Aug. 2022, doi: 10.1002/adhm.202201203.
- [445] E. Braungart, M. Gerlach, P. Riederer, R. Baumeister, and M. C. Hoener, “Caenorhabditis elegans MPP<sup>+</sup> model of Parkinson’s disease for high-throughput drug screenings,” *Neurodegener Dis*, 2004, doi: 10.1159/000080983.
- [446] J. Lama, Y. Buhidma, E. J. R. Fletcher, and S. Duty, “Animal models of Parkinson’s disease: a guide to selecting the optimal model for your research,” *Neuronal Signal*, vol. 5, no. 4, Dec. 2021, doi: 10.1042/NS20210026.
- [447] A. Dovonou, C. Bolduc, V. Soto Linan, C. Gora, M. R. Peralta III, and M. Lévesque, “Animal models of Parkinson’s disease: bridging the gap between disease hallmarks and research questions,” *Transl Neurodegener*, vol. 12, no. 1, p. 36, Jul. 2023, doi: 10.1186/s40035-023-00368-8.
- [448] E. A. Konnova and M. Swanberg, “Animal Models of Parkinson’s Disease,” in *Parkinson’s Disease: Pathogenesis and Clinical Aspects*, Codon Publications, 2018, pp. 83–106. doi: 10.15586/codonpublications.parkinsonsdisease.2018.ch5.

- [449] M. Ke *et al.*, “Comprehensive Perspectives on Experimental Models for Parkinson’s Disease,” *Aging Dis*, vol. 12, no. 1, p. 223, 2021, doi: 10.14336/AD.2020.0331.
- [450] T. Oz, A. Kaushik, and M. Kujawska, “Neural stem cells for Parkinson’s disease management: Challenges, nanobased support, and prospects,” *World J Stem Cells*, vol. 15, no. 7, pp. 687–700, Jul. 2023, doi: 10.4252/wjsc.v15.i7.687.
- [451] E. S. Ásgrímsdóttir and E. Arenas, “Midbrain Dopaminergic Neuron Development at the Single Cell Level: In vivo and in Stem Cells,” *Front Cell Dev Biol*, vol. 8, Jun. 2020, doi: 10.3389/fcell.2020.00463.
- [452] J. Piao *et al.*, “Preclinical Efficacy and Safety of a Human Embryonic Stem Cell-Derived Midbrain Dopamine Progenitor Product, MSK-DA01,” *Cell Stem Cell*, vol. 28, no. 2, pp. 217–229.e7, Feb. 2021, doi: 10.1016/j.stem.2021.01.004.
- [453] Y. Yuan *et al.*, “Dopaminergic precursors differentiated from human blood-derived induced neural stem cells improve symptoms of a mouse Parkinson’s disease model,” *Theranostics*, vol. 8, no. 17, pp. 4679–4694, 2018, doi: 10.7150/thno.26643.
- [454] R. Lara-Rodarte *et al.*, “Mouse Embryonic Stem Cells Expressing GDNF Show Enhanced Dopaminergic Differentiation and Promote Behavioral Recovery After Grafting in Parkinsonian Rats,” *Front Cell Dev Biol*, vol. 9, Jun. 2021, doi: 10.3389/fcell.2021.661656.
- [455] J. L. Biedler, S. Roffler-Tarlov, M. Schachner, and L. S. Freedman, “Multiple neurotransmitter synthesis by human neuroblastoma cell lines and clones.,” *Cancer Res*, vol. 38, no. 11 Pt 1, pp. 3751–7, Nov. 1978.
- [456] H. Xie, L. Hu, and G. Li, “SH-SY5Y human neuroblastoma cell line: in vitro cell model of dopaminergic neurons in Parkinson’s disease.,” *Chin Med J (Engl)*, vol. 123, no. 8, pp. 1086–92, Apr. 2010.
- [457] M. Şahin, G. Öncü, M. A. Yılmaz, D. Özkan, and H. Saybaşılı, “Transformation of SH-SY5Y cell line into neuron-like cells: Investigation of electrophysiological and biomechanical changes,” *Neurosci Lett*, vol. 745, p. 135628, Feb. 2021, doi: 10.1016/j.neulet.2021.135628.
- [458] S. Wen, T. Aki, K. Unuma, and K. Uemura, “Chemically Induced Models of Parkinson’s Disease: History and Perspectives for the Involvement of Ferroptosis,” *Front Cell Neurosci*, vol. 14, Dec. 2020, doi: 10.3389/fncel.2020.581191.
- [459] D. S. Cassarino, J. K. Parks, W. D. Parker, and J. P. Bennett, “The parkinsonian neurotoxin MPP+ opens the mitochondrial permeability transition pore and releases cytochrome c in isolated mitochondria via an oxidative mechanism,” *Biochimica et Biophysica Acta (BBA) - Molecular Basis of Disease*, vol. 1453, no. 1, pp. 49–62, Jan. 1999, doi: 10.1016/S0925-4439(98)00083-0.
- [460] C. Christensen, H. Þorsteinsson, V. H. Maier, and K. Æ. Karlsson, “Multi-parameter Behavioral Phenotyping of the MPP+ Model of Parkinson’s Disease in Zebrafish,” *Front Behav Neurosci*, vol. 14, Dec. 2020, doi: 10.3389/fnbeh.2020.623924.
- [461] R. Kumaran and M. R. Cookson, “Pathways to Parkinsonism Redux: convergent pathobiological mechanisms in genetics of Parkinson’s disease,” *Hum Mol Genet*, vol. 24, no. R1, pp. R32–R44, Oct. 2015, doi: 10.1093/hmg/ddv236.

- [462] Y. Wang *et al.*, “Astrocyte-to-neuron reprogramming and crosstalk in the treatment of Parkinson’s disease,” *Neurobiol Dis*, vol. 184, p. 106224, Aug. 2023, doi: 10.1016/j.nbd.2023.106224.
- [463] Y. Yang *et al.*, “Therapeutic functions of astrocytes to treat  $\alpha$ -synuclein pathology in Parkinson’s disease,” *Proceedings of the National Academy of Sciences*, vol. 119, no. 29, Jul. 2022, doi: 10.1073/pnas.2110746119.
- [464] A. de Rus Jacquet *et al.*, “The contribution of inflammatory astrocytes to BBB impairments in a brain-chip model of Parkinson’s disease,” *Nat Commun*, vol. 14, no. 1, p. 3651, Jun. 2023, doi: 10.1038/s41467-023-39038-8.
- [465] C. Pistono, N. Bister, I. Stanová, and T. Malm, “Glia-Derived Extracellular Vesicles: Role in Central Nervous System Communication in Health and Disease,” *Front Cell Dev Biol*, vol. 8, Jan. 2021, doi: 10.3389/fcell.2020.623771.
- [466] E. GOKCAL, V. E. GUR, R. SELVITOP, G. BABACAN YILDIZ, and T. ASIL, “Motor and Non-Motor Symptoms in Parkinson’s Disease: Effects on Quality of Life,” *Noro Psikiyatrs Ars*, vol. 54, no. 2, pp. 143–148, Jun. 2017, doi: 10.5152/npa.2016.12758.
- [467] A. Elkouzi, V. Vedam-Mai, R. S. Eisinger, and M. S. Okun, “Emerging therapies in Parkinson disease — repurposed drugs and new approaches,” *Nat Rev Neurol*, vol. 15, no. 4, pp. 204–223, Apr. 2019, doi: 10.1038/s41582-019-0155-7.
- [468] H. Metoki and S. Kuriyama, “Combination of genetic and environmental factors for childhood hypertension: a simple indicator of family history remains useful,” *Hypertension Research*, vol. 46, no. 4, pp. 1061–1063, Apr. 2023, doi: 10.1038/s41440-022-01165-y.
- [469] X.-Y. Gao, T. Yang, Y. Gu, and X.-H. Sun, “Mitochondrial Dysfunction in Parkinson’s Disease: From Mechanistic Insights to Therapy,” *Front Aging Neurosci*, vol. 14, Jun. 2022, doi: 10.3389/fnagi.2022.885500.
- [470] D. N. Hauser and T. G. Hastings, “Mitochondrial dysfunction and oxidative stress in Parkinson’s disease and monogenic parkinsonism,” *Neurobiol Dis*, vol. 51, pp. 35–42, Mar. 2013, doi: 10.1016/j.nbd.2012.10.011.
- [471] M. Y. Batiuk *et al.*, “Identification of region-specific astrocyte subtypes at single cell resolution,” *Nat Commun*, vol. 11, no. 1, p. 1220, Mar. 2020, doi: 10.1038/s41467-019-14198-8.
- [472] N. Iraci, L. Leggio, A. Lombardo, C. Panarello, F. Pappalardo, and G. Paternó, “An Analytical Model for the Inference of the EV Reception Process Parameters in Cell-to-Cell Communication,” in *Proceedings of the 10th ACM International Conference on Nanoscale Computing and Communication*, New York, NY, USA: ACM, Sep. 2023, pp. 136–141. doi: 10.1145/3576781.3608716.

## 6. Research articles

Attached files:

- Article 1. *“High-Resolution Respirometry Reveals MPP<sup>+</sup> Mitochondrial Toxicity Mechanism in a Cellular Model of Parkinson’s Disease”*;
- Article 2. *“Small Extracellular Vesicles Secreted by Nigrostriatal Astrocytes Rescue Cell Death and Preserve Mitochondrial Function in Parkinson's Disease”*;
- Article 3. *“An Analytical Model for the Inference of the EV Reception Process Parameters in Cell-to-Cell Communication”*.



Article

# High-Resolution Respirometry Reveals MPP<sup>+</sup> Mitochondrial Toxicity Mechanism in a Cellular Model of Parkinson's Disease

Pierpaolo Risiglione <sup>1,†</sup>, Loredana Leggio <sup>2,†</sup>, Salvatore A. M. Cubisino <sup>1</sup>, Simona Reina <sup>3,4</sup>,  
Greta Paternò <sup>2</sup>, Bianca Marchetti <sup>2,5</sup> , Andrea Magri <sup>3,4,\*</sup> , Nunzio Iraci <sup>2,‡</sup>   
and Angela Messina <sup>3,4,\*,‡</sup>

<sup>1</sup> Department of Biomedical and Biotechnological Sciences, University of Catania, V.le Andrea Doria 6, 95125 Catania, Italy; pierpaolo.risiglione@phd.unict.it (P.R.); salvatore.cubisino@phd.unict.it (S.A.M.C.)

<sup>2</sup> Department of Biomedical and Biotechnological Sciences, University of Catania, Torre Biologica, Via Santa Sofia 97, 95125 Catania, Italy; loredanaleggio@unict.it (L.L.); greta.paterno.gp@gmail.com (G.P.); biancamarchetti@libero.it (B.M.); nunzio.iraci@unict.it (N.I.)

<sup>3</sup> Department of Biological, Geological and Environmental Sciences, University of Catania, V.le Andrea Doria 6, 95125 Catania, Italy; simona.reina@unict.it

<sup>4</sup> we.MitoBiotech S.R.L., C.so Italia 172, 95125 Catania, Italy

<sup>5</sup> Neuropharmacology Section, OASI Research Institute-IRCCS, 94018 Troina (EN), Italy

\* Correspondence: andrea.magri@unict.it (A.M.); mess@unict.it (A.M.)

† These authors contributed equally to this work.

‡ These authors share the last authorship.

Received: 20 September 2020; Accepted: 20 October 2020; Published: 22 October 2020



**Abstract:** MPP<sup>+</sup> is the active metabolite of MPTP, a molecule structurally similar to the herbicide Paraquat, known to injure the dopaminergic neurons of the nigrostriatal system in Parkinson's disease models. Within the cells, MPP<sup>+</sup> accumulates in mitochondria where it inhibits complex I of the electron transport chain, resulting in ATP depletion and neuronal impairment/death. So far, MPP<sup>+</sup> is recognized as a valuable tool to mimic dopaminergic degeneration in various cell lines. However, despite a large number of studies, a detailed characterization of mitochondrial respiration in neuronal cells upon MPP<sup>+</sup> treatment is still missing. By using high-resolution respirometry, we deeply investigated oxygen consumption related to each respiratory state in differentiated neuroblastoma cells exposed to the neurotoxin. Our results indicated the presence of extended mitochondrial damage at the inner membrane level, supported by increased LEAK respiration, and a drastic drop in oxygen flow devoted to ADP phosphorylation in respirometry measurements. Furthermore, prior to complex I inhibition, an enhancement of complex II activity was observed, suggesting the occurrence of some compensatory effect. Overall our findings provide a mechanistic insight on the mitochondrial toxicity mediated by MPP<sup>+</sup>, relevant for the standardization of studies that employ this neurotoxin as a disease model.

**Keywords:** MPP<sup>+</sup>; mitochondria; Parkinson's disease; high-resolution respirometry; SH-SY5Y cells

## 1. Introduction

Parkinson's disease (PD) is a progressive age-related neurodegenerative disorder (ND) whose symptoms include motor system faults, such as resting tremors, rigidity and bradykinesia, and cognitive dysfunctions. These symptoms are the result of dopaminergic (DAergic) neurons loss within the *substantia nigra pars compacta* in the ventral midbrain and their terminal in the striatum, which lead consequently to striatal dopamine (DA) depletion [1]. The appearance of big spherical intraneuronal



inclusions in the brainstem and cortex, called Lewy bodies (LBs) that contain protein aggregates in which  $\alpha$ -synuclein ( $\alpha$ -syn) is the main structural component, is one of the most common histopathological PD features [2]. Neuroinflammation is another important hallmark of the disease. In this context, the glial compartment—astrocytes and microglia—are pivotal in PD onset and progression. Notably, depending on the signals released in the microenvironment, glia may have a dual role, either beneficial or detrimental for DAergic neurons and neural stem cells exposed to harmful stimuli [3].

As for the other NDs, the cause(s) of PD are ill-defined and currently, there is no cure to stop or reverse PD progression [4]. The transplantation of relevant cell types represents a promising therapeutic strategy. On the other hand, new cell-free approaches, such as those based on extracellular vesicles, are emerging as innovative nanotherapeutics [5,6]. In this context, the definition at the molecular level of toxicity mechanisms in PD is crucial to support the development of potential therapeutic avenues.

To date, about 90 genes were linked to familial PD onset [7]. Despite this, the etiology of the vast majority (up to 90%) of so-called “idiopathic” cases is multifactorial, recognized to arise from a combination of polygenic inheritance and environmental exposures [8,9]. Notably, a wide panel of environmental factors including neurotoxicants, commonly used as herbicides or pesticides, have long been recognized as critical risk factors for PD [10].

MPTP (1-methyl-4-phenyl-1,2,3,6-tetrahydropyridine) is a molecule structurally similar to the herbicide Paraquat and was the first neurotoxicant shown to induce in humans a profound parkinsonian syndrome [11,12]. MPTP injures, in a selective manner, the dopaminergic neurons in the nigrostriatal system, and when tested in various animal species, including non-human primates, it showed the ability to recapitulate most PD-like symptoms [13,14]: i.e., the long exposure to low MPTP doses promotes the increase of oxidative stress,  $\alpha$ -syn fibrillization, and loss of mitochondrial functionality [15–17]. Since MPTP is a highly lipophilic compound, it rapidly crosses the blood–brain barrier and after systemic exposure, the toxin levels are already detectable in the brain within minutes. By itself, MPTP is not a toxic substance, however, once in the brain, it is metabolized to 1-methyl-4-phenyl-2,3-dihydropyridinium (MPDP) by the enzyme monoamine oxidase B (MAO-B) in non-dopaminergic cells (i.e., the astrocytes) [18]. Next, MPDP is oxidized to the active 1-methyl-4-phenylpyridinium (MPP<sup>+</sup>) which is then released into the extracellular space, where it is taken up by the dopamine transporter (DAT) and is concentrated within the dopaminergic neurons, causing the specific loss of nigrostriatal neurons [19–21].

Within the cells, MPP<sup>+</sup> exerts its toxicity gathering in mitochondria, where it blocks the activity of NADH-ubiquinone oxidoreductase (complex I) of the mitochondrial electron transport system (ETS), leading to ATP depletion and reactive oxygen species (ROS) production [22–24]. Moreover, the prolonged exposure to the toxin causes a drastic inhibition of mtDNA-encoded respiratory subunits synthesis [25]. Despite these events having long been thought to be strictly related to DAergic neuronal loss in PD, another report suggests that neuronal death induced by MPP<sup>+</sup> is independent from complex I inhibition [26].

Neuroblastoma SH-SY5Y cells exposed to MPP<sup>+</sup> are one of the most used in vitro models in PD research. These cells, deriving from the SK-N-SH line, show a moderate activity of tyrosine hydroxylase (TH) and dopamine- $\beta$ -hydroxylase, conferring to the line a catecholaminergic phenotype [27,28]. SH-SY5Y cells may be differentiated in order to induce a “more-neuronal” phenotype: the addition of retinoic acid (RA) to the cell culture medium, in a concentration ranging from 5 to 20  $\mu$ M, represents the best approach [29]. The differentiation time may vary from 1 to 21 days during which cells switch toward a neuronal and DAergic phenotype [29]. All these variations found in protocols for SH-SY5Y culture and differentiation possibly contribute to the different functional outcomes [30]: for instance, in specific circumstances, differentiation treatment increases susceptibility to neurotoxins exposure [31], while in others no change or even a decrease was observed [32].

The large use of this in vitro model, however, was not accompanied in the years by a detailed characterization of the mitochondrial respiration. By delivering MPP<sup>+</sup> to differentiated SH-SY5Y cells, in this work, we performed an in-depth analysis of oxygen flows corresponding to each respiratory

state using high-resolution respirometry (HRR). Beyond an expected slight decrease in complex I activity, an accentuated raise of the dissipative component of respiration was observed, indicating the presence of extended damage in the inner mitochondrial membrane (IMM). Moreover, we uncovered a previously unknown compensatory effect of succinate dehydrogenase (complex II) as a response to the partial block of complex I activity exerted by toxin treatment. Overall, our findings depict a more intricate mechanism of MPP<sup>+</sup> mitochondrial toxicity.

## 2. Results

### 2.1. MPP<sup>+</sup> Toxicity Assessment in Differentiated SH-SY5Y Cells

Neuroblastoma SH-SY5Y cells were differentiated with RA and serum reduction for nine days prior to MPP<sup>+</sup> treatment, using the protocol schematized in Figure 1A. The differentiation induced morphological changes as highlighted in the brightfield and immunofluorescence images. In comparison with undifferentiated cells, RA-differentiated SH-SY5Y displayed thin and branching neurites usually resulting in a network formation (Figure 1B,C) [33]. Moreover, immunofluorescence analysis on RA-treated cells showed a decreased expression of the non-differentiated cell marker nestin (Figure 1D,F for quantification) and a higher expression of TH (Figure 1E,G for quantification), which plays a central role in DA synthesis [31]. In order to evaluate MPP<sup>+</sup> mitochondrial toxicity on a DAergic model, RA-differentiated SH-SY5Y cells were exposed to increasing toxin concentration and cell viability was determined after 24 h, performing a dose–response curve. As shown in Figure 1H, cell viability varied from 89% to 64% ranging from 1 to 3 mM of MPP<sup>+</sup>. Based on this result, we selected the lowest MPP<sup>+</sup> dose for further experiments assuming that, in this condition, any mitochondrial impairment is not ascribed to a consistent cell death but rather to the direct organelle damage caused by the neurotoxin.

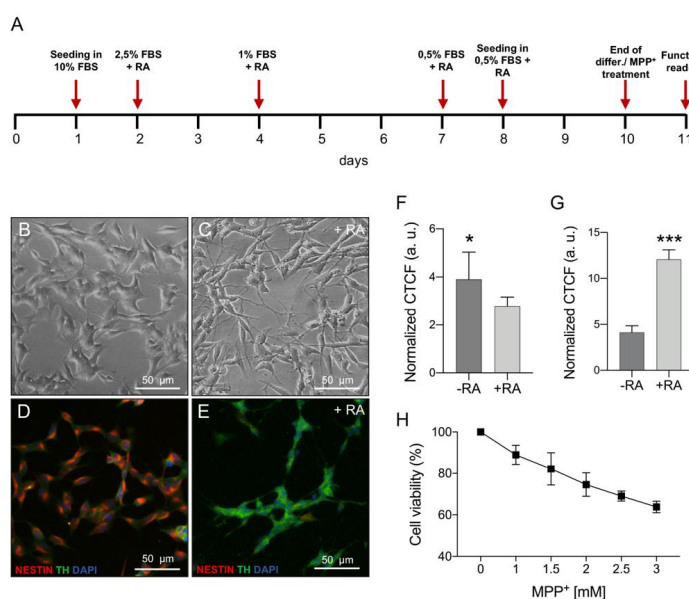


**Figure 1.** Phenotypic characterization of undifferentiated vs. differentiated SH-SY5Y cells and MPP<sup>+</sup> dose–response curve. (A) Timeline of the differentiation protocol. (B,C) Brightfield images showing morphological differences between undifferentiated cells on day zero (B) and differentiated cells at day nine (C); RA, retinoic acid. (D,E) Immunofluorescence images showing the different expression of nestin (red) and TH (green) in undifferentiated (D) and differentiated (E) cells. (F,G) Relative quantification of nestin (F) and TH (G) in undifferentiated and differentiated cells. (H) Dose–response curve for selected MPP<sup>+</sup> concentrations on differentiated SH-SY5Y cells. \*  $p < 0.05$  and \*\*\*  $p < 0.001$ .

## 2.2. $MPP^+$ Drastically Reduces Oxygen Consumption Associated with the Main Respiratory States

The oxygen consumption profile of RA-differentiated SH-SY5Y cells was analyzed by HRR using a specific substrate-uncoupler-inhibitor titration (SUIT) protocol. This protocol allows the investigation of the main respiratory states exploiting both endogenous and externally added substrates, that reached mitochondria after cell permeabilization [34]. In Figure 2A, a representative trace of oxygen consumption of untreated cells (control) illustrates the SUIT protocol. Briefly, the physiological oxygen consumption, corresponding to ROUTINE state, was measured in intact cells. Then, endogenous substrates (including ADP) were forced to leave the cells by permeabilization of the plasma membrane. Therefore, the remaining oxygen consumption was related to the non-phosphorylating or LEAK state. The OXPHOS state, indicating the oxygen flow sustained by the mitochondrial respiratory chain, was achieved in the presence of pyruvate, malate, glutamate, succinate, and ADP, the last in saturating concentration. Next, the maximal respiratory ETS capacity was obtained at the optimal uncoupler concentration. Finally, the specific inhibition of complex I and III with rotenone and antimycin respectively, allowed for the determination of the residual respiration or ROX [34,35].

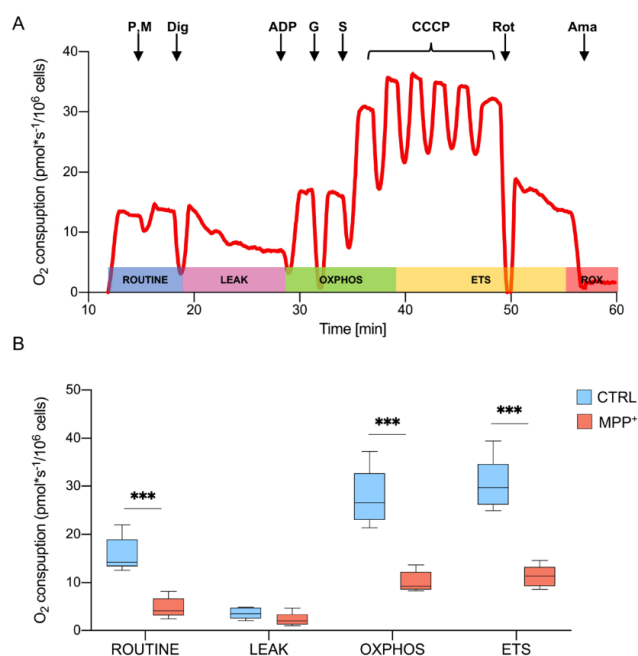


**Figure 2.** Oxygen consumption in differentiated SH-SY5Y cells. **(A)** The representative curve of mitochondrial respiratory function of untreated RA-differentiated SH-SY5Y cells assayed in MiR05 respiration medium at 37 °C. The respiratory states ROUTINE, LEAK, OXPHOS, ETS, and ROX were analyzed after the addition of specific substrates and inhibitors. P, pyruvate; M, malate; Dig, digitonin; G, glutamate; S, succinate; Rot, rotenone; Ama, antimycin. **(B)** Quantitative analysis of the oxygen consumption rate expressed as pmol/second per million cells of control and  $MPP^+$  treated cells calculated for ROUTINE, LEAK, OXPHOS, ETS. Data are shown as mean with standard deviation, with \*\*\*  $p < 0.001$ .

Oxygen consumption, corresponding to each respiratory state in cells treated with 1 mM  $MPP^+$  for 24 h, was monitored and compared to the control. The obtained values were corrected for the ROX and are reported in Figure 2B (see Supplementary Materials Table S1 for raw data). As shown, a dramatic reduction of oxygen flow was detected in ROUTINE (−70%,  $p = 0.0004$ ,  $n = 5$ ), OXPHOS (−70%,  $p = 0.0003$ ,  $n = 5$ ) and ETS (−62.7%,  $p < 0.0001$ ,  $n = 5$ ). Prior to a very moderate cell death,

as previously observed in the same condition, these results indicate that MPP<sup>+</sup> severely affects the respiratory capacity of mitochondria.

### 2.3. MPP<sup>+</sup> Increases the Dissipative Ratio of Oxygen Flux

The oxygen consumption depends on a sum of different factors, including obviously ETS activity but also mitochondrial mass and biogenesis, all features subjected to change upon MPP<sup>+</sup> exposure. For instance, MPP<sup>+</sup> increases autophagy and mitochondria degradation in SH-SY5Y cells [36,37], affects organelle morphology, mass and protein expression in RA-differentiated SH-SY5Y [25], and the mitochondrial dynamic in vivo [38].

Flux control ratios (FCRs), instead, express respiratory states independently of mitochondrial content since they are obtained by normalizing each flux for the maximum flux [34,35,39]. In Figure 3A (see also Supplementary Materials Table S2), ROUTINE, LEAK, and OXPHOS respiration are indicated as the ratio of maximal ETS capacity. As shown in the left panel, MPP<sup>+</sup> treatment affected specifically the LEAK state: a significant increase (+63%) was observed in treated cells ( $0.19 \pm 0.05$  in control vs.  $0.31 \pm 0.09$  in treated cells,  $p = 0.046$ ,  $n = 5$ ), while no significant differences were detected for ROUTINE and OXPHOS respiration between the samples. Since the LEAK state represents the amount of dissipative flux, this result suggests the presence of some injury at the IMM level which impinges on the proton gradient maintenance and, in turn, on ATP production [40]. As reported in the right panel, the phosphorylation-related flux is severely affected in ROUTINE ( $-71.9\%$ ,  $p = 0.0009$ ,  $n = 4$ ) and in a less dramatic manner in OXPHOS ( $-18.3\%$ ,  $p = 0.0039$ ,  $n = 4$ ). Accordingly, the respiratory reserve (RR), consisting of the extra ATP produced by oxidative phosphorylation in case of an increased energy demand [41,42] was found more than halved in MPP<sup>+</sup> treated cells (Figure 3B,  $-55\%$ ,  $p = 0.0002$ ,  $n = 4$ ) (see also Supplementary Materials Table S3).

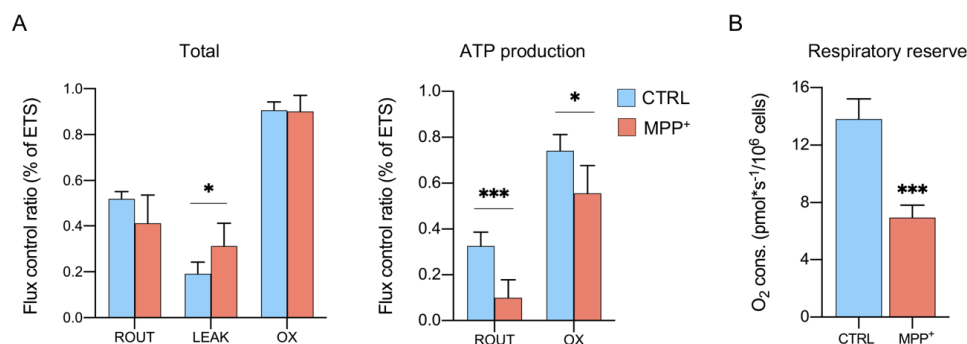


**Figure 3.** MPP<sup>+</sup> effect on mitochondrial respiration. (A) Oxygen consumption measured in different respiratory states in the presence or not of MPP<sup>+</sup>, expressed as the total or ATP-related flux. Data are displayed as the flux control ratio (FCR) of the maximal ETS capacity. (B) Oxygen flux related to the respiratory reserve of cells in the presence or not of MPP<sup>+</sup>. All data are shown as means with standard deviation; \*  $p < 0.05$  and \*\*\*  $p < 0.001$ .

Taken together, these results suggest that neurotoxin affects IMM integrity decreasing substantially the phosphorylation processes.

### 2.4. MPP<sup>+</sup> Reduces Coupling Efficiency in Each Respiratory State

Coupling efficiency represents another important parameter to evaluate MPP<sup>+</sup> effect on mitochondrial respiration. It indicates the ratio of oxygen flux coupled to ADP phosphorylation in a specific respiratory state [35].

Figure 4A shows the coupling degree of the ROUTINE state. In control cells, about 63% of oxygen consumption is coupled with the phosphorylation process, while only 28% of the flux is coupled in

MPP<sup>+</sup> treated cells ( $-62.9\%$ ,  $p = 0.0026$ ,  $n = 4$ ). Similarly, the coupling efficiency of OXPHOS and ETS was significantly decreased upon neurotoxin exposure, even if in a less dramatic manner. In particular, phosphorylation-related oxygen flux decreased from 78% (control cells) to 65% (MPP<sup>+</sup> treated) in OXPHOS ( $-16.7\%$ ,  $p = 0.0488$ ,  $n = 4$ ) and from 80% to 68% in ETS ( $-15\%$ ,  $p = 0.0426$ ,  $n = 5$ ) as reported in Figure 4B,C.

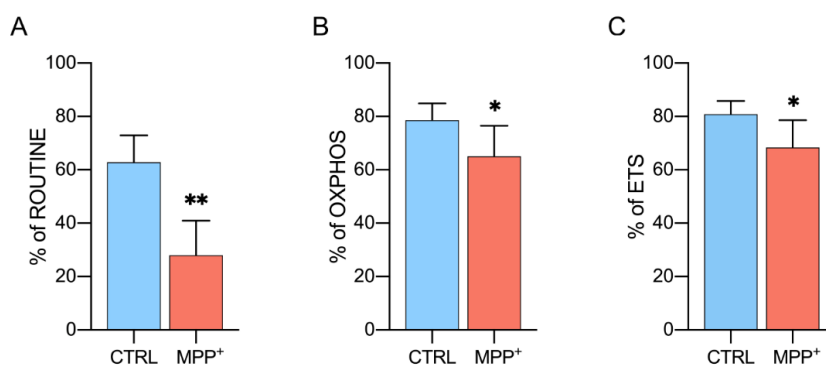


**Figure 4.** Coupling efficiency of different respiratory states. Rate of oxygen flux during ROUTINE (A), OXPHOS (B), and ETS (C) coupled with the ADP phosphorylation. Data are shown as the percentage of the reference state and expressed as means with standard deviation; \*  $p < 0.05$  and \*\*  $p < 0.01$ .

Overall, the observed reduction of coupling degree in all respiratory states confirms the strong impact of MPP<sup>+</sup> on the phosphorylating flows previously described.

#### 2.5. Activity of Complex II Is Increased Upon Complex I Inhibition

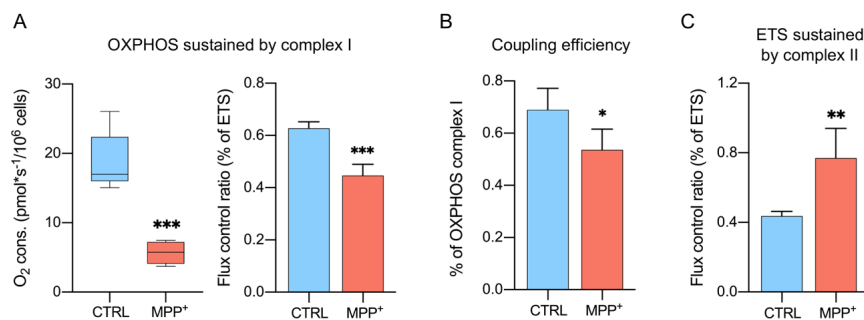
Since NADH-ubiquinone oxidoreductase is a specific target of MPP<sup>+</sup> [22], HRR was used to evaluate the contribution of this specific complex to the OXPHOS respiration. This was achieved in the presence of pyruvate, malate, glutamate, and ADP but not of succinate, which conversely stimulates complex II. Figure 5A shows both the oxygen consumption level and the corresponding FCRs. As occurred for the other respiratory states, the oxygen level of OXPHOS sustained by complex I was found substantially lowered after MPP<sup>+</sup> addition ( $-63.1\%$ ,  $p = 0.0002$ ,  $n = 5$ ). Similarly, a moderate decline of FCR was observed ( $-18\%$ ,  $p = 0.0003$ ,  $n = 4$ ). Accordingly, the degree of ATP-coupled respiration sustained exclusively by complex I was found significantly reduced (Figure 5B), varying from 69% of the control to 53% of MPP<sup>+</sup> treated cells ( $-23\%$ ,  $p = 0.043$ ,  $n = 4$ ).

After total OXPHOS stimulation and ETS measurement, complex I was inhibited by using rotenone. With ETS calculated in the presence of all substrates (including succinate), the measurement was related to the specific contribution of complex II to ETS. Despite a general reduction of oxygen flux in the presence of MPP<sup>+</sup> ( $-38.3\%$ ,  $p = 0.0156$ ,  $n = 5$ , Table S1), Figure 5C indicates a significant increase (+81%) in the FCR compared to control ( $p = 0.0084$ ,  $n = 4$ , Table S2) suggesting the existence of some compensatory mechanism(s) put in place by succinate dehydrogenase as a response to complex I inhibition.

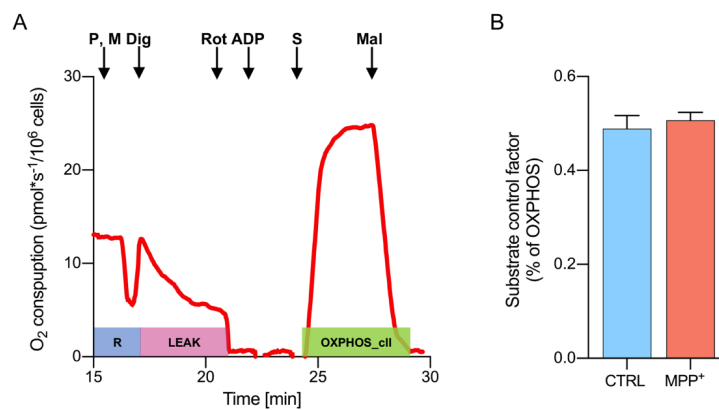
To further investigate this aspect and clarify whether a direct link between complex II and the toxin exists, the activity of succinate dehydrogenase was specifically assayed with a distinct HRR protocol aimed to evaluate the electron flow into the Q-junction occurring independently from complex I. It is indeed known that, when complex I is stimulated (as occurred in the protocol in Figure 2A), oxaloacetate rapidly accumulates within mitochondria, acting as a potent inhibitor of complex II, already at low doses [39,43].

Figure 6A shows a representative oxygen consumption curve of untreated differentiated SH-SY5Y cells, along with the protocol used for complex II stimulation. Briefly, cells were permeabilized in the

presence of pyruvate and malate but complex I was immediately inhibited by rotenone, thus avoiding oxaloacetate accumulation. Next, the addition of ADP did not induce any response, as demonstrated by the oxygen flow curve kept around zero (Figure 6A). Then, complex II was activated by succinate. As a counter-proof, the addition of the succinate dehydrogenase inhibitor malonic acid brought the oxygen curve back to zero. The complex II-linked oxygen flows were analyzed for control and MPP<sup>+</sup> treated cells, normalizing values for the convergent complex I + complex II electron supply flows [35,39]. The results are displayed in Figure 6B as substrate control factor (SCF). As reported, no significant difference in complex II activity was observed between samples ( $0.49 \pm 0.03$  in control vs.  $0.52 \pm 0.01$  in treated cells,  $p = 0.442$ ,  $n = 3$ ). These data indicate that the enhancement of succinate dehydrogenase activity, previously observed in MPP<sup>+</sup> treated cells (Figure 5C) likely depends on the inhibition of complex I activity, rather than from the toxin itself.



**Figure 5.** Specific contribution of complex I and complex II to different respiratory states. (A) Quantitative analysis of the oxygen consumption rate and the relative FCR of OXPHOS state sustained by complex I. Data were obtained by measuring OXPHOS respiration in the absence of succinate. (B) Rate of oxygen flux OXPHOS respiration sustained by complex I coupled with the ADP phosphorylation. (C) Quantitative analysis of the oxygen consumption rate and the relative FCR of ETS sustained by complex II. Data were obtained by measuring ETS after inhibition of complex I activity with rotenone. Data are shown as percentage of the reference state and expressed as means with standard deviation; \*  $p < 0.05$ , \*\*  $p < 0.01$ , and \*\*\*  $p < 0.001$ .



**Figure 6.** Activity of complex II assayed by HRR. (A) Representative curve of mitochondrial respiratory function of untreated RA-differentiated SH-SY5Y cells assayed in MiR05 respiration medium at 37 °C. The respiratory states ROUTINE, LEAK, and OXPHOS driven by complex II were obtained after the addition of specific substrates and inhibitors. P, pyruvate; M, malate; Dig, digitonin; Rot, rotenone; S, succinate; Mal, malonic acid. (B) Quantitative analysis of the oxygen consumption rate of control or MPP<sup>+</sup> treated cells of OXPHOS sustained by complex II. Data are expressed as the percentage of the total OXPHOS and shown as SCRs (mean with standard deviation).



### 3. Discussion

Mitochondrial dysfunction is an important hallmark of PD, together with protein aggregation and oxidative stress. These features, however, are common to all NDs and are strictly interconnected. Protein aggregates interact with the cytosolic surface of mitochondria and impair metabolic exchanges with the organelle. A $\beta$  oligomers in Alzheimer's disease [44,45], SOD1 mutants in Amyotrophic Lateral Sclerosis (ALS) [46–48], and  $\alpha$ -syn in PD [49], all associate with the Voltage-Dependent Anion Channels (VDAC) isoform 1, reducing dramatically the mitochondria synthesized ATP availability [50]. VDACS are the most abundant mitochondrial porin, evolutionarily conserved from yeast to humans, playing a fundamental role for organelle physiology [51–53]. It has been recently demonstrated that a reduction of VDAC1 function affects mtDNA synthesis and, in turn, the expression of mitochondrial genes encoding for essential subunits of ETS enzymes [54]. Also, in PD models, VDAC1 favors  $\alpha$ -syn translocation within mitochondria [55] where it is believed responsible for the impairment of complex I and IV activity [56,57]. Therefore, ETS damage represents a key event in mitochondrial dysfunction onset in PD.

Although, in a different way, the lipophilic cation MPP<sup>+</sup> accumulates in mitochondria and inhibits the electron flow from complex I to coenzyme Q, contributing to ATP depletion and ROS increase [17,24,58]. For this reason, MPP<sup>+</sup> is widely used for the induction of a PD-like phenotype in different in vitro models, such as the RA-differentiated SH-SY5Y cell line used herein, as a valid alternative to neuronal cells treatment with  $\alpha$ -syn oligomers and fibrils, or to genetic models. Thus, it is crucial to understand the precise changes in mitochondrial respiration upon the MPP<sup>+</sup> treatment. To this end, here we applied HRR technology highly sensitive and capable to deeply analyze oxygen consumption levels associated with each respiratory state and to ETS complexes.

We found that the treatment with 1 mM MPP<sup>+</sup> on RA-differentiated cells resulted in a slight decrease of cell viability (~10%) in front of a drop of oxygen consumption associated with the main respiratory states, up to 70%. These data indicate that MPP<sup>+</sup> exerts a specific mitochondrial toxicity, possibly depending on a reduction of both mitochondrial functionality and organelle mass [22,33,34]. Focusing on the specific differences within mitochondria, we performed a rigorous analysis of FCRs from which at least two intriguing results came out.

First, a significant increase of the dissipative flux, the LEAK state, was observed in cells upon MPP<sup>+</sup> exposure. The LEAK state depends mainly on the IMM integrity and on proton and electron leaking. In the case of IMM injury, protons by-pass ATP synthases, promoting a decrease in ATP production, and electrons escape the ETS pathway, as they are addressed to other substrates, increasing thus ROS formation [59]. The rise in LEAK respiration indicates the presence of extensive IMM damage in MPP<sup>+</sup> treated cells and this explains data in the literature about ATP depletion and oxidative stress induction [37,60]. Accordingly, oxygen flows devoted to ATP synthesis (the so-called net respiration) were found significantly decreased, drastically in ROUTINE and in a moderate manner during OXPHOS. This result was strengthened by a similar reduction in the coupling degree measured in all respiratory states.

Second, in the presence of MPP<sup>+</sup> the contribution of complex I to the OXPHOS respiration was remarkably reduced, as expected. At the same time, a significant increase in complex II activity during ETS was detected, indicating a compensatory mechanism put in place by complex II as a response to the partial inhibition of NADH-ubiquinone oxidoreductase and/or to the toxin. However, the same effect was not as strong as when the complex II activity was tested in association with the complete inhibition of complex I. Nonetheless, this result is not so surprising. It is known that a reduction of complex I activity, as found in MPP<sup>+</sup> treated cells, negatively impacts on malate dehydrogenase (MDH) activity, as a result of NAD<sup>+</sup> to NADH redox shift, affecting in turn oxaloacetate synthesis [39]. Since oxaloacetate is a potent inhibitor/modulator of succinate dehydrogenase, especially in nervous tissues [43], it is reasonable to speculate that complex II is less subjected to oxaloacetate inhibition in MPP<sup>+</sup> treated cells, due to the low activity of complex I. Notably, the main difference in the SUIT protocols applied here consists in the use of saturating rotenone concentration at different stages. Accordingly, in Figure 2A,

rotenone was added after complex I stimulation, allowing oxaloacetate to accumulate, whereas in Figure 6A complex I was directly inhibited, in order to avoid any eventual increase of oxaloacetate concentration. Therefore, the higher activity of complex II observed in the Parkinson's-like phenotype, i.e., where complex I is only partially inhibited by MPP<sup>+</sup> (as in Figure 5C) and not completely with the saturating rotenone concentration (as technically required for Figure 6 experiments), likely represents a response to complex I inhibition, rather than a direct effect of the neurotoxin. Other studies showed results in agreement with those found here. For example, Calabria and colleagues have found a compensatory effect ascribed to complex II, as well as an increase in LEAK respiration in NSC-34 cells expressing the SOD1 G93A mutant, a model of ALS [61]. Notably, this was explained as a response to the decreased activity of complex I, exerted by the SOD1 mutant [61]. Taken together, these findings depict the existence of a common rescue mechanism put in place by complex II in response to different stimuli (toxins, protein aggregates) affecting complex I activity. Furthermore, these effects can be only partially ascribed to the direct complex I impairment promoted by MPP<sup>+</sup>. In fact, it is known that cells use LEAK respiration as a protective strategy under certain circumstances. IMM contains a group of transporters called uncoupling proteins (UCPs), whose function is to partially dissipate the mitochondrial membrane potential in the form of heat [62,63]. The inhibition of complex I increases oxygen radical formation that is counteracted by the dissipation of a part of hyperpolarized IMM potential, a process known as “mild uncoupling”, with the final aim to neutralize the ROS effect [64]. Not coincidentally, a time- and dose-dependent induction of UCP2, 4, and 5 expression in neuronal cells was observed after exposure to MPP<sup>+</sup> [65]. Notably, UCP4 overexpression exerts a neuroprotective effect on SH-SY5Y upon MPP<sup>+</sup> treatment and stimulates complex II activity by its direct interaction, thus promoting an ATP level increase [66–68]. A cartoon depicting our proposed model is displayed in Figure 7.

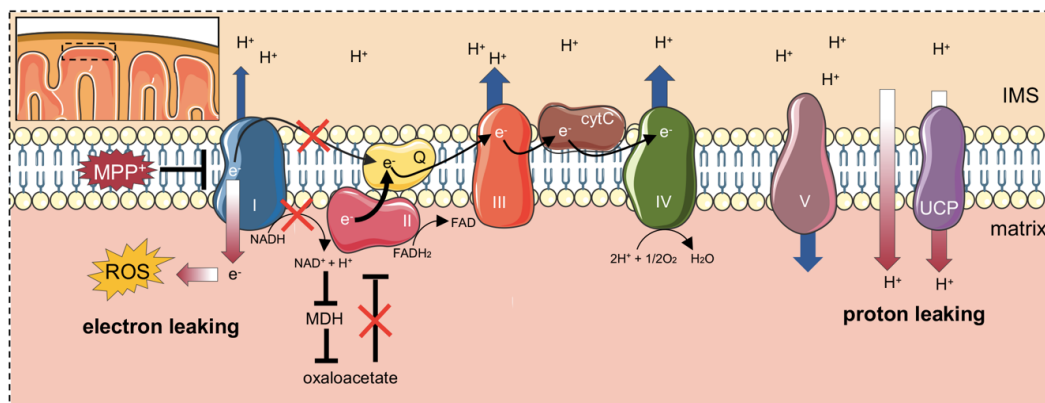


**Figure 7.** Proposed mechanism of MPP<sup>+</sup> toxicity at the IMM level. MPP<sup>+</sup> promotes the impairment of complex I activity. Electrons are then addressed towards other substrates, increasing ROS production (electron leaking). The reduced activity of complex I affects MDH activity as well as the accumulation of the Krebs cycle intermediates and complex II inhibitor oxaloacetate. In this perspective, the activity of complex II raises since it is less subjected to oxaloacetate inhibition. MPP<sup>+</sup> also induces UCPs gene expression. The increased activity of UCP proteins dissipates partially the proton gradients (proton leaking), a mechanism called “mild uncoupling” and aimed to counteract ROS damage. Original figure (created with <https://smart.servier.com> tools).

In any case, although moderate, the MPP<sup>+</sup> dose regimen here applied in SH-SY5Y cells was higher compared to those generally used in the highly vulnerable primary dopaminergic neurons, that are severely injured upon exposure to ≤50 μM MPP<sup>+</sup> or to the false neurotransmitter 6-hydroxydopamine [69]. Therefore, further studies are needed to disclose the herein described



mitochondrial effects of MPP<sup>+</sup> on primary mesencephalic neuronal cultures, that will be relevant for dopaminergic neuron physiopathology.

In conclusion, by using high-resolution respirometry tools we have identified and explained the bioenergetics fault and recovery found in MPP<sup>+</sup> treated cells, where mitochondria complex I was inhibited. By a precise analysis, we demonstrated the relevance of complex II in this recovery mechanism. These results are relevant to understand the mitochondria dysfunction in PD, and possibly in other NDs.

## 4. Materials and Methods

### 4.1. Cell Culture and Differentiation

The neuroblastoma cell line SH-SY5Y was purchased from ICLC (Interlab Cell Line Collection, accession number ICLC HTL95013; obtained from depositor European Collection of Authenticated Cell Cultures (ECACC)) and maintained in MEM/F12 medium supplemented with 10% fetal bovine serum, 2 mM L-glutamine and 1% penicillin/streptomycin. For cell differentiation, the protocol was adapted from [31,70]. Briefly, MEM/F12 was replaced with DMEM/F12 and 10  $\mu$ M all-trans RA (Sigma Aldrich, St. Louis, MO, USA) was added. The medium was changed every three days, lowering the serum amount to reach the final concentration of 0.5% by the seventh day. Cells were seeded at a density of  $3 \times 10^5$  cells/cm<sup>2</sup> in 6, 24, or 96 well plates.

### 4.2. Immunofluorescence

Cells seeded on poly-L-lysine coated glass coverslips (Sigma Aldrich) were fixed after treatment with 4% paraformaldehyde and stained with primary mouse anti-nestin antibody (sc-23927, Santa Cruz, 1:50) and with rabbit anti-TH (Tyrosine hydroxylase) antibody (AB152, Sigma-Aldrich, 1:250). Nuclei were stained with DAPI (Merck, Kenilworth, NJ, USA). Donkey anti-mouse Alexa Fluor 546 or donkey anti-rabbit Alexa Fluor 488 secondary antibodies were used (Thermo Fisher, Waltham, MA, USA). Fluorescence intensity was quantified using ImageJ software. Values are indicated as normalized corrected total cell fluorescence (CTCF) expressed as arbitrary units (A.U.).

### 4.3. MPP<sup>+</sup> Treatment and Cell Viability

Treatment with MPP<sup>+</sup> (Sigma Aldrich) was performed on day 10 of the differentiation protocol. Cells seeded in 96-well black microplates were treated for 24 h with the reported final concentrations of neurotoxin. The dose–response curve was performed using the following doses: 1, 1.5, 2, 2.5, and 3 mM. Cell viability was determined using the Celltitre-Blue Cell Viability Assay (Promega, Madison, WI, USA) according to the manufacturers' recommendations. Fluorescence intensity was measured using the microplate reader Varioskan (Thermo Scientific, Waltham, MA, USA).

### 4.4. High-Resolution Respirometry (HRR) Analysis

Mitochondrial respiration capacity of RA-differentiated SH-SY5Y was analyzed by HRR using the two-chamber system O2k-FluoRespirometer (Oroboros Instruments, Innsbruck, Austria). Cells were harvested, counted, and resuspended in the mitochondrial respiration buffer Mir05 (Oroboros Instrument). All the experiments were performed at 37 °C under constant stirring of 750 rpm. Oxygen consumption in the various respiratory states was determined using a SUIIT modified protocol [31] and the contribution of specific mitochondrial complexes to respiratory capacity was investigated.

ROUTINE respiration was measured in intact cells. Permeabilization of the plasma membrane was achieved by using the mild detergent digitonin (Sigma Aldrich) at the final concentration of 4.07  $\mu$ M. This concentration was previously determined in order to allow the access of substrates across the plasma membranes but without compromising mitochondrial membranes integrity. LEAK was measured after plasma membrane permeabilization and in the presence of previously added pyruvate and malate. A total of 5 mM pyruvate (P), 2 mM malate (M), and 10 mM glutamate (G) (Sigma Aldrich) were added

in order to activate complex I. OXPHOS capacity was recorded at saturating concentrations of 2.5 mM ADP (Sigma Aldrich) after the addition of 10 mM succinate (S) (Sigma Aldrich). The simultaneous presence of all substrates in the cuvette allowed the determination of the total OXPHOS activity. The uncoupled maximal ETS capacity was determined by titration with the uncoupler carbonyl cyanide 3-chlorophenylhydrazone, CCCP (Sigma Aldrich, 0.5  $\mu$ M) up to the complete dissipation of the proton gradient. The residual oxygen consumption (ROX) respiration was achieved by addition of rotenone and antimycin (Sigma Aldrich, 2 and 2.5  $\mu$ M respectively).

#### 4.5. Complex II Activity Analysis

Independent activity of complex II (succinate dehydrogenase) was measured by HRR with a specific protocol modified from [39]. Permeabilized cells were treated with 2  $\mu$ M rotenone in the presence of pyruvate and malate (5 and 2 mM respectively) [39]. Activity of complex II (OXPHOS sustained by complex II) was achieved by stimulation with 10 mM succinate in the presence of saturating ADP concentrations (2.5 mM). As counter-proof, the complex II inhibitor malonic acid (Sigma Aldrich, 5 mM) was added at the end of the experiment. In parallel, a control experiment performed without rotenone was carried out to achieve the total OXPHOS respiration. This state was used as a reference for normalization.

#### 4.6. Data Analysis

Instrumental and chemical background fluxes were opportunely calibrated as a function of oxygen concentration using DatLab software (Oroboros Instruments). Rate of oxygen consumption in the respiratory states ROUTINE, LEAK, OXPHOS, maximal ETS capacity was corrected for the ROX. The oxygen respiratory flux was expressed as pmol/s per million cells or as FCRs calculated for each state relative to the maximal uncoupled ETS capacity (used in this work as the reference state) [34,35]. Oxygen flux coupled to ATP synthesis was determined by correcting each state for the LEAK respiration and expressed as FCRs [34,35]. Coupling efficiencies were calculated by correcting each state for LEAK respiration and expressing it as a ratio of the total capacity in that specific state, as indicated [34,35]. The activity of complex II was calculated as SCFs normalizing the oxygen flux linked to complex II for the convergent flux of complex I + complex II, both measured during OXPHOS stimulation [39].

#### 4.7. Statistical Analysis

All data are expressed as means with standard deviation. At least three independent experiments were performed. Data were statistically analyzed by t-test using GraphPad Prism software. The following values \*  $p < 0.05$ , \*\*  $p < 0.01$ , \*\*\*  $p < 0.001$  were taken as significant.

**Supplementary Materials:** Supplementary materials can be found at <http://www.mdpi.com/1422-0067/21/21/7809/s1>. Table S1. Oxygen flux calculated for each respiratory state corrected for the ROX respiration in untreated (CTRL) and MPP+ treated cells; Table S2. FCR calculated for each respiratory state as ETS percentage in untreated (CTRL) and MPP+ treated cells; Table S3. FCR calculated for net and coupling respiration and E-R capacity factor.

**Author Contributions:** Conceptualization, A.M. (Andrea Magri), N.I., and A.M. (Angela Messina); methodology, A.M. (Andrea Magri), N.I., and A.M. (Angela Messina); analysis, P.R. and A.M. (Andrea Magri); investigation, P.R., L.L., S.A.M.C., G.P., and A.M. (Andrea Magri); resources, A.M. (Andrea Magri), N.I., and A.M. (Angela Messina); data curation, P.R., L.L., S.R., and A.M. (Andrea Magri); writing—original draft preparation, A.M. (Andrea Magri); writing—review and editing, S.R., B.M., A.M. (Angela Messina), and N.I.; supervision, N.I. and A.M. (Angela Messina); project administration, A.M. (Andrea Magri), N.I., and A.M. (Angela Messina); funding acquisition, A.M. (Andrea Magri), N.I., and A.M. (Angela Messina). All authors have read and agreed to the published version of the manuscript.

**Funding:** This research was funded by AIM Linea 1 Salute (AIM1833071) to A. Magri, Brains2South (Fondazione con il Sud—Bando Capitale Umano ad Alta Qualificazione 2015, grant no. 2015-PDR-0219) to N.I., PIACERI (grant no. ARVEST) and Proof of Concept (grant no. PEPSLA POC 01\_00054) to A. Mess.

**Acknowledgments:** The authors acknowledge Fondi di Ateneo 2020–2022, Università di Catania, linea Open Access. The authors acknowledge Vito De Pinto (University of Catania) for the useful discussion.

**Conflicts of Interest:** The authors declare no conflict of interest.

## Abbreviations

PD	Parkinson's disease
ND	Neurodegenerative disease
DA	Dopamine
LBS	Lewy's bodies
MPTP	1-methyl-4-phenyl-1,2,3,6-tetrahydropyridine
MPP <sup>+</sup>	1-methyl-4-phenylpyridinium ion
ETS	Electron transport system
HRR	High-resolution respirometry
RA	Retinoic acid
TH	Tyrosine hydroxylase
SUIT	Substrate-uncoupler-inhibitor titration
FCR	Flux control ratio
SCF	Substrate control factor
IMM	Inner mitochondrial membrane
OMM	Outer mitochondrial membrane

## References

1. Kalia, L.V.; Lang, A.E. Parkinson's disease. *Lancet* **2015**, *386*, 896–912. [[CrossRef](#)]
2. Kim, W.S.; Kagedal, K.; Halliday, G.M. Alpha-synuclein biology in Lewy body diseases. *Alzheimer's Res. Ther.* **2014**, *6*, 73. [[CrossRef](#)] [[PubMed](#)]
3. Marchetti, B.; Leggio, L.; L'Episcopo, F.; Vivarelli, S.; Tirolo, C.; Paternò, G.; Giachino, C.; Caniglia, S.; Serapide, M.F.; Iraci, N. Glia-Derived Extracellular Vesicles in Parkinson's Disease. *J. Clin. Med.* **2020**, *9*, 1941. [[CrossRef](#)]
4. Hirsch, E.C.; Jenner, P.; Przedborski, S. Pathogenesis of Parkinson's disease. *Mov. Disord.* **2013**, *28*, 24–30. [[CrossRef](#)] [[PubMed](#)]
5. Leggio, L.; Paternò, G.; Vivarelli, S.; Episcopo, F.L.; Tirolo, C.; Raciti, G.; Pappalardo, F.; Giachino, C.; Caniglia, S.; Serapide, M.F.; et al. Extracellular Vesicles as Nanotherapeutics for Parkinson's Disease. *Biomolecules* **2020**, *10*, E1327. [[CrossRef](#)]
6. Leggio, L.; Arrabito, G.; Ferrara, V.; Vivarelli, S.; Paternò, G.; Marchetti, B.; Pignataro, B.; Iraci, N. Mastering the Tools: Natural versus Artificial Vesicles in Nanomedicine. *Adv. Healthc. Mater.* **2020**, e2000731. [[CrossRef](#)] [[PubMed](#)]
7. Bandres-Ciga, S.; Diez-Fairen, M.; Kim, J.J.; Singleton, A.B. Genetics of Parkinson's disease: An introspection of its journey towards precision medicine. *Neurobiol. Dis.* **2020**, *137*, 104782. [[CrossRef](#)]
8. Marchetti, B. Nrf2/Wnt resilience orchestrates rejuvenation of glia-neuron dialogue in Parkinson's disease. *Redox Biol.* **2020**, *36*, 101664. [[CrossRef](#)]
9. Toffoli, M.; Vieira, S.R.L.; Schapira, A.H.V. Genetic causes of PD: A pathway to disease modification. *Neuropharmacology* **2020**, *170*, 108022. [[CrossRef](#)]
10. Marchetti, B. Wnt/ $\beta$ -catenin signaling pathway governs a full program for dopaminergic neuron survival, neurorescue and regeneration in the MPTP mouse model of Parkinson's disease. *Int. J. Mol. Sci.* **2018**, *19*, 3743. [[CrossRef](#)]
11. William Langston, J.; Ballard, P.; Tetrud, J.W.; Irwin, I. Chronic parkinsonism in humans due to a product of meperidine-analog synthesis. *Science* **1983**, *219*, 979–998. [[CrossRef](#)] [[PubMed](#)]
12. Langston, J.W.; Forno, L.S.; Tetrud, J.; Reeves, A.G.; Kaplan, J.A.; Karluk, D. Evidence of active nerve cell degeneration in the substantia nigra of humans years after 1-methyl-4-phenyl-1,2,3,6-tetrahydropyridine exposure. *Ann. Neurol.* **1999**, *46*, 598–605. [[CrossRef](#)]
13. Jackson-Lewis, V.; Przedborski, S. Protocol for the MPTP mouse model of Parkinson's disease. *Nat. Protoc.* **2007**, *2*, 141–151. [[CrossRef](#)]
14. Langston, J.W. The MPTP story. *J. Parkinsons. Dis.* **2017**, *7*, S11–S19. [[CrossRef](#)] [[PubMed](#)]
15. Baltazar, M.T.; Dinis-Oliveira, R.J.; de Lourdes Bastos, M.; Tsatsakis, A.M.; Duarte, J.A.; Carvalho, F. Pesticides exposure as etiological factors of Parkinson's disease and other neurodegenerative diseases-A mechanistic approach. *Toxicol. Lett.* **2014**, *230*, 85–103. [[CrossRef](#)] [[PubMed](#)]

16. Vaccari, C.; El Dib, R.; de Camargo, J.L.V. Paraquat and Parkinson's disease: A systematic review protocol according to the OHAT approach for hazard identification. *Syst. Rev.* **2017**, *6*, 98. [[CrossRef](#)] [[PubMed](#)]
17. Maiti, P.; Manna, J.; Dunbar, G.L.; Maiti, P.; Dunbar, G.L. Current understanding of the molecular mechanisms in Parkinson's disease: Targets for potential treatments. *Transl. Neurodegener.* **2017**, *6*, 28. [[CrossRef](#)]
18. Di Monte, D.A.; Wu, E.Y.; Irwin, I.; Delaney, L.E.; Langston, J.W. Biotransformation of 1-methyl-4-phenyl-1,2,3,6-tetrahydropyridine in primary cultures of mouse astrocytes. *J. Pharmacol. Exp. Ther.* **1991**, *258*, 594–600.
19. Heikkila, R.E.; Hess, A.; Duvoisin, R.C. Dopaminergic neurotoxicity of 1-methyl-4-phenyl-1,2,5,6-tetrahydropyridine in mice. *Science* **1984**, *224*, 1451–1453. [[CrossRef](#)]
20. Javitch, J.A.; D'Amato, R.J.; Strittmatter, S.M.; Snyder, S.H. Parkinsonism-inducing neurotoxin, N-methyl-4-phenyl-1,2,3,6-tetrahydropyridine: Uptake of the metabolite N-methyl-4-phenylpyridine by dopamine neurons explains selective toxicity. *Proc. Natl. Acad. Sci. USA* **1985**, *82*, 2173–2177. [[CrossRef](#)]
21. Watanabe, Y.; Himeda, T.; Araki, T. Mechanisms of MPTP toxicity and their implications for therapy of Parkinson's disease. *Med. Sci. Monit.* **2005**, *11*, RA17–RA23. [[PubMed](#)]
22. Nicklas, W.J.; Vyas, I.; Heikkila, R.E. Inhibition of NADH-linked oxidation in brain mitochondria by 1-methyl-4-phenyl-pyridine, a metabolite of the neurotoxin, 1-methyl-4-phenyl-1,2,5,6-tetrahydropyridine. *Life Sci.* **1985**, *36*, 2503–2508. [[CrossRef](#)]
23. Bose, A.; Beal, M.F. Mitochondrial dysfunction in Parkinson's disease. *J. Neurochem.* **2016**, *139*, 216–231. [[CrossRef](#)]
24. Mapa, M.S.T.; Le, V.Q.; Wimalasena, K. Characteristics of the mitochondrial and cellular uptake of MPP+, as probed by the fluorescent mimic, 4'I-MPP+. *PLoS ONE* **2018**, *13*, e0197946. [[CrossRef](#)] [[PubMed](#)]
25. Zhu, J.H.; Gusdon, A.M.; Cimen, H.; Van Houten, B.; Koc, E.; Chu, C.T. Impaired mitochondrial biogenesis contributes to depletion of functional mitochondria in chronic MPP+ toxicity: Dual roles for ERK1/2. *Cell Death Dis.* **2012**, *3*, e312. [[CrossRef](#)]
26. Choi, W.S.; Kruse, S.E.; Palmiter, R.D.; Xia, Z. Mitochondrial complex I inhibition is not required for dopaminergic neuron death induced by rotenone, MPP+, or paraquat. *Proc. Natl. Acad. Sci. USA* **2008**, *105*, 15136–15141. [[CrossRef](#)]
27. Biedler, J.L.; Schachner, M. Multiple Neurotransmitter Synthesis by Human Neuroblastoma Cell Lines and Clones. *Cancer Res.* **1978**, *38*, 3751–3757.
28. Ross, R.A.; Biedler, J.L. Presence and Regulation of Tyrosinase Activity in Human Neuroblastoma Cell Variants in Vitro. *Cancer Res.* **1985**, *45*, 1628–1632.
29. Pählman, S.; Ruusala, A.I.; Abrahamsson, L.; Mattsson, M.E.K.; Esscher, T. Retinoic acid-induced differentiation of cultured human neuroblastoma cells: A comparison with phorbol ester-induced differentiation. *Cell. Differ.* **1984**, *14*, 135–144. [[CrossRef](#)]
30. Xicoy, H.; Wieringa, B.; Martens, G.J.M. The SH-SY5Y cell line in Parkinson's disease research: A systematic review. *Mol. Neurodegener.* **2017**, *12*, 10. [[CrossRef](#)]
31. Lopes, F.M.; Schröder, R.; Júnior, M.L.C. da F.; Zanutto-Filho, A.; Müller, C.B.; Pires, A.S.; Meurer, R.T.; Colpo, G.D.; Gelain, D.P.; Kapczynski, F.; et al. Comparison between proliferative and neuron-like SH-SY5Y cells as an in vitro model for Parkinson disease studies. *Brain Res.* **2010**, *1337*, 85–94. [[CrossRef](#)]
32. Cheung, Y.T.; Lau, W.K.W.; Yu, M.S.; Lai, C.S.W.; Yeung, S.C.; So, K.F.; Chang, R.C.C. Effects of all-trans-retinoic acid on human SH-SY5Y neuroblastoma as in vitro model in neurotoxicity research. *Neurotoxicology* **2009**, *30*, 127–135. [[CrossRef](#)]
33. Teppola, H.; Sarkanen, J.R.; Jalonen, T.O.; Linne, M.L. Morphological Differentiation Towards Neuronal Phenotype of SH-SY5Y Neuroblastoma Cells by Estradiol, Retinoic Acid and Cholesterol. *Neurochem. Res.* **2016**, *41*, 731–747. [[CrossRef](#)]
34. Pesta, D.; Gnaiger, E. High-resolution respirometry: OXPHOS protocols for human cells and permeabilized fibers from small biopsies of human muscle. *Methods Mol. Biol.* **2012**, *810*, 25–58.
35. Gnaiger, E.; MitoEAGLE Task Group. Mitochondrial physiology. *Bioenerg. Commun.* **2020**, *1*. [[CrossRef](#)]
36. Zhu, J.H.; Horbinski, C.; Guo, F.; Watkins, S.; Uchiyama, Y.; Chu, C.T. Regulation of autophagy by extracellular signal-regulated protein kinases during 1-methyl-4-phenylpyridinium-induced cell death. *Am. J. Pathol.* **2007**, *170*, 75–86. [[CrossRef](#)]
37. Zilocchi, M.; Finzi, G.; Lualdi, M.; Sessa, F.; Fasano, M.; Alberio, T. Mitochondrial alterations in Parkinson's disease human samples and cellular models. *Neurochem. Int.* **2018**, *118*, 61–72. [[CrossRef](#)]

38. Dukes, A.A.; Bai, Q.; Van Laar, V.S.; Zhou, Y.; Ilin, V.; David, C.N.; Agim, Z.S.; Bonkowsky, J.L.; Cannon, J.R.; Watkins, S.C.; et al. Live imaging of mitochondrial dynamics in CNS dopaminergic neurons in vivo demonstrates early reversal of mitochondrial transport following MPP<sup>+</sup> exposure. *Neurobiol. Dis.* **2016**, *95*, 238–249. [[CrossRef](#)] [[PubMed](#)]
39. Gnaiger, E. Capacity of oxidative phosphorylation in human skeletal muscle. New perspectives of mitochondrial physiology. *Int. J. Biochem. Cell Biol.* **2009**, *41*, 1837–1845. [[CrossRef](#)] [[PubMed](#)]
40. Djafarzadeh, S.; Jakob, S.M. High-resolution respirometry to assess mitochondrial function in permeabilized and intact cells. *J. Vis. Exp.* **2017**, *120*, 54985. [[CrossRef](#)]
41. Pfleger, J.; He, M.; Abdellatif, M. Mitochondrial complex II is a source of the reserve respiratory capacity that is regulated by metabolic sensors and promotes cell survival. *Cell Death Dis.* **2015**, *6*, e1835. [[CrossRef](#)] [[PubMed](#)]
42. Evinova, A.; Cizmarova, B.; Hatokova, Z.; Racay, P. High-Resolution Respirometry in Assessment of Mitochondrial Function in Neuroblastoma SH-SY5Y Intact Cells. *J. Membr. Biol.* **2020**, *253*, 12–136.
43. Stepanova, A.; Shurubor, Y.; Valsecchi, F.; Manfredi, G.; Galkin, A. Differential susceptibility of mitochondrial complex II to inhibition by oxaloacetate in brain and heart. *Biochim. Biophys. Acta Bioenerg.* **2016**, *1857*, 1561–1568. [[CrossRef](#)] [[PubMed](#)]
44. Manczak, M.; Reddy, P.H. Abnormal interaction of VDAC1 with amyloid beta and phosphorylated tau causes mitochondrial dysfunction in Alzheimer's disease. *Hum. Mol. Genet.* **2012**, *21*, 5131–5146. [[CrossRef](#)]
45. Smilansky, A.; Dangoor, L.; Nakdimon, I.; Ben-Hail, D.; Mizrahi, D.; Shoshan-Barmatz, V. The voltage-dependent anion channel 1 mediates amyloid  $\beta$  toxicity and represents a potential target for Alzheimer disease therapy. *J. Biol. Chem.* **2015**, *290*, 30670–30683. [[CrossRef](#)]
46. Israelson, A.; Arbel, N.; Da Cruz, S.; Ilieva, H.; Yamanaka, K.; Shoshan-Barmatz, V.; Cleveland, D.W. Misfolded mutant SOD1 directly inhibits VDAC1 conductance in a mouse model of inherited ALS. *Neuron* **2010**, *67*, 575–587. [[CrossRef](#)] [[PubMed](#)]
47. Magri, A.; Belfiore, R.; Reina, S.; Tomasello, M.F.; Di Rosa, M.C.; Guarino, F.; Leggio, L.; De Pinto, V.; Messina, A. Hexokinase i N-terminal based peptide prevents the VDAC1-SOD1 G93A interaction and re-establishes ALS cell viability. *Sci. Rep.* **2016**, *6*, 34802. [[CrossRef](#)]
48. Shteinfer-Kuzmine, A.; Argueti, S.; Gupta, R.; Shvil, N.; Abu-Hamad, S.; Gropper, Y.; Hoeber, J.; Magri, A.; Messina, A.; Kozlova, E.N.; et al. A VDAC1-Derived N-Terminal Peptide Inhibits Mutant SOD1-VDAC1 Interactions and Toxicity in the SOD1 Model of ALS. *Front. Cell. Neurosci.* **2019**, *13*, 346. [[CrossRef](#)] [[PubMed](#)]
49. Rostovtseva, T.K.; Gurnev, P.A.; Protchenko, O.; Hoogerheide, D.P.; Yap, T.L.; Philpott, C.C.; Lee, J.C.; Bezrukov, S.M.  $\alpha$ -synuclein shows high affinity interaction with voltage-dependent anion channel, suggesting mechanisms of mitochondrial regulation and toxicity in Parkinson disease. *J. Biol. Chem.* **2015**, *290*, 18467–18477. [[CrossRef](#)]
50. Magri, A.; Messina, A. Interactions of VDAC with proteins involved in neurodegenerative aggregation: An opportunity for advancement on therapeutic molecules. *Curr. Med. Chem.* **2017**, *24*, 4470–4487. [[CrossRef](#)]
51. Leggio, L.; Guarino, F.; Magri, A.; Accardi-Gheit, R.; Reina, S.; Specchia, V.; Damiano, F.; Tomasello, M.F.; Tommasino, M.; Messina, A. Mechanism of translation control of the alternative *Drosophila melanogaster* Voltage Dependent Anion-selective Channel 1 mRNAs. *Sci. Rep.* **2018**, *8*, 5347. [[CrossRef](#)] [[PubMed](#)]
52. Magri, A.; Di Rosa, M.C.; Tomasello, M.F.; Guarino, F.; Reina, S.; Messina, A.; De Pinto, V. Overexpression of human SOD1 in VDAC1-less yeast restores mitochondrial functionality modulating beta-barrel outer membrane protein genes. *Biochim. Biophys. Acta Bioenerg.* **2016**, *1857*, 789–798. [[CrossRef](#)] [[PubMed](#)]
53. Messina, A.; Reina, S.; Guarino, F.; De Pinto, V. VDAC isoforms in mammals. *Biochim. Biophys. Acta Biomembr.* **2012**, *1818*, 1466–1476. [[CrossRef](#)] [[PubMed](#)]
54. Magri, A.; Di Rosa, M.C.; Orlandi, I.; Guarino, F.; Reina, S.; Guarnaccia, M.; Morello, G.; Spampinato, A.; Cavallaro, S.; Messina, A.; et al. Deletion of Voltage-Dependent Anion Channel 1 knocks mitochondria down triggering metabolic rewiring in yeast. *Cell. Mol. Life Sci.* **2020**, *77*, 3195–3213. [[CrossRef](#)] [[PubMed](#)]
55. Hoogerheide, D.P.; Gurnev, P.A.; Rostovtseva, T.K.; Bezrukov, S.M. Mechanism of  $\alpha$ -synuclein translocation through a VDAC nanopore revealed by energy landscape modeling of escape time distributions. *Nanoscale* **2017**, *9*, 183–192. [[CrossRef](#)]
56. Devi, L.; Raghavendran, V.; Prabhu, B.M.; Avadhani, N.G.; Anandatheerthavarada, H.K. Mitochondrial import and accumulation of  $\alpha$ -synuclein impair complex I in human dopaminergic neuronal cultures and Parkinson disease brain. *J. Biol. Chem.* **2008**, *283*, 9089–9100. [[CrossRef](#)]



57. Elkon, H.; Don, J.; Melamed, E.; Ziv, I.; Shirvan, A.; Offen, D. Mutant and wild-type  $\alpha$ -synuclein interact with mitochondrial cytochrome C oxidase. *J. Mol. Neurosci.* **2002**, *18*, 229–238. [[CrossRef](#)]
58. Fritz, R.R.; Abell, C.W.; Patel, N.T.; Gessner, W.; Brossi, A. Metabolism of the neurotoxin in MPTP by human liver monoamine oxidase B. *FEBS Lett.* **1985**, *186*, 224–228. [[CrossRef](#)]
59. Jastroch, M.; Divakaruni, A.S.; Mookerjee, S.; Treberg, J.R.; Brand, M.D. Mitochondrial proton and electron leaks. *Essays Biochem.* **2010**, *47*, 53–67.
60. Ramonet, D.; Perier, C.; Recasens, A.; Dehay, B.; Bové, J.; Costa, V.; Scorrano, L.; Vila, M. Optic atrophy 1 mediates mitochondria remodeling and dopaminergic neurodegeneration linked to complex I deficiency. *Cell Death Differ.* **2013**, *20*, 77–85. [[CrossRef](#)]
61. Calabria, E.; Scambi, I.; Bonafede, R.; Schiaffino, L.; Peroni, D.; Potrich, V.; Capelli, C.; Schena, F.; Mariotti, R. Ascs-exosomes recover coupling efficiency and mitochondrial membrane potential in an in vitro model of ALS. *Front. Neurosci.* **2019**, *13*, 1070. [[CrossRef](#)]
62. Ricquier, D.; Bouillaud, F. The uncoupling protein homologues: UCP1, UCP2, UCP3, StUCP and AtUCP. *Biochem. J.* **2000**, *345*, 161–179. [[CrossRef](#)] [[PubMed](#)]
63. Porter, R.K. Mitochondrial proton leak: A role for uncoupling proteins 2 and 3? *Biochim. Biophys. Acta Bioenerg.* **2001**, *1504*, 120–127. [[CrossRef](#)]
64. Cannon, B.; Shabalina, I.G.; Kramarova, T.V.; Petrovic, N.; Nedergaard, J. Uncoupling proteins: A role in protection against reactive oxygen species-or not? *Biochim. Biophys. Acta Bioenerg.* **2006**, *1757*, 449–458. [[CrossRef](#)] [[PubMed](#)]
65. Ho, P.W.L.; Chan, D.Y.L.; Kwok, K.H.H.; Chu, A.C.Y.; Ho, J.W.M.; Kung, M.H.W.; Ramsden, D.B.; Ho, S.L. Methyl-4-phenylpyridinium ion modulates expression of mitochondrial uncoupling proteins 2, 4, and 5 in catecholaminergic (SK-N-SH) cells. *J. Neurosci. Res.* **2005**, *81*, 261–268. [[CrossRef](#)]
66. Chu, A.C.Y.; Ho, P.W.L.; Kwok, K.H.H.; Ho, J.W.M.; Chan, K.H.; Liu, H.F.; Kung, M.H.W.; Ramsden, D.B.; Ho, S.L. Mitochondrial UCP4 attenuates MPP<sup>+</sup> and dopamine-induced oxidative stress, mitochondrial depolarization, and ATP deficiency in neurons and is interlinked with UCP2 expression. *Free Radic. Biol. Med.* **2009**, *46*, 810–820. [[CrossRef](#)] [[PubMed](#)]
67. Kwok, K.H.H.; Ho, P.W.L.; Chu, A.C.Y.; Ho, J.W.M.; Liu, H.F.; Yiu, D.C.W.; Chan, K.H.; Kung, M.H.W.; Ramsden, D.B.; Ho, S.L. Mitochondrial UCP5 is neuroprotective by preserving mitochondrial membrane potential, ATP levels, and reducing oxidative stress in MPP<sup>+</sup> and dopamine toxicity. *Free Radic. Biol. Med.* **2010**, *49*, 1023–1035. [[CrossRef](#)] [[PubMed](#)]
68. Ho, P.W.L.; Ho, J.W.M.; Tse, H.M.; So, D.H.F.; Yiu, D.C.W.; Liu, H.F.; Chan, K.H.; Kung, M.H.W.; Ramsden, D.B.; Ho, S.L. Uncoupling protein-4 (UCP4) increases ATP supply by interacting with mitochondrial complex II in neuroblastoma cells. *PLoS ONE* **2012**, *7*, e32810. [[CrossRef](#)]
69. L'Episcopo, F.; Serapide, M.F.; Tirolo, C.; Testa, N.; Caniglia, S.; Morale, M.C.; Pluchino, S.; Marchetti, B. A Wnt1 regulated Frizzled-1/ $\beta$ -catenin signaling pathway as a candidate regulatory circuit controlling mesencephalic dopaminergic neuron-astrocyte crosstalk: Therapeutical relevance for neuron survival and neuroprotection. *Mol. Neurodegener.* **2011**, *6*, 49. [[CrossRef](#)]
70. Shipley, M.M.; Mangold, C.A.; Szpara, M.L. Differentiation of the SH-SY5Y human neuroblastoma cell line. *J. Vis. Exp.* **2016**, *108*, 53193. [[CrossRef](#)]

**Publisher's Note:** MDPI stays neutral with regard to jurisdictional claims in published maps and institutional affiliations.



© 2020 by the authors. Licensee MDPI, Basel, Switzerland. This article is an open access article distributed under the terms and conditions of the Creative Commons Attribution (CC BY) license (<http://creativecommons.org/licenses/by/4.0/>).

## Supplemental Materials

**Table S1.** Oxygen flux calculated for each respiratory state corrected for the ROX respiration in untreated (CTRL) and MPP<sup>+</sup> treated cells. Data are reported as mean  $\pm$  standard deviation of  $n = 5$  independent experiments.

	<i>CTRL</i>	<i>MPP<sup>+</sup></i>
ROUTINE	15.75 $\pm$ 3.68	4.77 $\pm$ 2.14
LEAK	5.62 $\pm$ 0.95	3.64 $\pm$ 1.86
OXPHOS sustained by complex I	18.74 $\pm$ 4.28	5.68 $\pm$ 1.60
OXPHOS sustained by complex I & II	27.57 $\pm$ 5.97	10.15 $\pm$ 2.16
ETS	30.27 $\pm$ 5.49	11.29 $\pm$ 2.24
ETS sustained by complex II	12.96 $\pm$ 2.41	7.99 $\pm$ 2.71

**Table S2.** FCR calculated for each respiratory state as ETS percentage in untreated (CTRL) and MPP<sup>+</sup> treated cells. Data are reported as mean  $\pm$  standard deviation of  $n = 5$  independent experiments.

	<i>CTRL</i>	<i>MPP<sup>+</sup></i>
ROUTINE	0.51 $\pm$ 0.03	0.41 $\pm$ 0.12
LEAK	0.19 $\pm$ 0.05	0.31 $\pm$ 0.09
OXPHOS sustained by complex I	0.61 $\pm$ 0.03	0.50 $\pm$ 0.13
OXPHOS sustained by complex I & II	0.90 $\pm$ 0.03	0.90 $\pm$ 0.07
ETS sustained by complex II	0.42 $\pm$ 0.02	0.76 $\pm$ 0.18

**Table S3.** FCR calculated for net and coupling respiration, and E-R capacity factor. All data are expressed as ETS percentage in untreated (CTRL) and MPP<sup>+</sup> treated cells. Data are reported as mean  $\pm$  standard deviation of  $n = 5$  independent experiments.

	<i>CTRL</i>	<i>MPP<sup>+</sup></i>
netROUTINE control ratio	0.32 $\pm$ 0.05	0.09 $\pm$ 0.07
netOXPOS control ratio	0.71 $\pm$ 0.08	0.58 $\pm$ 0.12
ROUTINE coupling efficiency	0.62 $\pm$ 0.10	0.23 $\pm$ 0.15
OXPHOS coupling efficiency	0.78 $\pm$ 0.06	0.65 $\pm$ 0.11
OXPHOS complex I coupling efficiency	0.69 $\pm$ 0.08	0.53 $\pm$ 0.08
ETS coupling efficiency	0.80 $\pm$ 0.05	0.68 $\pm$ 0.09
<i>E-R</i> capacity factor	0.48 $\pm$ 0.03	0.58 $\pm$ 0.12


# Small Extracellular Vesicles Secreted by Nigrostriatal Astrocytes Rescue Cell Death and Preserve Mitochondrial Function in Parkinson's Disease

Loredana Leggio, Francesca L'Episcopo, Andrea Magri, María José Ulloa-Navas, Greta Paternò, Silvia Vivarelli, Carlos A. P. Bastos, Cataldo Tirolo, Nunzio Testa, Salvatore Caniglia, Pierpaolo Risiglione, Fabrizio Pappalardo, Alessandro Serra, Patricia García-Tárraga, Nuno Faria, Jonathan J. Powell, Luca Peruzzotti-Jametti, Stefano Pluchino, José Manuel García-Verdugo, Angela Messina, Bianca Marchetti,\* and Nunzio Iraci\*

Extracellular vesicles (EVs) are emerging as powerful players in cell-to-cell communication both in healthy and diseased brain. In Parkinson's disease (PD)—characterized by selective dopaminergic neuron death in ventral midbrain (VMB) and degeneration of their terminals in striatum (STR)—astrocytes exert dual harmful/protective functions, with mechanisms not fully elucidated. Here, this study shows that astrocytes from the VMB-, STR-, and VMB/STR-depleted brains release a population of small EVs in a region-specific manner. Interestingly, VMB-astrocytes secreted the highest rate of EVs, which is further exclusively increased in response to CCL3, a chemokine that promotes robust dopaminergic neuroprotection in different PD models. The neuroprotective potential of nigrostriatal astrocyte-EVs is investigated in differentiated versus undifferentiated SH-SY5Y cells exposed to oxidative stress and mitochondrial toxicity. EVs from both VMB- and STR-astrocytes counteract H<sub>2</sub>O<sub>2</sub>-induced caspase-3 activation specifically in differentiated cells, with EVs from CCL3-treated astrocytes showing a higher protective effect. High resolution respirometry further reveals that nigrostriatal astrocyte-EVs rescue neuronal mitochondrial complex I function impaired by the neurotoxin MPP<sup>+</sup>. Notably, only EVs from VMB-astrocyte fully restore ATP production, again specifically in differentiated SH-SY5Y. These results highlight a regional diversity in the nigrostriatal system for the secretion and activities of astrocyte-EVs, with neuroprotective implications for PD.

## 1. Introduction

Extracellular vesicles (EVs) are nanometric (30–1000 nm) lipid membranous structures released by virtually all cell types into the extracellular milieu, where they can be captured by adjacent or distal cells.<sup>[1–4]</sup> EVs is a general term used to describe a complex set of vesicles with distinct biogenesis and release mechanisms. Exosomes, microvesicles and apoptotic bodies partially overlap in terms of dimension and composition, making it difficult to identify specific EV subclasses.<sup>[5]</sup> Based on size, EVs are referred to as medium-large (>200 nm) or small (<200 nm, sEVs).<sup>[5–7]</sup> The importance of EVs in mediating cell-to-cell communication resides in their ability to deliver different cargoes (i.e., nucleic acids, proteins, metabolites, lipids) to target cells, thus influencing the cellular fate.<sup>[8–12]</sup> EVs have been identified in body fluids as potential new biomarkers for several diseases and are also exploited as advanced nanotherapeutics in regenerative medicine.<sup>[13–25]</sup> Like their synthetic liposomal counterpart, EVs protect their payloads from the action of nucleases and proteases, allowing the delivery

 The ORCID identification number(s) for the author(s) of this article can be found under <https://doi.org/10.1002/adhm.202201203>

© 2022 The Authors. Advanced Healthcare Materials published by Wiley-VCH GmbH. This is an open access article under the terms of the Creative Commons Attribution License, which permits use, distribution and reproduction in any medium, provided the original work is properly cited.

DOI: 10.1002/adhm.202201203

L. Leggio, G. Paternò, S. Vivarelli, F. Pappalardo, B. Marchetti, N. Iraci  
Department of Biomedical and Biotechnological Sciences  
University of Catania  
Catania 95123, Italy  
E-mail: biancamarchetti@libero.it nunzio.iraci@unicat.it  
F. L'Episcopo, C. Tirolo, N. Testa, S. Caniglia, B. Marchetti  
Oasi Research Institute-IRCCS  
Troina 94018, Italy



to distant sites.<sup>[20]</sup> Also, EVs display innate properties, such as the ability to cross biological barriers (e.g., blood brain barrier, although the mechanisms are not fully elucidated),<sup>[26,27]</sup> and a potential low immunogenicity.<sup>[28,29]</sup> Moreover, EVs possess a fingerprint, inherited from their donor cells, that distinguishes vesicles derived from different cell types.<sup>[20,30–32]</sup> Importantly, the EV content: i) reflects the “status” of the donor cell; and ii) it can change in response to specific modifications in the microenvironment.<sup>[33]</sup>

EVs have been demonstrated to play several roles in physiopathological conditions.<sup>[34]</sup> In the context of neurodegenerative diseases, including Parkinson’s disease (PD), EVs were initially identified as vehicles of misfolded proteins,<sup>[35–37]</sup> but in line with the dual role played by glial cells, EVs have been demonstrated to play also important neuroprotective functions.<sup>[38,39]</sup>

In particular, astrocyte (AS) dysfunction is increasingly emerging as a critical feature of PD,<sup>[40–51]</sup> the second most common neurodegenerative disorder, with no available cure to stop or reverse its progression.<sup>[52]</sup> PD is characterized by the selective and unrestrained death of dopaminergic (DAergic) cell bodies of the substantia nigra pars compacta (SNpc), residing in the ventral midbrain (VMB).<sup>[52–54]</sup> As a consequence, in the striatum (STR), DAergic terminals slowly degenerate leading to the classical motor features of PD (i.e., bradykinesia, rest tremor, rigidity, and postural instability).<sup>[52–55]</sup> Along with the chronic, age-dependent nigrostriatal degeneration, the abnormal accumulation of intraneuronal inclusions enriched in aggregated  $\alpha$ -synuclein ( $\alpha$ -syn), known as Lewy bodies (LBs) and Lewy neurites (LNs), as well as a massive astrogliosis, represent the major histopathologic hallmarks of the disease.<sup>[55–58]</sup> The causes and mechanisms of DAergic neuron death still remain elusive, albeit current evidence implicate a complex interplay between several genes and many environmental factors, especially ageing, inflammation and oxidative stress, all robustly impacting the astroglial cell compartment.<sup>[40,41,44–46,48,59–63]</sup> Converging data point to mitochondrial dysfunction as the pivotal final pathway for PD neurodegeneration, closely related to the selective

vulnerability of nigrostriatal neurons and to the specific properties of the astroglial microenvironment.<sup>[63–74]</sup> In fact, AS are active mediators of either beneficial or detrimental functions during neuronal degeneration, via the expression of a plethora of proinflammatory/anti-inflammatory molecules and neurotoxic/neuroprotective mediators.<sup>[41,44,45,71,72,75,76]</sup> The balance between these messengers, together with the bidirectional signaling with microglial cells, will determine the fate either toward a reparative process or a neuronal failure.

In this context, growing evidence highlights regional AS heterogeneity, at both molecular and functional levels, with important consequences for neuronal function and/or vulnerability.<sup>[77–87]</sup> Of note, AS display unique features within the nigrostriatal system, since within the central nervous system (CNS), VMB and STR are highly sensitive to oxidative stress, environmental toxins, inflammatory challenges, and ageing.<sup>[40,44,85,87–90]</sup> Also, AS exhibit regional heterogeneity in response to cytokines and chemokines during neuroinflammation and neurodegeneration/neuroprotection, with increasing evidence pointing at chemokines as major mediators of glia-neuron crosstalk.<sup>[91–93]</sup>

Accordingly, within the VMB, AS exert potent neuroprotective effects toward the vulnerable SNpc-DAergic neurons (reviewed in Ref. [73]). In particular, reactive VMB-AS were identified as main actors linking neuroinflammation to DAergic neuroprotection and repair in the 1-methyl, 4-phenyl, 1,2,3,6 tetrahydropyridine (MPTP) mouse model of basal ganglia injury.<sup>[94]</sup> In this context, a wide gene expression analysis identified a major upregulation of certain chemokines, in particular the CC chemokine ligand 3 (CCL3), shown to play important roles for DAergic neurogenesis, survival, and immunomodulation.<sup>[94–96]</sup> Notably, in vitro studies revealed CCL3-activated AS-neuron crosstalk as a critical element promoting both neuroprotection and neurogenesis of adult neural stem cells (NSCs).<sup>[44,73,94]</sup> However, the molecular details of this complex intercellular signaling are still a matter of intense debate. Here, we scrutinized the secretion of AS-derived extracellular vesicles (AS-EVs) from the VMB versus STR brain regions, in both basal and CCL3-activated conditions, as a likely way of communication with injured DAergic neurons. For the first time, our study demonstrates that AS-EVs in the nigrostriatal system propagate specific neuroprotective intercellular signaling, targeting neural oxidative damage and mitochondrial dysfunction, with region-dependent functional implications. This potential may be exploited to enhance the neuroprotection of DAergic neurons in PD.

## 2. Results

### 2.1. Astrocytes from the Nigrostriatal System Secrete Small EVs in a Region-Specific Manner

To assess potential differences in AS-EVs between the two principal brain regions affected in PD, primary AS cultures were established from the VMB and STR (Figure S1, Supporting Information).<sup>[94]</sup> Also, AS were grown from brains depleted of these two regions (hereafter called  $\Delta$ VS-AS), as control cells external to the nigrostriatal system (Figure S1, Supporting Information). AS were characterized under both basal and CCL3-treated (24 h) conditions, to test whether the latter confers additional pro-

A. Magri, P. Risiglione, A. Messina  
Department of Biological, Geological and Environmental Sciences  
University of Catania  
Catania 95125, Italy

M. J. Ulloa-Navas, P. García-Tárraga, J. M. García-Verdugo  
Laboratory of Compared Neurobiology  
University of Valencia-CIBERNED  
Paterna 46980, Spain

M. J. Ulloa-Navas  
Department of Neuroscience  
Mayo Clinic  
Jacksonville, FL 32257, USA

C. A. P. Bastos, N. Faria, J. J. Powell  
Department of Veterinary Medicine  
University of Cambridge  
Cambridge CB3 0ES, UK

A. Serra  
Luminex B.V.  
’s-Hertogenbosch 5115 MV, The Netherlands

L. Peruzzotti-Jametti, S. Pluchino  
Department of Clinical Neurosciences  
University of Cambridge  
Cambridge CB2 0QQ, UK

tective effects to AS-EVs.<sup>[94]</sup> All primary cultures produced high purity AS ( $\geq 98\%$  of GFAP<sup>+</sup> cells), without any differences in terms of proliferation rate upon CCL3 treatment (Figure S1A–D, Supporting Information). Moreover, in order to evaluate the health of AS at the time of EV isolation, the cell viability/death levels were investigated, and no significant differences were found between experimental groups, demonstrating that these factors are not in play to influence the production rate of AS-EVs from different brain regions (Figure S1E, Supporting Information).

Next, EVs were isolated from AS supernatants by differential centrifugation<sup>[97,98]</sup> and analyzed using a combination of different techniques, in order to evaluate dimensions, secretion rates, and specific markers. As a first line of characterization, we performed nanoparticle tracking analysis (NTA) on all EV samples. The data displayed an enriched population of vesicles with a peak size  $\approx 100$  nm, in the range of sEVs (Figure 1A). Interestingly, we observed that brain region of origin impacts on the EV secretion rate of astrocytes, since VMB-AS released 2- to 4-fold more vesicles per million cells compared to STR and  $\Delta$ VS, with an increased trend following CCL3 treatment (Figure 1B).

To further investigate this finding, we performed transmission electron microscopy (TEM) analysis on the same EV samples. The images show the presence of sEVs with the cup shapes, a typical result of the ultracentrifugation process (Figure 1C), with an average diameter between 60 and 70 nm (Figure 1D and Table S1, Supporting Information). Again, we found that VMB-AS released more vesicles than astrocytes from STR and  $\Delta$ VS (Figure 1E), corroborating the NTA results. Interestingly, we observed that the treatment with CCL3 stimulated VMB-AS to secrete more EVs (Figure 1E), while the other two regions did not show any significant change in the secretion rate following the CCL3 treatment (Figure 1E).

To study the differential responses to CCL3 between the three types of astrocytes, we evaluated the expression of the main chemokine receptors, Ccr1 and Ccr5,<sup>[99,100]</sup> by quantitative real-time PCR (qPCR). Ccr1 and Ccr5 levels were comparable between VMB and STR, and unchanged after treatment with CCL3 (Figure S2A, Supporting Information). In contrast, Ccr1 and Ccr5 expression in  $\Delta$ VS-AS samples was  $\approx 100$  times lower than in VMB- and STR-AS, with no change upon chemokine treatment (Figure S2A, Supporting Information). These data suggest that only the main regions involved in PD, namely VMB and STR, have the potential to respond to treatment with CCL3, corroborating previous findings.<sup>[40,94,101–103]</sup> (Figure S2A, Supporting Information). Such a limited capacity of  $\Delta$ VS-AS to respond to our stimulation protocol, prompted us to focus on the nigrostriatal system to further explore whether CCL3 elicits any cellular response in VMB- and STR-AS. Histological analysis performed in 1.5  $\mu$ m sections showed that CCL3 induces STR-AS to shift to a more pronounced irregular membrane morphology compared to VMB-AS (Figure S2B, Supporting Information). Moreover, scanning electron microscopy (SEM) analyses evidenced the remarkable presence of connectivity/secretory structures (e.g., microvilli-like processes) at the cellular surface of both VMB- and STR-AS (Figure S2C, Supporting Information). Again, STR-CCL3-AS exhibit a higher number of these membrane protrusions, suggesting that both brain regions are able to respond to CCL3, but with a different outcome (Figure S2C, Supporting Information). Interestingly, this

responsiveness involves changes in membrane dynamics, in line with published evidences regarding CCL3.<sup>[104,105]</sup>

Overall, these data demonstrate that AS-EV secretion characteristics are defined by their brain area origins.

## 2.2. Both VMB- and STR-AS-Derived Vesicles Are Enriched in sEV Markers

Next, we investigated the protein profiles of AS-EVs from the nigrostriatal system. We applied immunogold-labelling TEM (IG-TEM) for the tetraspanins CD63 and CD9, as sEV markers. The images in Figure 2A,B revealed the presence of both proteins, visualized as well-defined 6 nm gold nanoparticles at the EV surface. In order to extend these results to other sEV markers, and exclude contamination from other cellular components, we used western blotting (WB) (Figure 2C,D). In line with the immunogold-labelling TEM (IG-TEM) data, we found a specific enrichment of the tetraspanins CD63/CD9 and Pcd61p (Alix) in all EV samples compared to donor AS. In contrast, the cellular markers Golga2 (for Golgi), calnexin (for endoplasmic reticulum), SDHA (for mitochondria) and actin (for cytoplasm), were mainly retained in the cells (Figure 2C,D). These results confirm that our vesicular preparations are enriched in sEVs.

## 2.3. Both VMB- and STR-AS-Derived Vesicles Are Internalized by SH-SY5Y Cells

Before examining the effects of the sEVs on target neurons, we evaluated their internalization using the human neuroblastoma SH-SY5Y cells differentiated with retinoic acid (RA), as a model of tyrosine hydroxylase positive (TH<sup>+</sup>) neuronal target cells.<sup>[106–108]</sup> To follow AS-EVs, we used two different labeling approaches: i) both VMB- and STR-AS were treated with the PKH26 membrane dye, followed by ultracentrifugation to isolate labelled EVs (Figure 3A and Figure S3A,B, Supporting Information); and ii) PKH26 were applied directly to AS-EVs after ultracentrifugation (Figure S3C, Supporting Information). Both approaches led to PKH26-labelled AS-EVs, which were then administered to target cells at a ratio of 5:1 (EVs derived from five astrocytes used to treat one target cells), in line with the local brain tissue architecture.<sup>[109,110]</sup> First, the capacity of differentiated SH-SY5Y cells to internalize AS-EVs was evaluated by confocal microscopy. As shown by the orthogonal view analyses reported in Figure 3A and Figure S3A, Supporting Information, PKH26-labelled AS-EVs were efficiently taken up by cells and partially co-localized with TH, which has a high affinity for phospholipid membranes.<sup>[111]</sup> A volumetric 3D reconstruction of the intracellular distribution of AS-EVs confirms the effective enrichment of vesicles within the cytoplasmic compartment (Figure S3B and Movies S1 and S2, Supporting Information). Moreover, the bright field/IF combined view suggests that AS-EVs are distributed in the whole cytoplasm, including neurite protrusions (Figure S3C, Supporting Information). Thus, AS-EVs can be efficiently transferred to neuronal target cells.

Next, in order to quantify the internalization of the different vesicle samples by target cells, PKH26-labelled AS-EVs were administered to differentiated SH-SY5Y followed by imaging flow

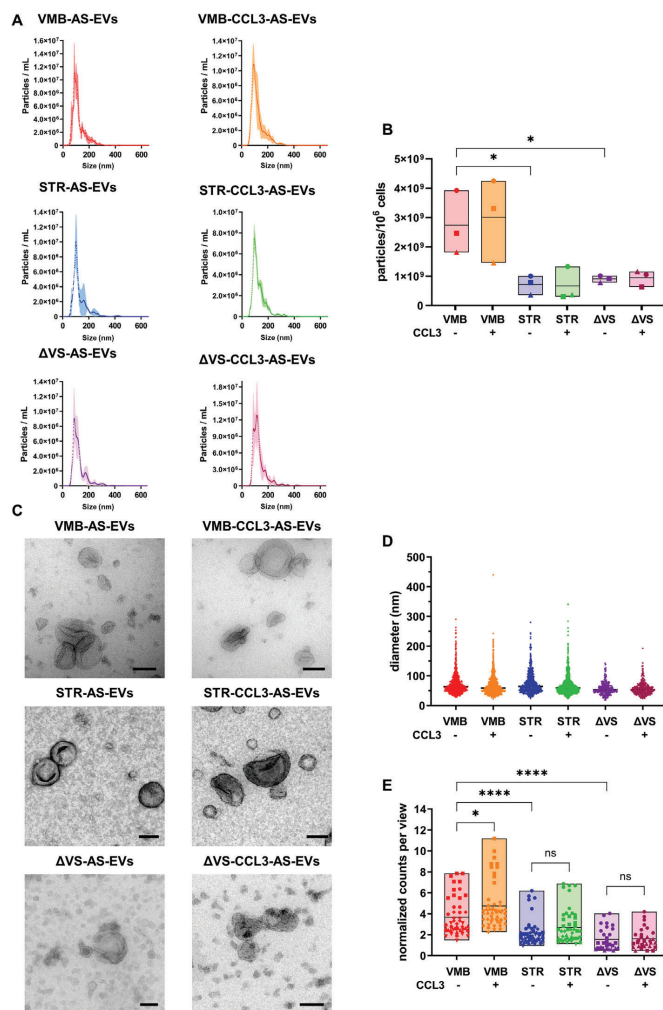


**Figure 1.** Brain region influences the rate of secretion of AS-sEVs and responsiveness to CCL3 treatment. **A)** NTA analysis for size distribution displays a peak  $\approx 100$  nm. Error bars represent SD from  $n = 3$  independent replicates. **B)** EV concentration, determined by NTA, was normalized over the number of cells. The mean of particles/10<sup>6</sup> cells shows that astrocytes from VMB region secrete more EVs than STR and ΔVS regions. Data are presented as floating bars with line at mean from  $n = 3$  independent replicates, indicated with different symbols. One-way ANOVA with Tukey's multiple comparison  $*p < 0.05$  (VMB-AS-EVs versus STR-AS-EVs; VMB-AS-EVs versus ΔVS-AS-EVs). **C)** TEM ultrastructural analysis reveals the presence of sEVs secreted by AS in every condition. Scale bars: 100 nm. **D)** In all AS-EV samples the average diameter is  $\approx 60/70$  nm. Raw data (diameter values) are presented as scatter dot plots with line at median  $\pm$  SD from  $n = 5$  (for VMB- and STR-AS-EVs) and  $n = 3$  (for ΔVS-AS-EVs) independent experiments. **E)** Quantitative analysis from TEM showed that astrocytes from VMB secrete more EVs than STR and ΔVS regions; the treatment with CCL3 stimulates VMB-AS to release more EVs. Data are normalized considering the number of starting cells, the resuspension volume after ultracentrifugation, the volume used in the microscope grid, and the area ( $\mu\text{m}^2$ ) of each field in the grid. Data are presented as floating bars with line at mean plus individual data points based on 50 images over 5 independent replicates (for VMB- and STR-AS-EVs) and on 30 images over 3 independent replicates (for ΔVS-AS-EVs), indicated with different symbols. One-way ANOVA with Tukey's multiple comparison: in **(B)**  $*p < 0.05$  (VMB-AS-EVs versus STR-AS-EVs and versus ΔVS-AS-EVs; in **(E)**  $*p < 0.05$  (VMB-AS-EVs versus VMB-CCL3-AS-EVs),  $****p < 0.0001$  (VMB-AS-EVs versus STR-AS-EVs and ΔVS-AS-EVs), ns: not significant.

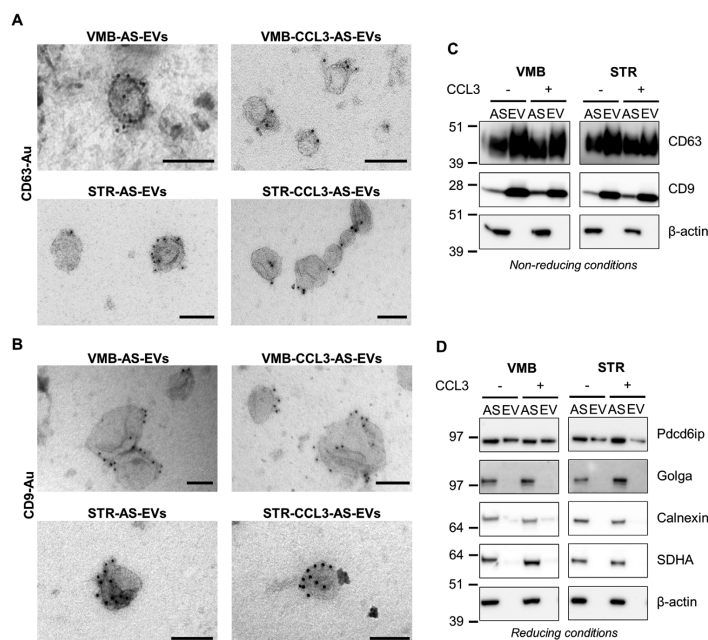


**Figure 2.** AS secrete vesicles enriched in sEV markers. A,B) IG-TEM on EV samples with  $\alpha$ -CD63 (A) and  $\alpha$ -CD9 (B). Scale bars: 100 nm. C,D) WB analyses on EV lysates and corresponding AS donor cells. WBs for  $\alpha$ -CD63/CD9 (C), in non-reducing conditions and for Pcd6ip (D), in reducing conditions show an enrichment in the EV samples versus donor AS. On the contrary, the cellular markers (i.e., Golga, Calnexin, SDHA, and Actin) are mostly enriched in AS (D). All panels are representative of  $n = 3$  independent experiments showing the same trend.

cytometry (IFC),<sup>[112]</sup> and their fluorescence intensity was measured after 2, 6 and 24 h (Figure 3B). Fluorescence increased in time dependent manner: i) at 2 h there was no significant difference between untreated (CTRL) and treated cells; ii) at 6 h fluorescence intensity increased significantly by 1.4- to 1.7-fold versus CTRL; and iii) at 24 h PKH26 intensity further increased (Figure 3C), suggesting that AS-EVs continued to enter target neurons (Figure 3C), in line with previous reports.<sup>[113]</sup>

Although it is not possible to exclude that PKH26 can label certain contaminant proteins in EV preparations,<sup>[114,115]</sup> it is unlikely that dye self-aggregation interfered with the analysis of vesicle uptake, as dye-only samples failed to label SH-SY5Y cells at all time points and with both techniques (i.e., IFC and IF) (Figure 3C and Figure S3C, Supporting Information).

Finally, in order to evaluate whether the differentiation process may influence the uptake of AS-EVs, we performed the same IFC analysis using undifferentiated SH-SY5Y target cells. As shown in Figure S3D, Supporting Information, a similar uptake time-course was observed for these cells (fluorescence intensity significantly rising by 1.4- to 1.8-fold after 6 h, with the uptake at 24 h higher than at 6 h). Thus, AS-EVs are internalized to a similar extent by SH-SY5Y cells, regardless of the regional identity of donor astrocytes, or the differentiation state of target neurons.

#### 2.4. EVs from CCL3-Activated Astrocytes Prevent $H_2O_2$ -Induced Caspase-3 Activation in Differentiated SH-SY5Y Neurons

To evaluate the effects of AS-EVs on target differentiated SH-SY5Y cells under oxidative stress/neurodegenerative conditions, we used the hydrogen peroxide ( $H_2O_2$ ),<sup>[116]</sup> a general source of ROS, and the neurotoxin MPP<sup>+</sup>, both used as well-established *in vitro* models of PD.<sup>[117–119]</sup> Based on preliminary time-course and dose-response experiments, we applied 35  $\mu M$   $H_2O_2$  or 1 mM MPP<sup>+</sup> for 24 h, treatments which consistently reduced cell viability by  $\approx 40\%$  and  $\approx 10\%$ , respectively—without inducing an acute and massive cell death (Figure S4A,B, Supporting Information).<sup>[120–122]</sup> Considering the internalization data, target cells were incubated with a 5:1 ratio of AS-EVs 6 h prior to the challenge with  $H_2O_2$  or MPP<sup>+</sup>, to allow a significant uptake of vesicles.

First, the extent of apoptosis was measured in differentiated SH-SY5Y cells using cleaved caspase-3 (c-Casp-3), whose levels were evaluated 24 h after  $H_2O_2$  treatment via IF (Figure 4A). Analysis of fluorescence intensity revealed that  $H_2O_2$  induced a 3-fold increase of c-Casp-3 compared to untreated cells (CTRL, Figure 4B). The presence of both VMB- and STR-AS-EVs significantly reduced apoptosis levels, with the EVs from CCL3-treated

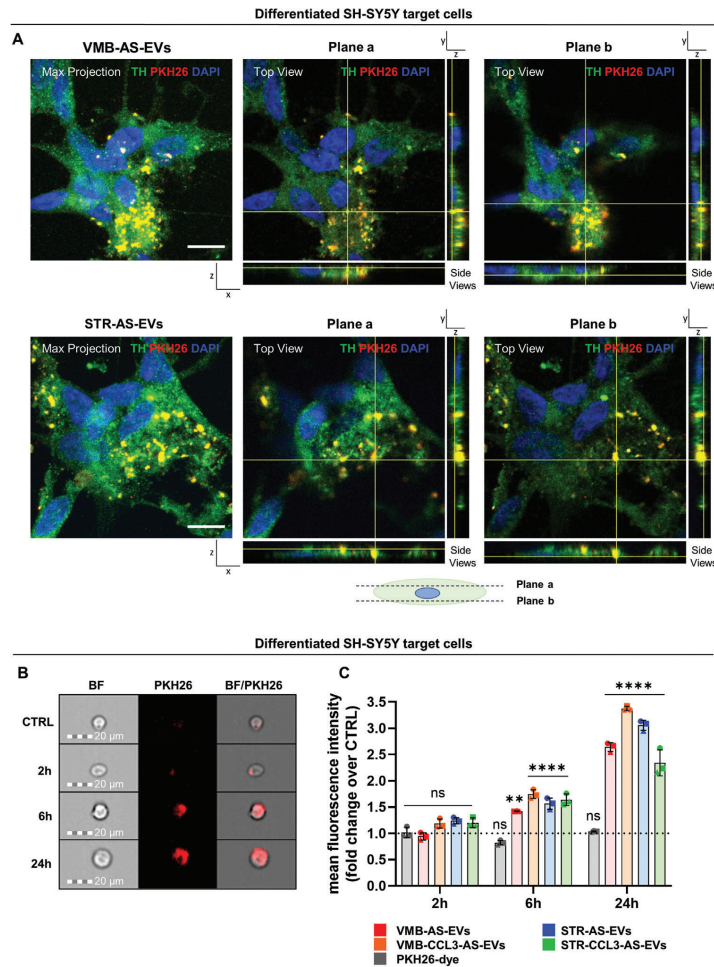


**Figure 3.** PKH26-labelled AS-EVs are internalized by differentiated, TH<sup>+</sup> SH-SY5Y neuronal cells. A) Max projection and orthogonal views of representative fields show the uptake of both VMB-AS- and STR-AS-PKH26-labelled EVs by differentiated SH-SY5Y. Each max projection is composed of a stack of 15 individual z planes, acquired every 0.4 μm along the z axis. Scale bar 10 μm. Plane a and Plane b orthogonal views represent, respectively, two selected planes located above and below the cellular nuclei (along the z axis), as represented by the cellular schematic. In all panels PKH26 is in red, TH in green, whereas nuclear DAPI counterstain is in blue. Confocal images show that PKH26 labelled EVs are present within the cellular bodies of SH-SY5Y target cells upon 6 h of incubation. B) Representative images from IFC of differentiated SH-SY5Y treated with PKH26-AS-EVs for 2, 6, and 24 h. Magnification 20×, scale bar 20 μm. C) IFC analysis of differentiated SH-SY5Y cells treated with PKH26-AS-EVs and PKH26-dye-only at different time points. Data are expressed as fold change of the mean fluorescence intensity ± SD over CTRL set to 1 for comparison (dotted line), from n = 3 independent experiments, indicated with different symbols. One-way ANOVA with Tukey's multiple comparison versus CTRL. \*\*p < 0.01, \*\*\*\*p < 0.0001, ns: not significant.



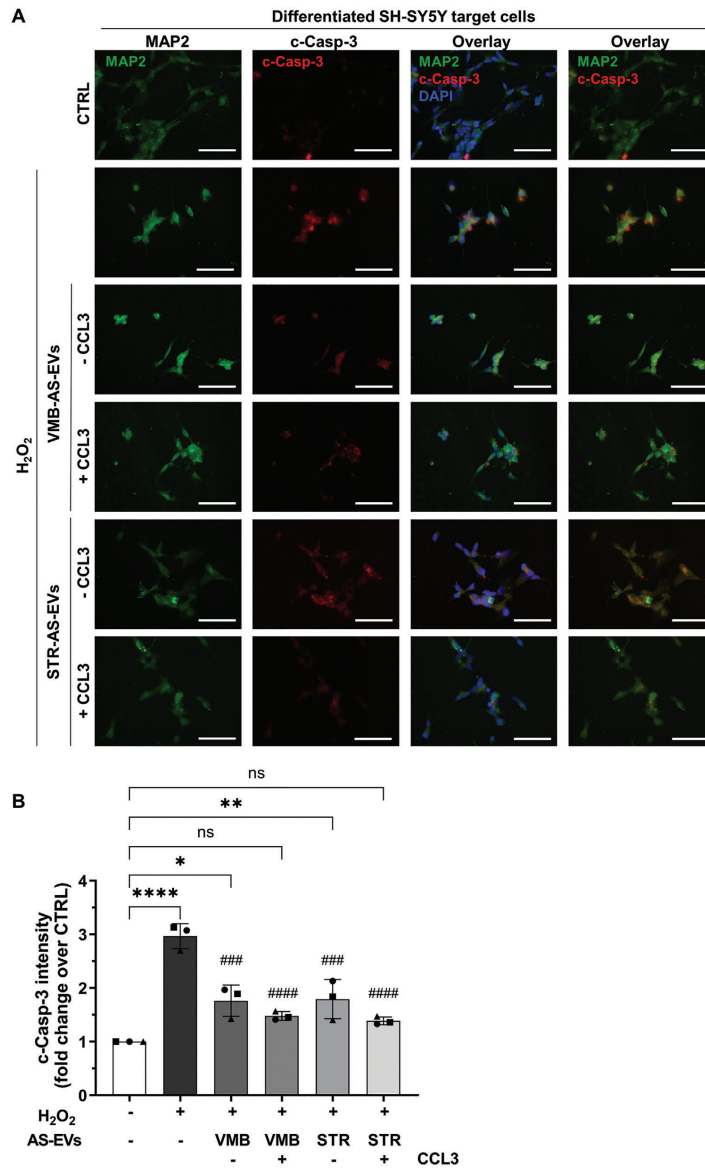


**Figure 4.** AS-EVs significantly reduce apoptosis in differentiated SH-SY5Y neurons challenged with  $H_2O_2$ . **A)** IF staining for MAP2 (in green), c-Casp-3 (in red), and DAPI (in blue), on differentiated SH-SY5Y exposed to AS-EVs and treated with  $35 \mu M H_2O_2$ . Scale bars:  $50 \mu m$ . **B)** Quantification of the c-Casp-3 staining in (A). The fluorescent intensities were normalized over the cell number. Data are expressed as mean  $\pm$  SD over CTRL set to 1 for comparison, from  $n = 3$  independent replicates, indicated with different symbols. One-way ANOVA with Tukey's multiple comparison  $*p < 0.05$ ,  $**p < 0.01$ ,  $***p < 0.0001$  versus CTRL, ns: not significant;  $###p < 0.001$ ,  $####p < 0.0001$  versus  $H_2O_2$ .

AS showing a full rescue of the c-Casp-3 levels induced by H<sub>2</sub>O<sub>2</sub> (Figure 4B). As a control, we applied CCL3 directly to H<sub>2</sub>O<sub>2</sub>-injured SH-SY5Y cells, without any rescue of cell viability (Figure S4C,D, Supporting Information). The same negative result was obtained by treating differentiated SH-SY5Y cells with contaminant EVs (cont-EVs) isolated from the complete medium only (i.e., medium that was not in contact with cells) (Figure S4E,F, Supporting Information).

To understand if the neuroprotective effect was specific for H<sub>2</sub>O<sub>2</sub>-injured differentiated SH-SY5Y cells, we measured caspase activity in undifferentiated SH-SY5Y cells treated with the AS-EVs, by using the same protocols (Figure S4G, Supporting Information). While H<sub>2</sub>O<sub>2</sub> induced a 2.5-fold increase of caspase activity, pre-exposure to AS-EVs did not reduce apoptosis induced by H<sub>2</sub>O<sub>2</sub> (Figure S4G, Supporting Information). Together, these results further identify AS-EVs as specific and effective mediators that deliver protective cargoes to H<sub>2</sub>O<sub>2</sub>-injured differentiated SH-SY5Y cells. The data also support the usefulness of CCL3-activated astrocytes as neuroprotective agents in nigrostriatal degeneration.<sup>[94]</sup>

### 2.5. Both VMB- and STR-AS-Derived EVs Preserve the Activity of Mitochondrial Complex I in Differentiated SH-SY5Y Neurons Injured by the Neurotoxin MPP<sup>+</sup>

Next, we extended the study of the neuroprotective potential of AS-EVs to the same target cells when exposed to the neurotoxin MPP<sup>+</sup>. MPP<sup>+</sup> affects DAergic neurons through the induction of a parkinsonian-like phenotype mainly by inhibiting the activity of the mitochondrial NADH-ubiquinone oxidoreductase (complex I, CI) of the electron transport chain.<sup>[117,123]</sup> Furthermore, as we recently demonstrated, the toxin compromises the overall integrity of the inner mitochondrial membrane (IMM), affecting ATP production via a mechanism which is independent from CI inhibition.<sup>[106]</sup> As mentioned above, we selected the dose of 1 mM MPP<sup>+</sup>, which causes only a small (~10%) reduction of cell viability after a 24 h incubation,<sup>[106]</sup> thus excluding non-specific mitochondrial deficits caused by a massive cell death process (Figure S4B, Supporting Information). EVs were applied on target cells (ratio 5:1) 6 h before the MPP<sup>+</sup> challenge, and mitochondrial functionality was analyzed by high-resolution respirometry (HRR) 24 h later.<sup>[124,125]</sup> We obtained the complete respiratory profile (i.e., the cellular O<sub>2</sub> consumption upon addition of substrates/inhibitors) (see Figure 5A for a representative trace of CTRL cells alongside a detailed protocol), and the main respiratory states of the different experimental groups were analyzed. This was achieved by two distinct steps: i) the mild permeabilization of plasma membranes, which allows the exit of substrates and thus the complete inhibition of OXPHOS respiration; and ii) the stimulation of CI activity with pyruvate, malate, glutamate, and ADP at saturating concentration (Figure 5A). This set-up allows the electrons to flow from CI—but not from CII—to CIII, through the Q junction (Figure 5A,B). Only the subsequent addition of succinate enables CII to participate to the total OXPHOS respiration (Figure 5A,F).

MPP<sup>+</sup> treatment did not change O<sub>2</sub> consumption in both intact (ROUTINE state) or permeabilized and fully stimulated cells (OXPHOS state) (Figure S5A,B, Supporting Information). Con-

trariwise, it specifically affected the contribution of CI to the OXPHOS respiration (Figure 5B–E), as expected.

As shown in Figure 5C, in CTRL cells CI accounted for ~73% of the overall OXPHOS, while MPP<sup>+</sup> reduced its activity up to a value of ~53%. In this context, all AS-EV samples promoted a significant increase of CI activity in MPP<sup>+</sup>-injured cells, up to full rescue (Figure 5C). Considering that the ultracentrifugation process may damage EVs with the consequent leakage of their content,<sup>[126]</sup> control experiments were performed using both the astrocyte conditioned media (ACM, still containing EVs, but ~50 times more diluted), or the same media depleted of EVs, obtained after ultracentrifugation (supernatant, SNT) (Figure 5D). In both cases, no significant rescue of CI activity was observed in MPP<sup>+</sup>-injured cells, thereby confirming that only purified intact EVs are able to revert the MPP<sup>+</sup>-induced complex I inhibition.

Because the EV uptake was similar in both differentiated and undifferentiated SH-SY5Y, we next repeated HRR measurements in undifferentiated SH-SY5Y exposed to 1 mM MPP<sup>+</sup>.

Although undifferentiated SH-SY5Y showed slight differences in the overall respirometry profile in terms of absolute values, MPP<sup>+</sup> treatment did not affect significantly ROUTINE or OXPHOS (Figure S5C,D, Supporting Information), but only CI activity, as for the differentiated cells. In particular, O<sub>2</sub> consumption linked to CI ranged from ~54% of CTRL cells to ~36% of MPP<sup>+</sup>-injured cells, but the treatment with AS-EVs was ineffective in improving CI activity (Figure 5E).

Together, these data indicate the ability of AS-EVs from both VMB and STR to efficiently preserve CI activity, specifically in differentiated SH-SY5Y cells, at a concentration far below MPP<sup>+</sup>-induced massive cytotoxicity.

### 2.6. Only EVs Secreted by VMB-AS Ameliorate ATP Production in Differentiated, MPP<sup>+</sup>-Injured SH-SY5Y Neurons

Given the potential of all AS-EV samples to protect CI activity from MPP<sup>+</sup>, we further assessed whether they positively impact on other critical features of MPP<sup>+</sup>-induced mitochondrial dysfunction. As already shown in Figure S5A,B, Supporting Information, the neurotoxin does not affect the total O<sub>2</sub> consumption recorded in the presence of endogenous substrates in intact cells, neither the one observed in the presence of externally added substrates in permeabilized cells. On the other hand, the neurotoxin treatment dramatically reduces the ATP-related fluxes, also known as net fluxes.<sup>[106]</sup> With this perspective, HRR was used to analyze the effect of AS-EVs on the O<sub>2</sub> flux exclusively devoted to ATP production in intact cells. As displayed in Figure 5G, MPP<sup>+</sup> drastically reduced the net flux up to ~75% in comparison to CTRL cells. Remarkably, treatment with EVs from VMB-AS—but not from STR-AS—significantly ameliorated the reduction in ADP phosphorylation of MPP<sup>+</sup>-injured differentiated SH-SY5Y cells, with no significant differences between basal and CCL3 conditions (Figure 5G). In line with these data, the degree of coupling between oxidative phosphorylation and electron flows (the coupling efficiency) was fully restored alongside with the increased ATP-related flows with VMB-AS-EVs only (Figure 5H). Again, no significant variation in the net flux or coupling efficiency was observed neither upon treatment with ACM/SNT (Figure S5E,F, Supporting Information), nor when AS-EVs were

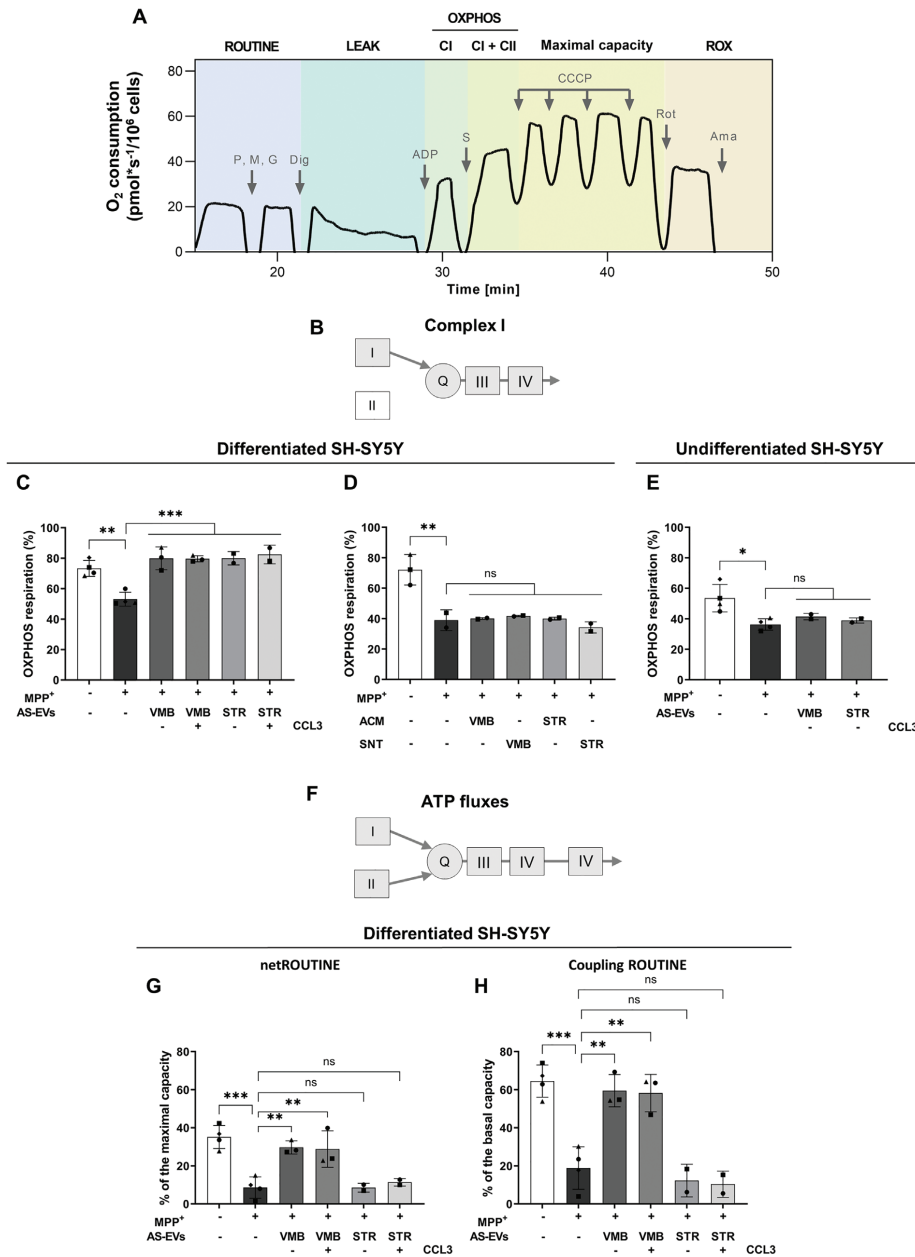


**Figure 5.** AS-EVs recover mitochondrial functions in differentiated SH-SY5Y neurons challenged with MPP<sup>+</sup>. **A)** Representative oxygraphic trace in untreated differentiated SH-SY5Y (control) cells alongside the specific protocol used. First, in intact cells, the physiological O<sub>2</sub> consumption, corresponding



given to undifferentiated SH-SY5Y cells (Figure S5G,H, Supporting Information).

Overall, these data indicate a regional specificity of VMB- versus STR-AS-EVs in their ability to rescue the mitochondrial functional capacity of differentiated SH-SY5Y cells under MPP<sup>+</sup> injury.

### 3. Discussion

Reactive AS are increasingly emerging as key players in the Parkinsonian brain, exerting both “beneficial” and “detrimental” effects.<sup>[40–42,44–50,73,89,94,127,128]</sup> Especially, the heterogeneous nature of AS has been emphasized, showing regional AS differential responses to both genetic and environmental factors, including ageing, inflammatory or neurotoxin exposures, all crucial conditions of vulnerability for PD.<sup>[40,41,44,45,73,81,88,129]</sup> Yet, the modality of the intricate AS-neuron crosstalk still remains undefined. Among the multiple modes of intercellular communication, the secretion of EVs has emerged as a powerful tool for the exchange of information.<sup>[39,130,131]</sup> EVs are released by most cell types of the brain and they have also been identified in body fluids as potential new biomarkers for PD and other neurodegenerative diseases (NDs).<sup>[13,14,18–21,132]</sup> Also, they are exploited as advanced nanotherapeutics in regenerative medicine.<sup>[13,15,20,22,23,25]</sup>

Here, we show for the first time that AS derived from the nigrostriatal system communicate via a population of vesicles enriched in sEVs, in line with the presence of exosomes and small microvesicles. Moreover, we elucidated specific EV properties according to the brain region of origin, both in terms of secretion rate and functions. Interestingly, the EV secretion rate was specific for each brain area, with VMB-AS releasing a higher number of vesicles compared to STR- and ΔVS-AS (i.e., AS from brains depleted of VMB and STR), which showed a similar rate of secretion. Also, we found that CCL3 played a critical role in the regulation of EV production, with only VMB-AS secreting more vesicles

in response to the chemokine. This AS activation strategy stems from a recent discovery made by our research team, identifying a 6-fold upregulation of CCL3 in the VMB of PD mice, in vivo, during nigrostriatal degeneration and self-recovery, whereby reactive AS were defined as the key components of DAergic neurorescue pathways against MPTP/MPP<sup>+</sup> injury.<sup>[94]</sup> In contrast, CCL3 did not increase EV secretion from STR- and ΔVS-AS. However, our expression analysis of the main CCL3 receptors (i.e., Ccr1 and Ccr5), suggests that the nigrostriatal system (both VMB- and STR-AS) had a specific potential to respond to the chemokine, while the expression of Ccr1 and Ccr5 in ΔVS-AS was ≈100 times lower. Indeed, STR-AS also responded to CCL3, but by extruding more membrane protrusions rather than increasing EV secretion. Therefore, in both nigrostriatal regions, CCL3 was able to influence the dynamics of cell membranes, in line with the membrane remodeling abilities of this chemokine.<sup>[104,105]</sup>

Our data showing differential intrinsic and extrinsic responses of VMB- and STR-AS fit with the reported high level of AS heterogeneity in the CNS, whose regulatory mechanisms (e.g., transcriptional versus epigenetic programs) remain as outstanding open questions for the field.<sup>[77,129,133,134]</sup> Indeed, the molecular machinery which orchestrates the distinct EV secretion rates—according to the brain region and the specific exposure to inflammatory triggers—needs to be further elucidated. Also, these findings call for a deeper understanding of the functional implications of such a specific response to microenvironmental cues between VMB (where the DAergic neurons reside) versus STR (where they project) for the pathogenesis of PD and, eventually, for the development of new therapeutic avenues. In fact, while a plethora of studies has identified AS harmful factors, little is known about both the mechanisms driving the induction of pro-reparative states and their cellular/molecular effectors.<sup>[135,136]</sup>

Initially identified as possible neurodegeneration’s Trojan horse, AS-EVs recently emerged as important mediators of “beneficial messages” to target neurons.<sup>[137]</sup> However, regional dif-

to ROUTINE state, was measured. Second, adenylates were forced to leave the cells by a mild plasma membrane permeabilization in order to analyze the LEAK state. Third, the contribution of CI to the OXPHOS respiration was assayed in the presence of the previous addition of the appropriate substrates (pyruvate, malate, glutamate) and a saturating ADP concentration. Then, addition of succinate allowed the activation of CII (CI + CII) and the achievement of total OXPHOS respiration. Fourth, the maximal capacity of ETS was obtained after CCCP titration. Fifth, the ROX was acquired after inhibition of ETS complexes with rotenone and antimycin A. P, pyruvate; M, malate; G, glutamate; Dig, digitonin; S, succinate; Rot, rotenone; Ama, antimycin A. B) Schematic representation of complex I activity measurement through mitochondrial ETS complexes. C) The effects of MPP<sup>+</sup> and EVs were tested in the same experimental conditions. The toxin reduces CI activity (CI-linked OXPHOS) of ≈30% compared to CTRL while AS-EVs fully recover CI functionality of MPP<sup>+</sup>-treated SH-SY5Y cells. The OXPHOS respiration linked to CI was expressed as flux control ratio using the total OXPHOS respiration as reference state. One-way ANOVA with Tukey’s multiple comparison *\*\*p* < 0.01 (CTRL versus MPP<sup>+</sup>), and *\*\*\*p* < 0.001 (MPP<sup>+</sup> versus MPP<sup>+</sup> + VMB-AS-EVs ± CCL3 and versus MPP<sup>+</sup> + STR-AS-EVs ± CCL3). D) The effects of ACM/SNT were tested as before. No significant differences were observed in MPP<sup>+</sup>-injured cells treated with ACM or SNT samples. The OXPHOS respiration linked to CI was expressed as flux control ratio using the total OXPHOS respiration as reference state. One-way ANOVA with Tukey’s multiple comparison *\*\*p* < 0.01 (CTRL versus MPP<sup>+</sup>), ns: not significant. E) The effects of AS-EVs were tested in undifferentiated SH-SY5Y cells. The toxin treatment significantly reduces CI activity versus CTRL, while no significant effect was observed in presence of AS-EV samples. The OXPHOS respiration linked to CI was expressed as flux control ratio using the total OXPHOS respiration as reference state. One-way ANOVA with Tukey’s multiple comparison *\*p* < 0.05 (CTRL versus MPP<sup>+</sup>), ns: not significant. In panels (C–E) data are expressed as the ratio between OXPHOS driven by CI and total OXPHOS (driven by CI + CII) ± SD. F) Schematic representation of mitochondrial ETS and ATP synthase complexes. G) MPP<sup>+</sup> reduces O<sub>2</sub> flux devoted to ATP production compared to CTRL in ROUTINE. Only VMB-AS-EVs promote a significant recovery of the flux in differentiated SH-SY5Y cells. Net ROUTINE was expressed as flux control ratio using the maximal capacity as reference state. Data are expressed as percentage of the maximal ETS capacity ± SD. One-way ANOVA with Tukey’s multiple comparison, *\*\*p* < 0.01 (MPP<sup>+</sup> versus MPP<sup>+</sup> + VMB-AS-EVs ± CCL3), *\*\*\*p* < 0.001 (CTRL versus MPP<sup>+</sup>), ns: not significant. H) Coupling efficiency in basal state (ROUTINE) of differentiated SH-SY5Y cells in the same experimental conditions. According to the ATP production data, only VMB-AS-EVs were able to significantly increase the rate of coupling between the oxidative phosphorylation and ATP production. Data are expressed as percentage of each specific state. Coupling efficiency was expressed as flux control ratio using the basal respiration (ROUTINE) as reference state. Data are expressed as means ± SD. One-way ANOVA with Tukey’s multiple comparison, *\*\*p* < 0.01 (MPP<sup>+</sup> versus MPP<sup>+</sup> + VMB-AS-EVs ± CCL3), *\*\*\*p* < 0.001 (CTRL versus MPP<sup>+</sup>), ns: not significant.

ferences were not taken into account, since AS-EV preparations were mostly derived from the cerebral cortex, whole brain, or immortalized glioma cells. Also, several protocols for target neuronal cultures and/or neuron differentiation/enrichment have been reported, which make it difficult to draw firm conclusions.<sup>[138–141]</sup>

Here, we used nigrostriatal AS-EVs to investigate their specific functional roles when transferred to RA-differentiated versus undifferentiated SH-SY5Y cells. We showed that the EV uptake for both target cell types was similar, regardless of the regional identity/treatment of donor astrocytes. In spite of this homogeneity, we uncovered relevant functional differences in terms of their neuroprotective potential. First, differentiated SH-SY5Y cells were exposed to two distinct sources of toxicity— $H_2O_2$  and MPP<sup>+</sup>—mimicking oxidative stress and mitochondrial dysfunction found in PD. Intriguingly, we found that depending on the challenge used, AS-EVs differentially mediated neuroprotection on these target cells. In particular, both VMB- and STR-AS secreted EVs able per se to counteract the cell death induced by  $H_2O_2$ . However, EVs derived from CCL3-treated astrocytes showed a higher efficacy in preventing the activation of caspase-3 in differentiated SH-SY5Y cells, by mechanisms that warrant further investigation. Importantly, the treatment with CCL3 directly on target neurons was not able to recapitulate the neuroprotective effects of AS-EVs. This novel finding sheds light on the mechanism of chemokine-mediated neuroprotection previously documented for nigrostriatal AS,<sup>[94]</sup> and further implicates a relevant role played by the inflammatory microenvironment in amplifying the “beneficial” AS-mediated neuroprotection. It is important to note in this respect, that, depending on the context, chemokines can trigger either harmful or protective effects.<sup>[91,92,94]</sup> In fact, our previous *in vitro* studies showed that AS exposure to CCL3 (but not to TNF- $\alpha$  or IL-1 $\beta$ ): i) reverted aging-induced loss of AS neuroprotective properties against MPP<sup>+</sup> cytotoxicity,<sup>[43]</sup> ii) promoted neuroprotection and DAergic neurogenesis from adult midbrain NSCs,<sup>[94]</sup> and iii) reverted the aged-AS to a pro-regenerative state.<sup>[96]</sup> On the contrary, the harmful microglial environment inhibited subventricular zone NSCs, further emphasizing the capacity of chemokine-activated AS in promoting DAergic neuron plasticity.<sup>[44,45,94,95]</sup>

Considering AS protective response to basal ganglia injury,<sup>[41–43,45,50,94,142]</sup> we also used MPP<sup>+</sup>—a well-recognized neurotoxin recapitulating Parkinsonian symptoms<sup>[117,143–145]</sup>—to investigate the ability of AS-EVs to target mitochondrial function. MPP<sup>+</sup> is sequestered in mitochondria where it selectively inhibits CI. Indeed, the well described deficiency of mitochondrial CI activity in the SNpc of patients with sporadic PD accounts for the majority of neuronal loss.<sup>[68]</sup> We found that a preventive treatment with AS-EVs from both VMB and STR efficiently restored CI activity in neuronal cells, severely affected by the toxin treatment. On the other hand, only VMB-AS-EVs fully preserved mitochondrial functionality, as demonstrated by the analysis of  $O_2$  flows devoted to ATP synthesis. In fact, MPP<sup>+</sup> compromised the net respirations via a general reduction of the inner mitochondrial membrane (IMM) integrity,<sup>[106]</sup> a critical feature for the maintenance of the proton gradient and therefore essential for the ADP phosphorylation process. In MPP<sup>+</sup>-injured neurons, a part of the gradient was dissipated, by-passing ATP synthase, and the positive effect exerted on CI was either nullified or not

culminated in ATP production, as in STR-AS-EVs treated cells. Different intriguing factors may contribute to this novel distinct effect of VMB- versus STR-AS-EVs. Again, this specificity may depend on the particular brain area facing region-specific neuronal vulnerabilities and/or specific tasks. For example, in the VMB, SNpc neurons are selectively vulnerable to mitochondrial CI inhibitors, versus the exquisite and “mysterious” sensitivity of STR neurons to succinate dehydrogenase (SDH, mitochondrial complex-II) inhibitors, such as the plant-derived mitochondrial toxin, 3-nitropropionic acid, causing striatal damage reminiscent of Huntington’s disease.<sup>[146]</sup> Also, besides neuroinflammation, a peculiar striatal AS vulnerability to metabolic impairments, protein aggregation, and mitochondrial instability<sup>[88,146–149]</sup> may at least in part explain this lack of “full beneficial response” observed with STR-AS-EVs. Further studies are needed to verify whether AS-EV heterogeneity—in VMB versus STR—can be the result of intrinsic regional differences and/or it might be promoted by external factors present in the microenvironmental milieu. Indeed, a key aspect to be deeply explored will involve the nature of AS-driven EV cargoes and their possible link with the mechanism(s) regulating the selection/trafficking of specific effectors toward EVs. A very long list of molecules (DNA, RNAs, proteins, lipids, metabolites, etc.) have been identified over the years within EVs, whose relative abundance changes based on the identity of the donor cell and in response to specific stimuli. Our data claim for a comprehensive multi-omics profiling of AS-EVs to clarify how: i) the regional identity of donor astrocytes may impact on the composition of vesicles; and ii) the relationship between potential EV-shuttled candidates and key mitochondrial pathways in neuronal target cells. Even if we did not observe an enrichment of SDHA in AS-EVs (see Figure 2D), different mitochondrial components may be transferred via astrocyte-derived vesicles. Several recent reports indicate the presence of both mtDNA and fully active mitochondrial proteins, from all of the five respiratory complexes, associated with EVs, including ATP synthase, cytochrome c oxidase subunits and others.<sup>[150,151]</sup> However, the mechanisms by which these proteins may play a functional role in recipient cells is not fully understood. Other findings suggest the possibility that mitochondrial-derived vesicles (MDVs)—involved in the mitochondrial quality control (MQC) system—may be rearranged within the multivesicular bodies and released in the microenvironment as exosomes.<sup>[152]</sup> Interestingly, a lower secretion of MDV-derived proteins was detected in sEVs from serum samples of PD patients versus controls, suggesting that the mitochondrial quality control (MQC) flux is impaired in PD.<sup>[153]</sup> The presence of specific ncRNAs (e.g., miRNAs, tRNA-derived fragments) and transcription factors (as mRNA or protein) within VMB versus STR AS-EVs—able to differentially regulate mitochondrial pathways in target cells—add further layers of complexity to the AS-neuron crosstalk.<sup>[154–156]</sup> Indeed, understanding the relative contribution of each potential candidate responsible for distinct functional effects on target cells remains a challenge for the field. Also, the way(s) used by AS-EVs to interact with target cells need(s) to be further characterized.

Remarkably, the positive effects exerted by AS-EVs were observed only when EVs were isolated from the ACM. ACM per se still contains EVs, although at a concentration approximately 50-fold lower in comparison to the purified vesicles. This may ex-

plain the lack of any significant rescue of mitochondrial parameters when ACM was used to challenge MPP<sup>+</sup> toxicity. Also, the fact that the SNT (ACM depleted of EVs) did not show any protective effect demonstrate that, in our hands, the ultracentrifugation process did not damage the vesicles, further excluding possible EV leakage.<sup>[126]</sup> Although we cannot rule out the possibility that other molecules might be co-purified with EVs, the lack of intracellular proteins—used to denote EV purity—in our vesicle preparations indicate that the AS-EV functions are most likely due to EVs.

Finally, we showed that the same vesicle samples applied to undifferentiated SH-SY5Y cells—exposed to either H<sub>2</sub>O<sub>2</sub> or MPP<sup>+</sup>—did not exert any neuroprotective effects, in contrast to their differentiated counterparts. This specificity in the AS-EV responsiveness points to a greater protective activity toward the dopamine neuronal phenotype, which merits further investigations. Retinoic acid (RA) is recognized to induce a neuronal differentiation program in SH-SY5Y cells which allows the development of a predominantly mature DAergic-like neurotransmitter phenotype.<sup>[157]</sup> Accordingly, in our experimental conditions, we found that in comparison with undifferentiated cells, differentiated SH-SY5Y displayed: i) neuron morphological and neuronal differentiation markers; and ii) a higher expression of TH (the rate limiting step in dopamine biosynthesis).<sup>[106]</sup>

Our data then support the notion that characteristics of AS dictated by their regional identity play important roles in modulating specifically DAergic neuron vulnerability. In fact, nigrostriatal AS display unique features, being sensitive to environmental stressors and PD neurotoxins, ageing and neuroinflammatory challenges.<sup>[73,88,90,147]</sup> Hence, under neurodegenerative conditions, many adaptive changes occur within the astroglial compartment, aimed to improve mitochondrial performance, to provide neurotrophic support, and/or to activate adult neurogenesis.<sup>[44,45,72,73,89,94]</sup>

Overall, it seems tempting to suggest the involvement of EVs in the AS-neuron crosstalk, in a region-specific and context-dependent way. More work is needed to clarify to what extent AS-EVs contribute to AS neuroprotective effects highlighted in experimental PD models.<sup>[158]</sup>

This knowledge will be crucial to fully understand the functions of AS-EVs, thus facilitating the diagnosis of CNS diseases and the identification of vesicle therapeutic potential.

#### 4. Conclusion

This study provides, for the first time, an in-depth phenotypic and functional characterization of AS-EVs from the two main brain regions affected in PD, that is, the VMB and the STR. We demonstrate that AS from both areas produce a population of vesicles highly enriched in sEVs (~70 nm). The EV secretion rate is specific for each brain region, with VMB astrocytes releasing more EVs per cell compared to the STR. Notably, only VMB-AS responded to CCL3 chemokine by producing more EVs, while STR-AS undergo plasma membrane modifications, in the absence of any effect due to cellular viability or proliferation.

Next, we showed the functional implications of these nigrostriatal-specific differences in AS-EV secretion, in the context of neurodegeneration. Indeed, only CCL3-stimulated AS-EVs are able to fully protect differentiated SH-SY5Y cells from

H<sub>2</sub>O<sub>2</sub>-induced apoptosis. On the other hand, only VMB-derived EVs ameliorated ATP production in the same cells injured with MPP<sup>+</sup>, further supporting the importance of the brain region for the accomplishment of specific functions within the brain. However, vesicles obtained from the same brain regions were not able to protect the undifferentiated SH-SY5Y cells, thus adding a further layer of complexity to the neuroprotective program dictated by AS-EVs.

In conclusion, our results highlight a novel role for AS-EVs in the propagation of specific intercellular signaling, with region-specific and inflammatory-dependent functional implications in targeting neuroprotection. Our data further unveil the multiple levels of interaction that are established between different types of cells populating the brain. In the long term, patient-tailored AS-EV treatments aimed to prevent disease progression and to promote neurological recovery may be foreseen, with implications for both the etiopathology and the treatment of PD, and other NDs.

#### 5. Experimental Section

**Primary Astrocyte Cultures and Treatments:** Wild type C57BL/6 animals were purchased from Charles River (animal experiments were approved by the Italian Ministry of Health authorization number 442/2020-PR). Primary astroglial cell cultures were prepared as described in Ref. [94]. Briefly, AS were obtained from mice at postnatal days P2-P4 and isolated from VMB and STR brain regions, and from brains depleted of these two regions ( $\Delta$ VS). AS were cultured in DMEM (1 g L<sup>-1</sup> glucose, Sigma Aldrich, D6046) supplemented with 10% FBS (Biowest, S1810), 2 mM L-glutamine (Sigma Aldrich, G7513), 2.5  $\mu$ g mL<sup>-1</sup> amphotericin B (Sigma Aldrich, A2942), and 1% penicillin/streptomycin (Sigma Aldrich, P0781) at 37 °C and 5% CO<sub>2</sub> for 13–17 days in 10 cm dishes specific for primary cultures (Corning, 353 803). Loosely adherent microglial cells were then removed by shaking. Cells were washed with sterile PBS 1x and allowed to grow for another two days or reseeded onto glass coverslips in 24-well plates for immunofluorescence (IF) analyses, or in 96-well plates for viability and cytotoxicity analyses. Cells were washed and then treated or not with the CCL3 300 ng mL<sup>-1</sup> (R&D, 450MA050), in DMEM medium supplemented with 10% FBS depleted of exosomes (System Biosciences, EXO-FBS-250A-1). CCL3 concentration was based on previously published time-course and dose-response studies.<sup>[43,94,96,102]</sup> Cells were maintained in this medium for 24 h before supernatant collection for EV purification.

For IF analyses, AS were labelled with rabbit anti-GFAP antibody (Dako, Z0334), while microglial cells were stained with goat anti-Iba1 antibody (Novus, NB100-1028). AS proliferation was evaluated by 5-Bromo-2'-deoxyuridine (BrdU) incorporation assay. The day before fixation, BrdU 5  $\mu$ M (Sigma Aldrich, 19-160) was added to cells for 24 h. Proliferative cells were stained with mouse anti-BrdU antibody (Sigma Aldrich, B8434). Donkey Alexa fluor secondary antibodies were used, and nuclei were stained with DAPI (Sigma Aldrich, 32670-5MG-F). IF images were acquired using a Leica microscope (DM5500) and analyzed with Fiji Image J software 1.51n.

For cytotoxicity analysis, 10  $\mu$ L of AS supernatants were collected and analyzed by LDH-Cytotoxicity Assay Kit (Fluorometric) (Abcam, ab197004), following the instruction provided by the kit. For viability analysis, CellTiter Blue reagent (Promega, G8080) (diluted 1:4 with PBS 1x) was added to each well of 96 well plates and incubated at 37 °C for 4 h. Then, for both kits, the fluorescent signal was measured by Varioskan flash plate reader (Thermo Fisher).

RNA was isolated from AS using the miRNeasy Mini Kit (Qiagen, 217004). Total RNA quantity and purity were assessed with the NanoDrop ND-1000 instrument (Thermo Scientific) and cDNA synthesis was performed using the High-capacity cDNA reverse transcription kit (Applied Biosystem, 4368814). Gene expression was studied via qPCR with

PowerUp SYBR Green Master Mix (Applied Biosystem, A25742), using the following primers:

Ccr1-forward: 5'-AGGTTGGGACCTTGAACCTTG-3',  
5'-CCGACCTCTCGAACACCC-3',  
Ccr1-reverse: 5'-ACAGTGAGTCTGTGTTCCAGA; and  
Ccr5-forward: 5'-TGAGACATCCGTTCCCTA-3',

Ccr5-reverse: 5'-GCTGAGCCGCAATTTGTTTC-3'. mRNA levels were normalized relative to Gusb: Gusb-forward: 5'-CCGACCTCTCGAACACCC-3', Gusb-reverse: 5'-GCTTCCCGTTCATACCACACC-3'. Samples were tested in triplicate on a QuantStudio 3 Real-Time PCR System (Applied Biosystem) and expressed as  $\Delta\Delta C_t$ .

**Scanning Electron Microscopy (SEM) Processing:** Cells were fixed in 3% glutaraldehyde (Sigma Aldrich, G5882) for 1 h. Samples were then post-fixed in 1% osmium tetroxide for 45 min at 4 °C. Samples were washed with deionized water and partially dehydrated in increasing concentrations of ethanol up to 100% ethanol. Subsequently, critical point drying and sputtering with gold/palladium alloy was performed at the Central Service for Experimental Research of the University of Valencia. SEM images were obtained on a Hitachi S4800 microscope.

**Histological Processing:** Cells were fixed in 3% glutaraldehyde for 1 h, then they were post fixed with 2% osmium tetroxide (Electron Microscopy Sciences) for 2 h. Sections were then washed in deionized water, and partially dehydrated in 70% ethanol. Afterward, the samples were contrasted in 2% uranyl acetate (Electron Microscopy Sciences) in 70% ethanol for 2 h at 4 °C. The samples were further dehydrated and infiltrated in Durcupan ACM epoxy resin (Sigma) at room temperature overnight, and then at 60 °C for 72 h. 1.5  $\mu\text{m}$  sections were obtained using an Ultracut UC7 ultramicrotome (Leica Biosystems). Sections were stained with 1% Toluidine Blue. Images were taken with an i80 Nikon Microscope.

**EVs Isolation and Characterization:** AS supernatants were collected and immediately centrifuged at  $1000 \times g$  at 4 °C for 15 min in order to pull down residual cells/cell debris. Next, the supernatants were subjected to ultracentrifugation in a Sorvall WX100 (Thermo Scientific). The first ultracentrifugation was performed at 100 000 g at 4 °C for 75 min, in ultra-cone polyclear centrifuge tubes, each containing the supernatant deriving from  $\approx 15 \times 10^6$  astrocytes (Seton, 7067), using the swing-out rotor SureSpin 630 (k-factor: 216, RPM: 23 200). Then the pellet was washed with cold PBS 1x and ultracentrifuged again at the same speed for 40 min in thick wall polycarbonate tubes (Seton, 2002), using the fixed-angle rotor T-8100 (k-factor: 106, RPM: 41 000). The resulting pellets, containing AS-EVs, were resuspended in PBS 1x (for NTA, EM and functional experiments), in RIPA buffer (for WB characterization), or in Diluent C (for PKH26 staining).

**Nanoparticle Tracking Analysis (NTA):** AS-EVs were diluted in PBS 1x and analyzed for particle size distribution and concentration on a Nanosight NS500 (Malvern Instruments Ltd, UK) fitted with an Electron Multiplication-Couple Device camera and a 532 nm laser. The sample concentration was adjusted to  $10^8$ – $10^9$  particles/mL and measurements were performed in static mode (no flow) at an average temperature of  $21 \pm 1$  °C. A total of 3 to 5 videos of 60 s were recorded for each independent replicate, loading a fresh sample for each measurement. Videos were processed on NTA software v3.2 and a detection threshold of 8 was used. The remaining settings were set to automatic. Total particle concentration for each EV sample was determined by NTA and used to calculate the number of EVs released per  $10^6$  cells.

**EV Negative Staining for Transmission Electron Microscopy (TEM):** AS-EVs were fixed with 2% paraformaldehyde (PFA) (Sigma Aldrich, P6148) in PBS 1x for 30 min. 200 mesh formvar and carbon coated nickel grids were glow-discharged to make the surface grid hydrophilic. Fixed samples were placed on the grids for 7 min, samples were washed with ultrapure water and stained with 2% uranyl acetate for 7 min and examined at 80 kV on a FEI Tecnai G2 Spirit (FEI Company, Hillsboro, OR) transmission electron microscope equipped with a Morada CCD digital camera (Olympus, Tokyo, Japan). To obtain the number of vesicles in EM, 10 random fields (from 60 000  $\times$  magnification) were counted, each from a different square of the 200-mesh grid, per each condition.<sup>[159]</sup> The results were normalized taking into account the following parameters: the number of starting cells,

the resuspension volume after ultracentrifugation, the volume used in the microscope grid, and the area ( $\mu\text{m}^2$ ) of each field in the grid.

**EV Immunogold Labelling for Transmission Electron Microscopy (TEM):** To increase the hydrophobic properties of the grids 200 mesh formvar and carbon coated nickel grids were glow-discharged. Grids were placed on a 10  $\mu\text{L}$  drop of each sample for 7 min and washed with PBS 1x. Nonspecific reactions were avoided using blocking solution containing 0.3% BSA for 30 min. Then, samples were washed in 0.1% BSAc (Aurion, Wageningen, the Netherlands) in PBS 1x. The samples were incubated in 10  $\mu\text{L}$  of 1:50 primary antibody (rat anti-CD9 or rat anti-CD63, see Table 1) in 0.1% BSAc (Electron Microscopy Sciences) for 1 h. After, the samples were washed in 0.1% BSAc and incubated in 1:20 goat anti-rat 6 nm gold particles (Abcam, ab105300) in 0.1% BSAc for 1 h in the dark. Grids were rinsed with 0.1% BSAc and fixed with 2% glutaraldehyde for 5 min and washed with ultrapure water. Finally, negative staining with 2% uranyl acetate was performed for 5 min. The samples were examined at 80 kV on a FEI Tecnai G2 Spirit (FEI Company, Hillsboro, OR) transmission electron microscope equipped with a Morada CCD digital camera (Olympus, Tokyo, Japan).

**Western Blotting:** AS and EVs extracts were processed as in Ref.[97, 98]. Briefly, AS and EVs were lysed in RIPA buffer (10 mM Tris HCl pH 7.2 (Fisher Scientific, BP152); 1% sodium deoxycholate (Sigma Aldrich, 30970); 1% Triton X-100 (Sigma Aldrich, T8787); 0.1% (for cells) or 3% (for EVs) SDS (Sigma Aldrich, 71736); 150 mM NaCl (Sigma Aldrich, S7653); 1 mM EDTA pH 8 (VWR chemicals, E177-100ML); 1 mM phenylmethanesulfonyl fluoride solution (PMSF, Sigma Aldrich, 93482); 1x Halt Complete Protease inhibitor cocktail (Roche, 04693116001), 1x Halt Phosphatase inhibitor cocktail (Thermo Fisher Scientific, 78420)), and protein concentration was measured with DC Protein Assay (Biorad, 500-0116), using BSA (Pierce, 23210) as standard (AS-EV protein yield: 0.5–1.5  $\mu\text{g}/10^6$  cells). The same amount of cell or EV lysates was then loaded into 4–12% Bis-Tris plus gels (Invitrogen, NWO4125BOX) in reducing or non-reducing conditions. Afterward, proteins were transferred onto PVDF membrane. All primary and secondary antibodies are listed in Table 1.

**SH-SY5Y Culture, Differentiation, and Treatments:** SH-SY5Y cells were purchased from ICLC (Interlab Cell Line Collection, accession number ICLC HTL95013; obtained from depositor European Collection of Authenticated Cell Cultures [ECACC]) and cultured and differentiated as described in Ref. [106]. Briefly, cells were maintained in MEM/F12 medium (Bioclon GmbH, F0325 and Sigma Aldrich, N4888). For cell differentiation, MEM/F12 was replaced with DMEM/F12 and 10  $\mu\text{M}$  retinoic acid (Sigma Aldrich, R2625), and cultivated for 8 days with gradual serum deprivation until 0.5% FBS. At the end of differentiation, cells were detached and seeded at the density of  $3 \times 10^5$  cells/cm<sup>2</sup> in 12-well (for IFC analysis, see Section 5.10 for EV labeling), 96-well (for dose response curve), 24-well (for c-Casp-3 IF staining), or 6-well (for HRR analysis, see Section 5.11) plates. For all the experiments where EVs were applied on target cells, the authors used the ratio 5:1 (i.e., EVs derived from five AS used to treat one SH-SY5Y cell).

For IFC analysis, labelled AS-EVs were applied on differentiated and undifferentiated SH-SY5Y cells (see below) seeded on 12 well plates. Internalization was evaluated at different time points (i.e., 2, 6, and 24 h) at 20 $\times$  magnification by using the Amnis FlowSight Imaging Flow Cytometer (Luminex). At the end of each time point, cells were trypsinized and collected in 1 mM EDTA + 1% BSA. For all passages cells were kept on ice. Fluorescence intensity of PKH26 was measured by using 488 nm laser. Flow cytometric gating was used to select focused single cells and the mean fluorescence intensity of treated cells was compared with that of untreated cells. For normalization, the authors analyzed the first 1000 single cells, in order of acquisition, with an optimal focus, using IDEAS software version 6.2 T83.0 (Amnis, part of Luminex).

Two dose-response curves, one for H<sub>2</sub>O<sub>2</sub> (Sigma Aldrich, H1009) and one for MPP<sup>+</sup> (Sigma Aldrich, D048), were performed at 24 h, using CellTiter Blue (Promega, C8080), as described in the Primary Astrocyte Cultures and Treatments section.

For IF, cells were seeded on poly-L-lysine coated glass coverslips. After two days, EVs were applied on target cells. As a control, the vesicles eventually present as contaminants in the medium used to culture AS (cont-EVs) were also tested following the same experimental steps used for AS-EVs.

**Table 1.** List of antibodies used in WB.

Antibody	Dilution	Brand	Catalog number
Rat monoclonal anti-CD63	1:5000	MBL	D263-3
Rat monoclonal anti-CD9	1:5000	BD Pharmingen	553758
Mouse monoclonal anti-Pdcd6ip	1:500	BD transduction lab	611620
Mouse monoclonal anti-SDHA	1:1000	Abcam	ab14715
Rabbit polyclonal anti-Caxx	1:10 000	Abcam	ab22595
Mouse monoclonal anti-GM130	1:1000	BD transduction lab	610823
Mouse monoclonal anti- $\beta$ -actin	1:10 000	Sigma Aldrich	A1978
HRP-conjugated anti-mouse secondary antibody	1:10 000	Dako	P0447
HRP-conjugated anti-rabbit secondary antibody	1:10 000	Invitrogen	31460
HRP-conjugated anti-rat secondary antibody	1:10 000	Invitrogen	31470

Following ultracentrifugation, cont-EVs were resuspended in PBS 1x and used to treat SH-SY5Y maintaining the same ratio with the starting volume of medium, as for the purification of AS-EVs. 6 h later, cells were treated with 35  $\mu$ M H<sub>2</sub>O<sub>2</sub> for a further 24 h. Coverslips were fixed with 4% PFA and stained with rabbit polyclonal anti-c-Caspase-3 (Cell Signaling, 9664) primary antibody and with mouse monoclonal anti-map2 primary antibody (Merck Millipore, MAB3418). The secondary antibodies used were the anti-Rabbit Alexa Fluor 546 (Thermo Fisher Scientific, A10040), and the anti-Mouse Alexa fluor 488 secondary antibodies (Thermo Fisher Scientific, R37114). Nuclei were counterstained with DAPI. IF images were acquired using a Leica microscope (DM5500) and analyzed with Fiji ImageJ software. The intensity of the c-Casp-3 signal was measured by using the following steps in ImageJ software: i) analyze; ii) measure; and iii) integrated density, as in Ref. [160]. Integrated density was normalized for the number of DAPI<sup>+</sup> nuclei.

As a further control, the chemokine CCL3 (at 30 and 300 ng mL<sup>-1</sup>) was added directly to SH-SY5Y cell cultures on 96-well plate 6 h before H<sub>2</sub>O<sub>2</sub> exposure. Cell viability/death was evaluated 24 h after the H<sub>2</sub>O<sub>2</sub> treatment with CellTiter Blue and Caspase-Glo 3/7 Assay (Promega, G8091).

Undifferentiated SH-SY5Y cells were seeded at a density of 1  $\times$  10<sup>5</sup> cells/cm<sup>2</sup> in 96, 12 and 6-well plates. For apoptosis analysis, cells were seeded in 96-well plates. Two days after, cells were treated with AS-EVs, then after 6 h with 35  $\mu$ M H<sub>2</sub>O<sub>2</sub> and finally analyzed with the Caspase-Glo 3/7 Assay after a further 24 h. For IFC and HRR analysis (see below), cells were seeded in 12 and 6-well plates, respectively, and processed like differentiated SH-SY5Y cells.

**EV Labelling:** EV internalization was analyzed with two different approaches of labelling. First, AS were treated with the lipophilic dye PKH26 (Sigma Aldrich, MINI26-1KT), following the protocol suggested by the manufacturer. After 3 days cells were washed, and medium changed with DMEM supplemented with 10% FBS depleted of exosomes. EVs were isolated from AS supernatants after 24 h by ultracentrifugation. The resulting EVs were applied on differentiated SH-SY5Y cells seeded onto poly-L-lysine (Sigma Aldrich, P9155) coated glass coverslips in 24 well plates. Target cells were stained with  $\alpha$ -TH primary antibody (Millipore, AB152) as in Ref. [106]. Imaging was performed using the confocal laser scanning microscope Leica TCS SP8. Image acquisitions were performed through LAS X software (Leica Microsystems). Image analyses were done using the open-source Java image processing program Fiji is Just ImageJ (Fiji). 3D reconstruction was done with the Fiji 3D Viewer dedicated plugin.

For the second approach, EVs were directly labelled with the same lipophilic dye, following the protocol suggested by the manufacturer, with some modification. Briefly, EVs derived from 90 mL of AS supernatant were ultracentrifuged, and the resulting pellets were resuspended in 0.3 mL of Diluent C plus 4  $\mu$ L of dye, and incubated at room temperature for 5 min, mixing every 30 s. The labeling was quenched by adding 1% BSA in PBS 1x and again ultracentrifuged. The resulting pellet, containing the labelled EVs, were resuspended in 100  $\mu$ L PBS 1x. Residual PKH26 was eliminated

into the Exosome Spin Column (Thermo Fisher Scientific, 4484449) according to the manufacturer's recommendations. Again, eluted EVs were applied on differentiated SH-SY5Y cells seeded onto glass coverslips in 24 well plates. At the end of the treatment cells were fixed with 4% PFA. As a control, PBS 1x with the same concentration of PKH26 dye was centrifuged under the same conditions and added to target cells. IF images were acquired using a Leica microscope (DM5500) and analyzed with Fiji ImageJ software 1.51n. For IFC analysis see the SH-SY5Y Culture, Differentiation, and Treatments section.

**High-Resolution Respirometry (HRR):** The capacity of different respiratory states in differentiated or undifferentiated SH-SY5Y cells was assayed by High-Resolution Respirometry (HRR) using the O2k-FluoRespirometer (Oroboros Instruments). Cells were seeded in 6-well plates and, after two days, AS-EVs were applied on the top of SH-SY5Y cells, as before. As control, 30% of ACM or supernatant (ACM after ultracentrifugation, SNT) were applied on target cells. 6 h later, cells were treated with MPP<sup>+</sup> 1 mM and analyzed after further 24 h. All the experiments were performed in mitochondrial respiration buffer Mir05 (Oroboros Instrument, 60101-01) at 37 °C under constant stirring (750 RPM). A specific Substrate-Uncoupler-Inhibitor Titration (SUIT) protocol was used for the determination of the O<sub>2</sub> consumption in each specific respiratory state, as detailed in Ref. [106]. Briefly, respiration in the presence of endogenous substrates or ROUTINE was measured in intact cells. The mild-detergent digitonin (Sigma Aldrich, D5628) was added at the final concentration of 4  $\mu$ M in order to obtain the permeabilization of plasma membrane without compromising the mitochondrial membranes' integrity. The O<sub>2</sub> consumption after permeabilization or LEAK was determined in the presence of 5 mM pyruvate (Sigma Aldrich, P2256) and 2 mM malate (Sigma Aldrich, M1000), but not adenylates. The contribution of complex I to the OXPHOS respiration was achieved by the addition of 10 mM glutamate (Sigma Aldrich, G1626) in the presence of a saturating concentration of ADP (2.5 mM, Sigma Aldrich, 117105). The OXPHOS respiration was then stimulated with the addition of 10 mM succinate (Sigma Aldrich, S2378). The uncoupled maximal capacity of the electron transport system (ETS) was obtained after titration with 0.5  $\mu$ M of uncoupler carbonyl cyanide 3-chlorophenylhydrazone (CCCP, Sigma Aldrich, C2759) up to the complete dissipation of the proton gradient. Finally, the residual O<sub>2</sub> consumption or ROX was obtained upon addition of 2  $\mu$ M rotenone (Sigma Aldrich, R8875) and 2.5  $\mu$ M antimycin A (Sigma Aldrich, A8674). The O<sub>2</sub> consumption in ROUTINE, LEAK, OXPHOS, and ETS capacity was corrected for the ROX. Values were then expressed as Flux Control Ratio (FCR) of the maximal respiration, using ETS capacity as a reference state.<sup>[161]</sup> The O<sub>2</sub> flux related to ATP synthesis was determined by correcting ROUTINE and OXPHOS for the LEAK respiration. Coupling efficiencies were calculated by correcting each state for LEAK respiration and expressing it as a percentage of the capacity in that specific state.<sup>[161]</sup> Instrumental and chemical background fluxes were calibrated as a function of the O<sub>2</sub> concentration using DatLab software (version 7.4.0.1, Oroboros Instruments).



**Statistical Analysis:** Pre-processing of data are described in each figure legend. The statistical analyses were performed with GraphPad Prism software (version 9.2.0). For all the analyses, differences among groups were analyzed by one-way ANOVA followed by a Tukey's multiple comparisons test. The values are expressed as mean ( $\pm$  SD) and a  $p < 0.05$  was accepted as significant. For IF on AS, data were obtained from  $n = 4$  (for VMB- and STR-AS) or  $n = 3$  (for  $\Delta$ VS-AS) independent biological replicates (from 4 to 10 images for each replicate). For cell viability/cytotoxicity on AS, data were obtained from  $n = 3$  independent replicates. For NTA, data were obtained from  $n = 3$  independent biological replicates (a total of 3 to 5 videos of 60 s recorded for each biological replicate). For EM, data were obtained from  $n = 5$  (for VMB- and STR-AS) or  $n = 3$  (for  $\Delta$ VS-AS) independent biological replicates (10 fields for each replicate). For qPCR, data were obtained from  $n = 3$  independent biological replicates. For IFC analysis on SH-SY5Y cells data were obtained from  $n = 3$  independent biological replicates. For the dose-response curve of  $H_2O_2$  and MPP<sup>+</sup>, data were obtained from  $n = 3$  independent biological replicates were analyzed by nonlinear regression, dose-response-inhibition ([Inhibitor] versus response—variable slope [four parameters]). For IF on SH-SY5Y, data were obtained from  $n = 3$  independent biological replicates (from 4 to 8 images for each biological replicate). For cell viability and apoptosis on differentiated and undifferentiated SH-SY5Y cells, data were obtained from at least  $n = 2$  independent biological replicates. For HRR measurement on differentiated SH-SY5Y treated with AS-EVs, the following independent biological replicates have been performed:  $n = 4$  for CTRL and MPP<sup>+</sup>,  $n = 3$  for +/- VMB-AS-EVs,  $n = 2$  for +/- STR-AS-EVs. For HRR measurement on differentiated SH-SY5Y treated with ACM/SNT, the following independent biological replicates have been performed:  $n = 3$  for CTRL and  $n = 2$  for MPP<sup>+</sup>, VMB-ACM/SNT, STR-ACM/SNT. For HRR measurement on undifferentiated SH-SY5Y treated with AS-EVs, the following independent biological replicates have been performed:  $n = 3$  for CTRL and  $n = 2$  for MPP<sup>+</sup>, VMB-AS-EVs, and STR-AS-EVs.

All relevant data of the experiments are available at the EV-TRACK knowledgebase (EV-TRACK ID: EV220106).<sup>[162]</sup>

## Supporting Information

Supporting Information is available from the Wiley Online Library or from the author.

## Acknowledgements

A. Messina, B.M. and N.I. contributed equally to this work. The authors thank Aviva M. Tolkovsky, Vito De Pinto, Massimo Libra, and Tommaso Leonardi for critically discussing the article. They acknowledge the support and technical assistance of Nunzio Vicario, Gabriele Raciti, Patrizia Caruso, and Fabrizio Cavallaro. They are grateful to CAPIR (Center for Advanced Preclinical in vivo Research) Team for maintenance and care of animals. They acknowledge the PON project Bio-nanotech Research and Innovation Tower (BRIT), financed by the Italian Ministry for Education, University and Research (MIUR) (Grant no. PONa3\_00136). They acknowledge the technical assistance of the BRIT Team with essential instruments. They are grateful to the Pharmacology section at the BIOMETEC Department which hosts the authors' laboratory. The project has been supported by the "Brain to South" grant (Fondazione con il Sud – Bando Capitale Umano ad Alta Qualificazione 2015). The research program also received support from the Italian Ministry of Health (Cur. Res. And Finalized Res projects 2010–2020), from University of Catania ("Bando-Chance", PRIN-2015, PIACERI and Ph.D. program in Biotechnology). The authors acknowledge "AIM Linea 1 Salute" (AIM1833071) to A. Magri. They acknowledge the Nano-scaffolding for neuronal migration and generation project (PCI2018-093062) granted by the Spanish Ministry of Science, Innovation and Universities and Red de Terapia Celular (TerCel-RD16/0011/0026). After initial online publication, the "United Kingdom" was changed to "UK" in affiliations 6 and 8 on October 19, 2022, as per journal style.

Open access funding provided by universita degli Studi di Catania within the CRUI-CARE agreement.

## Conflict of Interest

A.S. is an employee of Luminex B.V., which is a subsidiary of Luminex Corporation a DiaSorin Company. Luminex Corporation is the manufacturer of the Amnis FlowSight Imaging Flow Cytometer.

## Authors Contribution

L.L., F.L.E., A.Ma., N.F., L.P.-J., S.P., J.M.G.-V, A.Me., B.M., and N.I. conceived and designed the experiments; L.L., F.L.E., G.P., N.T., F.P., and N.I. performed primary astrocyte cultures; L.L., F.L.E., G.P., S.V., F.P., and N.I. performed SH-SY5Y cultures and treatments; L.L., G.P., S.V., F.P., L.P.-J., S.P., and N.I. carried out EV isolation and labeling; L.L., F.L.E., G.P., S.V., C.T., B.M., and N.I. carried out immunofluorescence and confocal microscopy; L.L., G.P., S.V., A.S., and N.I. performed IFC analyses; L.L., G.P., S.C., and N.I. performed WB analysis; L.L., C.A.P.B., J.J.P., N.F., and N.I. performed nanoparticle tracking analysis; L.L., M.J.U.-N., J.M.G.-V., and N.I. performed electron microscopy analysis; L.L., A.Ma., G.P., P.R., A.Me., and N.I. performed high-resolution respirometry analysis; L.L., F.L.E., A.Ma., M.J.U.-N., G.P., S.V., C.A.P.B., and N.I. performed statistical analyses; L.L., A.Ma., B.M., and N.I. wrote the original draft; L.L., A.Ma., S.V., L.P.-J., S.P., J.M.G.-V., A.Me., B.M., and N.I. performed review and revision of the paper. All authors contributed to the preparation of the figures and to the final version of the manuscript. All authors read and approved the final manuscript.

## Data Availability Statement

The data that support the findings of this study are available from the corresponding author upon reasonable request.

## Keywords

astrocytes, exosomes, extracellular vesicles, high-resolution respirometry, mitochondria, Parkinson's disease

Received: May 20, 2022

Revised: July 5, 2022

Published online: August 15, 2022

- [1] L. A. Mulcahy, R. C. Pink, D. R. F. Carter, *J. Extracell. Vesicles* **2014**, 3, 24641.
- [2] B. L. Deatherage, B. T. Cookson, *Infect. Immun.* **2012**, *80*, 1948.
- [3] D. G. Robinson, Y. Ding, L. Jiang, *Protoplasma* **2016**, *253*, 31.
- [4] R. Kalluri, V. S. LeBleu, *Science* **2020**, *367*, eaau6977.
- [5] D. K. Jeppesen, A. M. Fenix, J. L. Franklin, J. N. Higginbotham, Q. Zhang, L. J. Zimmerman, D. C. Liebler, J. Ping, Qi Liu, R. Evans, W. H. Fissell, J. C. Patton, L. H. Rome, D. T. Burnette, R. J. Coffey, *Cell* **2019**, *177*, 428.
- [6] C. Théry, K. W. Witwer, E. Aikawa, M. J. Alcaraz, J. D. Anderson, R. Andriantsitohaina, A. Antoniou, T. Arab, F. Archer, G. K. Atkin-Smith, D. C. Ayre, J.-M. Bach, D. Bachurski, H. Baharvand, L. Balaj, S. Baldacchino, N. N. Bauer, A. A. Baxter, M. Bebawy, C. Beckham, A. Bedina Zavec, A. Benmoussa, A. C. Berardi, P. Bergese, E. Bielska, C. Blenkiron, S. Bobis-Wozowicz, E. Boilard, W. Boireau, A. Bongiovanni, et al., *J. Extracell. Vesicles* **2018**, *7*, 1535750.
- [7] K. W. Witwer, D. C. Goberdhan, L. O'Driscoll, C. Théry, J. A. Welsh, C. Blenkiron, E. I. Buzás, D. Di Vizio, U. Erdbrügger, J. M. Falcón-Pérez, Q. L. Fu, A. F. Hill, M. Lenassi, J. Lötvall, R. Nieuwland, T. Ochiai, S. Rome, S. Sahoo, L. Zheng, *J. Extracell. Vesicles* **2021**, *10*, e12182.

- [8] N. Iraci, T. Leonardi, F. Gessler, B. Vega, S. Pluchino, *Int. J. Mol. Sci.* **2016**, *17*, 171.
- [9] S. El-Andaloussi, Y. Lee, S. Lakkhal-Littleton, J. Li, Y. Seow, C. Gardiner, L. Alvarez-Erviti, I. L. Sargent, M. J. A. Wood, *Nat. Protoc.* **2012**, *7*, 2112.
- [10] O. G. de Jong, D. E. Murphy, I. Mäger, E. Willms, A. Garcia-Guerra, J. J. Gitz-Francois, J. Lefferts, D. Gupta, S. C. Steenbeek, J. van Rheenen, S. El-Andaloussi, R. M. Schiffelers, M. J. A. Wood, P. Vader, *Nat. Commun.* **2020**, *11*, 1113.
- [11] I. K. Herrmann, M. J. A. Wood, G. Fuhrmann, *Nat. Nanotechnol.* **2021**, *16*, 748.
- [12] G. van Niel, D. R. F. Carter, A. Clayton, D. W. Lambert, G. Raposo, P. Vader, *Nat. Rev. Mol. Cell Biol.* **2022**, *23*, 369.
- [13] L. Leggio, S. Vivarelli, F. L'Episcopo, C. Tirollo, S. Caniglia, N. Testa, B. Marchetti, N. Iraci, *Int. J. Mol. Sci.* **2017**, *18*, 2698.
- [14] M. Shi, C. Liu, T. J. Cook, K. M. Bullock, Y. Zhao, C. Ghingina, Y. Li, P. Aro, R. Dator, C. He, M. J. Hipp, C. P. Zabetian, E. R. Peskind, S.-C. Hu, J. F. Quinn, D. R. Galasko, W. A. Banks, J. Zhang, *Acta Neuropathol.* **2014**, *128*, 639.
- [15] R. Kojima, D. Bojar, G. Rizzi, G. C. El Hamri, M. D. El-Baba, P. Saxena, S. Ausländer, K. R. Tan, M. Fussenegger, *Nat. Commun.* **2018**, *9*, 1305.
- [16] A. Fuster-Matanzo, F. Gessler, T. Leonardi, N. Iraci, S. Pluchino, *Stem Cell Res. Ther.* **2015**, *6*, 227.
- [17] D. Buschmann, V. Mussack, J. B. Byrd, *Adv. Drug Delivery Rev.* **2021**, *174*, 348.
- [18] Z. H. Zhao, Z. T. Chen, R. L. Zhou, X. Zhang, Q. Y. Ye, Y. Z. Wang, *Front. Aging Neurosci.* **2019**, *10*.
- [19] S. Wang, Z. Liu, T. Ye, O. S. Mabrouk, T. Maltbie, J. Aasly, A. B. West, *Acta Neuropathol. Commun.* **2017**, *5*, 86.
- [20] L. Leggio, G. Arrabito, V. Ferrara, S. Vivarelli, G. Paternò, B. Marchetti, B. Pignataro, N. Iraci, *Adv. Healthcare Mater.* **2020**, *9*, 2000731.
- [21] A. Clayton, E. Boilard, E. I. Buzas, L. Cheng, J. M. Falcón-Perez, C. Gardiner, D. Gustafson, A. Gualerzi, A. Hendrix, A. Hoffman, J. Jones, C. Lässer, C. Lawson, M. Lenassi, I. Nazarenko, L. O'Driscoll, R. Pink, P. R.-M. Siljander, C. Soekmadji, M. Wauben, J. A. Welsh, K. Witwer, L. Zheng, R. Nieuwland, *J. Extracell. Vesicles* **2019**, *8*, 1647027.
- [22] A. Jarmalavičiute, V. Tunaitis, U. Pivoraite, A. Venalis, A. Pivoriunas, *Cytotherapy* **2015**, *17*, 932.
- [23] K. Narbutė, V. Pilipenko, J. Pupure, Z. Dzirkale, U. Jonavičė, V. Tunaitis, K. Kriaučiūnaitė, A. Jarmalavičiūtė, B. Jansone, V. Kluša, A. Pivoriunas, *Stem Cells Transl. Med.* **2019**, *8*, 490.
- [24] M. J. Haney, Y. Zhao, E. B. Harrison, V. Mahajan, S. Ahmed, Z. He, P. Suresh, S. D. Hingtgen, N. L. Klyachko, R. L. Mosley, H. E. Gendelman, A. V. Kabanov, E. V. Batrakova, *PLoS One* **2013**, *8*, e61852.
- [25] M. J. Haney, N. L. Klyachko, Y. Zhao, R. Gupta, E. G. Plotnikova, Z. He, T. Patel, A. Piroyan, M. Sokolsky, A. V. Kabanov, E. V. Batrakova, *J. Controlled Release* **2015**, *207*, 18.
- [26] G. C. Terstappen, A. H. Meyer, R. D. Bell, W. Zhang, *Nat. Rev. Drug Discovery* **2021**, *20*, 362.
- [27] J. Saint-Pol, F. Gosselet, S. Duban-Deweir, G. Pottiez, Y. Karamanos, *Cells* **2020**, *9*, 851.
- [28] X. Zhu, M. Badawi, S. Pomeroy, D. S. Sutaria, Z. Xie, A. Baek, J. Jiang, O. A. Elgarnal, X. Mo, K. L. Perle, J. Chalmers, T. D. Schmittgen, M. A. Phelps, *J. Extracell. Vesicles* **2017**, *6*, 1324730.
- [29] W.-C. Wu, J. Tian, D. Xiao, Y.-X. Guo, Y. Xiao, X.-Y. Wu, G. Casella, J. Rasouli, Y.-P. Yan, A. Rostami, L.-B. Wang, Y. Zhang, X. Li, *Nanoscale* **2022**, *14*, 2393.
- [30] Z. Yan, S. Dutta, Z. Liu, X. Yu, N. Mesgarzadeh, F. Ji, G. Bitan, Y. H. Xie, *ACS Sens.* **2019**, *4*, 488.
- [31] A. Hoshino, H. S. Kim, L. Bojmar, K. E. Gyan, M. Cioffi, J. Hernandez, C. P. Zambirinis, G. Rodrigues, H. Molina, S. Heissel, M. T. Mark, L. Steiner, A. Benito-Martin, S. Lucotti, A. Di Giannatale, K. Offer, M. Nakajima, C. Williams, L. Nogués, F. A. P. Vatter, A. Hashimoto, A. E. Davies, D. Freitas, C. M. Kenific, Y. Araso, W. Buehring, P. Lauritzen, Y. Ogitani, K. Sugiura, N. Takahashi, et al., *Cell* **2020**, *182*, 1044.
- [32] H. Zhang, D. Freitas, H. S. Kim, K. Fabijanic, Z. Li, H. Chen, M. T. Mark, H. Molina, A. B. Martin, L. Bojmar, J. Fang, S. Rampersaud, A. Hoshino, I. Matei, C. M. Kenific, M. Nakajima, A. P. Mutvei, P. Sansone, W. Buehring, H. Wang, J. P. Jimenez, L. Cohen-Gould, N. Paknejad, M. Brendel, K. Manova-Todorova, A. Magalhães, J. A. Ferreira, H. Osório, A. M. Silva, A. Massey, et al., *Nat. Cell Biol.* **2018**, *20*, 332.
- [33] M. Durcin, A. Fleury, E. Taillebois, G. Hilairet, Z. Krupova, C. Henry, S. Truchet, M. Trötz Müller, H. Köfeler, G. Mabileau, O. Hue, R. Andriantsitohaina, P. Martin, S. Le Lay, *J. Extracell. Vesicles* **2017**, *6*, 1305677.
- [34] G. Van Niel, G. D'Angelo, G. Raposo, *Nat. Rev. Mol. Cell Biol.* **2018**, *19*, 213.
- [35] M. Sardar Sinha, A. Ansell-Schultz, L. Civitelli, C. Hildesjö, M. Larsson, L. Lannfelt, M. Ingelsson, M. Hallbeck, *Acta Neuropathol.* **2018**, *136*, 41.
- [36] J. M. Silverman, S. M. Fernando, L. I. Grad, A. F. Hill, B. J. Turner, J. J. Yerbury, N. R. Cashman, *Cell. Mol. Neurobiol.* **2016**, *36*, 377.
- [37] K. M. Danzer, L. R. Kranich, W. P. Ruf, O. Cagsal-Getkin, A. R. Winslow, L. Zhu, C. R. Vanderburg, P. J. McLean, *Mol. Neurodegener.* **2012**, *7*, 42.
- [38] A. Vogel, R. Upadhyaya, A. K. Shetty, *eBioMedicine* **2018**, *38*, 273.
- [39] B. Marchetti, L. Leggio, F. L'Episcopo, S. Vivarelli, C. Tirollo, G. Paternò, C. Giachino, S. Caniglia, M. F. Serapide, N. Iraci, *J. Clin. Med.* **2020**, *9*, 1941.
- [40] F. L'Episcopo, C. Tirollo, M. F. Serapide, S. Caniglia, N. Testa, L. Leggio, S. Vivarelli, N. Iraci, S. Pluchino, B. Marchetti, *Front. Aging Neurosci.* **2018**, *10*, 12.
- [41] B. Marchetti, M. P. Abbraccio, *Trends Pharmacol. Sci.* **2005**, *26*, 517.
- [42] K. Kuter, L. Olech, U. Glowacka, *Mol. Neurobiol.* **2018**, *55*, 3049.
- [43] F. L'Episcopo, C. Tirollo, L. Peruzzotti-Jametti, M. F. Serapide, N. Testa, S. Caniglia, B. Balzarotti, S. Pluchino, B. Marchetti, *Stem Cells* **2018**, *36*, 1179.
- [44] B. Marchetti, C. Tirollo, F. L'Episcopo, S. Caniglia, N. Testa, J. A. Smith, S. Pluchino, M. F. Serapide, *Aging Cell* **2020**, *19*, e13101.
- [45] F. L'Episcopo, C. Tirollo, N. Testa, S. Caniglia, M. C. Morale, B. Marchetti, *CNS Neurol. Disord.: Drug Targets* **2010**, *9*, 349.
- [46] P. L. McGeer, E. G. McGeer, *Mov. Disord.* **2008**, *23*, 474.
- [47] M. V. Sofroniew, H. V. Vinters, *Acta Neuropathol.* **2010**, *119*, 7.
- [48] H. D. E. Booth, W. D. Hirst, R. Wade-Martins, *Trends Neurosci.* **2017**, *40*, 358.
- [49] J. E. Burda, M. V. Sofroniew, *Neuron* **2014**, *81*, 229.
- [50] M. Bélanger, P. J. Magistretti, *Dialogues Clin. Neurosci.* **2009**, *11*, 281.
- [51] P. C. Chen, M. R. Vargas, A. K. Pani, R. J. Smeyne, D. A. Johnson, Y. W. Kan, J. A. Johnson, *Proc. Natl. Acad. Sci. USA* **2009**, *106*, 2933.
- [52] E. C. Hirsch, P. Jenner, S. Przedborski, *Mov. Disord.* **2013**, *28*, 24.
- [53] C. M. Tanner, S. M. Goldman, *Neurol. Clin.* **1996**, *14*, 317.
- [54] O. Hornykiewicz, *Neurology* **1998**, *51*, S2.
- [55] J. T. Bendor, T. P. Logan, R. H. Edwards, *Neuron* **2013**, *79*, 1044.
- [56] A. H. V. Schapira, C. W. Olanow, J. T. Greenamyre, E. Bezard, *Lancet* **2014**, *384*, 545.
- [57] J. Jankovic, *Mov. Disord.* **2019**, *34*, 41.
- [58] V. S. Van Laar, J. Chen, A. D. Zharikov, Q. Bai, R. Di Maio, A. A. Dukes, T. G. Hastings, S. C. Watkins, J. T. Greenamyre, C. M. St Croix, E. A. Burton, *Redox Biol.* **2020**, *37*, 101695.
- [59] J. Drouin-Ouellet, F. Cicchetti, *Trends Pharmacol. Sci.* **2012**, *33*, 542.
- [60] E. C. Hirsch, S. Vyas, S. Hunot, *Parkinsonism Relat. Disord.* **2012**, *18*, S210.
- [61] J. R. Cannon, J. T. Greenamyre, *Neurobiol. Dis.* **2013**, *57*, 38.
- [62] E. C. Hirsch, D. G. Standaert, *Mov. Disord.* **2021**, *36*, 16.

- [63] B. Marchetti, P. A. Serra, C. Tirolò, F. L'Episcopo, S. Caniglia, F. Gennuso, N. Testa, E. Miele, S. Desole, N. Barden, M. C. Morale, *Brain Res. Rev.* **2005**, *48*, 302.
- [64] A. H. Schapira, *Lancet Neurol.* **2008**, *7*, 97.
- [65] M. Szelechowski, A. Bétourné, Y. Monnet, C. A. Ferré, A. Thourard, C. Foret, J. M. Peyrin, S. Hunot, D. Gonzalez-Dunia, *Nat. Commun.* **2014**, *5*, 5181.
- [66] P. P. Michel, E. C. Hirsch, S. Hunot, *Neuron* **2016**, *90*, 675.
- [67] S. R. Subramaniam, M. F. Chesselet, *Prog. Neurobiol.* **2013**, *106*, 17.
- [68] J. Blesa, I. Trigo-Damas, A. Quiroga-Varela, V. R. Jackson-Lewis, *Front. Neuroanat.* **2015**, *9*.
- [69] S. J. Chinta, C. A. Lieu, M. Demaria, R. M. Laberge, J. Campisi, J. K. Andersen, *J. Intern. Med.* **2013**, *273*, 429.
- [70] J. Blesa, S. Przedborski, *Front. Neuroanat.* **2014**, *8*.
- [71] B. Marchetti, P. A. Serra, F. L'Episcopo, C. Tirolò, S. Caniglia, N. Testa, S. Cioni, F. Gennuso, G. Rocchitta, M. S. Desole, M. C. Mazzarino, E. Miele, M. C. Morale, *Ann. N. Y. Acad. Sci.* **2005**, *1057*, 296.
- [72] M. C. Morale, P. A. Serra, F. L'Episcopo, C. Tirolò, S. Caniglia, N. Testa, F. Gennuso, G. Giachinta, G. Rocchitta, M. S. Desole, E. Miele, B. Marchetti, *Neuroscience* **2006**, *138*, 869.
- [73] B. Marchetti, *Redox Biol.* **2020**, *36*, 101664.
- [74] E. C. Hirsch, *Ann. Neurol.* **1992**, *32*, S88.
- [75] M. C. Morale, P. A. Serra, M. R. Delogu, R. Migheli, G. Rocchitta, C. Tirolò, S. Caniglia, N. Testa, F. L'Episcopo, F. Gennuso, G. M. Scoto, N. Barden, E. Miele, M. Speranza Desole, B. Marchetti, *FASEB J.* **2004**, *18*, 164.
- [76] L. Maatouk, C. Yi, M.-A. Carrillo-de Sauvage, A.-C. Compagnon, S. Hunot, P. Ezan, E. C. Hirsch, A. Koulakoff, F. W. Pfrieger, F. Tronche, L. Leybaert, C. Giaume, S. Vyas, *Cell Death Differ.* **2019**, *26*, 580.
- [77] B. E. Clarke, D. M. Taha, G. E. Tyzack, R. Patani, *Glia* **2021**, *69*, 20.
- [78] L. Soreq, J. Rose, E. Soreq, J. Hardy, D. Trabzuni, M. R. Cookson, C. Smith, M. Ryten, R. Patani, J. Ule, *Cell Rep.* **2017**, *18*, 557.
- [79] M. Asanuma, N. Okumura-Torigoe, I. Miyazaki, S. Murakami, Y. Kitamura, T. Sendo, *Int. J. Mol. Sci.* **2019**, *20*, 598.
- [80] L. Morel, M. S. R. Chiang, H. Higashimori, T. Shoneye, L. K. Iyer, J. Yelick, A. Tai, Y. Yang, *J. Neurosci.* **2017**, *37*, 8706.
- [81] M. V. Sofroniew, *Trends Immunol.* **2020**, *41*, 758.
- [82] L. Ben Hairn, D. H. Rowitch, *Nat. Rev. Neurosci.* **2017**, *18*, 31.
- [83] L. M. De Biase, K. E. Schuebel, Z. H. Füsfield, K. Jair, I. A. Hawes, R. Cimbro, H.-Y. Zhang, Q.-R. Liu, H. Shen, Z.-X. Xi, D. Goldman, A. Bonci, *Neuron* **2017**, *95*, 341.
- [84] H. Chai, B. Diaz-Castro, E. Shigetomi, E. Monte, J. C. Oceau, X. Yu, W. Cohn, P. S. Rajendran, T. M. Vondriska, J. P. Whitelegge, G. Coppola, B. S. Khakh, *Neuron* **2017**, *95*, 531.
- [85] W. Xin, K. E. Schuebel, K. Jair, R. Cimbro, L. M. De Biase, D. Goldman, A. Bonci, *Neuropsychopharmacology* **2019**, *44*, 344.
- [86] A. V. Molofsk, R. Krenick, E. Ullian, H. H. Tsai, B. Deneen, W. D. Richardson, B. A. Barres, D. H. Rowitch, *Genes Dev.* **2012**, *26*, 891.
- [87] E. W. Kostuk, J. Cai, L. Iacovitti, *Glia* **2019**, *67*, 1542.
- [88] L. E. Clarke, S. A. Liddelow, C. Chakraborty, A. E. Münch, M. Heiman, B. A. Barres, *Proc. Natl. Acad. Sci. USA* **2018**, *115*, E1896.
- [89] M. F. Serapide, F. L'Episcopo, C. Tirolò, N. Testa, S. Caniglia, C. Giachino, B. Marchetti, *Front. Aging Neurosci.* **2020**, *12*, 24.
- [90] I. Miyazaki, M. Asanuma, *Cells* **2020**, *9*, 2623.
- [91] F. Trettel, M. A. Di Castro, C. Limatola, *Neuroscience* **2020**, *439*, 230.
- [92] C. Lauro, M. Catalano, F. Trettel, C. Limatola, *Ann. N. Y. Acad. Sci.* **2015**, *1351*, 141.
- [93] B. Marchetti, S. Pluchino, *Trends Mol. Med.* **2013**, *19*, 144.
- [94] F. L'Episcopo, C. Tirolò, N. Testa, S. Caniglia, M. C. Morale, C. Cossetti, P. D'Adamo, E. Zardini, L. Andreoni, A. E. C. Ihekweba, P. A. Serra, D. Franciotta, G. Martino, S. Pluchino, B. Marchetti, *Neurobiol. Dis.* **2011**, *41*, 508.
- [95] F. L'Episcopo, C. Tirolò, N. Testa, S. Caniglia, M. C. Morale, M. Deleidi, M. F. Serapide, S. Pluchino, B. Marchetti, *J. Neurosci.* **2012**, *32*, 2062.
- [96] F. L'Episcopo, C. Tirolò, N. Testa, S. Caniglia, M. C. Morale, M. F. Serapide, S. Pluchino, B. Marchetti, *Stem Cells* **2014**, *32*, 2147.
- [97] C. Cossetti, N. Iraci, T. R. Mercer, T. Leonardi, E. Alpi, D. Drago, C. Alfaro-Cervello, H. K. Saini, M. P. Davis, J. Schaeffer, B. Vega, M. Stefanini, C. J. Zhao, W. Muller, J. M. Garcia-Verdugo, S. Mathivanan, A. Bachi, A. J. Enright, J. S. Mattick, S. Pluchino, *Mol. Cell* **2014**, *56*, 193.
- [98] N. Iraci, E. Gaude, T. Leonardi, A. S. H. Costa, C. Cossetti, L. Peruzzotti-Jametti, J. D. Bernstock, H. K. Saini, M. Gelati, A. L. Vescovi, C. Bastos, N. Faria, L. G. Occhipinti, A. J. Enright, C. Frezza, S. Pluchino, *Nat. Chem. Biol.* **2017**, *13*, 951.
- [99] A. Mueller, P. G. Strange, *FEBS Lett.* **2004**, *570*, 126.
- [100] L. Cartier, O. Hartley, M. Dubois-Dauphin, K.-H. Krause, *Brain Res. Rev.* **2005**, *48*, 16.
- [101] F. L'Episcopo, M. F. Serapide, C. Tirolò, N. Testa, S. Caniglia, M. C. Morale, S. Pluchino, B. Marchetti, *Mol. Neurodegener.* **2011**, *6*, 49.
- [102] F. L'Episcopo, C. Tirolò, N. Testa, S. Caniglia, M. C. Morale, F. Impagnatiello, S. Pluchino, B. Marchetti, *J. Neurosci.* **2013**, *33*, 1462.
- [103] F. L'Episcopo, C. Tirolò, S. Caniglia, N. Testa, M. C. Morale, M. F. Serapide, S. Pluchino, B. Marchetti, *J. Mol. Cell Biol.* **2014**, *6*, 13.
- [104] C. A. Reichel, M. Rehberg, P. Bihari, C. M. Moser, S. Linder, A. Khandoga, F. Krombach, *J. Leukocyte Biol.* **2008**, *83*, 864.
- [105] C. A. Reichel, M. Rehberg, M. Lerchenberger, N. Berberich, P. Bihari, A. G. Khandoga, S. Zahler, F. Krombach, *Arterioscler., Thromb., Vasc. Biol.* **2009**, *29*, 1787.
- [106] P. Risiglion, L. Leggio, S. A. M. Cubisino, S. Reina, G. Paternò, B. Marchetti, A. Magri, N. Iraci, A. Messina, *Int. J. Mol. Sci.* **2020**, *21*, 7809.
- [107] F. M. Lopes, R. Schröder, M. L. C. da F. Júnior, A. Zanotto-Filho, C. B. Müller, A. S. Pires, R. T. Meurer, G. D. Colpo, D. P. Gelain, F. Kapczinski, J. C. Fonseca Moreira, M. da Cruz Fernandes, F. Klamt, *Brain Res.* **2010**, *1337*, 85.
- [108] R. A. Ross, J. L. Biedler, *Cancer Res.* **1985**, *45*, 1628.
- [109] J. Bahney, C. S. von Bartheld, *Anat. Rec.* **2018**, *301*, 697.
- [110] C. S. von Bartheld, J. Bahney, S. Herculano-Houzel, *J. Comp. Neurol.* **2016**, *524*, 3865.
- [111] A. Baumann, A. Jorge-Finnigan, K. Jung-Kc, A. Sauter, I. Horvath, L. A. Morozova-Roche, A. Martinez, *Sci. Rep.* **2016**, *6*, 39488.
- [112] E. Eitan, E. R. Hutchison, K. Marosi, J. Comotto, M. Mustapic, S. M. Nigam, C. Suire, C. Maharana, G. A. Jicha, D. Liu, V. Machairaki, K. W. Witwer, D. Kapogiannis, M. P. Mattson, *NPJ Aging Mech. Dis.* **2016**, *2*, 16019.
- [113] Z. Liao, H. Liu, L. Ma, J. Lei, B. Tong, G. Li, W. Ke, K. Wang, X. Feng, W. Hua, S. Li, C. Yang, *ACS Nano* **2021**, *15*, 14709.
- [114] K. Takov, D. M. Yellon, S. M. Davidson, *J. Extracell. Vesicles* **2017**, *6*, 1388731.
- [115] J. B. Simonsen, *J. Extracell. Vesicles* **2019**, *8*, 1582237.
- [116] D. B. Zorov, M. Juhaszova, S. J. Sollott, *Physiol. Rev.* **2014**, *94*, 909.
- [117] J. W. Langston, *J. Parkinson's Dis.* **2017**, *7*, S11.
- [118] P. Maiti, J. Manna, G. L. Dunbar, P. Maiti, G. L. Dunbar, *Transl. Neurodegener.* **2017**, *6*.
- [119] C. Christensen, H. Porsteinsson, V. H. Maier, K. Å. Karlsson, *Front. Behav. Neurosci.* **2020**, *14*.
- [120] N. Ismail, M. Ismail, M. U. Imam, N. H. Azmi, S. F. Fathy, J. B. Foo, M. F. Abu Bakar, *BMC Complementary Altern. Med.* **2014**, *14*, 467.
- [121] H. Guan, H. Yang, M. Yang, D. Yanagisawa, J.-P. Bellier, M. Mori, S. Takahata, T. Nonaka, S. Zhao, I. Tooyama, *Exp. Neurol.* **2017**, *291*, 51.
- [122] C.-F. Jhuo, S.-K. Hsieh, C.-J. Chen, W.-Y. Chen, J. T. C. Tzen, *Nutrients* **2020**, *12*, 3665.
- [123] W. J. Nicklas, I. Vyas, R. E. Heikkila, *Life Sci.* **1985**, *36*, 2503.
- [124] M. S. T. Mapa, V. Q. Le, K. Wimalasena, *PLoS One* **2018**, *13*, e0197946.



- [125] R. R. Fritz, C. W. Abell, N. T. Patel, W. Gessner, A. Brossi, *FEBS Lett.* **1985**, *186*, 224.
- [126] T. E. Whittaker, A. Nagelkerke, V. Nele, U. Kauscher, M. M. Stevens, *J. Extracell. Vesicles* **2020**, *9*, 1807674.
- [127] J. K. Sandhu, M. Gardaneh, R. Iwasio, P. Lanthier, S. Gangaraju, M. Ribocco-Lutkiewicz, R. Tremblay, K. Kiuchi, M. Sikorska, *Neurobiol. Dis.* **2009**, *33*, 405.
- [128] S. A. Liddel, K. A. Guttenplan, L. E. Clarke, F. C. Bennett, C. J. Bohlen, L. Schirmer, M. L. Bennett, A. E. Münch, W. S. Chung, T. C. Peterson, D. K. Wilton, A. Frouin, B. A. Napier, N. Panicker, M. Kumar, M. S. Buckwalter, D. H. Rowitch, V. L. Dawson, T. M. Dawson, B. Stevens, B. A. Barres, *Nature* **2017**, *541*, 481.
- [129] L. De Boni, A. H. Watson, L. Zaccagnini, A. Wallis, K. Zhelcheska, N. Kim, J. Sanderson, H. Jiang, E. Martin, A. Cantlon, M. Rovere, L. Liu, M. Sylvester, T. Lashley, U. Dettmer, Z. Jaunmuktane, T. Bartels, *Acta Neuropathol.* **2022**, *143*, 453.
- [130] C. Cossetti, J. A. Smith, N. Iraci, T. Leonardi, C. Alfaro-Cervello, S. Pluchino, *Front. Physiol.* **2012**, *3*.
- [131] J. A. Smith, T. Leonardi, B. Huang, N. Iraci, B. Vega, S. Pluchino, *Biogerontology* **2015**, *16*, 147.
- [132] L. Leggio, G. Paternò, S. Vivarelli, G. G. Falzone, C. Giachino, B. Marchetti, N. Iraci, *Aging Dis.* **2021**, *12*, 1494.
- [133] C. Escartin, E. Galea, A. Lakatos, J. P. O'Callaghan, G. C. Petzold, A. Serrano-Pozo, C. Steinhäuser, A. Volterra, G. Carmignoto, A. Agarwal, N. J. Allen, A. Araque, L. Barbeito, A. Barzilai, D. E. Bergles, G. Bonvento, A. M. Butt, W.-T. Chen, M. Cohen-Salmon, C. Cunningham, B. Deneen, B. De Strooper, B. Díaz-Castro, C. Farina, M. Freeman, V. Gallo, J. E. Goldman, S. A. Goldman, M. Götz, A. Gutiérrez, et al., *Nat. Neurosci.* **2021**, *24*, 312.
- [134] M. A. S. Pavlou, L. Grandbarbe, N. J. Buckley, S. P. Niclou, A. Michelucci, *Prog. Neurobiol.* **2019**, *174*, 36.
- [135] G. E. Tyzack, S. Sitnikov, D. Barson, K. L. Adams-Carr, N. K. Lau, J. C. Kwok, C. Zhao, R. J. M. Franklin, R. T. Karadottir, J. W. Fawcett, A. Lakatos, *Nat. Commun.* **2014**, *5*, 4294.
- [136] M. Sidoryk-Węgrzynowicz, Y. N. Gerber, M. Ries, M. Sastre, A. M. Tolkovsky, M. G. Spillantini, *Acta Neuropathol. Commun.* **2017**, *5*, 89.
- [137] A. Venturini, M. Passalacqua, S. Pelassa, F. Pastorino, M. Tedesco, K. Cortese, M. C. Gagliani, G. Leo, G. Maura, D. Guidolin, L. F. Agnati, M. Marcoli, C. Cervetto, *Front. Pharmacol.* **2019**, *10*.
- [138] R. Pascua-Maestro, E. González, C. Lillo, M. D. Ganfornina, J. M. Falcón-Pérez, D. Sanchez, *Front. Cell. Neurosci.* **2019**, *12*.
- [139] N. Shakespear, M. Ogura, J. Yamaki, Y. Homma, *Neurochem. Res.* **2020**, *45*, 1020.
- [140] A. Datta Chaudhuri, R. M. Dasgheyb, L. R. DeVine, H. Bi, R. N. Cole, N. J. Haughey, *Glia* **2020**, *68*, 128.
- [141] K. Guitart, G. Loers, F. Buck, U. Bork, M. Schachner, R. Kleene, *Glia* **2016**, *64*, 896.
- [142] L. Leggio, G. Paternò, S. Vivarelli, F. L'Episcopo, C. Tirolo, G. Raciti, F. Pappalardo, C. Giachino, S. Caniglia, M. F. Serapide, B. Marchetti, N. Iraci, *Biomolecules* **2020**, *10*, 1327.
- [143] A. H. V. Schapira, *Exp. Neurol.* **2010**, *224*, 331.
- [144] A. H. V. Schapira, J. M. Cooper, D. Dexter, J. B. Clark, P. Jenner, C. D. Marsden, *J. Neurochem.* **1990**, *54*, 823.
- [145] A. L. Bulteau, N. P. Mena, F. Auchère, I. Lee, A. Prigent, C. S. Lobsgier, J. M. Camadro, E. C. Hirsch, *Free Radic. Biol. Med.* **2017**, *108*, 236.
- [146] R. Morigaki, S. Goto, *Brain Sci.* **2017**, *7*, 63.
- [147] K. Kaur, J. S. Gill, P. K. Bansal, R. Deshmukh, *J. Neurol. Sci.* **2017**, *381*, 308.
- [148] S. Saxena, P. Caroni, *Neuron* **2011**, *71*, 35.
- [149] J. Creus-Muncunill, M. E. Ehrlich, *Neurotherapeutics* **2019**, *16*, 957.
- [150] D. Liu, Z. Dong, J. Wang, Y. Tao, X. Sun, X. Yao, *Mitochondrion* **2020**, *54*, 122.
- [151] K. Todkar, L. Chikhi, V. Desjardins, F. El-Mortada, G. Pépin, M. Germain, *Nat. Commun.* **2021**, *12*, 1971.
- [152] A. Picca, F. Guerra, R. Calvani, C. Bucci, M. R. Lo Monaco, A. R. Bentivoglio, H. J. Coelho-Júnior, F. Landi, R. Bernabei, E. Marzetti, *Int. J. Mol. Sci.* **2019**, *20*, 805.
- [153] A. Picca, F. Guerra, R. Calvani, F. Marini, A. Biancolillo, G. Landi, R. Beli, F. Landi, R. Bernabei, A. Bentivoglio, M. R. Lo Monaco, C. Bucci, E. Marzetti, *J. Clin. Med.* **2020**, *9*, 504.
- [154] A. J. Chu, J. M. Williams, *Front. Physiol.* **2022**, *12*.
- [155] M. Zhao, S. Liu, C. Wang, Y. Wang, M. Wan, F. Liu, M. Gong, Y. Yuan, Y. Chen, J. Cheng, Y. Lu, J. Liu, *ACS Nano* **2021**, *15*, 1519.
- [156] X. Wang, I. Weidling, S. Koppel, B. Menta, J. P. Ortiz, A. Kalani, H. M. Wilkins, R. H. Swerdlow, *Mitochondrion* **2020**, *55*, 100.
- [157] J. A. Korecka, R. E. van Kesteren, E. Blaas, S. O. Spitzer, J. H. Kamstra, A. B. Smit, D. F. Swaab, J. Verhaagen, K. Bossers, *PLoS One* **2013**, *8*, e63862.
- [158] A. Merlevede, E. M. Legault, V. Drugge, R. A. Barker, J. Drouin-Ouellet, V. Olariu, *Sci. Rep.* **2021**, *11*, 1514.
- [159] K. Wang, L. Ye, H. Lu, H. Chen, Y. Zhang, Y. Huang, J. C. Zheng, *J. Neuroinflammation* **2017**, *14*.
- [160] A. Ertürk, Y. Wang, M. Sheng, *J. Neurosci.* **2014**, *34*, 1672.
- [161] D. Pesta, E. Gnaiger, *Methods Mol. Biol.* **2012**, *810*, 25.
- [162] EV-TRACK Consortium, J. Van Deun, P. Mestdagh, P. Agostinis, Ö. Akay, S. Anand, J. Anckaert, Z. A. Martinez, T. Baetens, E. Beghein, L. Bertier, G. Berx, J. Boere, S. Boukouris, M. Bremer, D. Buschmann, J. B. Byrd, C. Casert, L. Cheng, A. Cmoch, D. Daveloose, E. De Smedt, S. Demirsoy, V. Depoorter, B. Dhondt, T. A. P. Driedonks, A. Dudek, A. Elsharawy, I. Floris, A. D. Foers, et al., *Nat. Methods* **2017**, *14*, 228.

# ADVANCED HEALTHCARE MATERIALS

## Supporting Information

for *Adv. Healthcare Mater.*, DOI 10.1002/adhm.202201203

Small Extracellular Vesicles Secreted by Nigrostriatal Astrocytes Rescue Cell Death and Preserve Mitochondrial Function in Parkinson's Disease

*Loredana Leggio, Francesca L'Episcopo, Andrea Magri, María José Ulloa-Navas, Greta Paternò, Silvia Vivarelli, Carlos A. P. Bastos, Cataldo Tirolo, Nunzio Testa, Salvatore Caniglia, Pierpaolo Risiglione, Fabrizio Pappalardo, Alessandro Serra, Patricia García-Tárraga, Nuno Faria, Jonathan J. Powell, Luca Peruzzotti-Jametti, Stefano Pluchino, José Manuel García-Verdugo, Angela Messina, Bianca Marchetti\* and Nunzio Iraci\**

Supporting Information

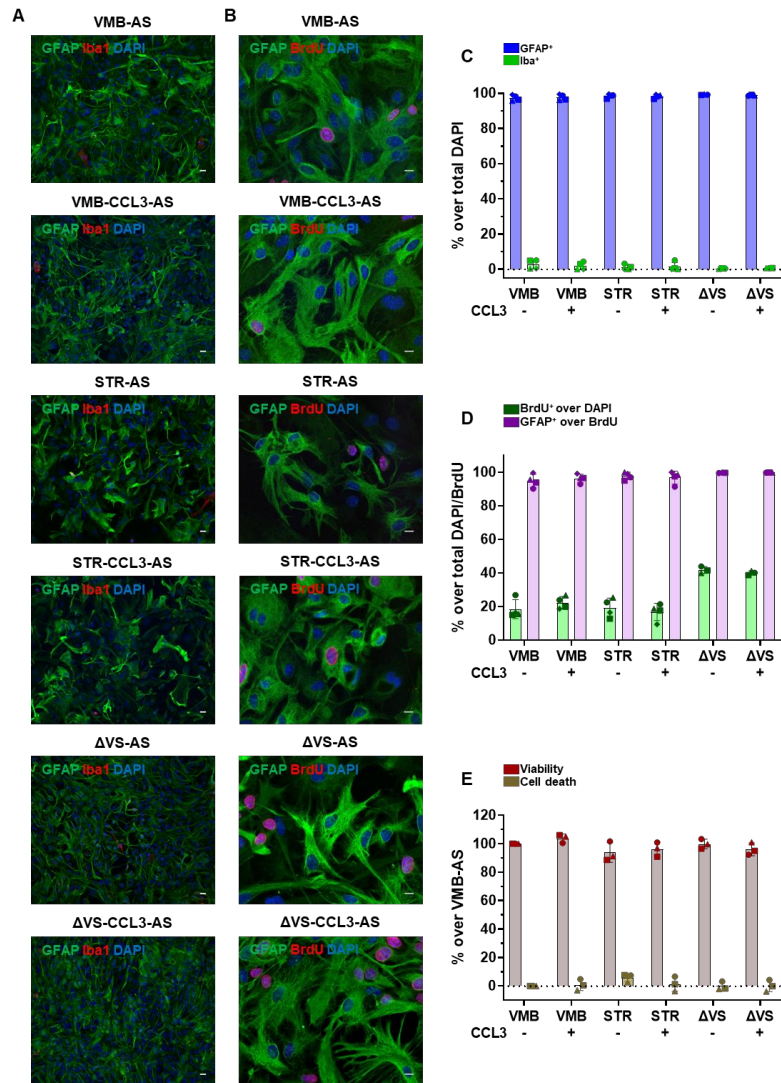
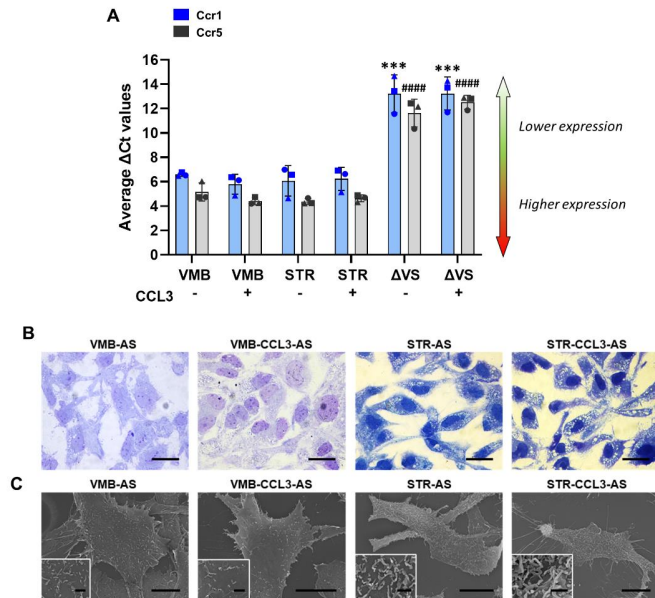


**Figure S1.** Characterization of AS primary cultures from VMB, STR and from VMB- and STR-depleted brain regions (ΔVS-AS), under basal and CCL3-treated conditions. A) Immunofluorescence (IF) images show the presence of AS (GFAP<sup>+</sup> cells, in green) and microglial cells (Iba1<sup>+</sup> cells, in red), with DAPI<sup>+</sup> nuclei (in blue). Scale bars: 20 μm. B) IF images show the presence of proliferative AS (GFAP<sup>+</sup>/BrdU<sup>+</sup> cells, in green and red respectively), with DAPI<sup>+</sup> nuclei (in blue). Scale bars: 10 μm. C) Quantification of the staining in A: the number of GFAP<sup>+</sup> and Iba1<sup>+</sup> cells are normalized over total DAPI<sup>+</sup> nuclei. Data are expressed as mean ± SD from n=4

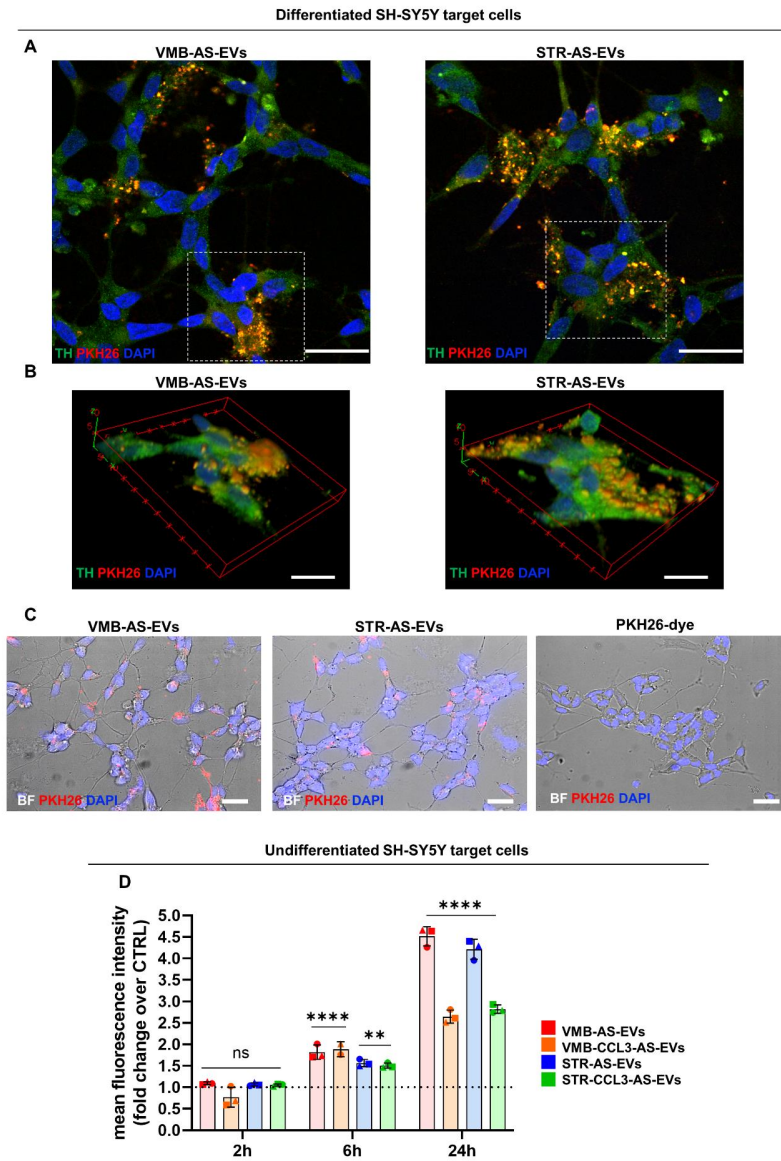
(for VMB- and STR-AS) and n=3 (for  $\Delta$ VS-AS) independent experiments, indicated with different symbols. D) Quantification of the staining in B: the number of BrdU<sup>+</sup> cells are normalized over total DAPI<sup>+</sup> nuclei, while GFAP<sup>+</sup> cells are normalized over BrdU<sup>+</sup> cells. Data are expressed as mean  $\pm$  SD from n=4 (for VMB- and STR-AS) and n=3 (for  $\Delta$ VS-AS) independent experiments, indicated with different symbols. E) Analysis of cell viability and death. Data are expressed as mean over VMB-AS  $\pm$  SD from n=3 independent experiments, indicated with different symbols.

Table S1. Diameter values of AS-EV samples.

Diameter (nm)	VMB-AS-EVs	VMB-CCL3-AS-EVs	STR-AS-EVs	STR-CCL3-AS-EVs	$\Delta$ VS-AS-EVs	$\Delta$ VS-CCL3-AS-EVs
Minimum	28,28	22,12	24,19	24,25	18,5	23,7
Maximum	290,8	440,1	280,3	340,9	142,5	192,7
Median	63,5	59,5	64,9	59,6	53,3	54,0
Mean	72,5	68,5	75	63,5	58,7	64
Std. Deviation	14,5	14,7	7	17,8	6,8	8,5



**Figure S2.** A) qPCR analyses of CCL3 receptors in AS, showing average  $\Delta C_t$  values for Ccr1 and Ccr5. Gusb was used as housekeeping gene. Data are presented as mean  $\pm$  SD from  $n=3$  independent replicates, indicated with different symbols. One-way ANOVA with Tukey's multiple comparison test shows that  $\Delta C_t$  values for Ccr1 in  $\Delta VS$ -AS are significantly higher compared to all the other groups ( $***p < 0.001$ );  $\Delta C_t$  values for Ccr5 in  $\Delta VS$ -AS are significantly higher compared to all the other groups ( $#####p < 0.0001$ ). B) Semithin sections stained with toluidine blue show differences in the membranes of STR-AS (CCL3 vs. basal) but not in VMB. C) SEM analysis shows that STR-AS bear more irregular membrane protrusions after CCL3 supplementation. Scale bars B: 50  $\mu m$ , C: 10  $\mu m$ , inserts: 1  $\mu m$ .



**Figure S3.** PKH26-labelled AS-EVs internalization by differentiated and undifferentiated SH-SY5Y cells. A) Single plan confocal images show the uptake of both VMB-AS- and STR-AS-PKH26-labelled EVs by differentiated SH-SY5Y (white dotted squares were shown as max projections in Figure 3A). Scale bar 20  $\mu$ m. B) 3D reconstruction from all z stacks (see Figure 3A). Scale bars 10  $\mu$ m. C) IF (in red PKH26 labelled AS-EVs and in blue DAPI counterstained nuclei) and bright field (whole cells) images of differentiated SH-SY5Y upon treatment with PKH26-labelled EVs. EVs are distributed in cell bodies and also in neurites. On the right, PKH26

dye-only were administered to target cells. Scale bars: 20  $\mu$ M. D) IFC analysis of undifferentiated SH-SY5Y cells treated with PKH26-AS-EVs at different time points. Data are expressed as fold change of the mean fluorescence intensity  $\pm$  SD over CTRL (dashed line at y axis =1) from n=3 independent experiment, indicated with different symbols. One-way ANOVA with Tukey's multiple comparison vs. CTRL. \*\*p < 0.01, \*\*\*\*p < 0.0001, ns: not significant.



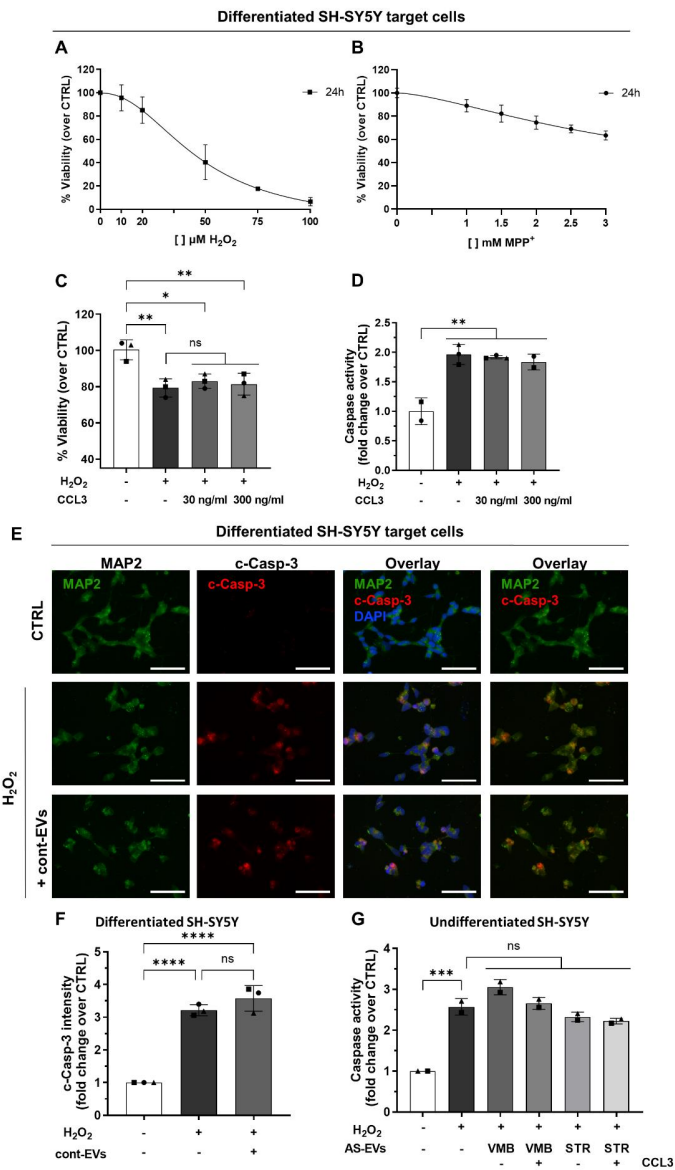


**Figure S4.** A) Dose response curve of  $H_2O_2$  on differentiated SH-SY5Y cells at 24 h. B) Dose response curve of  $MPP^+$  on differentiated SH-SY5Y cells at 24 h. C-D) Analysis of cell viability (C) and cell death (D) of differentiated SH-SY5Y neurons treated with CCL3 and challenged with  $H_2O_2$ , expressed as percentage (in C) or fold change (in D) over CTRL. Data are expressed as mean  $\pm$  SD from n=3 independent replicates, indicated with different symbols. One-way ANOVA with Tukey's multiple comparison \* $p < 0.05$ , \*\* $p < 0.01$  vs. CTRL, ns = not significant.

ns: not significant. E) IF staining for MAP2 (in green), c-Casp-3 (in red) and DAPI (in blue), on differentiated SH-SY5Y exposed to cont-EVs and treated with 35  $\mu\text{M}$   $\text{H}_2\text{O}_2$ . Scale bars: 50  $\mu\text{m}$ . F) Quantification of the c-Casp-3 staining in E. The fluorescent intensity values were normalized over total DAPI<sup>+</sup> nuclei. Data are expressed as mean  $\pm$  SD over CTRL, set to 1 for comparison. G) Caspase 3/7 activities in undifferentiated SH-SY5Y exposed to AS-EVs (ratio 5:1) for 6 h and then treated with 35  $\mu\text{M}$   $\text{H}_2\text{O}_2$  for 24 h. Data are expressed as mean  $\pm$  SD over CTRL, set to 1 for comparison. One-way ANOVA with Tukey's multiple comparison. In (F) \*\*\*\*p < 0.0001 (CTRL vs.  $\text{H}_2\text{O}_2$  and vs.  $\text{H}_2\text{O}_2$  + cont-EVs), ns: not significant. In (G) \*\*\*p < 0.001 (CTRL vs.  $\text{H}_2\text{O}_2$ ), ns: not significant.

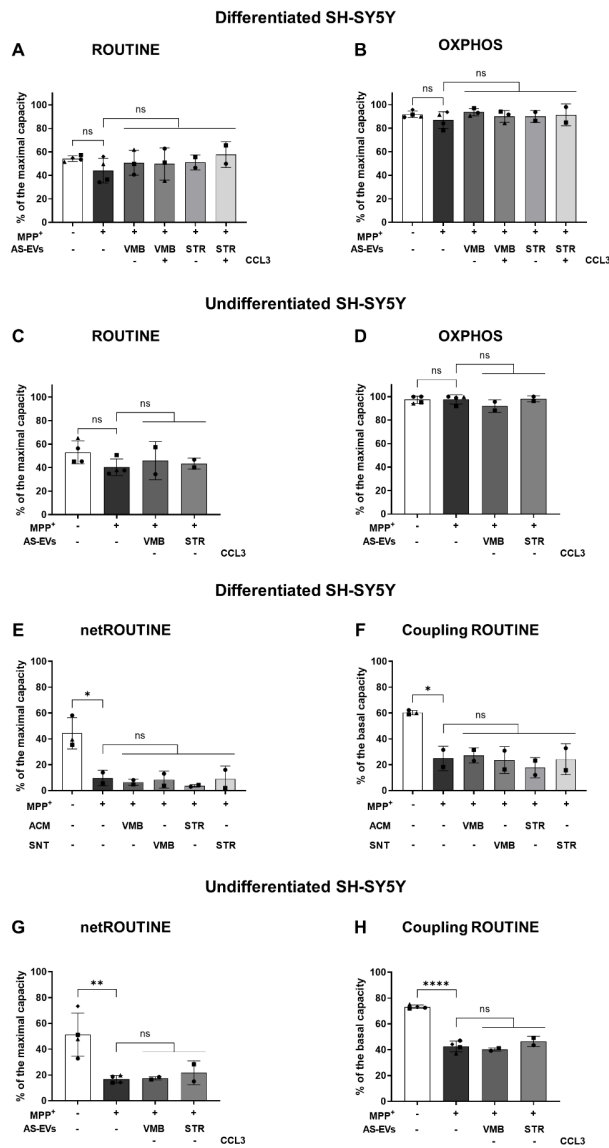


**Figure S5** A-D) Analysis of O<sub>2</sub> flows correspondent to the main respiratory states ROUTINE and OXPHOS achieved upon different experimental conditions and/or EV treatment in differentiated (A-B) or undifferentiated (C-D) SH-SY5Y cells. MPP<sup>+</sup> did not affected respiration in any condition tested. All data are expressed as flux control ratio, as percentage of the maximal respiratory capacity. E-F) Analysis of net and coupling ROUTINE achieved upon different experimental conditions and/or EVs, ACM or SNT treatment in differentiated SH-SY5Y. In this case, MPP<sup>+</sup> promoted a general and significative decrease of both net and coupling respirations.

However, no effect was observed upon EVs, ACM or SNT treatment. Data are expressed as a flux control ratio, as percentage of specific reference states maximal and basal respiratory capacity for net and coupling respiration, respectively. G-H) Analysis of net and coupling ROUTINE achieved upon different experimental conditions and/or EVs treatment in undifferentiated SH-SY5Y. As for differentiated cells, MPP<sup>+</sup> promoted a reduction of both parameters which is not restored by EVs. Data are expressed as a flux control ratio, as percentage of specific reference states maximal and basal respiratory capacity for net and coupling respiration, respectively. In (A-H) data are expressed as mean  $\pm$  SD. One-way ANOVA with Tukey's multiple comparison was performed, with \*p <0.05, \*\*p<0.01 and \*\*\*\*p<0.001 (CTRL vs. MPP<sup>+</sup>), ns: not significant.

# An Analytical Model for the Inference of the EV Reception Process Parameters in Cell-to-Cell Communication

Nunzio Iraci  
nunzio.iraci@unict.it  
BIOMETEC - University of Catania  
Catania, Italy

Loredana Leggio  
loredana.leggio@unict.it  
BIOMETEC - University of Catania  
Catania, Italy

Alfio Lombardo  
alfio.lombardo@unict.it  
DIEEI - University of Catania  
Catania, Italy

Carla Panarello  
carla.panarello@unict.it  
DIEEI - University of Catania  
Catania, Italy

Fabrizio Pappalardo  
fabrizio.pappalardo@phd.unict.it  
DIEEI - University of Catania  
Catania, Italy

Greta Paternó  
greta.paterno@phd.unict.it  
BIOMETEC - University of Catania  
Catania, Italy

## ABSTRACT

The communication mediated by extracellular vesicles (EVs) is recognized as an opportunity for delivering biological material to recipient cells, with the aim of developing innovative and more efficient therapeutic protocols. In this context, they can represent an effective alternative to unsuccessful drug delivery systems, for the treatment of several diseases. However, a deeper understanding of the dynamics regulating the uptake of EVs by target cells is necessary, yet challenging, for the development of novel therapeutic approaches. In fact, the technologies today available do not allow the direct visualization of EV uptake over time. On the contrary, an indirect reconstruction of the molecular events is only possible and the estimation of the parameters involved in this molecular process remains a difficult task. For this reason, in this article we propose the mathematical model of a generic uptake process, with the aim of providing a tool both for the inference of still unknown biological parameters and for the design of biological experiments, according to some desired results.

## CCS CONCEPTS

• **Applied computing** → **Telecommunications; Biological networks**; • **Mathematics of computing** → **Ordinary differential equations**.

## KEYWORDS

Extracellular Vesicles, Exosomes, Cell-to-cell Communication, Molecular Communication, Mathematical Model, EV Uptake, EV Labelling

## ACM Reference Format:

Nunzio Iraci, Loredana Leggio, Alfio Lombardo, Carla Panarello, Fabrizio Pappalardo, and Greta Paternó. 2023. An Analytical Model for the Inference of the EV Reception Process Parameters in Cell-to-Cell Communication. In *The 10th ACM International Conference on Nanoscale Computing and Communication (NANOCOM '23)*, September 20–22, 2023, Coventry, United Kingdom. ACM, New York, NY, USA, 6 pages. <https://doi.org/10.1145/3576781.3608716>



This work is licensed under a Creative Commons Attribution-NonCommercial International 4.0 License.  
NANOCOM '23, September 20–22, 2023, Coventry, United Kingdom  
© 2023 Copyright held by the owner/author(s).  
ACM ISBN 979-8-4007-0034-7/23/09.  
<https://doi.org/10.1145/3576781.3608716>

## 1 INTRODUCTION

Extracellular Vesicles (EVs) mediate a particular type of cell-to-cell communication that is gaining interest in the bio-medical community [20]. EVs are nano-sized (30-1000 nm), spherical particles, carrying several kinds of molecules, and delimited by a lipid membrane which protects their payload from the action of external proteases and nucleases (i.e. the enzymes that digest proteins and nucleic acids, respectively). EVs are secreted by donor cells, diffuse into the extracellular space, and are internalized by target cells through several uptake mechanisms [14]. Once reached the target cell, the EVs with their payload may induce profound changes in the biology of the target cells. Therefore, thanks to the advances in bio-nano-technology and the possibility of engineering EVs, it has been envisioned to engage natural or synthetic-engineered EVs for delivering drugs to target cells, in the treatment of diseases [12].

However, the molecular mechanisms involved in the uptake of EVs are not fully understood. Ideally, for understanding the whole process, it would be necessary to work at a single EV (even single molecule) resolution, over a dense set of time points [9]. However, this remains a technical challenge for the field, considering that it is possible to visualize and to estimate the internalization, but without any knowledge of the number or concentration of internalized EVs and their relationship with the effects observed after the treatment. Furthermore, the experiments carried out at different time points, require multiple replicates, since for each measurement the experiment need to be stopped for the analysis. For example, in the set of experiments carried out to generate the model describing the dynamics of EV internalization, target cells were seeded in several wells of 12-well plates, with 3 wells representing a single condition. Therefore, to produce different conditions at different time points, multiple wells were provided. At the end of the treatment, to perform the measurement of EV-derived fluorescence by the imaging flow cytometry, the cells were detached from the well, washed of their medium to eliminate both cellular debris and residual EVs, and then resuspended in a specific buffer to be finally analyzed at single cell level. All passages are repeated for every time point. As expected, this kind of experiments is, in general, very expensive (in particular in terms of EV production, other than for instruments' costs) and time-consuming, and it is hardly affordable to repeat them for a dense set of time points. For these reasons, a good design of the experiments, based on the estimation of the expected results, is crucial to avoid waste of resources.

To this purpose, several models of EV uptake are present in literature [11]. However, diverse pathways are used by cells to uptake the vesicles. Indeed, after reaching the target cell, EVs can be internalized via receptor-mediated endocytosis or lipid RAFTs [8], spontaneous and protein-mediated fusion [21], phagocytosis [7], macropinocytosis [17] or can signal to target cells with a juxtacrine mechanism [19]. The uptake models developed so far are specific of some particular mechanisms and would be useful on the design of selective uptake experiments. Unfortunately, considering that the internalization mechanisms are used by cells, not only for the EV uptake, but also for internalization of other molecules and for the physiological recycle of membranes, the inhibition or selection of specific uptake pathways may be toxic for the cells and the development of efficient pharmacological treatments is challenging.

With this in mind, in this paper we introduce an analytical model of a generic uptake process of EVs by a target cell. However, the model parameters, which correspond to the rate of chemical reactions involved in the absorption process, are not known. For this reason, based on laboratory data, an estimation of the unknown parameters is performed and used to design future experiments so reducing costs and time. More specifically, the model solutions describing the evolution of the process are compared with experimental data collected *in vitro* from a neuroblastoma cell line (SH-SY5Y) treated with EVs isolated from primary murine astrocytes (AS). From these experiments the values of the parameters associated with the uptake of EVs by SH-SY5Y are deduced. Then, the use of the model as a tool for the design of new biological experiments is assessed by comparing the EV internalization forecasted by the model with experimental data obtained in the same conditions.

The paper is organized as follows. The Section 2 gives an overview on the uptake of EVs from a target cell. In Section 3 the analytical model of a generic uptake process is derived. Section 4 describes the biological experiments that have been conducted. In Section 5 the comparison between collected data and model solutions provides values to the model parameters. Additionally, a model application example is provided. Finally, Section 6 draws some conclusions.

## 2 OVERVIEW OF EV UPTAKE

EVs are nanometric spherical particles, coated with a lipid membrane, enriched with transmembrane proteins that allow their recognition by recipient cells [4]. Once generated and released by donor cells, EVs meet different fates. Some EVs may undertake a long-term navigation in the extracellular fluids. Another fraction of EVs release their cargo in the extracellular space as the result of the dissolution of their membrane [21]. Other EVs remain local and establish various types of interaction with so-called target cells.

Interactions between EVs and target cells are based mainly on protein interactions (receptors, tetraspanins, integrins, clathrine, caveoline, etc.) [16], that mediate both a juxtacrine signaling or the EV internalization. The latter involves mechanisms classified in: i) endocytosis (both clathrin dependent, independent, and lipid-raft mediated) [15], ii) macropinocytosis [5], iii) phagocytosis [6], and iv) membrane fusion [21].

More in detail, endocytosis, macropinocytosis, phagocytosis and lipid-raft have a similar events evolution distinguished by the types of proteins involved and the response of the target cell membrane that causes the EV internalization. The process is sprung from a

high affinity binding of one or two pairs of surface proteins (one protruding from the EVs and the other from the plasma membrane of the target cell). This binding allows activation of cascading reactions, which bend, distort or prolong the membrane of the target cell. Due to that, EV is totally enveloped and internalized in the endosome, where it can then meet different fates [14].

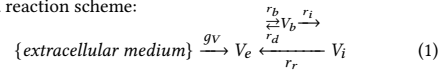
Juxtacrine signaling is a different strategy in which target cell is able to process information bound to the EV. The principal difference between endocytosis and juxtacrine way is that EVs bind with high affinity to the surface of the cell, to trigger a specific molecular process [19]. This strategy is not included into our model, since in the experimental data we have not an accumulation of EVs on the surface of the target cell, but only within the cell over time.

Finally, fusion is a well-known natural phenomenon taking place when two separated membrane portions come close and melt into each other. It seems to be activated by specific fusogenic proteins [18]. In general, phospholipidic membranes have a positive charge on the external surface, so spontaneous fusion is rare in nature. Thanks to the presence of two couples of fusogenic proteins, one on the surface of the EV and the other on the membrane of the target cell, depending on the values of pH and temperature, it is possible to force the charge pushback until the fusion between both membranes with release of the EV cargo within the cytoplasm [21].

The identity of the proteins involved in all of those processes are only partially known (caveolines, clathrins, receptors), while several proteins and mechanisms are still under investigation. For this reason, among others, the development of efficient pharmacological treatments for long-term inhibition or selection of specific uptake pathways in *in vitro* experiments, is not easy to be practically achievable, since also the uptake of other molecules would be inhibited with consequent side effects for the viability of the cells. Therefore, the experimental measures of the EV internalization rate in target cells, that, at the time, is possible to collect, do not discriminate among the possible uptake mechanisms.

## 3 UPTAKE MODEL

In this work we focus on a generic EV uptake process, which develops on two phases: *i*) the EVs in the extracellular medium are supposed to bind with some generic receptors, *ii*) they are internalized by the target cell. Let  $V_e$  indicate the number of available EVs in the extracellular space close to the plasma membrane of the target cell, and let  $V_b$  and  $V_i$  indicate the bound and internalized EVs, respectively. The dynamics of the binding and internalization processes are assumed to be regulated by the binding and internalization rate constants, denoted as  $r_b$  and  $r_i$ , respectively. Note that, a fraction of the EV-cell bonds may disassociate before the internalization is activated and the involved EVs come back to the extracellular medium. To take into account this occurrence, the bond disassociation rate constant  $r_d$  has been introduced. The evolution of the EV uptake can be summarized by the following simplified reaction scheme:



where  $g_V$  is the supply rate of EVs, i.e. the number of EV supplied to the cell by external sources in the time unit, and  $r_r$  indicates the recycling rate constant, i.e. the rate at which the target cell may recycle or release a fraction of the internalized EVs.

In order to model the evolution of the EV uptake process, we first focus on the time-dependent number of the available, bound and internalized EVs,  $V_e(t)$ ,  $V_b(t)$  and  $V_i(t)$ , respectively, and consider the events that affect their temporal variation. In particular, let us note that the binding of an EV to the target cell produces a decrease in the number of available EVs,  $V_e(t)$ , and a corresponding increase in the number of bound ones,  $V_b(t)$ . Similarly, the internalization of a bound EV, at the rate  $r_i$ , accounts for a negative contribution in the temporal variation of the bound EVs,  $V_b(t)$ , and a positive contribution to the temporal variation of the internalized ones,  $V_i(t)$ . Besides the binding and internalization events, also the recycling processes of EVs, as well as the possibility that a fraction of the EV-cell bonds disassociates before the fusion process is activated, affect the EV amount in the three considered states. More specifically, both events produce, at the rate  $r_r$  and  $r_i$ , respectively, an increase of the number of available EVs,  $V_e(t)$ , and a decrease of the internalized and bound ones,  $V_i(t)$  and  $V_b(t)$ , respectively. All the above considerations lead to the following equations:

$$\begin{cases} \frac{dV_e(t)}{dt} = -r_b V_e(t) + r_d V_b(t) + r_r V_i(t) + g_V(t) \\ \frac{dV_b(t)}{dt} = r_b V_e(t) - (r_d + r_i) V_b(t) \\ \frac{dV_i(t)}{dt} = r_i V_b(t) - r_r V_i(t) \end{cases} \quad (2)$$

Note that the number of EVs in the extracellular medium may not be spatially uniform. However, the fluid dynamics of EVs delivery to the cell surface [22] is out the scope of this work, since we are here interested on the dynamics of binding and internalization of the EVs to the plasma membrane. For this reason, we assume that there is a layer of fluid close to the plasma membrane of the target cell, where the number of the EVs can be considered spatially uniform and we define  $V_e$  as the number of EVs in this portion of extracellular fluid. Therefore, we can consider here the sole dependence of  $V_e$  from time. The number of EVs, close to the plasma membrane of the target cell, is supplied to the system from an external source at the delivery rate  $g_V(t)$ , which in general is a function of time.

### 3.1 Model solution

The set of ordinary differential equations (2) constitutes the model of the binding and internalization process of EVs by a target cell. In this section we provide the solution of this system, which is linear and solvable with standard methods.

As usual, we need to find three linearly independent solution of the homogeneous system associated to (2), i.e. for  $g_V(t) = 0$ . So let us look for solutions in the form:

$$\mathbf{V} = e^{\lambda t} \mathbf{v} \quad (3)$$

where  $\lambda$  and  $\mathbf{v}$  are the eigenvalues and eigenvectors, respectively, of the coefficient matrix  $\mathbf{A}$  of (2), and  $\mathbf{V}$  is the vectorial notation for the number of external, bound and internalized EVs, i.e.:

$$\mathbf{V} = \begin{bmatrix} V_e \\ V_b \\ V_i \end{bmatrix} \quad \mathbf{A} = \begin{bmatrix} -r_b & r_d & r_r \\ r_b & -(r_d + r_i) & 0 \\ 0 & r_i & -r_r \end{bmatrix} \quad (4)$$

As known, the eigenvalues  $\lambda$  are the roots of the characteristic equation of the matrix  $\mathbf{A}$ , i.e.  $|\mathbf{A} - \lambda \mathbf{I}| = 0$  (where  $|\cdot|$ , when applied to a matrix, denotes its determinant, and  $\mathbf{I}$  is the identity matrix), which is easy to verify that can be written as follows:

$$\lambda \left( \lambda^2 + (r_b + r_i + r_d + r_r) \lambda + r_r (r_d + r_i) + r_b (r_r + r_i) \right) = 0 \quad (5)$$

The roots of (5) are:

$$\begin{aligned} \lambda_1 &= 0 \\ \lambda_{2,3} &= -\frac{1}{2} (r_b + r_i + r_d + r_r) \pm \frac{1}{2} \sqrt{\Delta} \end{aligned} \quad (6)$$

where

$$\Delta = (r_b + r_i + r_d + r_r)^2 - 4 (r_r (r_d + r_i) + r_b (r_r + r_i)) \quad (7)$$

The eigenvector  $\mathbf{v}_i$  associated to the  $i$ -th eigenvalue  $\lambda_i$  must satisfy the following equation:

$$\mathbf{A} \mathbf{v}_i = \lambda_i \mathbf{v}_i \quad (8)$$

However, when  $\Delta = 0$ , the characteristic equation (5) presents a double root, i.e.  $\lambda_2 = \lambda_3$ , which means the eigenvalue is incomplete or defective, and a third linearly independent solution can be found in the form:

$$\mathbf{V} = e^{\lambda_2 t} (t \mathbf{v}_2 + \mathbf{v}_3) \quad (9)$$

where  $\mathbf{v}_2$  is found from (8), and  $\mathbf{v}_3$  is found from:

$$(\mathbf{A} - \lambda_2 \mathbf{I}) \mathbf{v}_3 = \mathbf{v}_2 \quad (10)$$

After some calculation, the eigenvectors associated to the eigenvalues in (6) are:

$$\begin{aligned} \mathbf{v}_1 &= \begin{bmatrix} r_r (r_d + r_i) \\ r_b r_r \\ r_i r_b \end{bmatrix} \quad \mathbf{v}_2 = \begin{bmatrix} (\lambda_2 + r_r) (\lambda_2 + r_d + r_i) \\ r_b (\lambda_2 + r_r) \\ r_i r_b \end{bmatrix} \\ \mathbf{v}_3 &= \begin{cases} \begin{bmatrix} (\lambda_3 + r_r) (\lambda_3 + r_d + r_i) \\ r_b (\lambda_3 + r_r) \\ r_i r_b \end{bmatrix} & \text{if } \Delta \neq 0 \\ \begin{bmatrix} 2\lambda_2 + r_d + r_i + r_r \\ r_b \\ 0 \end{bmatrix} & \text{if } \Delta = 0 \end{cases} \end{aligned} \quad (11)$$

The general solution of the system (2) is the linear combination of the solution (3) and (9) with the eigenvalues and eigenvectors found so far, and can be summarized, according to the sign of  $\Delta$ , as follows:

$$\mathbf{V} = \begin{cases} k_1 \mathbf{v}_1 + k_2 e^{\lambda_2 t} \mathbf{v}_2 + k_3 e^{\lambda_3 t} \mathbf{v}_3 & \text{if } \Delta > 0 \\ k_1 \mathbf{v}_1 + e^{\lambda_2 t} (k_2 \mathbf{v}_2 + k_3 \mathbf{v}_3 + k_3 \mathbf{v}_2 t) & \text{if } \Delta = 0 \\ k_1 \mathbf{v}_1 + e^{\mathcal{R}[\lambda_2] t} (\cos(\mathcal{I}[\lambda_2] t) (k_2 \mathcal{R}[\mathbf{v}_2] + k_3 \mathcal{I}[\mathbf{v}_2]) + \sin(\mathcal{I}[\lambda_2] t) (k_2 \mathcal{I}[\mathbf{v}_2] + k_3 \mathcal{R}[\mathbf{v}_2])) & \text{if } \Delta < 0 \end{cases} \quad (12)$$

where  $\mathcal{R}[\cdot]$  and  $\mathcal{I}[\cdot]$  indicate real and imaginary part of a complex number, respectively, and  $k_1$ ,  $k_2$ , and  $k_3$  are constants to be found according to the initial conditions.

Note that the solution found so far is the solution of the homogeneous system associated to (2). To find the complete solution of the system, the term  $g_V(t)$  has to be considered. However, the model solution will be compared with experimental results obtained in the case  $g_V(t) = 0$ ,  $\forall t$ . For this reason, the computation of the general solution of (2), with  $g_V(t) \neq 0$ , is out the scope of this work.

## 4 EXPERIMENTAL CASE STUDY

In this section, we describe the biological experiments for the measurement of the EV uptake evolution.

The methods of isolation, characterization and staining of the EVs, and the detailed description of the cellular treatments can be found in [10]. Briefly, EVs were isolated from primary murine astrocytes (AS) taken from wild-type newborn mice (C57BL/6, P2-P4)[10]. After maturation, AS were maintained in culture for further 24 hours and, subsequently, the EVs were isolated via differential ultracentrifugation [10]. The number of EVs obtained were  $2.73 \cdot 10^9$  per

million of AS (the donor cells), as measured by Nanoparticle Tracking Analysis [10]. EVs were labelled with the very stable (about 100 days) CellVue Claret Fluorescent Cell Linker Dye (Merck), using the protocol described in [10]. This dye is excited by a laser at a wavelength of 655 nm and emits at a wavelength of 675 nm corresponding to the far-red spectrum [2].

The target cells are SH-SY5Y, a human neuroblastoma cell line differentiated into dopaminergic-like neurons with retinoic acid and serum deprivation [10]. SH-SY5Y cells were seeded in a 12 well plate, in an amount of  $1 \cdot 10^6$  cells per well. 24 hours after seeding, target cells were treated with EVs using two ratios 5:1 and 0.5:1, that correspond to the EVs produced by 5 or 0.5 donor AS, respectively, and given to 1 target cell. In total,  $1.37 \cdot 10^{10}$  EVs were used for the 5:1 ratio, while for the 0.5:1 ratio  $1.37 \cdot 10^9$  EVs. In the following we refer to this two experiment conditions as *Exp1* and *Exp2* for the ratio 5:1 and 0.5:1, respectively. The time of EV treatment represent the time  $t_0$ . Then cells were left with EVs for 6, 24, 48 and 72h, to evaluate EV uptake over time. Target cells at each time points were detached by trypsinization, washed of their medium and cellular debris, and resuspended in 1 mm EDTA + 1% BSA [10].

The EV uptake by the target cells was detected with the imaging flow cytometer (IFC, Amnis FlowSight), using the IDEAS [13] software [1]. This approach allows to evaluate the amount of EV internalization at single cell level. The first 2000 single cells, in order of acquisition, were analyzed, and the data were expressed in terms of mean fluorescence intensity. In order to convert such a measure to number of internalized EVs, the fluorescence of a single EVs should be known. However, the Amnis FlowSight magnification does not allow the detection of single EV fluorescence, neither within the cells, nor as a sample to be directly measured by the instrument before the treatment on target cells. Therefore, a parallel set of experiments was carried out seeding cells in 96-well plates, in an amount of 85.000 cells per well. The treatment with EVs was performed following the same strategy as for the IFC analysis ( $1.16 \cdot 10^9$  EVs for the 5:1 ratio, and  $1.16 \cdot 10^8$  EVs for the 0.5:1 ratio). The EV-derived fluorescence was measured by using a plate reader (PR, Varioskan, Thermo Fisher Scientific), with use of SkanIt<sup>TM</sup> software [3]. To derive the fluorescence of the single EVs, the same amount of labelled vesicles has been measured with the PR in the 96-well plate, in the absence of cells. Note that the amount of EVs and cells in the 96 well plate differs from the ones in the 12 well plate (although a normalization per area/well has been used) for the analysis through the flow cytometer, while the ratio between EVs and cells is kept constant. Notably, the exclusive use of PR for the measurement of EV derived fluorescence in target cells is not possible since this instrument does not allow the analysis at single cell level. On the contrary, only the fluorescence of the whole well (including both cells and the medium) can be measured. For this reason, we used two different strategies to obtain the required unknown variables. Indeed, the measurements obtained through IFC and PR have been compared, and the fluorescence of a single EV (in the unit of measurement of the IFC) has been deduced through a simple proportion, in the assumption of linearity, as follows:

$$F(EV)_{IFC} = \frac{F(EV)_{PR} \cdot F(Cell+EVs)_{IFC}}{F(Cell+EVs)_{PR}} \quad (13)$$

where  $F(EV)_{IFC}$  and  $F(EV)_{PR}$  indicate the fluorescence intensity of a single EV for flow cytometer and plate reader, respectively, and

$F(Cell + EVs)_{IFC}$  and  $F(Cell + EVs)_{PR}$  indicate the fluorescence intensity of a single cell after EVs internalization for flow cytometer and plate reader, respectively.

By applying the results of (13) to the flow cytometer results, we obtain the temporal evolution, shown in Fig. 1b, of the number of EVs internalized by the target cells for two different initial conditions (namely the initial number of EVs the cells are treated with), above referred to as *Exp1* and *Exp2*. The initial number of EVs per cell, in the following indicated as  $V_0$ , has been calculated according to the percentage of cells detected as positive by the imaging flow cytometer (i.e. the cells that present a non negligible level of internalization). The values obtained are  $V_0 = \{16000, 3400\}$ , for the case *Exp1* and *Exp2*, respectively.

## 5 MODEL APPLICATION

In Section 3 we have derived an analytical model describing the uptake process of EVs from a target cell. In this model, the variables are the EV in different phases of the process, and the coefficients are the parameters regulating the processes, i.e. the rates of the chemical reactions involved in EV binding and internalization, as well as in the disassociation/recycling process of the EVs. However, as already said, poor information is available in literature about those parameters. On the contrary, through the biological experiments, as described in Section 4, the concentration of the external, bound and internalized EVs, i.e. the model variables  $V_e(t)$ ,  $V_b(t)$  and  $V_i(t)$ , can be measured over the time. Then, a change of perspective can be applied to the model, so that the  $V$ s are no more unknown variables, and instead the model parameters, are the unknowns in the equations (2). Therefore, we will exploit the model to infer, through a mathematical inverse process, the values for the model parameters that apply to the case under study, i.e. the administration of EVs from murine astrocytes to the target cells SH-SY5Y.

With this in mind, in this section we will first consider, in Section 5.1, which model assumption are needed, to make the model representative of the experimental conditions. Then in Section 5.2, we will compare the analytical solution of the model with experimental results, to infer the model parameter that apply for the case under study. Finally, in Section 5.3 we will use the model with the parameter values found in Section 5.2, to provide a forecasting of the results of a second experiment, and to demonstrate that the model could also be used for the design of new experiment, based on desired results.

### 5.1 From the model to lab experiments

In this section, we will consider the model assumptions that makes the model representative of the experiments described in Section 4.

Let us first focus on the initial condition of the experiment. In particular, let us note that the labelled EVs are placed all at once in the well at the beginning of the experiment, while the cells have not yet either bound or internalized EVs. In terms of the variables of the model, this means that at the initial time  $t_0 = 0$ , we can write:

$$V_e(0) = V_0, \quad V_b(0) = 0, \quad V_i(0) = 0 \quad (14)$$

where  $V_0$  indicates the initial amount of EVs per cell.

Moreover, no additional EVs are supplied during the duration of the experiment to the system under study. Therefore we can consider:

$$g_V(t) = 0 \quad \forall t \quad (15)$$



According to (14), the constants  $k_1$ ,  $k_2$  and  $k_3$  in (12), can now be calculated. Note, that we do not know yet which case we need to consider, according to the sign of  $\Delta$ . Nevertheless, as shown in Fig. 1b, the measurements of  $V_i$  do not show oscillating behaviour, which allows us to exclude, in our study, the case of  $\Delta < 0$ . Moreover, the case  $\Delta = 0$  is a singular case, for which the parameters need to be fine-tuned, and this occurrence can be reasonably considered unlikely in real-world experiments and meaningless from the biological/physical point of view. Therefore, in the following, if not otherwise specified, we will consider only the case  $\Delta > 0$ .

From (12), together with (11) and (14), we obtain the following expressions for the constants  $k_1$ ,  $k_2$  and  $k_3$ :

$$k_1 = \frac{V_0}{\lambda_2 \lambda_3}, \quad k_2 = \frac{V_0}{\lambda_2 (\lambda_2 - \lambda_3)}, \quad k_3 = \frac{V_0}{\lambda_3 (\lambda_3 - \lambda_2)} \quad (16)$$

By replacing (16), in (12), we obtain the general solution of the model for the experiments described in Section 4.

## 5.2 Model parameter inference

In this section, we will exploit the model to infer, through a mathematical inverse process, the values for the model parameters that apply to the case under study, i.e. the administration of EVs from murine astrocytes to the target cells SH-SY5Y.

To this purpose, let us consider the measurement of  $V_i$  from the experiment denoted as *Exp2* in Section 4, and let us look for the best fitting of this curve. According to (12), the best fitting function has to be in the following form:

$$V_i = a + b e^{\lambda_2 t} + c e^{\lambda_3 t} \quad (17)$$

with:

$$a = k_1 v_{31}, \quad b = k_2 v_{32}, \quad c = k_3 v_{33} \quad (18)$$

where  $v_{ij}$  indicates the  $i$ -th component of the vector  $\mathbf{v}_j$  of (11). It is easy to verify that from (11), together with (16), the following constraints between the coefficients  $a$ ,  $b$ , and  $c$  of (17) hold:

$$b = a \frac{\lambda_3}{\lambda_2 - \lambda_3}, \quad c = a \frac{\lambda_2}{\lambda_3 - \lambda_2} \quad (19)$$

Therefore, according to the coefficient constraints in (19), the best fitting function for  $V_i$  has to be in the form:

$$V_i = a \left( 1 + \frac{\lambda_3}{\lambda_2 - \lambda_3} e^{\lambda_2 t} + \frac{\lambda_2}{\lambda_3 - \lambda_2} e^{\lambda_3 t} \right) \quad (20)$$

where  $a$ ,  $\lambda_2$  and  $\lambda_3$  are to be determined by the fitting. Let us indicate as  $a_f$ ,  $\lambda_{f2}$  and  $\lambda_{f3}$ , the values obtained in this way. By replacing the above values in (18), and combining them with (6), (7), (11) and (16), we obtain the following system of equations:

$$\begin{cases} V_0 \frac{r_b r_i}{\lambda_{f2} \lambda_{f3}} = a_f \\ \sqrt{\Delta} = |\lambda_{f3} - \lambda_{f2}| \\ -\frac{1}{2} (r_b + r_i + r_d + r_r) = \frac{1}{2} (\lambda_{f2} + \lambda_{f3}) \end{cases} \quad (21)$$

where  $|\cdot|$ , when applied to a number, denotes its absolute value.

Let us recall that the unknowns in this problem are the model parameters  $r_b$ ,  $r_d$ ,  $r_i$ , and  $r_r$ , that regulates the internalization process. Therefore, we need to solve a system of four independent equations in those unknowns. The system (21), provides three of the four needed equations. The last equation is obtained considering the measurement of the number of EVs in the extracellular medium at a given time-point. In terms of the variables of the model, the measurement of the EVs in the extracellular medium correspond to the variable  $V_e$ . By equating the measured value of  $V_e(t_p)$ , at

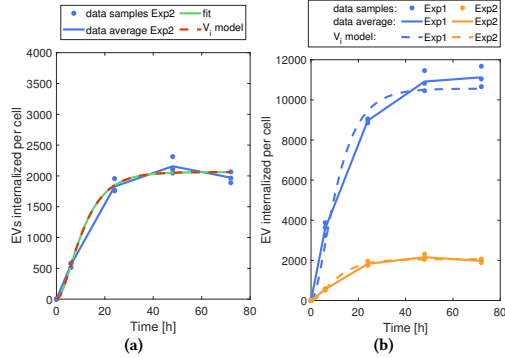


**Figure 1: (a) Comparison between the experimental data, curve fitting and model solution, for the case *Exp2* - (b) Comparison between the experimental data and the EVs internalization forecasted by the model**

the time point indicated here as  $t_p$ , to the analytical expression obtained from (12), together with (16), and solving the obtained equation together with (21), after some mathematical manipulation, we obtain the following formulas for the computation of the model parameters:

$$\begin{cases} P = \frac{a_f \lambda_{f2} \lambda_{f3}}{V_0} \\ r_r = -\frac{1}{2} (\lambda_{f2} + \lambda_{f3}) \pm \frac{1}{2} \sqrt{4P + (\lambda_{f2} - \lambda_{f3})^2} \\ S = \frac{V_e(t_p) - k_2 \lambda_{f2} (\lambda_{f2} + r_r) e^{\lambda_{f2} t_p} - k_3 \lambda_{f3} (\lambda_{f3} + r_r) e^{\lambda_{f3} t_p}}{k_1 r_r - k_2 (\lambda_{f2} + r_r) e^{\lambda_{f2} t_p} - k_3 (\lambda_{f3} + r_r) e^{\lambda_{f3} t_p}} \\ r_b = -(\lambda_{f2} + \lambda_{f3} + r_r + S) \\ r_i = \frac{P}{r_b} \\ r_d = S - r_i \end{cases} \quad (22)$$

where, for the sake of simplicity, we have introduced the quantities  $P$ , and  $S$ , defined as:

$$P = r_b r_i, \quad S = r_d + r_i \quad (23)$$

In Fig. 1a, the measurement of  $V_i$  from the experiment *Exp2* in Section 4 is shown together with the best fitting functions in the form of (20). The corresponding values of  $a_f$ ,  $\lambda_{f2}$ , and  $\lambda_{f3}$  are resumed in Table 1a. The fit has been performed with the curve-fitting toolbox in the statistical analysis package of Matlab (MathWorks), with the nonlinear least squares method, by using the default algorithm "Trust Region". The starting points have been empirically found to help the fit to be found.

According to the values in Table 1a, together with the measured value of the EVs in the extracellular medium for the experiment *Exp2*, which is  $V_e(t_p) = 1.3534 \cdot 10^3$ , for  $t_p = 6$ h, we proceed to calculate the model parameters from (22). Note that, as it is easy to verify, the expression of  $r_r$  in (22) comes from a second order equation, which provides in general two solutions. Accordingly, two theoretically possible combinations of parameters are found. Nevertheless, negative values of the model parameters do not have physical meaning. For this reason, if some negative theoretical value is found, the corresponding combination of parameters is discarded. With all this in mind, the computation of the parameter according to (22), for the values in Table 1a, provides one feasible combination of parameter values, which are provided in Table 1b.

**Table 1: (a) Parameters for the best fitting curve in Fig. 1a - (b) Model parameter values according to (22)**

(a)		(b)	
Name	Value	Name	Value
$a_f$	$2.0624 \cdot 10^3$	$r_b$	$1.68335 \cdot 10^{-1}$
$\lambda_{f2}$	$-2.395 \cdot 10^{-1}$	$r_d$	$4.8915 \cdot 10^{-2}$
$\lambda_{f3}$	$-1.228 \cdot 10^{-1}$	$r_i$	$1.14475 \cdot 10^{-1}$
		$r_r$	$3.0550 \cdot 10^{-2}$

The analytical solution, obtained according to (12), by replacing the values from Table 1b, is drawn in Fig. 1a. As expected, the figure shows that the analytical solution of the model describes with good approximation the experimental data.

### 5.3 Forecasting and Design

In this section we will exploit the model with the parameter values found in Section 5.2, to forecast the results of another experiment session. In particular, let us consider the case study, denoted as *Exp1* in Section 4, where the amount of initial EVs changes with respect to the experiment *Exp2*, used to infer the model parameters. Let us consider the solution of the model according to the new initial conditions. Fig. 1b shows the comparison between the experimental results and the model solutions. As we can see the model solution is close to the experimental results.

To show the potentiality of the model let us consider an example. Let us suppose we would like to know the initial amount  $V_0$  of EVs to provide at the time instant  $t_0 = 0$ , such that, at the time instant  $t^*$ , the amount of EVs inside the cell is  $V^*$ . In terms of the model variables, this condition can be written as:

$$V_i(t^*) = V^* \quad (24)$$

where the expression of  $V_i$  is given by the third component of (12). The change of  $V_0$  affects the values of the coefficients  $k_1$ ,  $k_2$ , and  $k_3$ , that have to be calculated again. Although this time  $V_0$  is the unknown, the initial condition is again expressed by (14). Therefore,  $k_1$ ,  $k_2$ , and  $k_3$  can be calculated through (16), as function of  $V_0$ .

For this example, let us choose  $t^* = 48h$  e let us suppose the desired number of EVs internalized by the target cell be the corresponding value in the *Exp1* series of data, i.e.  $V^* = 1.9 \cdot 10^4$ . By replacing these values in (24), together with the expression from (12), and (11) and solving the equation in  $V_0$ , we find that the initial number of EVs to be administered to the target cell is  $V_0 = 1.6745 \cdot 10^4$ , which in fact corresponds with good approximation to the initial number of  $1.6 \cdot 10^4$  EVs considered for the experiment *Exp1*.

## 6 CONCLUSIONS AND FUTURE WORKS

In this paper we have presented the analytical model of a generic EV uptake mechanisms from target cells, with the aim of providing an efficient tool for the design of biological experiments, which are often expensive and time consuming. However, since the biological parameter regulating the chemical reaction involved in the uptake process are not known, a comparison between experimental results and model solutions has been carried out, to infer characteristic values of those parameters. After that the model has been used to forecast the results of a second experiment session, showing how can be used for the design of new biological experiment, according to some desired results.

## REFERENCES

- [1] [n. d.]. Amnis Merck KGaA, Darmstadt. *FlowSight User's Manual* ([n. d.]).
- [2] [n. d.]. PBS Dulbecco's. *PKH26 Red Fluorescent Cell Linker Kit for General Cell Membrane Labeling* ([n. d.]).
- [3] [n. d.]. Scientific ThermoFisher. *Varioskan LUX multimode microplate reader* ([n. d.]).
- [4] Samir El Andaloussi, Imre Mäger, Xandra O Breakefield, and Matthew JA Wood. 2013. Extracellular vesicles: biology and emerging therapeutic opportunities. *Nature reviews Drug discovery* 12, 5 (2013), 347–357.
- [5] Cristina Escrivente, Sascha Keller, Peter Altevogt, and Julia Costa. 2011. Interaction and uptake of exosomes by ovarian cancer cells. *BMC cancer* 11 (2011), 1–10.
- [6] Du Feng, Wen-Long Zhao, Yun-Ying Ye, Xiao-Chen Bai, Rui-Qin Liu, Lei-Fu Chang, Qiang Zhou, and Sen-Fang Sui. 2010. Cellular internalization of exosomes occurs through phagocytosis. *Traffic* 11, 5 (2010), 675–687.
- [7] Kinsley C French, Marc A Antonyak, and Richard A Cerione. 2017. Extracellular vesicle docking at the cellular port: Extracellular vesicle binding and uptake. In *Seminars in cell & developmental biology*, Vol. 67. Elsevier, 48–55.
- [8] Bhagyashree S Joshi, Marit A de Beer, Ben NG Giepmans, and Inge S Zuhorn. 2020. Endocytosis of extracellular vesicles and release of their cargo from endosomes. *ACS nano* 14, 4 (2020), 4444–4455.
- [9] Brian J Jurgielewicz, Yao Yao, and Steven L Stice. 2020. Kinetics and specificity of HEK293T extracellular vesicle uptake using imaging flow cytometry. *Nanoscale research letters* 15 (2020), 1–11.
- [10] Loredana Leggio, Francesca L'Episcopo, Andrea Magri, María José Ulloa-Navas, Greta Paternò, Silvia Vivarelli, Carlos AP Bastos, Cataldo Tirolo, Nunzio Testa, Salvatore Caniglia, et al. [n. d.]. Small Extracellular Vesicles Secreted by Nigrostriatal Astrocytes Rescue Cell Death and Preserve Mitochondrial Function in Parkinson's Disease. *Advanced Healthcare Materials* ([n. d.]), 2201203.
- [11] Alfio Lombardo, Giacomo Morabito, Carla Panarello, and Fabrizio Pappalardo. 2022. Modeling Biological Receivers: The Case of Extracellular Vesicle Fusion to the Plasma Membrane of the Target Cell. In *Proceedings of the 9th ACM International Conference on Nanoscale Computing and Communication* (Barcelona, Catalunya, Spain) (NANOCOM '22). Association for Computing Machinery, New York, NY, USA, Article 9, 6 pages. <https://doi.org/10.1145/3558583.3558847>
- [12] L Loredanda, Gd Arrabito, V Ferrara, V Silvia, P Greta, M Bianca, Bg Pignataro, I Nunzio, et al. 2020. Mastering the Tools: Natural versus Artificial Vesicles in Nanomedicine. *ADVANCED HEALTHCARE MATERIALS* (2020).
- [13] Luminex. [n. d.]. IDEAS® Image Data Exploration and Analysis Software User's Manual. ([n. d.]).
- [14] Kelly J McKelvey, Katie L Powell, Anthony W Ashton, Jonathan M Morris, and Sharon A McCracken. 2015. Exosomes: mechanisms of uptake. *Journal of circulating biomarkers* 4 (2015), 7.
- [15] Angela Montecalvo, Adriana T Larregina, William J Shufesky, Donna Beer Stolz, Mara LG Sullivan, Jenny M Karlsson, Catherine J Baty, Gregory A Gibson, Geza Erdos, Zhiliang Wang, et al. 2012. Mechanism of transfer of functional microRNAs between mouse dendritic cells via exosomes. *Blood, The Journal of the American Society of Hematology* 119, 3 (2012), 756–766.
- [16] Laura Ann Mulcahy, Ryan Charles Pink, and David Raul Francisco Carter. 2014. Routes and mechanisms of extracellular vesicle uptake. *Journal of extracellular vesicles* 3, 1 (2014), 24641.
- [17] Kosuke Noguchi, Momoko Obuki, Haruka Sumi, Merlin Klussmann, Kenta Morimoto, Shinya Nakai, Takuya Hashimoto, Daisuke Fujiwara, Ikuo Fujii, Eiji Yuba, et al. 2021. Macropinocytosis-inducible extracellular vesicles modified with antimicrobial protein CAP18-derived cell-penetrating peptides for efficient intracellular delivery. *Molecular Pharmaceutics* 18, 9 (2021), 3290–3301.
- [18] Ashley E Russell, Alexandra Sneider, Kenneth W Witwer, Paolo Bergese, Suendra N Bhattacharyya, Alexander Cocks, Emanuele Cocucci, Uta Erdbrügger, Juan M Falcon-Perez, et al. 2019. Biological membranes in EV biogenesis, stability, uptake, and cargo transfer: an ISEV position paper arising from the ISEV membranes and EVs workshop. *Journal of Extracellular Vesicles* 8, 1 (2019), 1684862.
- [19] Saray Tabak, Sofia Schreiber-Avissar, and Elie Beit-Yannai. 2021. Influence of anti-glaucoma drugs on uptake of extracellular vesicles by trabecular meshwork cells. *International Journal of Nanomedicine* 16 (2021), 1067.
- [20] Guillaume van Niel, David RF Carter, Aled Clayton, Daniel W Lambert, Graça Raposo, and Pieter Vader. 2022. Challenges and directions in studying cell–cell communication by extracellular vesicles. *Nature Reviews Molecular Cell Biology* 23, 5 (2022), 369–382.
- [21] Amandine Vargas, Shufeng Zhou, Maude Éthier-Chiasson, Denis Flipo, Julie Lafond, Caroline Gilbert, and Benoit Barbeau. 2014. Syncytin proteins incorporated in placenta exosomes are important for cell uptake and show variation in abundance in serum exosomes from patients with preeclampsia. *The FASEB Journal* 28, 8 (2014), 3703–3719.
- [22] Mladen Veletić, Michael Taynann Barros, Ilangko Balasingham, and Sasitharan Balasubramanian. 2019. A molecular communication model of exosome-mediated brain drug delivery. In *Proceedings of the Sixth Annual ACM International Conference on Nanoscale Computing and Communication*. 1–7.

## 7. List of publications

Scopus ID: 57218667149

Web of Science ID: ITU-7834-2023

ORCID ID: 0000-0002-5568-8872

Citations: 123

H-Index: 6

- Leggio L.\*, **Paternò G.**\*, Cavallaro F., Vivarelli S., Manna C., Calogero A.E., Cannarella R., Iraci N. “*Sperm epigenetics and sperm RNAs as drivers of male infertility: truth or myth?*”. Status: Accepted. \* These authors contributed equally
- Pittalà M.G.G., Leggio L., **Paternò G.**, Cunsolo V., Vivarelli S., Di Francesco A., Alpi E., Iraci N., Saletti R. “*SPROUTS\_DB: an Implemented Database of Contaminants for Proteomic Studies of Extracellular Vesicles*”. Status: Under review.
- Leggio L., **Paternò G.**, Vivarelli S., Bonasera A., Pignataro B., Iraci N., Arrabito G. “*Label-free approaches for extracellular vesicles detection*”. iScience. September 30, 2023 (IF: 5.8; PMID: 37867957).
- Iraci, N., Leggio, L., Lombardo, A., Panarello, C., Pappalardo, F., **Paternò, G.** “*An Analytical Model for the Inference of the EV Reception Process Parameters in Cell-to-Cell Communication*”. In Proceedings of ACM Conference (Conference’17), 2023. <https://doi.org/10.1145/3576781.3608716>
- Leggio L., L’Episcopo F., Magrì A., Ulloa-Navas M., **Paternò G.**, Vivarelli S., Bastos C., Tirolo C., Testa N., Caniglia S., Risiglione P., Pappalardo F., Serra A., García-Tárraga P., Faria N., Powell J.J., Peruzzotti-Jametti L., Pluchino S., Garcia-Verdugo J.M., Messina A., Marchetti B., Iraci N. “*Small Extracellular Vesicles Secreted by Nigrostriatal Astrocytes Rescue Cell Death and Preserve Mitochondrial Function in Parkinson’s Disease*”. Adv. Healthcare Mater. 2022 Jul 20 (IF: 10.00; PMID: 35856921).
- Leggio L., **Paternò G.**, Vivarelli S., Falzone G.G., Giachino C., Marchetti B., Iraci N. “*Extracellular Vesicles as novel diagnostic and prognostic biomarkers for Parkinson’s Disease*”. Aging Dis. 2021 Sep 1 (IF: 7.4; PMID: 34527424).
- Risiglione P., Leggio L., Cubisino S.A.M., Reina S., **Paternò G.**, Marchetti B., Magrì A., Iraci N., Messina A. “*High-Resolution Respirometry Reveals MPP+ Mitochondrial Toxicity Mechanism in a Cellular Model of Parkinson’s Disease*”. Int J Mol Sci. 2020 Oct 22 (IF: 5.6; PMID: 33105548).
- Leggio L., **Paternò G.**, L’Episcopo F., Tirolo C., Raciti G., Pappalardo F., Vivarelli S., Giachino C., Caniglia S., Serapide M.F., Marchetti B., Iraci N. “*Extracellular Vesicles as Nanotherapeutics for Parkinson’s Disease*”. Biomolecules. 2020 Sep 16 (IF: 5.5; PMID: 32948090).

- Leggio L., Arrabito G., Ferrara V., Vivarelli S., **Paternò G.**, Marchetti B., Pignataro B., Iraci N. “*Mastering the Tools: Natural vs. Artificial Vesicles in Nanomedicine*”. Adv Healthc Mater. 2020 Aug 31 (IF: 10.00; PMID: 32864899).
- Marchetti B., Leggio L., L’Episcopo F., Vivarelli S., Tirolo C., **Paternò G.**, Giachino C., Caniglia S., Serapide M.F., Iraci N. “*Glia-derived extracellular vesicles in Parkinson’s Disease*”. J Clin Med. 2020 Jun 21 (IF: 3.9; PMID: 32575923).

## 8. Meetings and educational workshops

- *Co-author*: “An Analytical Model for the Inference of the EV Reception Process Parameters in Cell-to-Cell Communication”. (ACM NanoCom 2023. 20-22 September 2023, Coventry).
- *Co-author*: “Brain region specificity of astrocyte-derived extracellular vesicles: uncovering the mechanisms of neuroprotection in Parkinson’s disease”. (3rd EVIta Symposium. 13-15 September 2023, Urbino).
- *Poster – presenting author*: “Exploring the neuroprotective mechanisms of astrocyte-derived extracellular vesicles in the context of Parkinson’s disease.” (Glia 2023. 8-11 July 2023, Berlin).
- *Co-author*: “Brain region specificity of astrocyte-derived extracellular vesicles: molecular determinants for the preservation of mitochondrial functions in Parkinson’s Disease.” (AD/PD 2023. March 28 - April 1 2023, Gothenburg).
- *Oral presentation – presenting author*: “Brain region specificity of astrocyte-derived extracellular vesicles: preservation of mitochondrial function in a cellular model of Parkinson’s disease.” (SIB 2022. 20 December 2022, Catania).
- *Co-author*: “Uncovering the mechanisms of neuroprotection by astrocyte-derived extracellular vesicles in Parkinson’s disease.” (SIB 2022. 20 December 2022, Catania).
- *Oral presentation – presenting author*: “Secretion of extracellular vesicles from nigrostriatal astrocytes: implications for neuroprotection in the context of Parkinson’s disease.” (VIII Retreat of the Department of Biomedical and Biotechnological Sciences, University of Catania. 3 December 2022, Catania).
- *Poster – presenting author*: “Brain region specificity of astrocyte-derived extracellular vesicles: preservation of mitochondrial function in a cellular model of Parkinson’s disease.” (FENS forum 2022. 09-13 July 2022, Paris).
- *Co-author*: “Astrocyte-derived extracellular vesicles from specific brain regions rescue apoptosis and preserve mitochondrial function in a cellular model of Parkinson’s disease.” (2nd EVIta Symposium. 20-22 September 2021, Lucca).
- *Co-author*: “Astrocytes from distinct nigrostriatal brain regions secrete extracellular vesicles able to mediate neuroprotection in cellular models of Parkinson’s disease”. (XV European Meeting on Glial Cells in Health and Disease. Online, 5-9 July 2021).
- *Co-author*: “Phenotypic and functional analysis of nigrostriatal astrocyte-derived extracellular vesicles reveals an intrinsic brain area-dependent neuroprotective

potential in Parkinson's disease models". (ISEV2021, online conference, 18-21 May 2021).

- *Video Poster – presenting author*: “Astrocyte-derived extracellular vesicles from nigrostriatal brain regions differentially exert dopaminergic neuroprotection.” (BraYn Web Conference: 3rd Brainstorming Research Assembly for young neuroscientists. 25-26 November 2020).
- *Co-author*: “Characterization of exosomes as natural messengers of bioactive molecules in the glia-neuronal signaling in Parkinson’s disease.” (BraYn Conference: 2nd Brainstorming Research Assembly for young neuroscientists. 14-16 November 2019, Milano).
- *Co-author*: “Ultrastructural and molecular characterization of astrocyte-derived extracellular vesicles from nigrostriatal brain regions: implications for dopaminergic neuroprotection.” (1st EVIta Symposium. 6-8 November 2019, Palermo).
- *Co-author*: “Ultrastructural and molecular characterization of astrocyte-derived extracellular vesicles from nigrostriatal brain regions: implications for dopaminergic neuroprotection” (XIV European Meeting on Glial Cells in Health and Disease. 10-13 July 2019, Porto).
- *Training courses*: “Information Systems Security and Phishing”. (Institute Pasteur. 12 October 2023, Paris).
- *Training courses*: “Biological, Chemical and General Risks in lab”. (Institute Pasteur. 20-25 September 2023, Paris).
- *Training course*: “Introductory course of Glia Congress”. (Glia 2023. 7 July 2023, Berlin).
- *Training course*: “Alfatest: Introduction of Zetasizer Ultra, Nanosight e Exoview, and demonstration of Zetasizer Nano S90 instrument”. (University of Catania. 9 May 2023, Catania).
- *Training course*: “Smart Biotech 2022”. (EXPOLAB 2022. 21-22 September 2022, Catania).
- *Training course*: “Smart Safety 2022”. (EXPOLAB 2022. 28-30 September 2022, Catania).
- *Training course*: “Salute e sicurezza nei luoghi di lavoro”. (University of Catania. 3 March 2021, Catania).

- *Training course*: “Corso Base sulla sperimentazione Animale”. (University of Catania. 13 December 2019, Catania).
- *Training course*: “The Outer Mitochondrial membrane: biogenesis and functions at the interface between the organelle and the cytosol”. (University of Catania. 27 November 2018, Catania).
- *Training courses*: “Salute e sicurezza nei luoghi di lavoro”. (University of Catania. 21-23 February 2017// 15 December 2014, Catania).